78-8694

RODON, Ignacio, 1949-
FILTRATION OF DUSTS AT 150°C BY A PANEL BED FILTER WITH PUFFBACK.

City University of New York, Ph.D., 1978
Engineering, chemical

University Microfilms International, Ann Arbor, Michigan 48106

FILTRATION OF DUSTS AT 150°C BY A PANEL BED FILTER WITH PUFFBACK

by

Ignacio Rodon

A dissertation submitted to the Graduate Faculty in Chemical Engineering in partial fulfillment for the degree of Doctor of Philosophy, The City University of New York

1978

This manuscript has been read and accepted for the Graduate Faculty in Engineering in satisfaction of the dissertation requirement for the degree of Doctor of Philosophy.

January 4, 1978
Date

Arthur M. Squires
Chairman of Examining Committee

January 4, 1978
Date

Executive Officer

Prof. Arthur M. Squires (Chairman and Mentor
Prof. Robert A. Graff
Prof. Leslie Isaacs
Prof. Robert Pfeffer
Supervisory Committee

The City University of New York

ABSTRACT

This research was undertaken to test the filtration performance of the panel bed filter at 150°C in a laboratory unit.

Our goal was to determine the operational conditions which would provide high collection efficiencies, with practicable gas throughput and pressure drop, in the filtration of dusts of different characteristics.

The panel bed filter is a particulate collection device in which the constraint to a two-phase flow is a tall narrow bed of granular solids retained between two vertical porous walls. The dirty gas-entry wall comprises louvers that support and expose free surfaces of the solid.

The filtration performance of a panel bed is greatly improved if a surface layer deposit of dust is rapidly formed at each free surface. These "surface cakes" should have coherent "roots" which extend a short distance into the granular bed. This mode of operation requires the periodic removal of the cakes whenever resistance to gas throughput increases to an unacceptable level.

"Puffback"; a reverse surge flow of gas applied during a momentary interruption of filtration; causes deposited dust, together with a little of the granular solid, to spill from each of the free surfaces and therefore permits the cyclic operation of the filter with no permanent increase in pressure drop.

Filtration tests, conducted at 150°C and under suitable conditions, with representative samples of two coal fly ashes and clinker cooler cement dust, afforded overall efficiencies beyond 99.9 Wt%.

The results obtained with these three dusts suggest the use of 40-50 mesh angular sand as the filtration foundation medium for high efficiency operation. A face velocity of 11 cm/s appears to be a practicable design velocity. The clean bed pressure drop under these conditions would be about 9 cm of H_2O. The frequency of puffback cleaning should be equivalent to a pressure drop across the filter cakes between 12 and 15 cm of H_2O. The spills of sand originated from an efficient puffback cleaning of the filter, would imply the need of a sand recycle system handling between 8 and 11 kilograms of sand per kilogram of dust removed.

The penetration trends observed, with the filtration systems studied, suggest that the adhesivity and/or autohesivity of the dust being filtered can considerably alter the filter's reaction to changes in operating conditions (i.e., filtration velocity, frequency and intensity of cleaning).

Efficiency for removal of sub-micrometer particles, in tests conducted with one fly ash and at optimum conditions, was estimated at beyond 99 Wt%. During these tests the panel bed was an absolute filter for particles bigger than 5 micrometers.

Experiments performed in a horizontal bed of sand at 150°C suggest that visual observation of the formation of a

deposit of a given dust upon a granular solid can be a useful preliminary test to select a size of solid suitable for a panel bed filter to deal with the dust.

A new design for the gas-entry louvers was incorporated to the filter. This design was found to be appropriate for high-efficiency panel bed filtration of dusts of different characteristics. It was concluded that the size of the granules for the filtration of a given dust at preselected conditions should be such as to provoke the formation of surface filter cakes whose roots do not extend beyond the width of the front louver plate.

ACKNOWLEDGEMENTS

I wish to thank Professor Arthur M. Squires for his guidance and interest throughout this investigation.

I also wish to thank Professor Robert A. Graff, Dr. Kun Chieh Lee, Professor Leslie Isaacs and Professor Robert Pfeffer for their contribution to this research.

I thank the staff of the Marine Microbial Ecology Laboratory of the Biology Department for their assistance with the microscopy.

Thanks are also due to the Chemical Engineering Shop, especially John Bodnaruk, George DiIorio and John Spencer for their assistance in constructing the experimental apparatus.

My deep thanks to William P. Hoogsteden, Jesus Urbaez, and Jonah Smith for their assistance in the experimental work.

I am grateful to the Venezuelan Government which through La Universidad del Zulia supported me while pursuing my doctorate.

A grant from the Electric Power Research Institute supported a major part of this work.

DEDICATION

This research is dedicated to my wife, Isabel, to my parents, Dr. A. Raul Rodon and Carolina Gonzalez Rodon, and to my parents in law, Dr. Silvestre Rincon and Mary Vezga Rincon who provided me with the courage and patience that this effort required.

TABLE OF CONTENTS

LIST OF TABLES

LIST OF FIGURES

CHAPTER 1.0 INTRODUCTION

In many present-day advanced processing technologies dust removal has become a necessity. The ecological insult associated with its generation coupled with foreseen stricter regulations have developed great interest in the field of particulate collection.

The enormous advantages of gravel filters versus conventional dust collecting devices, for high temperature operation, have resulted in innovations and improvements of granular filters which have been used since the late 1800's.

Squire's idea of using a sand filter with intermittent cleaning for the high efficiency filtration of dusts at high temperature opened up a new line of effort in the field. The panel bed filter seemed to offer benefits which motivated the research needed for its development.

Some ten years ago a panel bed filter laboratory was created at the City College of New York.

At the outset, from work in the laboratory at room temperature, it was observed that a coherent deposit of fly ash, i.e. a "filter cake", can form upon sand that is "sufficiently fine". For example, at room temperature it was possible to deposit a coherent filter cake upon the surface of 20-30 mesh sand, but not upon 10-14 mesh sand.

A panel bed filter that exposes a large number of sand surfaces for supporting deposits of dust was developed. Louvered walls, somewhat resembling venetian blinds, hold a sand bed in a

tall, relatively narrow "panel". Gas flows in the horizontal direction across the sand bed, and dust in the gas tends to deposit upon sand surfaces at the gas-entry "face" of the panel.

The work of Lee, based on Squire's idea, led to the development of a technique for cleaning surfaces at the gas-entry face, which was called "puffback". It consists of interrupting the flow of gas to be filtered, and causing a surge flow of gas to move in the reverse direction across the panel. It was discovered that this reverse surge flow creates a mass movement of the sand bed toward the gas-entry face, causing sand from each gas-entry surface to spill and to carry with it the deposit of dust accumulated during a filtration step prior to cleaning.

The investigation of this cleaning technique in a small laboratory panel bed filter suggested that a successful puffback requires that the reverse surge flow of gas act over a suitable time scale, in general less than about 50 milliseconds.

The surge flow creates a reverse pressure difference across the panel bed, and studies of this difference with high-speed transducers proved useful. Unexpectedly, the size of the spill of sand from the gas-entry face does not depend upon the peak value of the reverse pressure difference. Rather the spill depends only upon the "active time" during which the reverse pressure difference is greater than the minimum pressure difference that just produces a tiny spill of sand.

From laboratory experiments it was found that a coherent filter cake of fly ash can filter micron-size particulate matter

at high efficiency. It was expected therefore that the panel bed filter might show an extremely high efficiency for removing power-station fly ash from gas toward the end of a filtration cycle, after a fly ash cake had developed. A surprise in this research was that after a few filtration cycles, the filtration efficiency is excellent even at the outset of a new cycle.

There is apparently a synergism between puffback cleaning and the micro-mechanics of the filter cake, which results in the unexpectedly high efficiencies obtained. The filter cake appears to have "roots" extending into the sand bed for a distance several times the diameter of a grain of the sand. Puffback cleaning, if properly monitored, can remove only one or two layers of sand grains and therefore leaves the roots behind. These evidently serve to promote high filtration efficiency of fly ash entering the sand bed at the start of a new filtration cycle.

The room temperature filtration experiments performed with a small laboratory panel bed, provided overall efficiencies beyond 99.99 Wt % in the filtration of redispersed fly ash. Experiments performed in a horizontal bed of sand with different dusts, indicated that the autohesivity of the dust and its adhesivity toward sand or another granular collection medium can drastically affect the conditions at which a coherent filter cake is formed.

Since both autohesivity and adhesivity could be expected to change with temperature it was decided to explore the filtration performance of a small panel bed at a relatively higher temperature, and with dusts of different characteristics.

The room temperature panel bed filter set-up was then modified to allow us the study of the different variables which affect the efficiency of collection of redispersed dusts at 150°C. This temperature, besides being a typical stack gas temperature, assured the removal of moisture and consequently the assistance of capillary forces in the filtration mechanism.

The objective of this research was to achieve the highest possible collection efficiencies in the filtration of redispersed dusts at 150°C.

CHAPTER 2.0: EFFORTS TO FILTER GAS BY A GRANULAR BED

Equipment and processes employing fixed granular beds of various materials including sand for the removal of particles from air streams have been reported as far back as the late 1800's and early 1900's. Sand bed filters were also an early expedient in the control of radioactive particle emissions from the Hanford processing plants. (Jackson, 1973).

An extensive coverage of the literature on fixed granular bed filtration of aerosols has been published (Juvinall et al., 1970) in which some designs and collection performance are described in detail.

The ruggedness that can be designed into a sand-bed filter for a variety of relatively severe conditions of operation (such as high temperature, thermal shock, air-pressure shock, ground acceleration and chemical attack) called upon the attention of those who at the beginning of this century became aware of the need for dust respirators and dust-removal devices.

2.01 Modes of Operation

There are two modes of operation which have characterized the application of granular beds as filters: 1) Deep bed filtration and 2) Surface cake filtration

1) Deep bed filtration

As Figure 2-1 illustrates "deep bed filtration" is characterized by cylindrical granular beds of sand arranged in layersof increasing fineness in the direction of flow. This concept was proposed for the filtration of very dilute suspensions of aerosols at high efficiency and for low velocity operation, providing relatively low pressure drops and a long operating interval between cleaning or renewal (usually years).

A typical industrial application of this mode of operation was the sand bed filter for removal of radiactive aerosols from the processing stacks at Hanford. The design was conceived by Lapple (Juvinall et al., 1970) and implied the removal of active particles of 0.5 to 20 micrometers in diameter from a 2.29×10^{-3} g/m^3 suspension. The permissible outlet concentration was smaller than 2.29×10^{-5} g/m^3 (99% overall efficiency by weight). Preliminary tests with a 0.61 meter deep bed of 20-40 mesh sand gave overall efficiencies greater than 99.0 wt % at superficial gas velocities up to 5.08 cm/s. The sand filters were put into operation in October 1948. Their inside dimensions are 14.02 by 32.92 m with 2.59 m total depth of sand and aggregate. One of the untis contains 0.914 m of 20-40 mesh sand (finest granule used in the multilayer filters) and is operated under negative pressures at average air flow of 12.41 m^3/s with 18.54 cm of H_2O pressure drop and affording overall collection efficiencies of 99.8-99.9 Wt%.

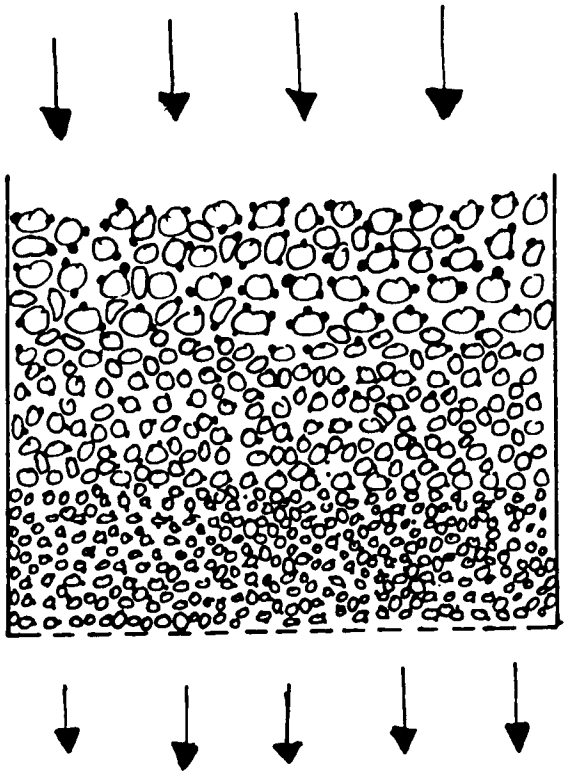

Figure 2-1 Deep Bed Filtration.

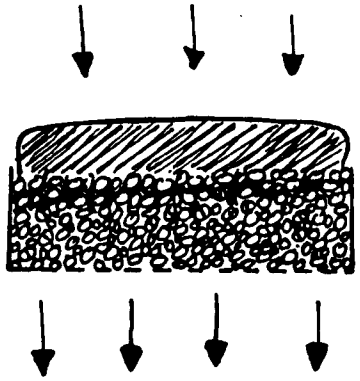

Figure 2-2 Surface Cake Filtration.

In 1968 (First, 1968) the filters had been in continuous operation for 20 years at Handford and 13 years at Savannah River without servicing or replacement. Such trouble-free service is an important advantage when intensively radioactive material is being collected; on the other hand a 1.524 m, 0.102 m-deep fiberglass filter at Hanford was operated with lower air-resistance and higher efficiency than the sand filters for 10 years before becoming plugged with ammonium chloride.

In spite of the advantages mentioned above, higher air flow resistance, lower efficiency, difficulty of final disposal when the bed is no longer functional, and higher initial cost have resulted in little current interest in deep bed sand filters as compared to fiberglass filters.

2) Surface cake filtration

As illustrated in Figure 2-2, "surface cake filtration" is characterized by shallow beds of particles stacked in a vertical array. For best performance, the unit is to be operated under conditions which provoke the rapid formation of a surface filter cake of the dust being filtered, cake which has to be periodically removed whenever resistance to gas throughput increases to an unacceptable level. This design is best suited for the filtration of relatively concentrated solid-gas mixtures at very high efficiencies, and affording higher velocity operation at similar pressure drops achieved in deep-bed sand filters.

An old idea is to treat a gas by causing it to flow in

a horizontal direction across a bed of granular solid disposed in a tall, narrow "panel." Such a bed is seen, for example, in Figure 2-3 where the bed is held in place by louvered walls which resemble venetian blinds.

The example shown in Figure 2-3 is the first we know of. At the time of Henry Deacon's death in 1876, the problem of finding a suitable reactor for his famous chlorine process had not yet been solved. Early in 1878, his assistant, F. Hurter, announced the solution illustrated in Figure 2-3 in a letter to Lunge (Lunge, 1880). Figure 2-3 provided Hurter's operators with a quick way to dump the short-lived Deacon catalyst a portion at a time, yet without having to shut down completely and cool the reactor. No doubt Hurter also appreciated the low pressure drop and high gas treating capacity inherent in equipment like Figure 2-3. It remained in use until about 1910, when chlorine byproduct of electrolytic caustic displaced the Deacon process.

Over the past century, many patents and publications have appeared that essentially go back to the idea of Figure 2-3, but relatively few applications have emerged (Squires and Pfeffer, 1970). A number of inventors have proposed improvements, combinations and innovations related to the application of the structure of Figure 2-3 to the problem of filtering dust from industrial gases, but with no general acceptance or success. It can easily be recognized that the complexities involved in just mechanically

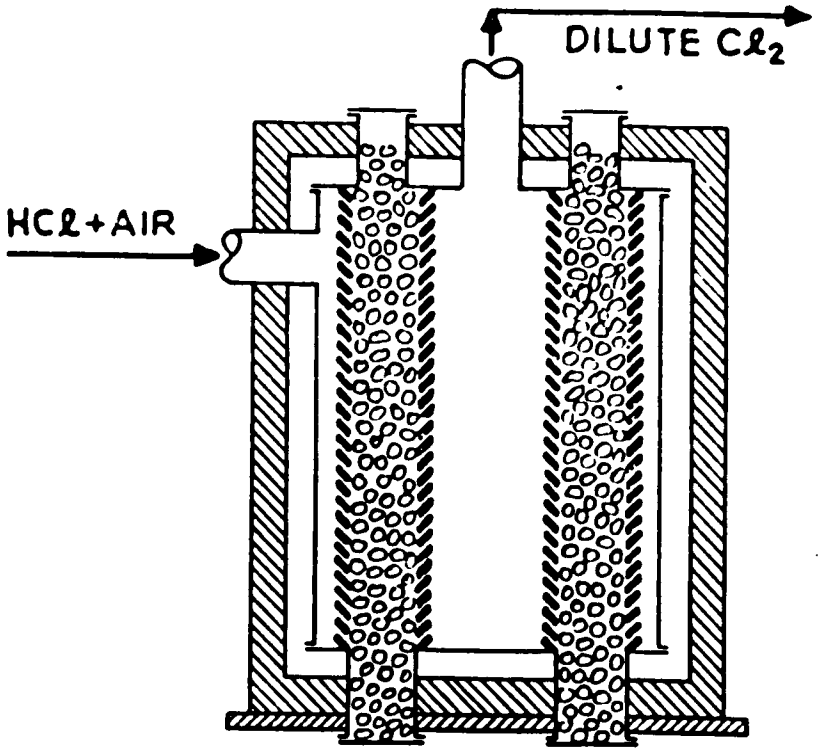

Figure 2-3 Panel Bed Reactor for Deacon Process. The twelve-sided, nearly circular panel was housed in a circular steel shell within a brick furnace. The catalyst space was 0.914 meters across, and both outer diameter and height were about 4.57 meters. The catalyst space was divided by partitions into six segments, one of which was dumped and renewed each fortnight.

supporting large quantities of heavy sand can hardly compete with the simplicity of light-weight cloth-bag filters reportedly offering equally efficient collection of fines. Besides weight consideration the in-situ ability to remove the filter cake of collected dust by flexing a cloth bag presents a considerable challenge to its counterpart in sand bed devices (Zenz and Krockta, 1972).

The past 20 to 30 years have now seen a renewed interest developing in this field as a result of the realization of the enormous advantages of "sand" versus cloth for high-temperature operations in many present-day advanced processing technologies.

Typical of the mainstream efforts are a) the Pall Fitler (Fixed Porous Metal Sintered Beds); b) the Mechanical Industries Filter (Continuous Moving Gravel Bed); c) the Lurgi Filter (Fixed Bed with Vibratory Cleaning); d) the Ducon Filter (Fixed Bed with Fluidized Expansion Cleaning); e) the Rex Gravel Bed Filter (Cyclone Fixed Bed Combination with Backflux Air and Smoothing Device Cleaning). A brief description of each will present the progressive improvements and the encountered difficulties.

a) The Pall Filter

As illustrated in Figure 2-4, Pall's design (Pall, 1953) consists of a thin bed of granules constructed by sintering a shallow layer of metallic granules in a high temperature furnace. Such sheets of sintered metal granules are sold commercially for filtration purposes. As depicted

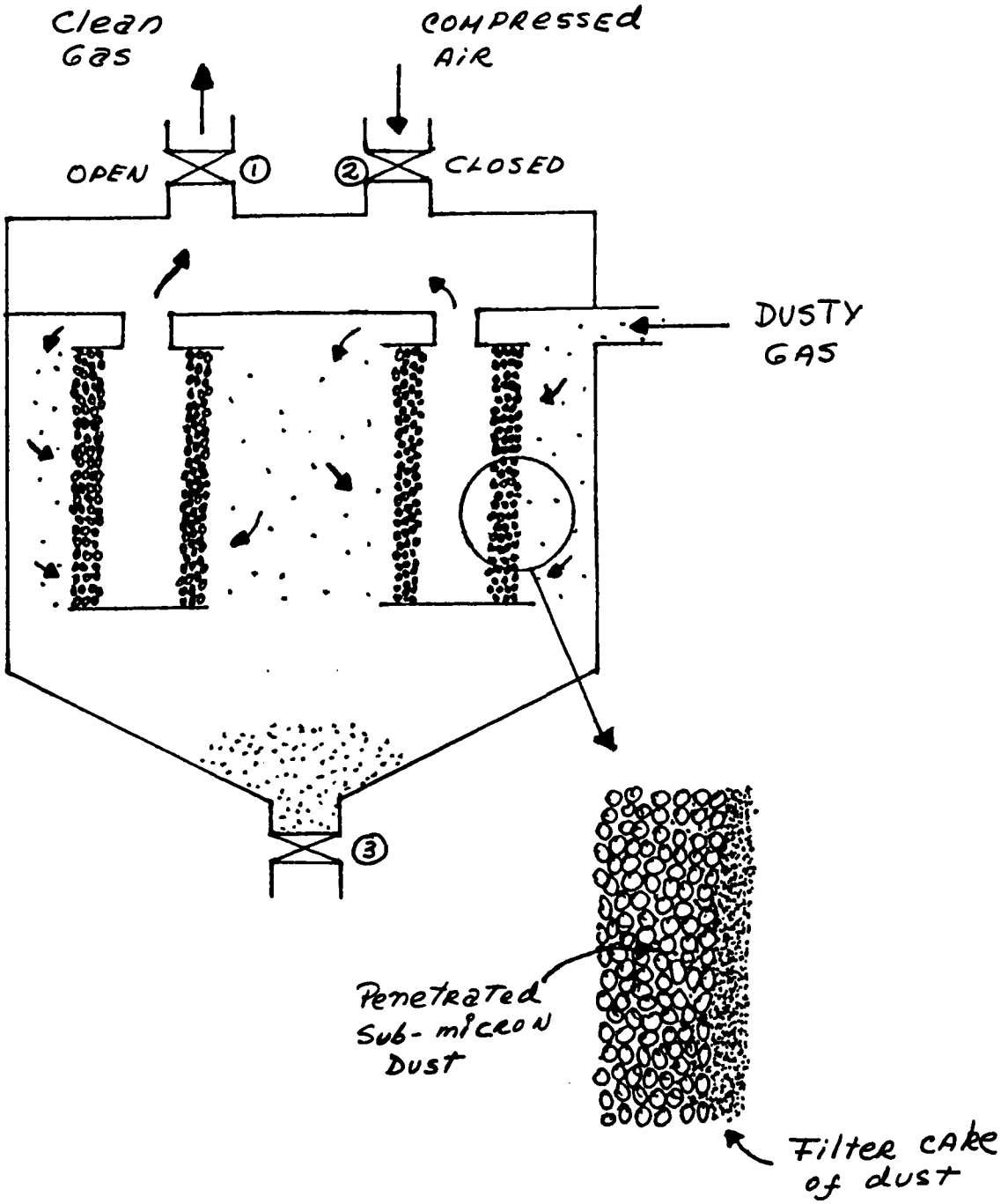

Figure 2-4 The Pall Filter.

in Figure 2-4, porous sintered metal filters are generally adapted to gas systems in tubular form. In normal operation valve 1 would be open, allowing dusty inlet gas to flow through the elements, depositing a filter cake on their outer upstream surfaces and leaving through the exhaust plenum. When the cake has grown to a thickness exhibiting high-pressure drop, valve 1 is closed, valve 2 is opened, and a short, high-pressure pulse of air is admitted in reverse flow through the porous elements to dislodge the filter cake which falls to the bottom of the containing vessel, to be eventually withdrawn through valve 3. In continuous use, the valves operate on a timed cycle and the containing vessel is provided with a multiplicity of porous elements and separate plenums for localized reverse cleaning. Zenz and Krockta (1972) point out that in order to obtain structural strength, the granules making up the porous element must be small in size to present sufficient bonding surface. This results in high-pressure drop or low gas capacity despite the only approximately 0.32 cm wall thickness of the elements. It is also mentioned (Zenz and Krockta, 1972) that the thin wall tubes are very subject to cracking as a result of repeated thermal shocks between high-temperature operation and relatively colder reverse-flow cleaning blasts.

b) The Mechanical Industries Filter

In the early 1950's Mechanical Industries Inc. introduced the Dorfan impingo filter. As Figure 2-5 illustrates the

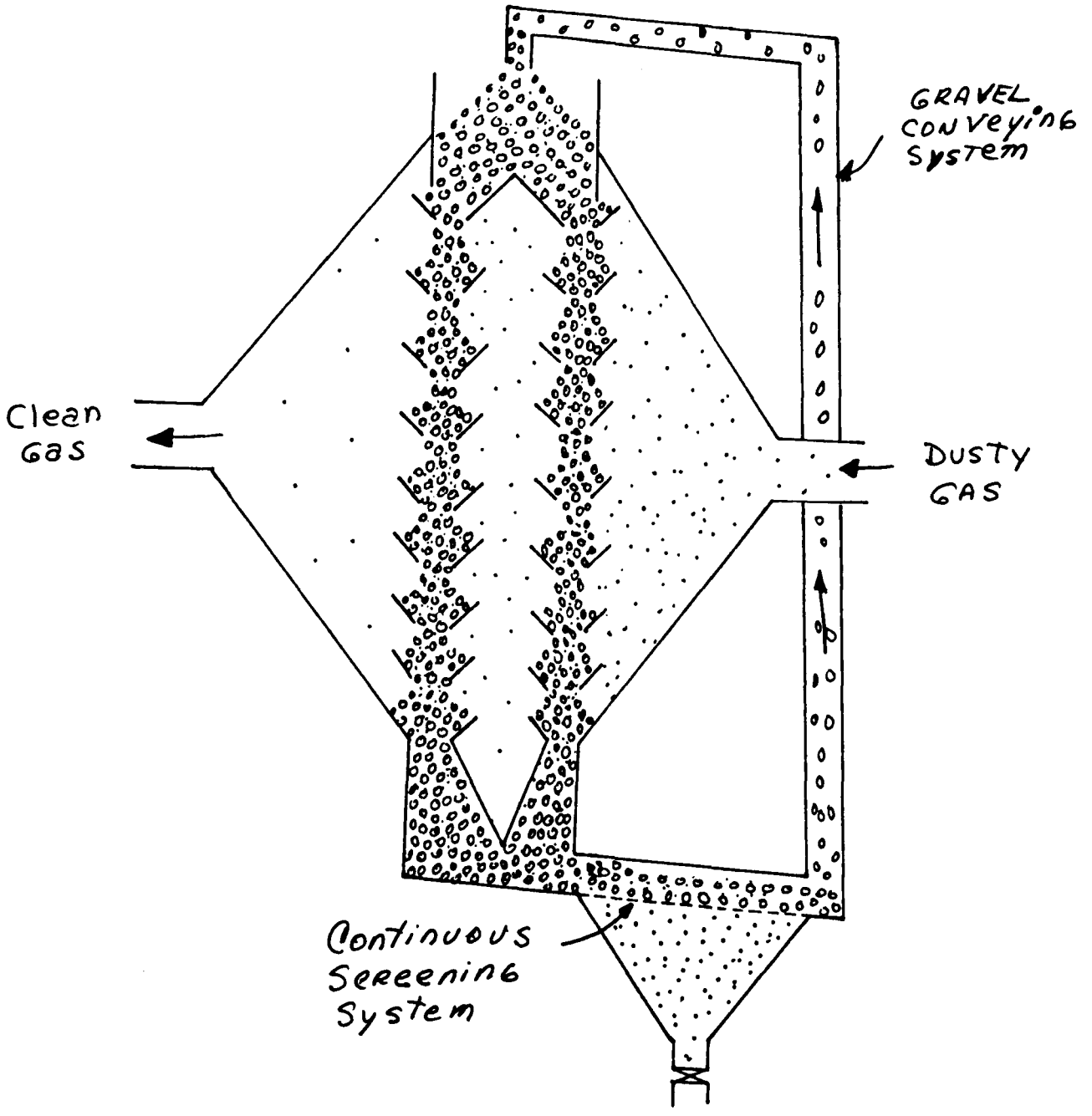

Figure 2-5 The Mechanical Industries Filter.

filter consisted basically of a down flowing bed of gravel retained between louvered walls. Dust laden gas was filtered by blowing through the bed normal to the direction of gravel flow and the filtered dust carried downward with the gravel, trapped within its interstices.

These filters were designed with relatively large granules (6.35 to 38.1 mm in diameter) in order to provide large gas throughput capacity at reasonable pressure drops. This mode of operation resulted in low collection efficiencies especially for the small particles present in the suspension. It was therefore suggested the use of staging beds in series as shown in Figure 2-5. Units of this type were installed in a number of asbestos plants, but they failed to find general applicability. (Zenz and Krockta, 1972.)

c) The Lurgi Filter

The Lurgi MB-Filter was developed by Messrs. Max and Wolfgang Berz in Germany (Engelbrecht, 1965). As Figure 2-6 illustrates the filter consists of several parallel compartments connected by a common raw gas duct and a common clean gas duct. Each individual compartment can be isolated from the gas stream by a butterfly damper (Figure 2-6). When an individual compartment is in filtering service, the raw gas passes upward through the filter bed of the horizontally arranged filter bed container. The dust in the gas will be retained by the filter bed and the clean gas will leave through the clean gas duct on top. When a compartment is to be cleaned the butterfly damper

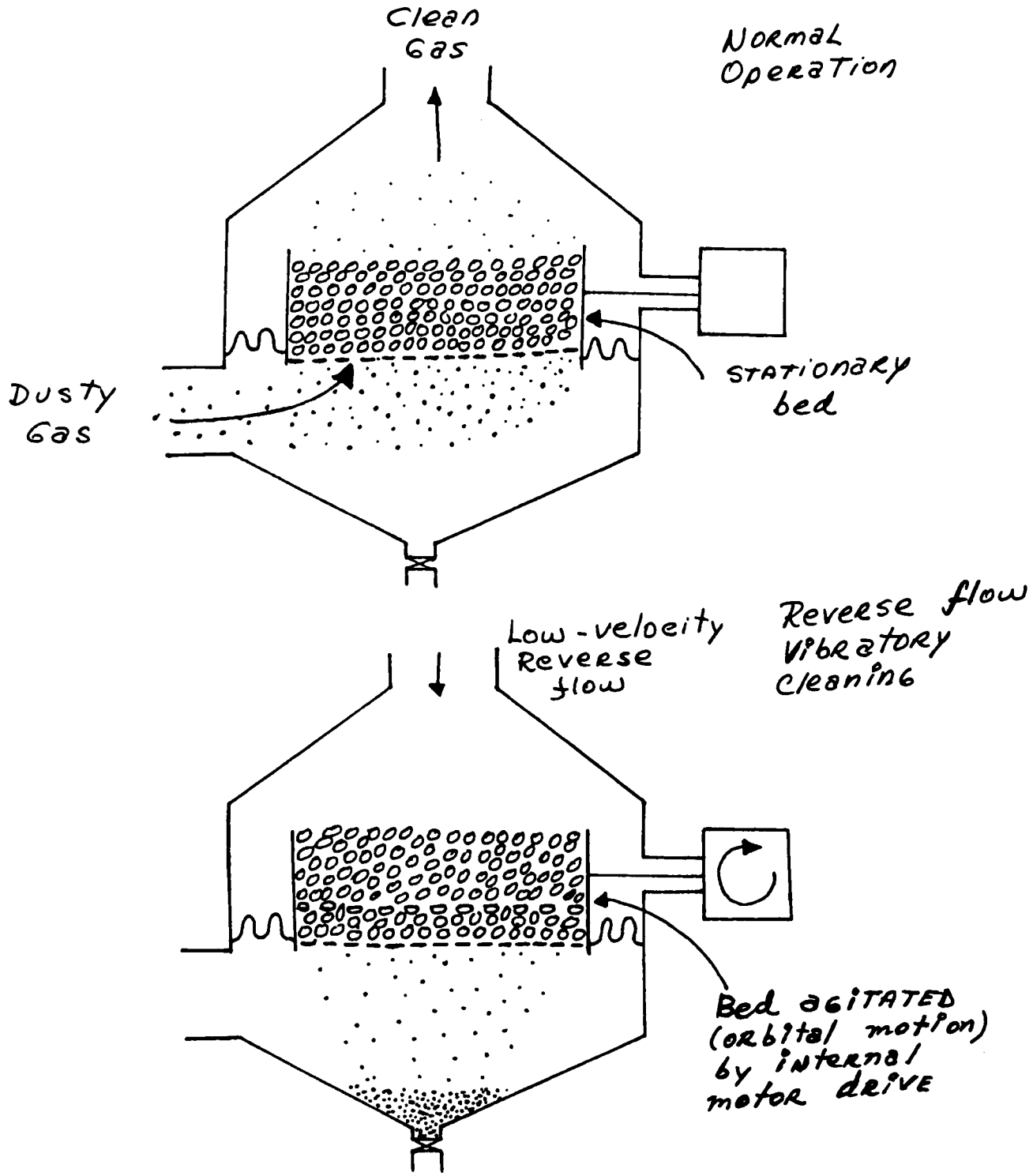

Figure 2-6 The Lurgi Filter.

in the clean gas duct will be closed so as to prevent raw gas from entering the compartment. A laterally arranged vibrator motor then goes into action vibrating the filter bed so that the retained dust will fall downward into the hopper from where it will be removed by a screw conveyor. When the butterfly damper is closed a sweep air damper is opened simultaneously so as to pass air or gas by suction to the filter hopper. The flow of this sweep air from top to bottom favors the downward movement of the dust during the cleaning period. At the end of the cleaning of the filter bed, the vibrating motor is stopped, the sweep air damper is closed and the butterfly damper is opened and again admits dust laden gas to the filter compartment. The units were usually designed with two superimposed filtering layers. The first layer consists of steel turnings or other suitable material with a negligible draft loss. The second filter layer is held on a horizontal sieve plate and consists of loosely packed material such as gravel with almost spherical pebbles of equal size and rough surface. Grain sizes between one and six mm (3-18 mesh) are used as filter bed fillings. Usually the specific load on the filter bed is, depending on application, between 0.278 and 0.83 $m^3/s/m^2$ of filter surface area. The draft loss of the filters, also depending on application, ranges between 5.08 and 15.24 cm of water.

Due to the need of using elastic seals which insulate the filter bed container from the filter casing, the maximum

continuous operating temperature is 246° C (Arras et al., 1972).

The first filter of this kind went into operation in 1959 for cleaning the waste air from Fuller coolers in a West German cement works. In 1970 (Zenz and Krockta, 1972) when the unit was reportedly withdrawn from the market almost two hundred plants in differend fields of application were cleaning about 1652 m^3/s (Arras et al., 1972).

Its shortcoming lies in several factors: 1) the strain imposed on the necessary flexing membranes associated with the vibrating mechanism shortens the life of the unit; 2) the unit could not be used continuously at temperatures higher than 246° C; 3) the unit could not handle high dust concentrations without a preliminary separator; 4) since the raw gas passes the gravel bed upwards, an excessive dust loading may lead to fluidization; 5) temporary excessive "upset" gas volumes above the design level causes the collection efficiency to deteriorate (Arras et al.,1972). Some typical applications of the Lurgi Filter were: 1) Cleaning of waste gas from a pulverizing and drying unit for cement raw materials; 2) cleaning of waste gas from lime kilns; 3) cleaning of waste air from a clinker cooler; 4) cleaning waste gas from a drying drum for road construction material (mobile unit).

c) The Ducon Filter

The Ducon Filter, introduced in 1966 by the Ducon Company, Inc., is illustrated in Figure 2-7. (Zenz and

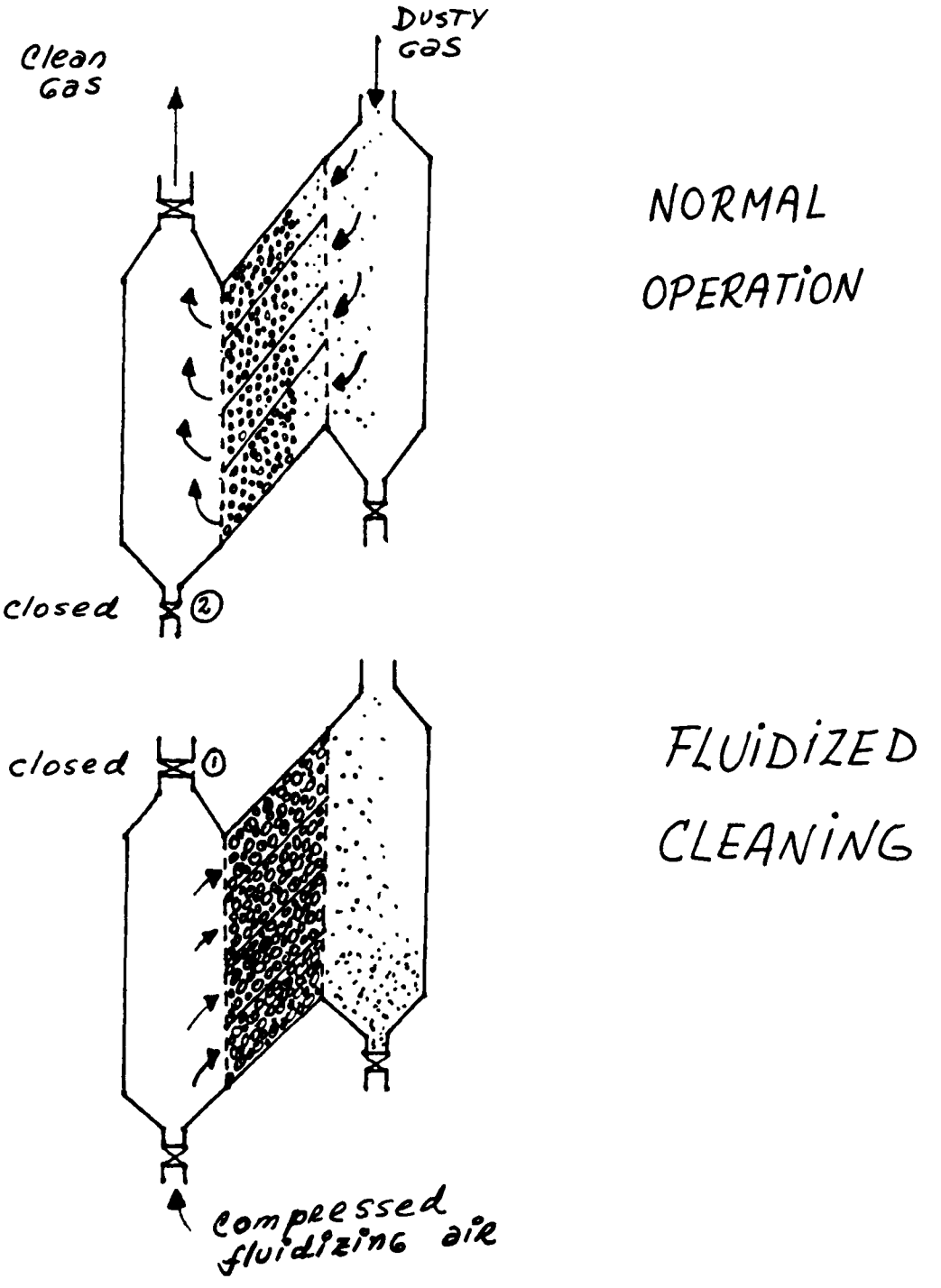

Figure 2-7 The Ducon Filter (First Generation)

Krockta, 1972). In normal operation dusty gas passes through vertical arrays of parallel shallow granular beds held within metal-walled compartments, shown as louvers, sealed at top and bottom by perforated meshes finer in aperture than the size of the bed granules. The dusty gas enters the beds at relatively high velocities in the range of 10.16 to 50.8 $cm^3/s/cm^2$ of bed surface area and deposits fines principally within their interstices. When flow resistance reaches a level requiring the bed to be cleaned, valve 1 is closed and valve 2 opened to admit a flow of compressed gas sufficient to fluidize the bed granules, and thus by entrainment expel the particles collected and agglomerated in the bed interstices. No loss of sand can occur since any granules which might reach the end of a compartment cannot escape through the perforated retaining mesh. This initial design was tested in numerous plant locations using a variety of particulate solids. A typical 260^oC continuous operation over a period of several months at 30.48 $cm^3/s/cm^2$ of bed surface showed reduction of Fluid Cracking Catalyst (F.C.C.) fines from an inlet loading of 2.29 g/m^3 to an outlet of less than 2.29×10^{-2} g/m^3 of which all was smaller than 3 micrometers. The size of the granules used in these tests was in the range of 30 U.S.S. mesh. One inherent disadvantage of a device like the one illustrated in Figure 2-7 is that there is the possibility of reentrainment of dust particles while cleaning the beds.

After a six year effort the Ducon Filter was modified

to match the characteristics desired of an F.C.C. regenerator flue gas filter (Kalen and Zenz, 1973). Figure 2-8 illustrates the new design. The basic concept that blowback fluidization of a shallow granular bed should dislodge interstitially trapped fine particles, by near analogy to the blowback flexing of the fibers of bag filters, led to the development of this commercially viable filter. Each cylindrical element of the granular bed filter consists essentially of multiple shallow beds of sand stacked vertically within two perforated concentric metal tubes. The elements are supported from a clean gas plenum within a housing. The basic arrangement is shown in Figure 2-8. Particle laden gas flows through the unit continuosly. Periodically a pulse of blowback gas is admitted for a fraction of a second, through ports provided for each element, to momentarily fluidize the filter medium and clear it of accumulated fines. A typical element is shown in Figure 2-8. The beds of sand grains rest on slotted inner screen supports having opening dimensions slightly smaller than the diameter of the sand grains. Above each bed there is an annular space with an outer screen similar to the inner screen. In operation, particle laden flue gas entering the dusty side of the filter housing passes through the element's outer retaining screens, flows downwardly through the inner or bed-supporting screens, and through the inner cylinder into the clean gas plenum to the vessel outlet nozzle. The bulk of the filtered catalyst

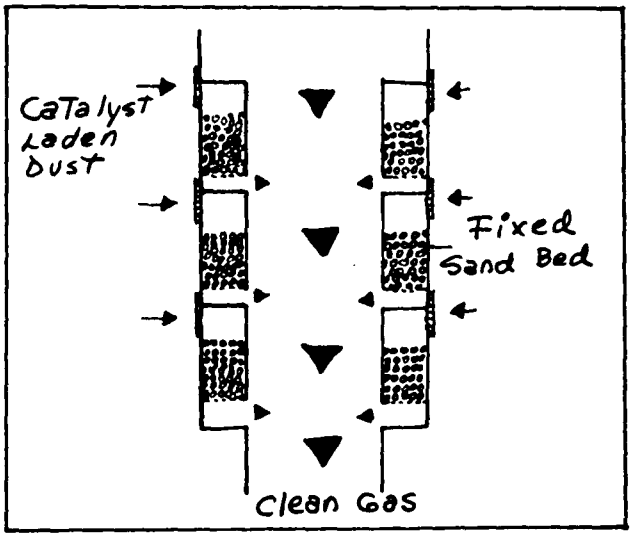

Figure 2-8 The Ducon Filter (Second Generation).

fines accumulate on the surface and within the interstices of the sand beds leading to a gradually increasing resistance to gas flow.

When the resistance to flow within an element reaches a predetermined level, a small volume of compressed blowback air is introduced to the element in a pulse, which induces blowback gas flow from the clean gas plenum, sufficient to momentarily fluidize all the sand beds within the element simultaneously. This blowback gas flexes the bed in fluidized expansion, expelling interstitially deposited agglomerated catalyst fines, as well as any accumulated catalyst fines on the bed surfaces, through the outer screen where they fall into the collection hopper for eventual drawoff. After the blowback pulse has passed, the sand grains fall back to their original fixed bed operating position. The short duration cleaning pulse consumes only a small amount of compressed air, and has no perceptible effect on the steady state gas flow through the filter.

A test unit was operated continuously for over 7 months filtering F.C.C. regenerator flue gas at a refinery. This unit has 2 elements each of which has 14 6.35 cm-deep beds of 760 micron-sand. The operating inlet temperature range was 371-482^{o}C for the filtration of a 0.34 to 1.95 g/m^{3} gas stream at 0.224 to 0.472 actual m^{3}/s. The total bed surface was 1.115 m^{2} and the measured overall efficiencies ranged from 85 to 98 Wt%. The inside and outside diameter of each element were 12.7 and 20.32 cm

respectively. The pressure drop through the unit varied from 15.24 to 30.48 cm of water.

It was predicted (Kalen and Zenz, 1973) that for achieving a 95.6 Wt% overall efficiency in the filtration of F.C.C. dust (at typical commercial operating conditions) at 25.4 cm/s upon 760 micrometer-sand, a pressure drop of 40.64 cm of H_2O is required. It was also indicated (Kalen and Zenz, 1973) that the presence of a small bypass of dirty gas during the moments when the sand beds were flexed or fluidized worked against obtaining higher collection efficiencies.

e) The Rex Gravel Bed Filter (Lurgi's second generation)

The experience gathered by Lurgi in the industrial operation of the MB filter was utilized when the cyclone-gravel bed filter combination was developed. In 1966, the first new GFE cyclone-gravel bed filter combination was installed in a cement works in South Germany and it was introduced in U.S.A. by Rexnord Inc. in 1971 (Schueler, 1972).

As illustrated in Figure 2-9 the Rex Gravel Bed Filter combination consists of parallel arrangement of several filter modules of equal size, connected by common raw gas and clean gas ducts. The raw gas enters the filter via a raw gas plenum in which some separation of the coarser fractions takes place by gravity-settling. From there the gas enters the cyclone separator where the medium fractions are partially separated and removed via a discharge airlock at the outlet. The pre-cleaned raw gas now rises from the

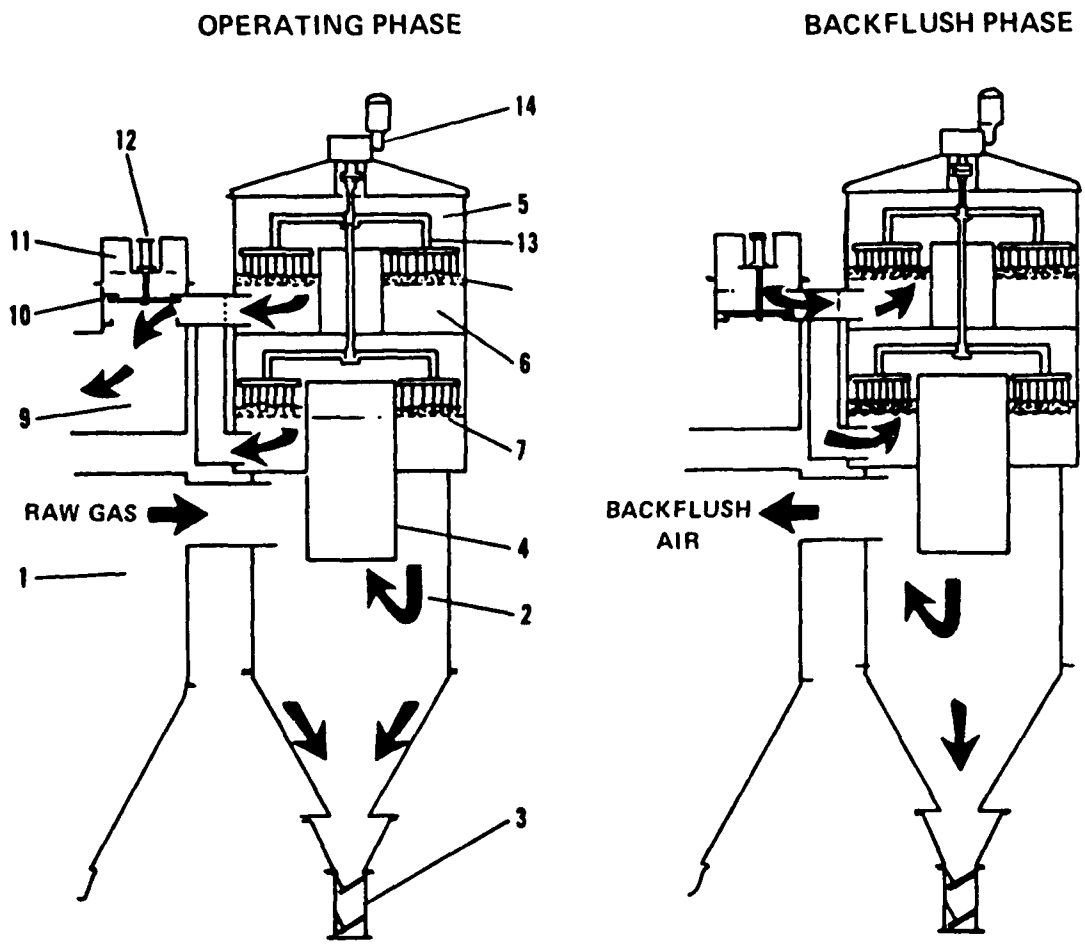

1. INLET CHAMBER
2. PRIMARY COLLECTOR (CYCLONE)
3. DOUBLE TIPPING GATE (DUST DISCHARGE)
4. VORTEX TUBE
5. FILTER CHAMBER
6. GRAVEL BED
7. SCREEN SUPPORT FOR BED
8. CLEAN GAS COLLECTION CHAMBER
9. EXHAUST PORT
10. BACKWASH CONTROL VALVE
11. BACKWASH AIR INLET
12. VALVE CYLINDER
13. STIRRING RAKE
14. STIRRING RAKE MOTOR/REDUCERS

Figure 2-9 The Rex Gravel Bed Filter.

cyclone through the vortex tube and enters the filter chamber. It passes through the horizontal filter bed from top to the bottom, so that most of the remaining fine dust is deposited on the quartz grains and in the interstices of this bed. The cleaned gas now flows through the clean gas collection chamber and passes through a valve into the clean gas duct. During the cleaning cycle, the unit is isolated from the gas stream by a disc valve. Then, backflush air is admitted to the filter chamber in a reverse flow direction to loosen the filter bed. This backflush air is forced in by using a backflush air blower. During the cleaning process a rake stirring device is rotated by a gear motor. After the dust is removed the backflux air and rakes are inactivated. Agglomerated dust particles are carried by the backflush air via the vortex tube back into the cyclone where the velocity is reduced and the gas stream deflected so that a large percentage of the dust settles out. The backflux air, containing the remaining dust, mixes with the raw gas and is then subjected to cleaning in the companion units of the filter. The unit is usually designed with two parallel-connected filter beds, one on top of the other (Figure 2-9) in order to minimize ground area requirements.

The unit is reported to be able to work at temporary peak temperatures of 482^{o} C, showing insensitivity, in terms of overall weight collection efficiency, to variations in the gas volume and in the raw gas dust burden. Overall

collection efficiencies around 99.7 Wt% in the filtration of clinker cooler dust have been reported (Arras et al., 1972). The pressure drop is typically between 7.62 to 12.7 cm of water.

In 1975 an evaluation of a Rex Gravel Filter was conducted by the Southern Research Institute under contract with E.P.A. (McCain, 1976). The tests were conducted on a gravel bed filter system controlling the emissions from clinker coolers on two 453.6×10^3 kg/day Portland cement kilns. The overall collection efficiency of the Rex gravel bed filter, determined by conventional techniques on a source producing particulate having a mass median diameter of about 200 microns ranged from 95 to 98 Wt% during three days of testing, throughout which the collector was said not to be operating in an optimum mode. Overall efficiencies determined from cascade impactor data during a second two-day test series were found to be 99.3 and 99.7 Wt%. The system pressure drops in the first test series ranged from 11.6 to 17.6 cm of water, while during the second test series the system pressure drop ranged from 9.6 to 14 cm of water. Measured fractional efficiencies were about 50 Wt% at 0.04 microns, zero or negative over the size interval from about 0.08 to 1.0 μm, approximately zero at 1 μm, 30% at 2 μm and about 97.5% at 5 μm. The system energy usage during the tests was approximately 1780 joules/SCM at a pressure drop of 11.8 cm W.C.

Table 2-1 summarizes the design specifications of the

system as tested. These tests suggested that the collection efficiency of the system is sensitive to the gas flow volume through the system, increasing markedly with decreasing flow over the range of values that were obtained during this series of tests.

In 1975 there were 25 units installed throughout the United States cleaning about 3870 actual m^3/s (Rexnord, 1976).

Typical applications of the Rex Gravel Filter for cleaning exhaust gases in U.S.A. are: 1) clinker cooler 2) lime kiln; 3) dolomite kiln; 4) windbox sinter machine; 5) refractory kiln; 6) cupola kiln.

Table 2.1

Design Specifications of a Rex Gravel Bed Filter

Inlet Volume Flow: 2266 ACM/min at 204°C
(80,000 ACFM at 400°F)

Backflush Volume Flow: 317 ACM/min at 66°C
(11,200 ACFM at 150°F)

Pressure Drop: 25.3 cm w.c. (10 inches w.c.)

Gravel Size: 4 mm (5/32 inch) x No. 6 mesh

Bed Depth: 11.4 cm (4-1/2 inch)

Bed Area: 3.72 m^2/Bed (40 ft^2/Bed)

(For a total of 59.5 m^2 of bed area with 52 m^2 actively filtering in normal operation.)

CHAPTER 3.0: PANEL BED FILTER: CONCEPTION AND PREVIOUS RESEARCH

3.01 Conception

Squires' idea (Squires, 1967) of using a sand bed filter with intermittent cleaning for the high efficiency filtration of dusts at high temperature emerged some fifteen years ago. Figure 3-1 shows the first version of the Panel Bed Filter in which, dust-laden gas flows horizontally across a tall narrow bed of a granular solid. Solid in each bed is retained between two vertical porous walls. The gas entry wall comprises louvers that support and expose free surfaces of the solid. A surface layer deposit of dust forms at each free surface, with roots that extend a short distance into the granular bed. After a time interval and during a momentary interruption of flow of gas being filtered, a reverse surge flow of clean gas (puffback) causes deposited dust together with a little of the granular solid to spill from each of the free surfaces. Squires and Pfeffer (1970) use the example of 16-30 mesh treating material, and gas throughputs around 6.1 $cm^3/s/cm^2$.

Figure 3-2 shows conceptually how Squires' idea might be applied in high temperature filtration. In this arrangement the dusty gas passes through a narrow bed of stationary sand held between a panel of louvers and a fine mesh screen The unit is to be operated under conditions

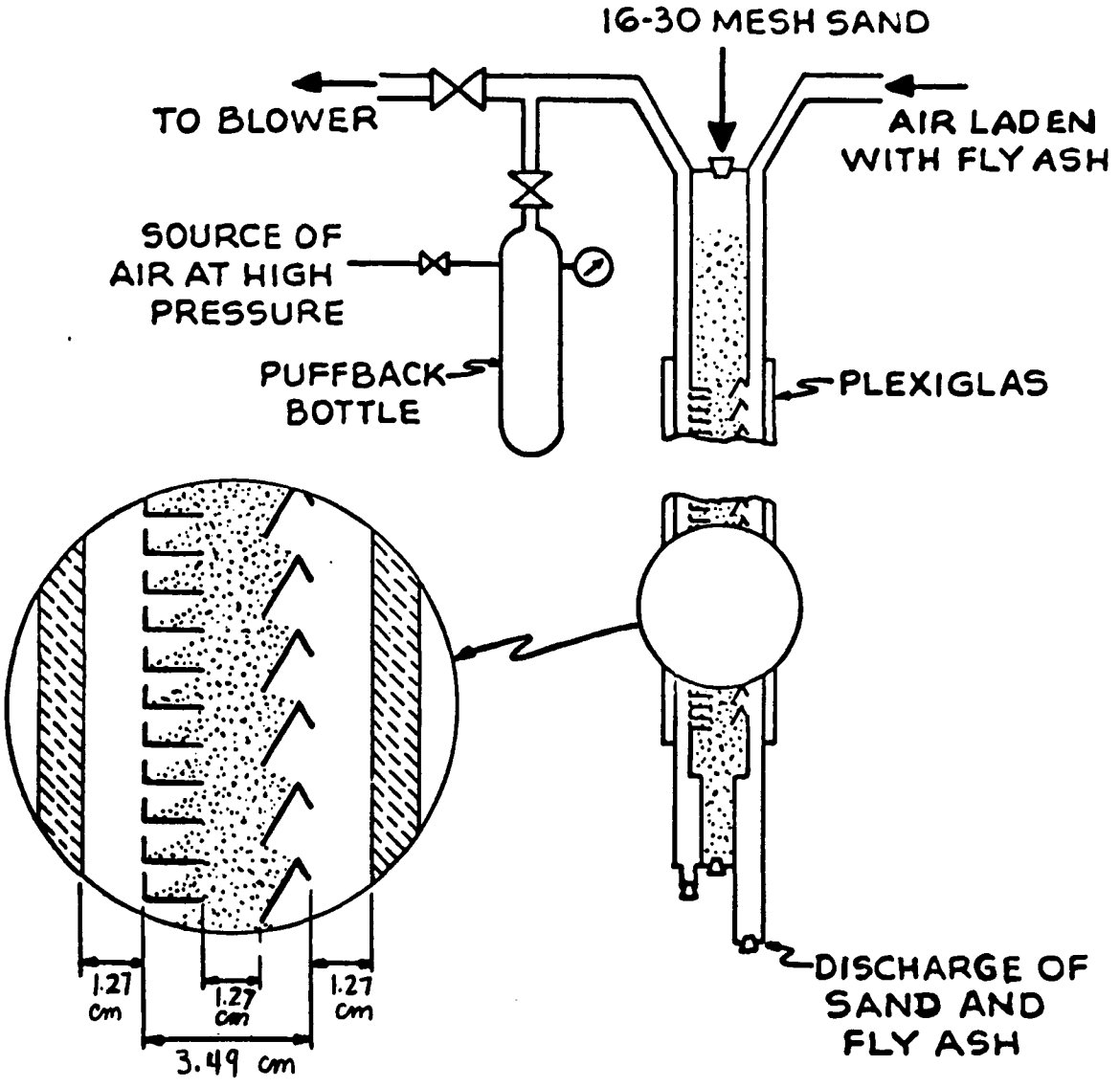

Figure 3-1 Arrangement of Unit LS-1.

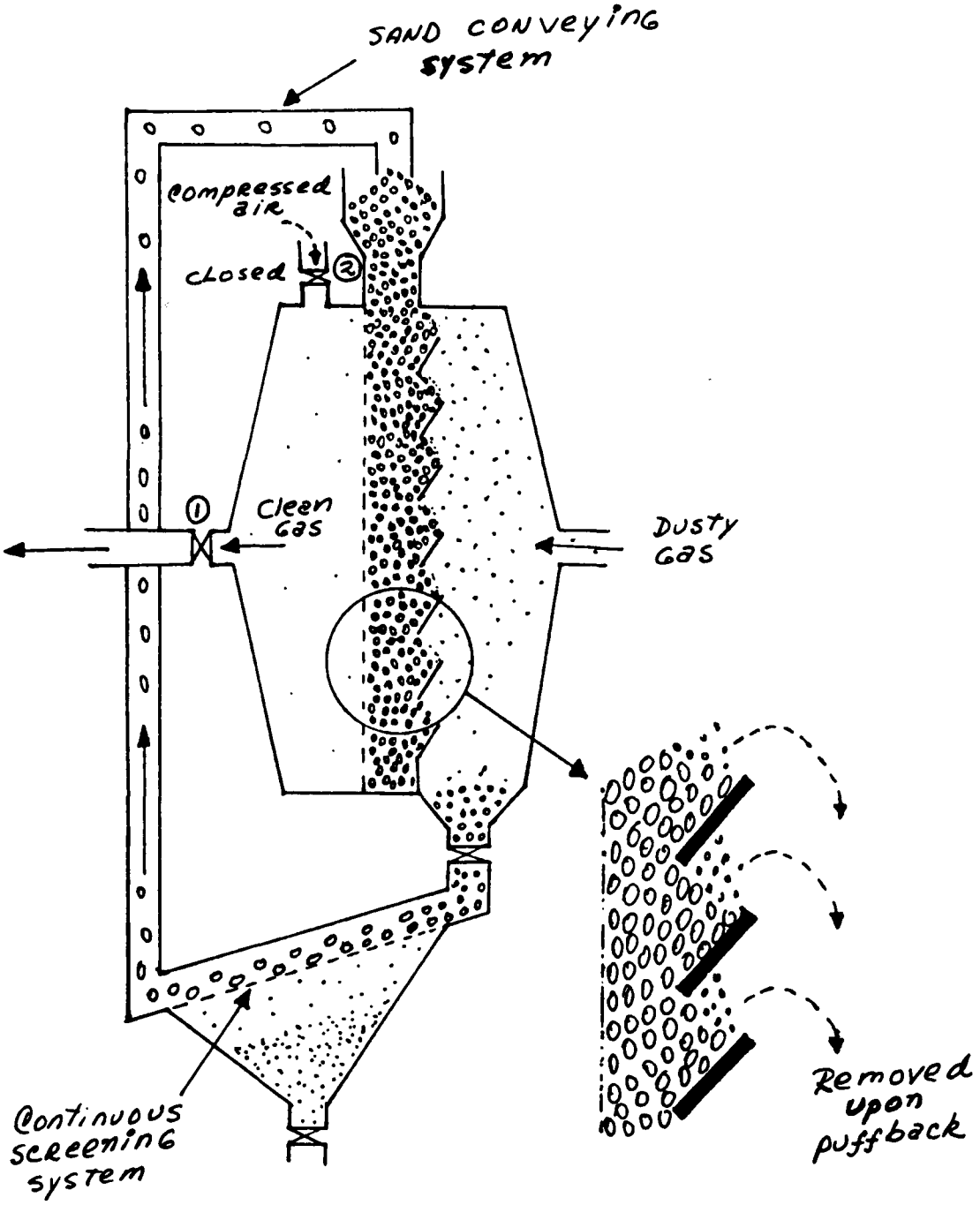

Figure 3-2 A Panel Bed Filter

which provoke the formation of a filter cake on the exposed bed surfaces. When the resistance of the cake has reached an undesirable level, the clean gas outlet valve 1 is closed and a short pulse of compressed air is blasted in reverse flow through the sand bed by opening valve 2. In continuous use, the valves operate on a timed cycle and the containing vessel is provided with a multiplicity of panels exhausting to a partitioned plenum, permitting localized reverse flow cleaning of individual panels.

The sharp puff of gas supplied to the clean face of the unit causes a mass movement of the sand toward the right and this causes the filter deposits to fall away from the dirty face together with a small amount of the sand. The expelled sand is immediately replaced by downward movement of fresh sand from the overhead hoppers. This only intermittent downward movement, coupled with a fine size of sand permits high efficiency collection and avoids the buildup of resistance due to subsequent penetration of fine deposited dust.

After several years of research efforts (Lee et al., 1977) the panel bed filter is believed to be ready for moderately rapid commercial exploitation. Figure 3-3 shows the preferred design for the support "louvers" of a panel bed filter. There are three columns of louvers. At the left in Figure 3-3 the "wishbone louvers" support gas entry surfaces of the fine granular solid which serves as a filter medium. This solid is supplied by gravity from an

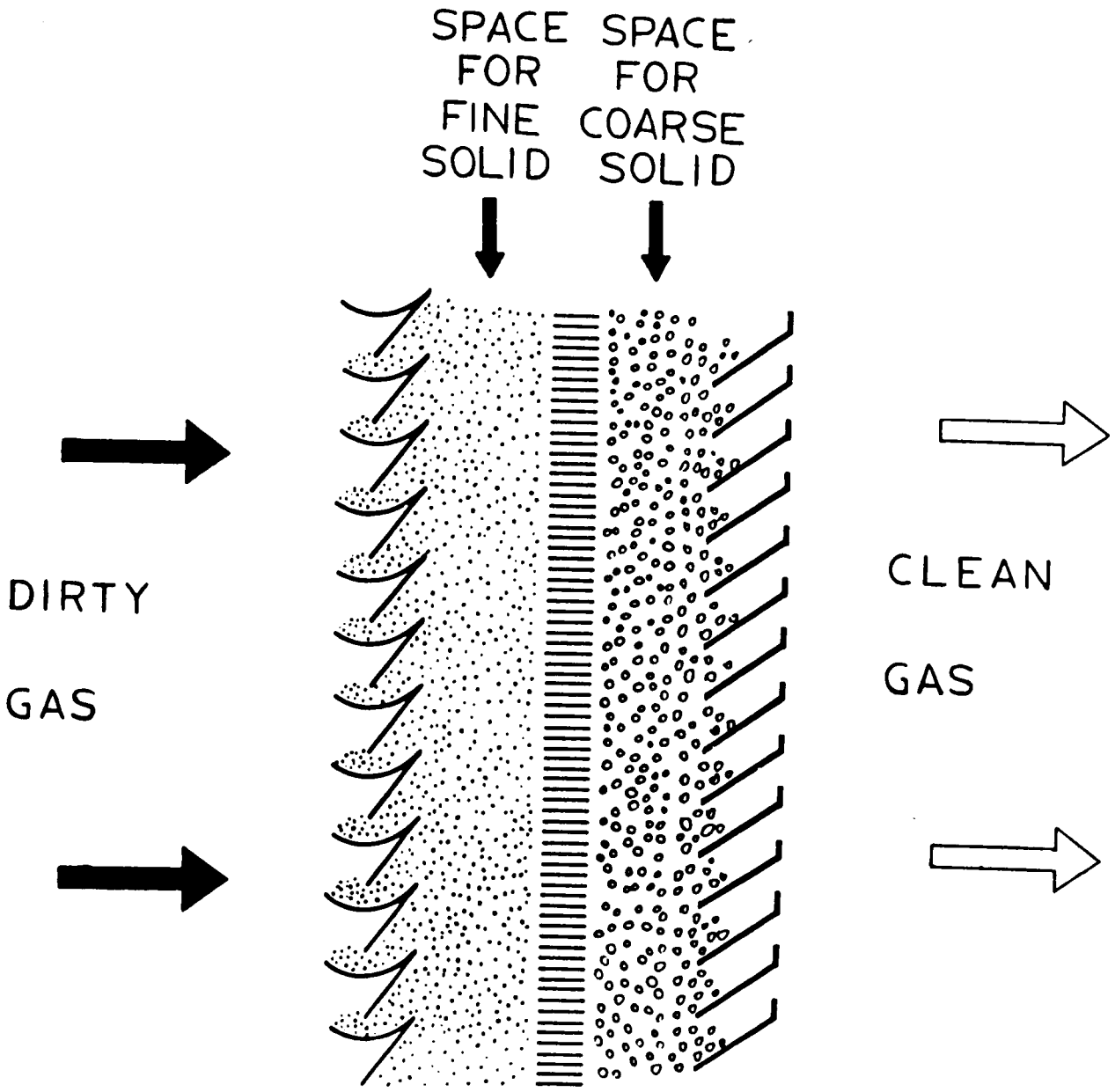

Figure 3-3 Preferred "Louvers" Design of a Panel Bed Filter.

overhead supply bin (not seen in Figure 3-3) to a tall, narrow space between wishbone louvers and a central column of closely spaced horizontal louvers. A coarse solid is held in place within a second tall, narrow space, between the central louvers and the inclined louvers at the right in Figure 3-3. In operation of the panel bed filter, coherent surface deposits form upon the gas entry surfaces of the dirty face. The coarser solid on the gas exit side is to prevent the smaller solid from blowing away from this side along with filtered gas. During cleaning, a sharp puff of gas supplied to the clean face of the unit causes a mass movement of the fine solid toward the left. This causes the filter deposits to fall away from the dirty face together with a small amount of the fine solid. The closely spaced louvers in the center of Figure 3-3 are designed to prevent the coarse solid from participating in the mass movement of the fine solid toward the left. Preliminary design studies (Lee et al., 1977) suggest that arrangements can be found providing overall gas filtering capacity on the order of 2.29 to 3.05 cubic meters per second per square meter of land area occupied by the filter. It was estimated (Lee et al., 1977) that the total power needed to operate a large-scale panel bed filter that serves a 344 megawatt coal-burning electricity station is about 0.01% of the electricity capacity of the station. (This figure does not include the power required to drive the flue gases through the filter.)

3.02 Squires' Work

Exploratory trials of three panel bed filters constructed by Squires (Squires and Pfeffer, 1970) gave the first indication of the inherent ability of this device for high efficiency filtration of dusts. It was concluded that such a device has a good probability of achieving overall efficiencies beyond 99.Wt% on power-station coal fly ash. It was estimated that a commercial design would provide a gas treating capacity per unit ground area on the order of four times greater than an electrostatic precipitator of comparable efficiency.

3.02.1 Room Temperature Filtration Data: Tests of Unit LS-1

Figure 3-1 is a schematic diagram of the first panel bed filter test unit, which was called LS-1. The unit was operated with 16-30 mesh angular sand. The panel was 3.5 cm wide in the horizontal direction of the gas flow across the bed, 30.48 cm wide in the horizontal direction perpendicular to the gas flow, and 147.32 cm in height. Dirty gas flowed downshot in a space 1.27 cm wide adjacent to the "dirty" face of the panel, and clean gas flowed upshot in a similar space next to the "clean face." The panel was used to remove electrostatically precipitated coal fly ash of unknown size distribution from air at ambient conditions. The sample of ash was obtained from a high-efficiency precipitator operating in the stack of a coal-fired power plant owned by Consolidated Edison Co. of

New York, Inc. The ash, after being dispersed in a fluidized bed, was mixed with air and drawn to the unit by a blower. The filter was cleaned by applying Squires' surge backflow or "puffback" technique. The overall mass collection efficiency was estimated from weight gains on sampling paper filters which were mounted on filter holders at the outlet of the device and from the amount of fly ash fed to the unit.

Table 3-1 summarizes the main features of the results obtained from tests conducted on unit LS-1.

It was observed (Squires and Pfeffer, 1970) that dirty sand could be used in the panel without danger of dust re-entrainment at the conditions tested.

3.02.2 Puffback Experiments: Test of Unit LS-2

Figure 3-4a shows a cross section of unit LS-2 which was constructed simply to study puffback. It was entirely made of plexiglas in order that the motion of the sand during puffback could be seen in cross section. Figure 3-4b shows that the effect of puffback is to cause the sand to move as a "plug" toward each dirty face surface, throughout the panel from top to bottom. Because of the plug-like character of the sand motion, puffback lifts each gas entry sand surface and causes both dust and a thin layer of sand to spill from each surface. The precision of this phenomenon may be appreciated from the fact that the average sand spill achieved during operation of unit LS-1 amounted to removing a layer of sand having a depth approximately

TABLE 3-1 Summary of tests of unit LS-1

Panel Area	= 0.45 m^2 (4.83 ft^2) (Projected Area)
Air throughput	28.32 10^{-3} m^3/s (60 ft^3/min) 6.1 cm/s (12 ft/min) Based upon panel area
Loading of fly ash in dirty air	4.6 to 9.2 g/m^3 (2 to 4 grains/ft^3)
Duration of run	1.8 to 3×10^3 s (30 to 50 min)
Quantity of fly ash collected in a run	283 to 425 g (10 to 15 oz.) 0.6 to 0.9 kg/m^2 (2 to 3 oz/ft^2)
Pressure Drop at start of run	24.91 Pa (0.1 inch of H_2O) (0.254 cm of H_2O)
Increae in pressure drop due to formation of fly ash filter cake	about 124.55 Pa (0.5 in. water) (1.27 cm of H_2O)
Crude Overall Filtration Efficiency	99.7-99.9Wt%
Puffback Bottle volume	5200 cm^3 (315 in^3)
Puffback Valve area	403.25 10^{-6} m^2 (0.625 in^2)
Puffback pressure	37.71×10^4 Pa (40 psig)
Weight ratio of sand to fly ash from puffback	about 2.5

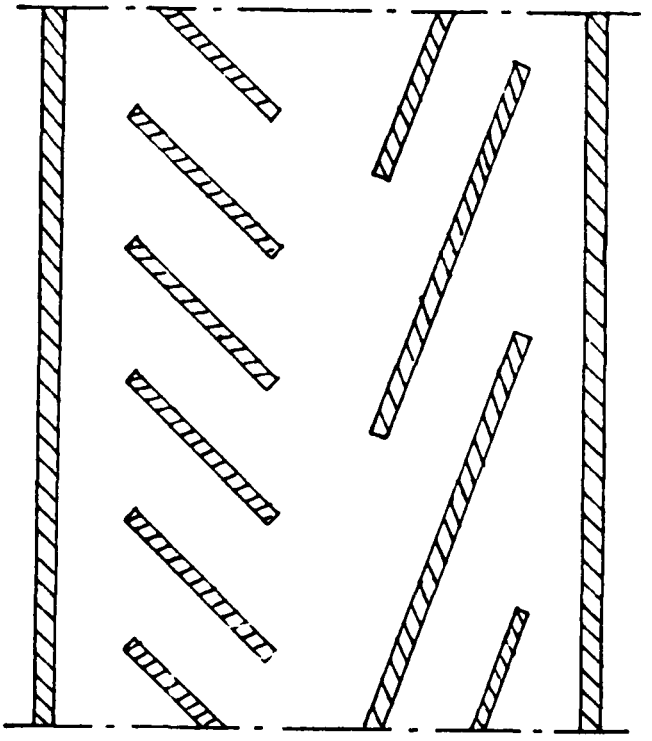

Figure 3-4a Cross Section of Panel of Unit LS-2.

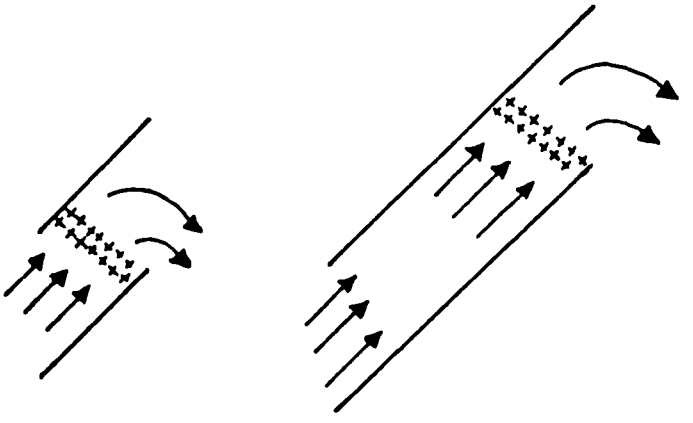

Figure 3-4b Effect of Surge Backflow of Gas (Puffback).
A surge backflow of gas of sufficient intensity produces a plug-like movement of sand toward gas-entry surfaces.

Fifure 3-4 Panel Bed Filter: Unit LS-2

equal to the width of two average grains of sand.

All attempts to clean unit LS-2 by means of a steady backflow of gas failed. It was observed (Squires and Pfeffer, 1970) that the spilled sand originated from deep within the bed and contained no detectable quantity of dust.

The work on the LS panels is apparently the first demonstration that shock cleaning can both clean filter cake from a filter having many loose, renewable surfaces and also renew each surface without undue loss of filter solid.

3.03 Paretsky's Work

Paretsky (Paretsky, 1972) conducted filtration runs in a panel bed filter laboratory unit which proved to be not suitable for consistent operation and later performed filtration experiments on a small representative section of a panel bed filter.

3.03.1 Room Temperature Filtration Data: Tests with a Representative Section of a Panel Bed Filter

Figure 3-5 (Paretsky, 1972) shows a cross section of the small panel bed filter used for filtration of coal fly ash redispersed in ambient air. The granular bed was 3.18 cm (1.25 in.) high by 43.18 cm (17 in.) wide, with an average thickness of about 8.89 cm (3.5 in.). The front louvers, inclined at an angle of 60^{o}, retain the sand at its angle of repose. The sand used was 20-30 mesh.

The overall fly ash collection efficiency (Wt.%) was determined from the weight gain on a filter paper contained

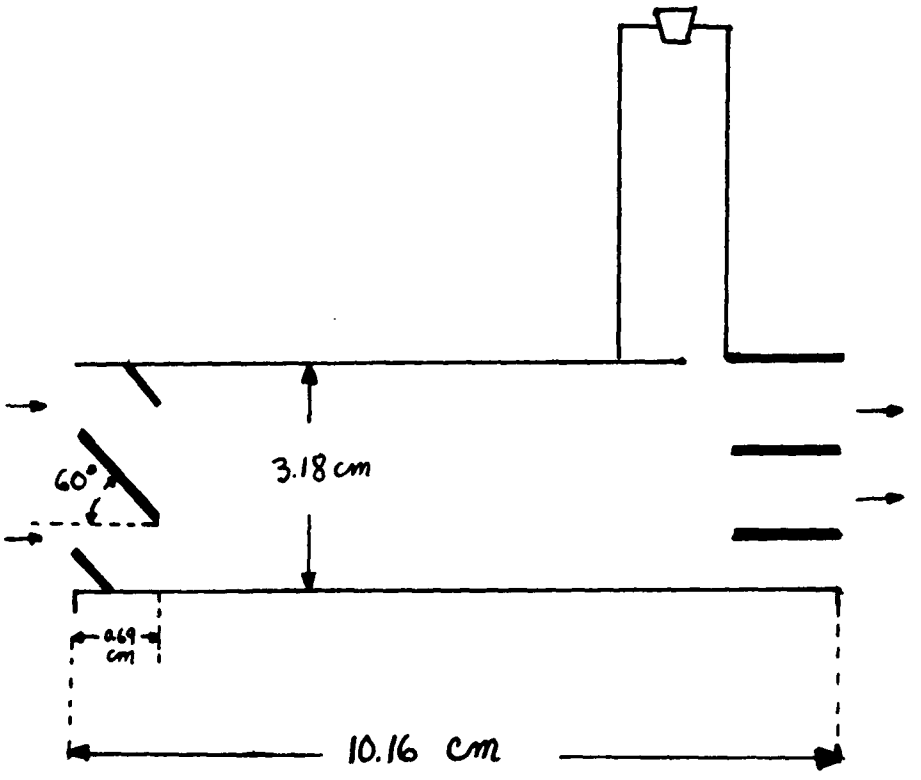

Figure 3-5 Cross-section of sand bed of panel.

in an isokinetic sampling probe at the outlet of the filter and from the amount of fly ash fed to the unit or recovered from puffback. The ash was obtained from a high efficiency electrostatic precipitator operating in the stack of a coal-fired power plant owned by Consolidated Edison Company of New York. Its particle size distribution, shown in Figure 3-6, is a typical log-normal distribution with a mass median diameter of about 15 micrometers and a geometric standard deviation of about 3.3. The ash was redispersed upstream of the sand bed by passing it through a critical drop created by a sharp edged venturi. The puffback tank had an effective volume of 278 cm^3(17 $in.^3$) while the puffback ball-valve afforded a port area of 2.52 cm^2 (0.39 in^2).

Table 3-2 shows typical filtration data obtained with this small section of a panel bed filter (Paretsky, 1972). As can be observed in Table 3-2 overall efficiencies beyond 99 Wt % were achieved for filtration of coal fly ash at velocities ranging from 2.59 to 16.05 cm/s.

3.03.2 Dilute Aerosol Penetration in Coal Fly Ash Cakes deposited on a Representative Section of a Panel Bed Filter

Since the efficiency data obtained in the section of a panel bed filter did not reflect the behavior of the unit for filtering small particles, it was decided to measure the efficiency of collection of 1.1 micrometer aerosols (Dow polystyrene microspheres) on previously deposited coal fly ash filter cakes.

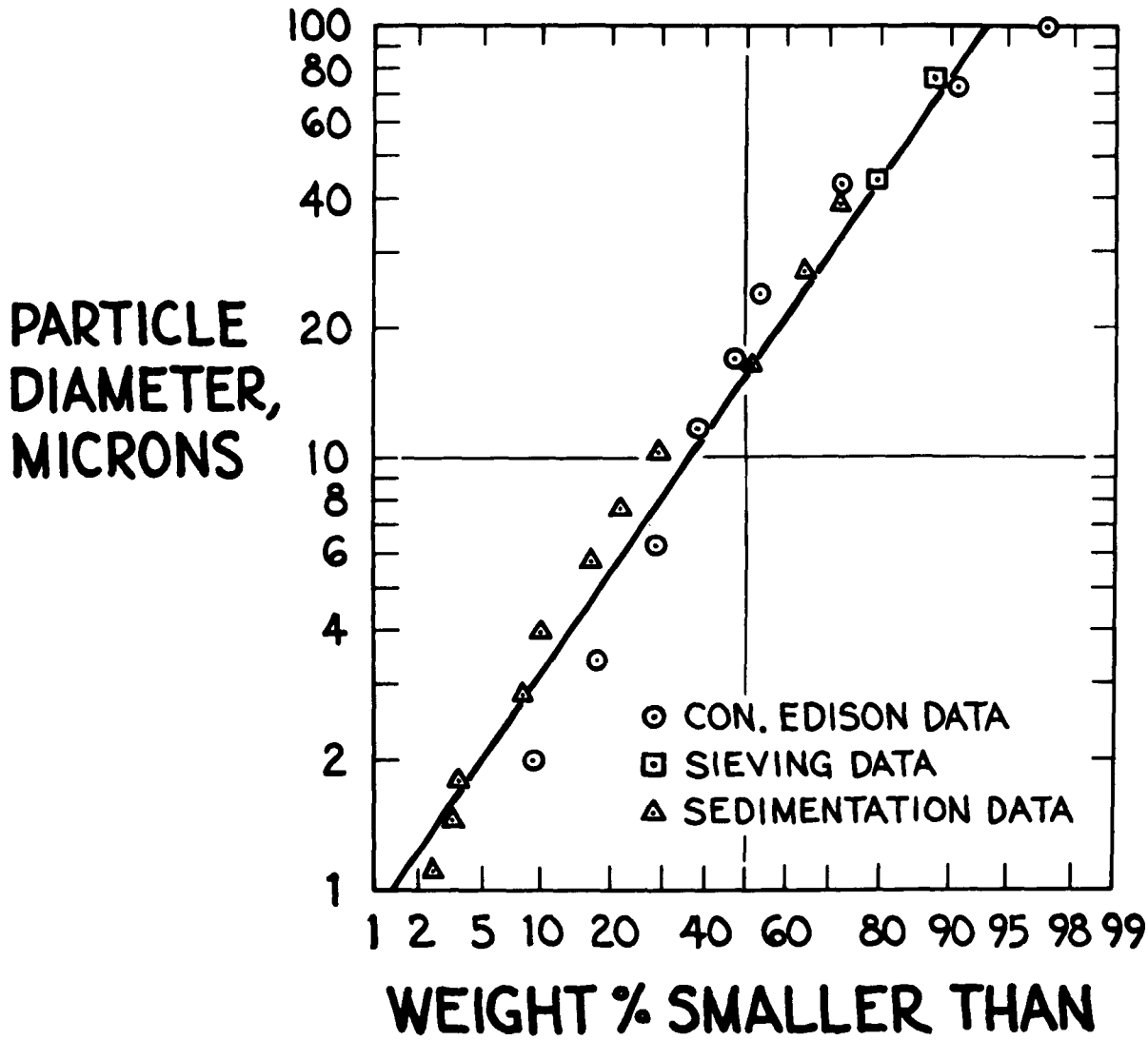

Figure 3-6 Distribution of particle size in fly ash supplied from electrostatic precipitator working at 99+ % efficiency.

TABLE 3-2 Typical Filtration Data Obtained in a Small Section of a Panel Bed Filter (Paretsky, 1972)

Run No.	P-34	P-01	P-22*	P-14
No. of Cycles	7	7	12	6
V bed (cm/s)	2.59	5.28	11.38	16.05
Inlet Fly Ash Loading (g/m^3)	14	6.5	2.5	1.7
Puffback Pressure (kPa) (Volume of Tank=278.6cm^3)	204.7	204.7	204.7	290.9
Fly Ash Areal Density (g/cm^2)**	0.178	0.149	0.058	0.161
Average Ash/Sand from puffback	0.38	0.48	0.28	0.24
Initial Cycle Overall Efficiency(Wt.%)	99.936	n.a.	97.7	99.47
Overall Efficiency (Wt.%)***	99.986	99.87	99.28	99.62
Initial Pressure Drop (cm H_2O)	0.279	0.483	1.143	2.032
Cake Pressure Drop (cm H_2O)	3.328	1.320	1.321	2.54
Initial ΔP at steady state (cm H_2O)	0.610	0.737	1.549	3.708

* A dilute aerosol penetration test was performed after the 8th cycle, therefore quantities listed in this table are based on the first 8 cycles.

** Grams of fly ash deposited per cm^2 of sand surface area.

*** Based on fly ash recovered from puffback.

Initial efforts were directed at performing most of the aerosol tests at a face velocity of about 0.35 cm/sec, even when the cakes had been deposited at much higher velocities (Paretsky, 1972). The selection of the above velocity was based on the fact that it is in the diffusion regime for aerosol filtration, region in which excellent agreement had been obtained between theory and experiment while filtering 1.1 micron aerosols with horizontal beds of sand (Paretsky, 1972; Paretsky et al., 1971.)

It was concluded (Paretsky, 1972) that filtering aerosol at much lower velocities than the ones used for deposition of the filtering media (cake) was unsuitable because: a) the large difference between the two velocities could conceivably cause fracture or rearrangement of the filter cake and this would affect the bed's cyclic behavior; b) the aerodynamic path of the aerosols is radically different from the path of the fly ash. Therefore the resultant collection efficiencies of the test aerosol do not reflect the collection efficiency of the 1.1 micrometer fly ash particles.

Table 3-3 illustrates this effect while showing fractional efficiencies obtained in the filtration of 1.1 micrometer aerosols at 0.35 cm/sec with coal fly ash filter cakes deposited at 11.38 cm/s upon 20-30 mesh sand in the representative section of the panel bed filter.

TABLE 3-3 Fractional Efficiencies vs. Cake Pressure Drops for Filtration of 1.1 micrometer Aerosol with Previously Deposited Coal Fly Ash Cakes in a Section of the Panel Bed

ΔP cake (cm of H_2O)	Ef.
1.35	0.27
2.31	0.70
4.83	0.80
9.6	0.81

ΔP initial for all runs was 1.14 cm of H_2O.

Superficial velocity: Cake deposition = 11.38 cm/s

Aerosol test = 0.35 cm/s

It was stated that the effect of better efficiencies with higher cake pressure drops was due to this velocity difference (Paretsky, 1972).

The table below shows results obtained from aerosol tests performed on coal fly ash filter cakes deposited at 2.54 cm/s. In both runs the initial pressure drop was 0.25 cm of H_2O, while the cake pressure drop was kept at 3.33 cm of H_2O.

Aerosol Test Velocity (cm/s)	Ef.
0.36	0.78
2.59	0.984

It was indicated (Paretsky, 1972) that the cakes deposited at this lower velocity were more losely packed and more susceptible to change. Severe cake fracture was believed

to be occuring while conducting the aerosol test at 0.36 cm/s, for the pressure drop after the aerosol test decreased substantially; this effect was not observed while filtering the aerosol at the same velocity at which the cakes had been deposited ($\approx$ 2.6 cm/sec). It was concluded that the aerosol test should be conducted at the same velocity at which the cake had been deposited and without interruption of the flow.

It was pointed out that the efficiencies obtained in the representative section of the panel bed filter were substantially smaller than the ones obtained, under same operating conditions, with filter cakes deposited upon horizontal beds of the same sand, (Paretsky, 1972). This was attributed to a large difference in porosity between the two beds. (A porosity of 0.43 was estimated for the horizontal bed of 20-30 mesh angular sand, while the panel bed section filled with the same sand was believed to have a porosity in between 0.55 and 0.61.)

3.04 Lee's Work

Lee (Lee, 1975 and Lee et al., 1977) designed the first successful panel bed filter laboratory units and concentrated the initial research to the study of puffback at room temperature.

After puffback was under control, he then conducted exploratory tests for the filtration of coal fly ash with sand in a laboratory unit at ambient conditions. Even when puffback proved to be an efficient way of cleaning the

laboratory unit for long-term operation, it was not at all obvious that it could work as smoothly in a typical commerical-size unit; as a result, Lee et al. (1977) designed a 3.048 meter tall panel bed unit for studying puffback.

3.04.1 Micro-Mechanics of Puffback: Experiments with a Laboratory Panel Bed

From the viewpoint of soil mechanics, the spill of sand from each gas entry surface of the dirty face of the panel bed during puffback reflects a failure of the sandy "soil." When cohesionless granules such as sand are subjected to a shearing displacement, a volume change usually occurs as the sand grains move relative to one another. The volume of a loose specimen undergoing shear will decrease, while on the other hand, a dense specimen will expand. Whatever the initial condition of the sand, after shear the specimen will approach a definite ultimate volume characteristic of the sand. Since soil strength depends upon porosity, this will also approach an ultimate value after sufficient shear. Figure 3-7 illustrates this effect.

Whitman et al. (1963, 1964) studied shear strength of sands during rapid loading, and showed that elastic or plastic deformation plays an important role if stress is imposed quickly. With slow loading, even slight motion of sand grains relative to one another can tend to relieve the stress. With rapid loading, slight readjustments of position of individual sand grains are less probable. Initiation of the movement of the sand tends to involve

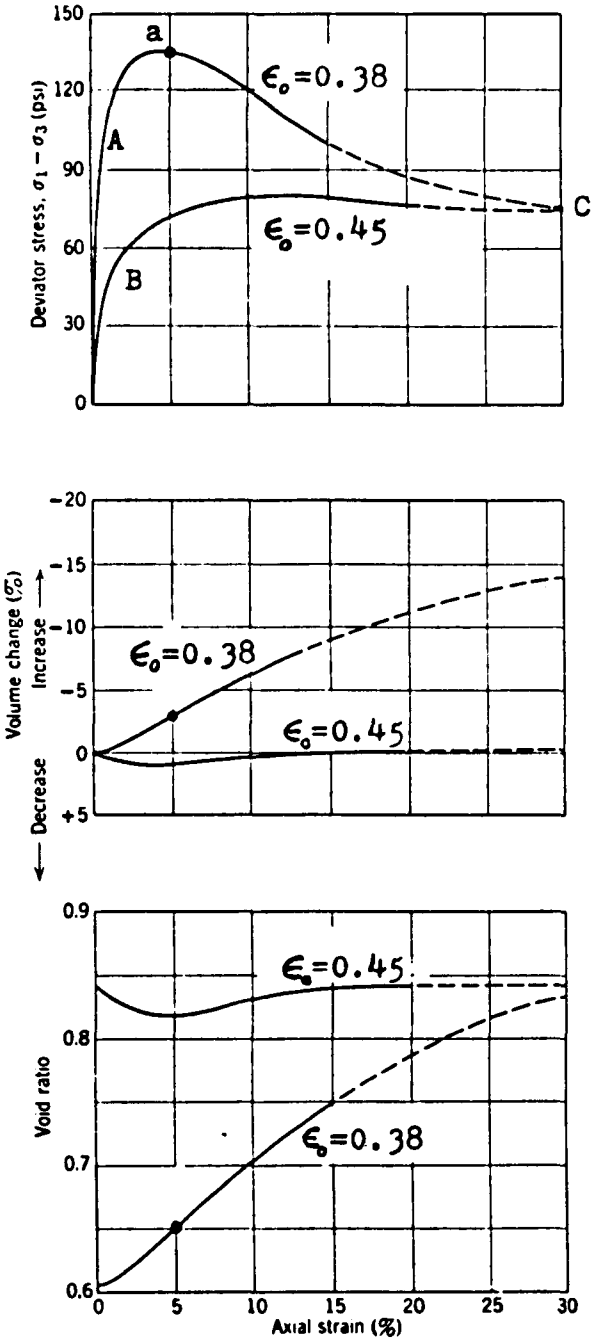

Figure 3-7 Stress-strain Curves for Loose and Dense Specimens, Medium-fine Sand.

particle deformation. Soil resistance is accordingly greater, and a larger force is needed to induce sand failure.

3.04.11 Experimental Arrangements and Procedures

Figures 3-8 and 3-9 show the mechanical design of the two panel bed filters developed by Lee (Lee, 1975; Lee et al., 1977) for studying puffback. The second unit shown in Figure 3-9 is substantially identical to the first unit, excepting that:

(1) a glass window was provided to permit visual observation of sand motion during puffback, and

(2) a vertical plate could be installed near the back face of the panel bed to reduce the volume on the clean side of the bed.

Figure 3-9 provides an isometric sketch illustrating the mechanical design of the second apparatus for studying puffback. This second design allowed the study of puffback with two widely different volumes of gas on the clean side of the panel bed. Thus, "downshot puffback" could be performed with the vertical metal plate in place at the right-hand side in Figure 3-9. "Sideshot puffback" could be performed if the metal plate was omitted and the horizontal part of the equipment of Figure 3-8 was fitted at the right in Figure 3-9. The volume on the clean side of the panel bed is 11,900 cubic centimeters for sideshot puffback, and 713 cubic centimeters for downshot. The side plate of the unit is 0.64 cm glass, with louvers

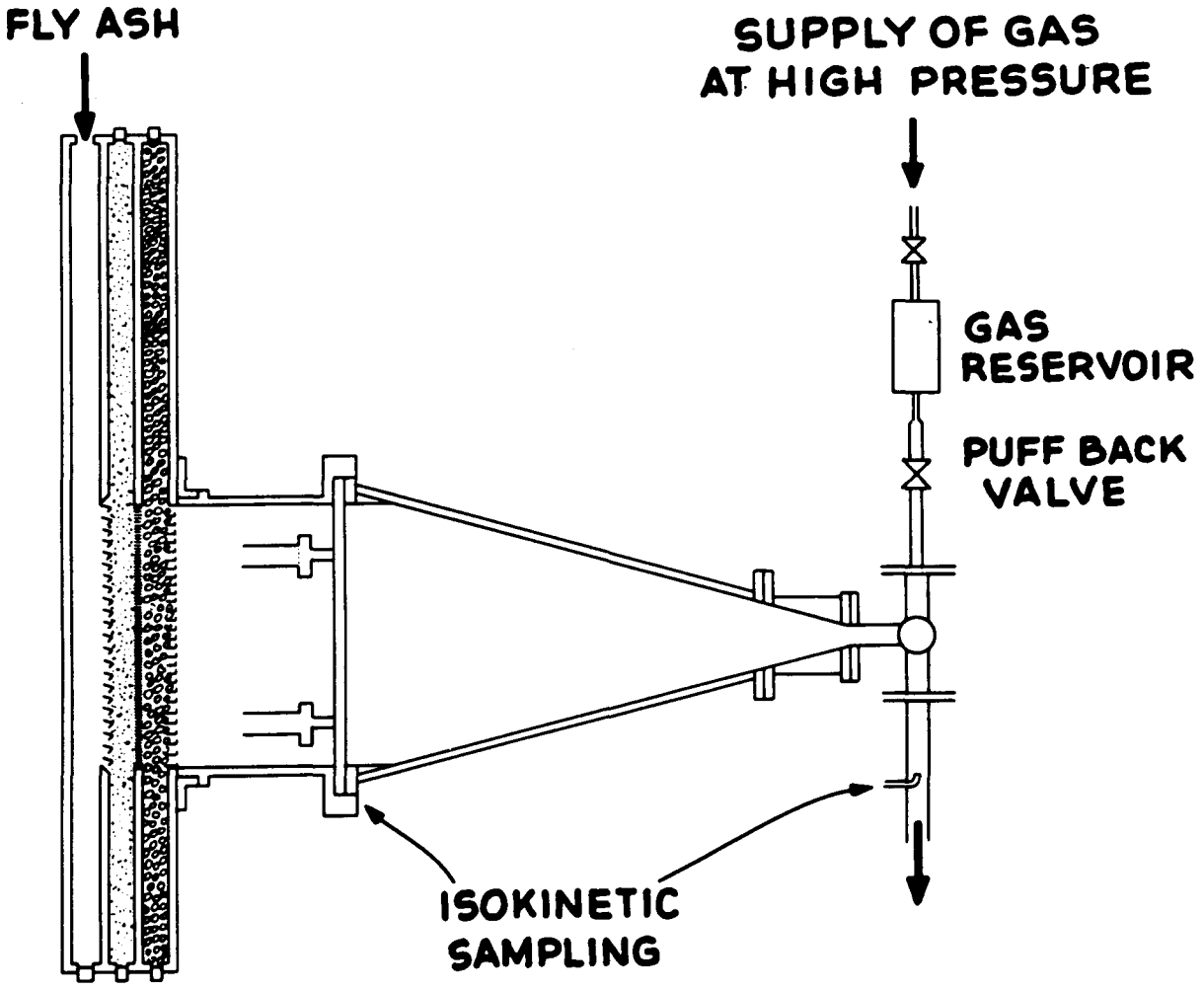

Figure 3-8 Schematic Cross-Sectional View of Apparatus for Test of Panel Bed Filter. The First Unit

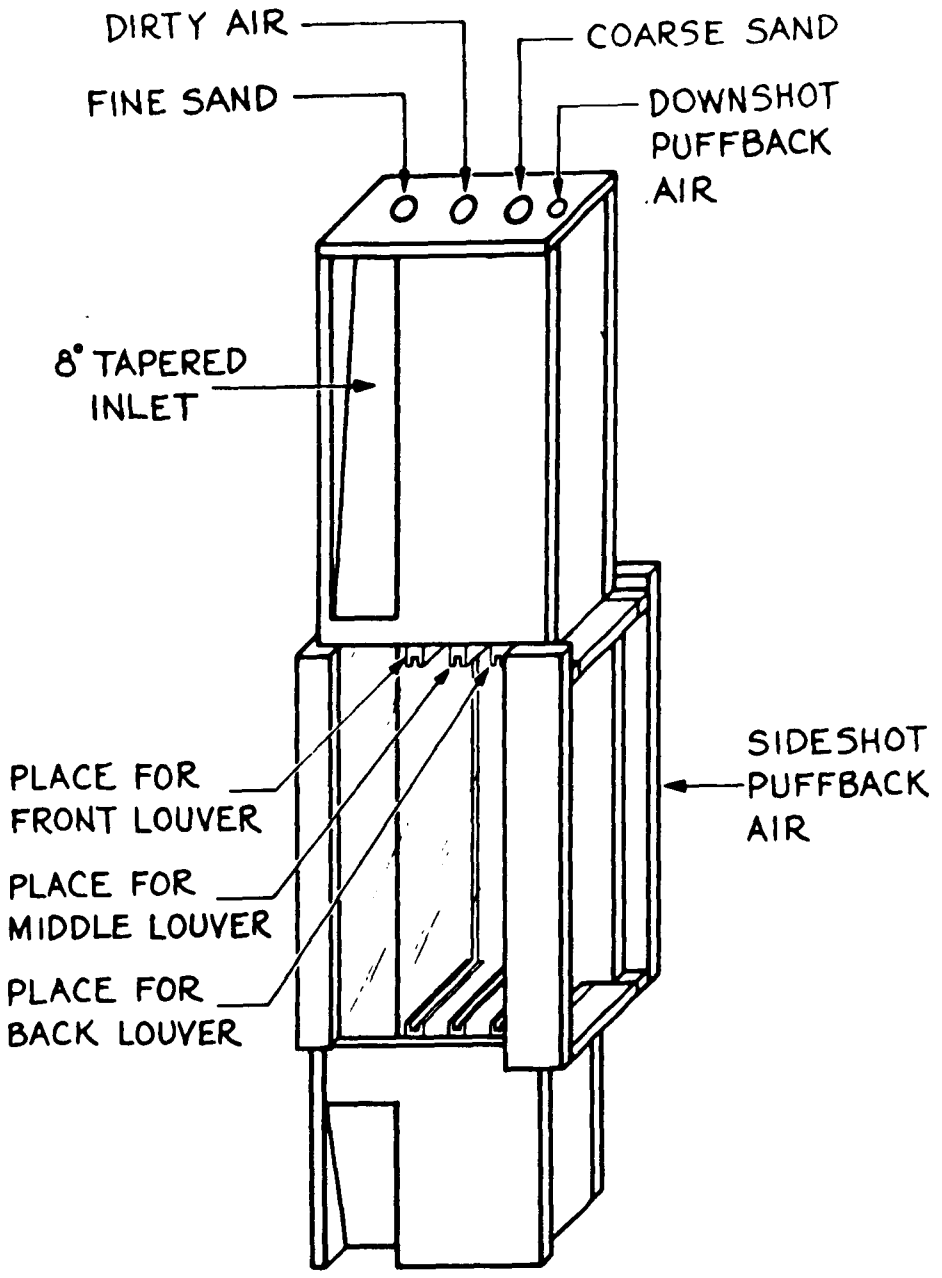

Figure 3-9 Second Apparatus for studying micro-mechanics of puffback, with glass side wall for visual observation

pressed directly against the glass to permit study of sand motion during puffback either by eye or by means of high-speed movies, which were taken at 3,000 frames per second. (Lee et al., 1977.)

Lee (1975) tested a series of dirty-face louvers (front louvers) in the panel bed filter. The louvers were designed so that the angle of the louver opening for the sand free surface with the horizontal (the louver surface angle) should be less than the angle of repose of sand. The louver surface angle was designed at 27^{o}. The angle of repose of sand ranges from 30^{o} to 35^{o} depending on the sand properties (Zenz and Othmer, 1960).

Figure 3-10 shows the details of the preferred arrangement of louvers for the panel bed filter at that time (Lee, 1975). The front louver design shown in Figure 3-10 was called the "chevron" louvers and with them most of the puffback and filtration experiments were carried out.

Two high-sensitivity, low-impedance quartz transducers (Kistler Model 206) were used to follow the pressure changes on clean and dirty sides of the panel during puffback. These transducers have a resolution of 5.587 Pa and a response time of 3 μs. Their signals were fed into a multi-channel oscilloscope fitted with a Polaroid camera.

High-speed motion pictures of puffback were taken at 3000 frames per second with a Hycam high speed movie camera while testing the second unit (Figure 3-9). The time

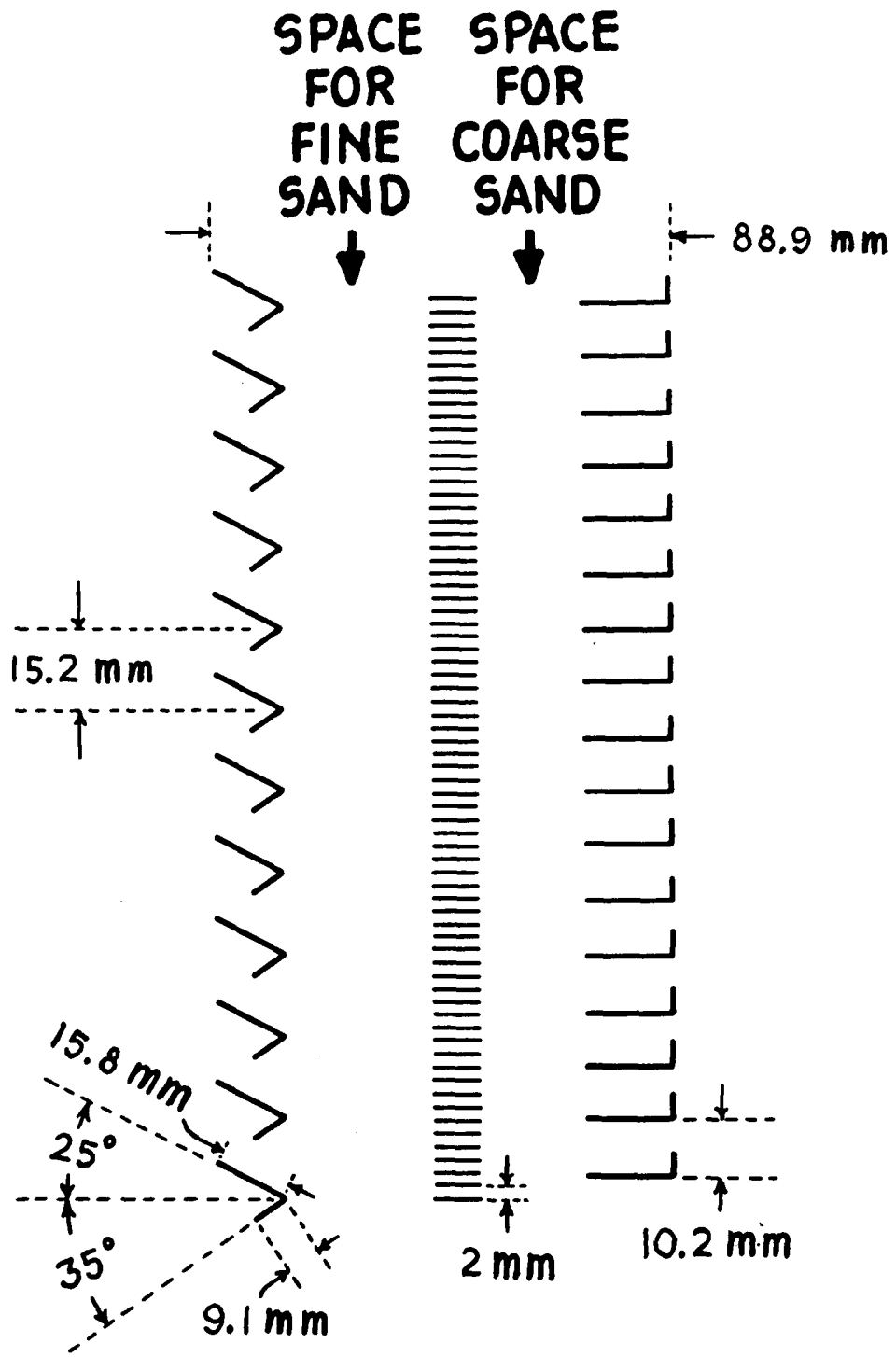

Figure 3-10 Arrangement of louvers used in tests of fly ash filtration at room temperature. The louvers at the dirty face are the "chevron" design.

period taken by each individual event of puffback was measured with the aid of a Lafayette movie analyzer. Variables tested were:

three sand sizes:	10-14, 20-30, and 40-50 mesh;
three solenoid valves:	0.476 cm gate valve (Cv=1.8);
	0.794 cm gate valve (Cv=3.4), and
	2.54 cm globe valve (Cv=9.9);
five puffback gas reservoir :	103, 206, 412, 1,370, and 2,550 cubic centimeters;
puffback gas reservoir pressure:	135.8 to 515 kPa.

The first two valves were supplied by Valcor Engineering Corp. of Kenilworth, New Jersey, and the third by Atkomatic Valve Co., of Indianapolis, Indiana. Each valve opened in about 15 to 20 ms. In all tests, the backing sand was 10-14 mesh.

Measurements were made of the sand spill over four segments of the height of the panel bed by installing collecting pans, resembling gutters, at the first, third, and twelfth louvers of the total twenty louvers. Tests were also conducted (Lee, 1975) in which a steady flow of air was furnished to the clean side.

3.04.12 Sand Motion During Puffback

Visual observation of puffback led to the conclusion that puffback sandspill was created by the aerodynamic force or the drag force on sand grains due to the air flow.

In both downshot and sideshot puffback, it was possible to achieve a reasonably uniform sand spill from each gas entry surface. The motion of the mass of sand toward each surface is a body movement of the sand--i.e., the sand moves in a mass.

High speed movies revealed three stages of sand "failure." First, sand jumps up from the inner edge of each sand surface, as illustrated in Figure 3-11a. A few milliseconds later, the bulk of the sand moves forward, as seen in Figure 3-11b. During the bulk movement of the sand, the "spouting" of sand at the inner edge of each surface stops.

When puffback intensity is high, there is a clear separation of fine sand from the middle louvers. The entire bed of sand has moved forward, as shown in Figure 3-11b. At the same time, the sand bed moves downward slightly to make good the loss of sand from the nearby gas-entry surface.

The second stage of sand motion, i.e., the bulk movement stage, lasts from about 10 to 100 milliseconds, according to the intensity of the puffback. Almost all of the spilled sand is removed during this stage. A third stage of sand motion lasts several times longer than the second stage. During the third stage, shown in Figure 3-11c, only a few grains of sand fall, i.e., from the outer edges of the surface-supporting louvers. At the same time, sand moves downward in the body of the sand bed to make good the loss of sand from the gas entry surfaces in the

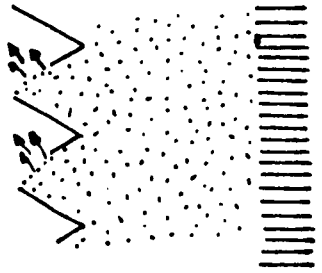

(a) First stage:
local failure near
inner edge of each
gas-entry surface.

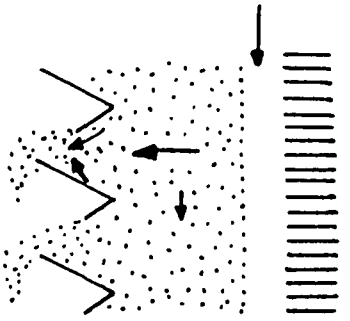

(b) Second stage:
body failure and
separation.

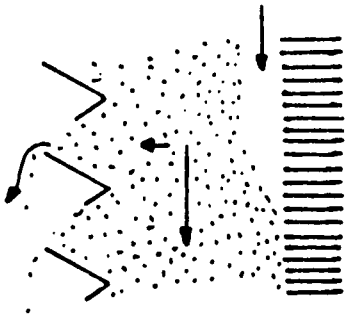

(c) Third stage:
gravity motion downward,
de-separation, and
afterspill.

Figure 3-11 Three Stages of Sand Motion During Puffback.

lower part of the panel bed.

From the point of view of soil mechanics, the first stage of motion is a result of local failure of the sand bed at the inner edge of each sand surface. The second stage is a body failure, and this is the more important phenomenon in respect to the practicable use of puffback to clean a panel bed filter.

No failure and no sand motion occurred in a puffback conducted with a sheet of plastic in place between the fine sand and the middle louvers. It is believed (Lee et al., 1977) that the body failure of the second stage occurs when aerodynamic forces acting on the sand bed overtake the soil strength of the bed.

Loss of sand during the third stage (local failure) was believed to be a result of an adjustment of the new sand surface to a configuration that is stable in respect to the angle of repose of the sand. It was mentioned (Lee, 1975 and Lee et al., 1977) that possibly the amount of this final spill is affected by the declining "tail" of the flow of puffback gas.

3.03.13 Results for Steady Blowback

Lee (Lee, 1975; Lee et al., 1977) while working with the transparent filtration unit (Figure 3-9) confirmed the earlier report of Squires and Pfeffer (1970) to the effect that experience seems to indicate that a steady blow back is not capable of removing sand uniformly over the height of a panel bed.

Tests were conducted with three grades of sand (10-14, 20-30, and 40-50 mesh) in the front column of the panel bed and for two initial conditions of the sand:

1. Fresh-filled sand (i.e., "loose packing" in the terminology of soil mechanics).
2. Loosened sand (looser than the above "loose packing") in which the sand was loosened by removing some sand from the bottom of the fine sand column.

For fresh-filled sand, a steady blowback causes a loss of sand to occur when the reverse air velocity reaches a critical velocity. However, the loss occurs only at the top edge of the top gas-entry sand surface, as illustrated in Figure 3-12a. In other words, sand failure occurs only along the line formed by the louver edge of the topmost louver of the column of louvers at the gas-entry face. When the blowback velocity is increased further, sand begins eventually to fall from the top edge of the second gas entry surface, as seen in Figure 3-12b.

For loosened sand, the spill behavior is not reproducible. A spill of sand occurs unpredictably at a louver at any elevation of the panel bed where the soil strength is weakest. No matter where the spill starts, however, once the sand begins to move, the greatest sand spill occurs at the top gas entry surface. For the three grades of sand used the same phenomena occured. It was observed that the starting of a continuous sand spill

(a) Start of the Failure.

(b) Failure at increased rate of air backflow.

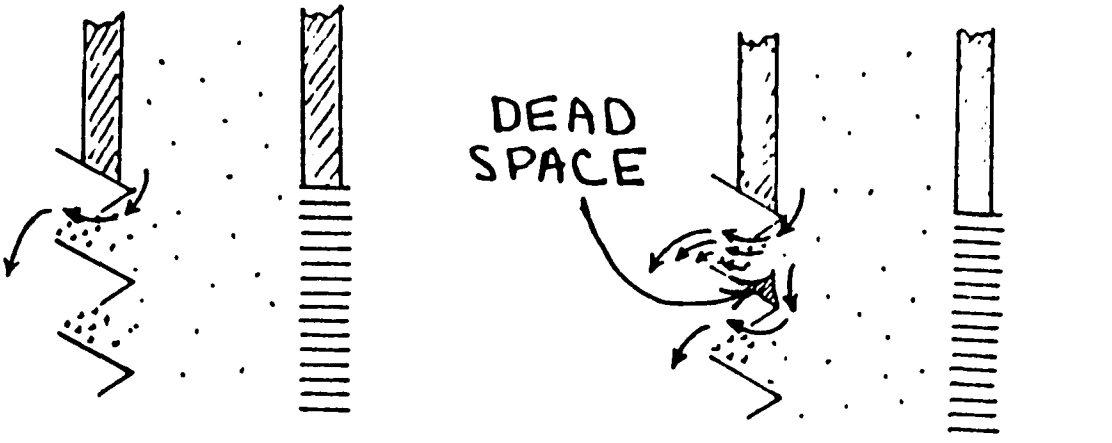

Figure 3-12 Local Failure of Sand in Steady Blowback of Air Across The Panel Bed.

always happened at about a constant pressure drop. Lee (1975) called this pressure drop the "failure pressure," and this increased with increasing size of sand. It was concluded (Lee, 1975) that steady blowback fails to do the job of cleaning the dirty sand surface uniformly, because the air flow has the time to find the weakest point in the bed, and the flow concentrates at that point. On the other hand, in puffback the failure pressure is reached so quickly that it will cause failure throughout the bed. The air flow at a given point does not have time to know what is happening elsewhere, or to find the weakest point of the bed.

3.04.14 Transient Pressure Results

Lee (Lee, 1975; Lee et al., 1977) used transducers for measuring the time variation of pressure during puffback on the clean and dirty side of the panel bed. After smoothing the curves and substracting one from the other, plots like the one shown in Figure 3-13 were obtained. It can be observed in Figure 3-13 that the time of rise of the pressure difference to a peak is between 10 and 20 ms. Lee (Lee, 1975) conducted these tests with a) three sand grades; b) three front louver designs; c) three puffback valves; d) five puffback bottles; e) two different puffback arrangements (downshot and sideshot); and f) a set of different puffback pressures.

Figure 3-14 gives the collected and weighed sand spilled from each puffback test as a function of the peak pressure difference reached in each test. For each

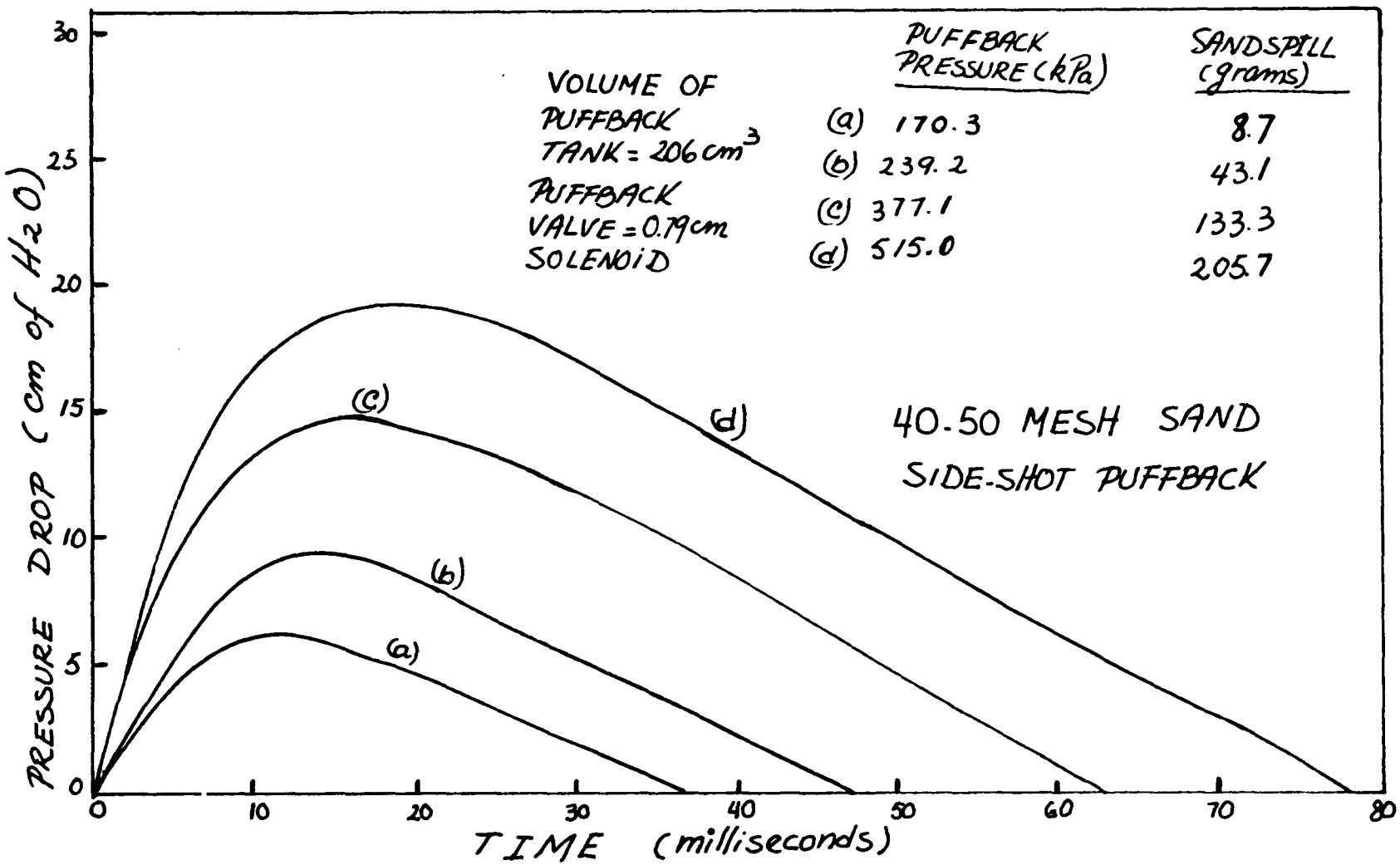

Figure 3-13 Typical Time Variation of Pressure Drop Across Panel Bed During Puffback.

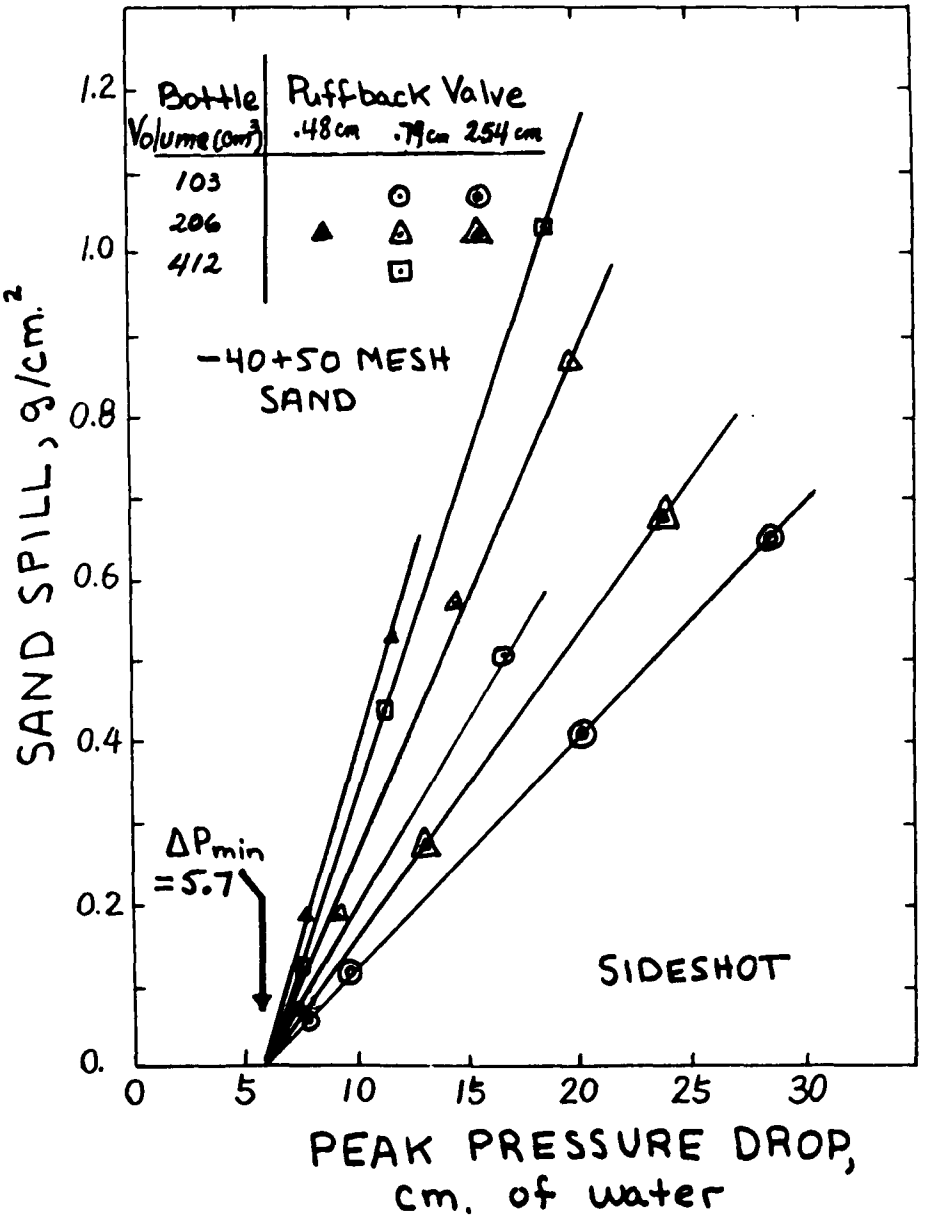

Figure 3-14 Sand spill (per unit projected vertical area of panel bed) versus peak pressure difference, for 40-50 mesh sand and sideshot puffback.

combination of puffback bottle and valve, the data defines a reasonably straight line.

The lines in Figure 3-14 suggest what is plausible, viz., that there is a minimum pressure difference that must be produced by the flow of puffback gas to produce a body movement of the sand in the second stage of puffback. It was observed (Lee, 1975; Lee et al., 1977) that the minimum pressure difference for body failure was not a function of sand size, phenomenon which was attributed to the fact that soil mechanical properties of cohesionless soils do not vary much with granule size.

A big surprise in this work (Lee, 1975) was the fact that for each sand tested, the size of the spill is apparently a function of just one variable, viz., the time during which the pressure difference exceeds the minimum pressure drop needed to cause body failure of the sand (ΔPmin). This time was called "active time" and is defined in terms of an idealized "triangular" curve of puffback pressure difference versus time shown in Figure 3-15. Figure 3-16 illustrates the dependence of sand spill upon active time for 40-50 mesh sand.

The fact that the sand spill does not depend upon the peak pressure drop was not expected at all. It was remarked (Lee, 1975; Lee et al., 1977) that the minimum pressure difference just required to cause local failure of the panel bed in a steady blow back is distinctly less than ΔPmin for body failure in puffback.

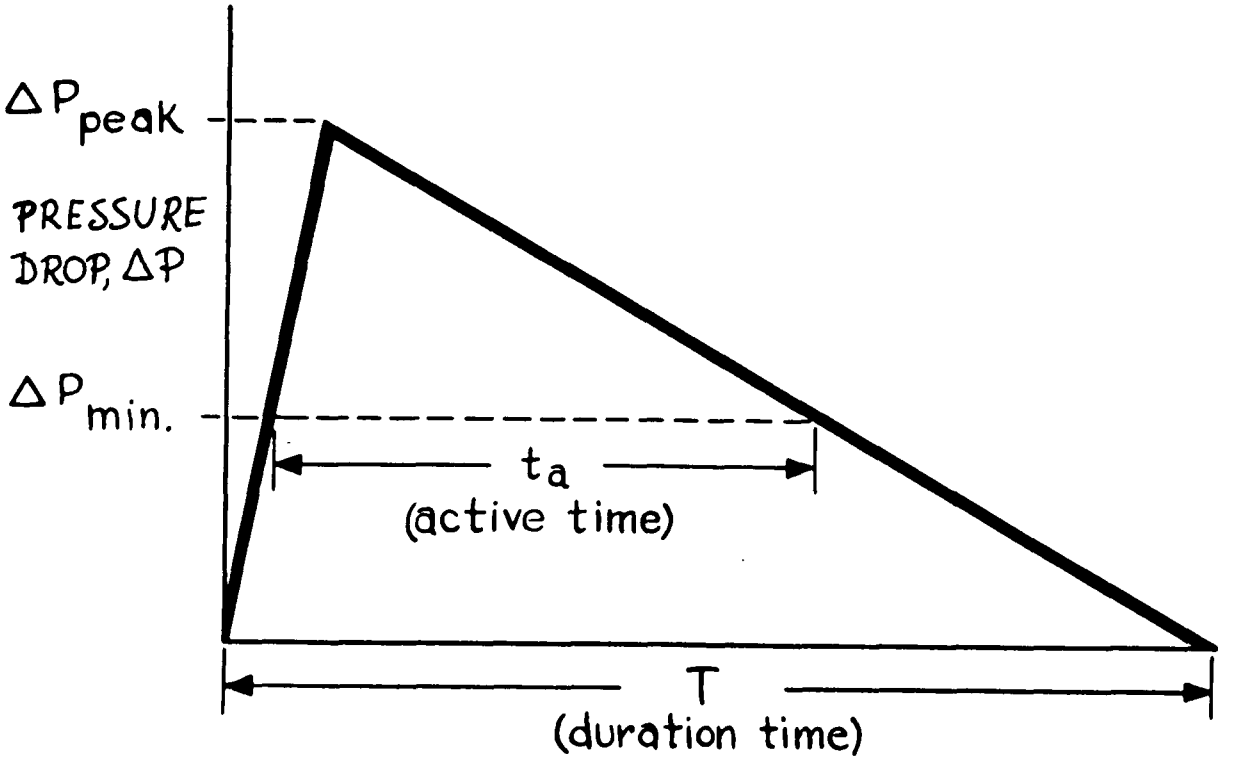

IDEAL TRIANGULAR SHAPED PRESSURE DROP CURVE

Figure 3-15 "Active time", t_a, is defined as the time during which the pressure difference across the panel bed exceeds the failure pressure, ΔP_{min}.

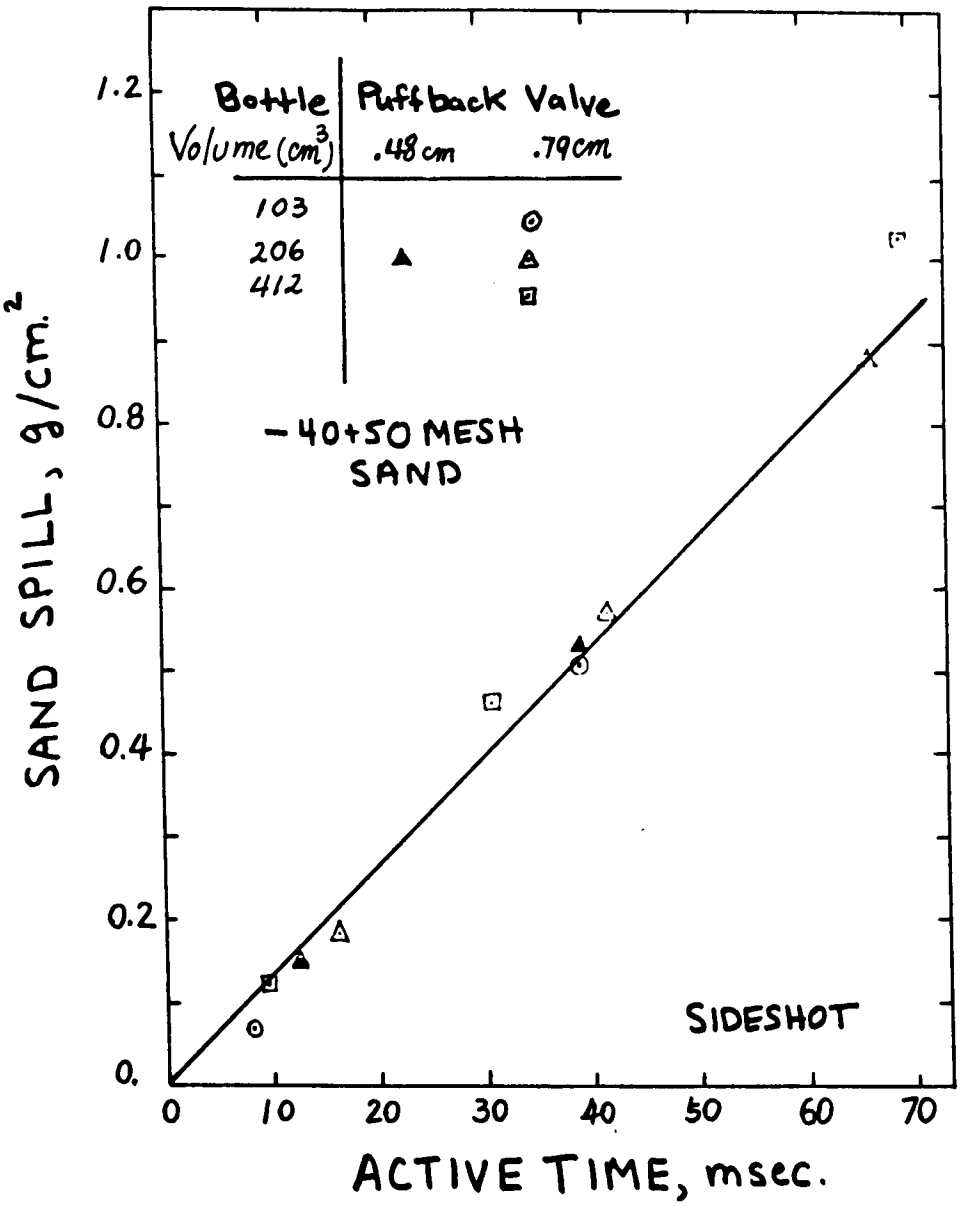

Figure 3-16 Correlation of sand spill (per unit area) and active time for 40-50 mesh sand and sideshot puffback.

3.04.15 Importance of Initial Bed Porosity

Puffback sandspill must be controlled in such a way as to produce a reproduceable, uniform spill across the height of the panel bed, and this was not a straightforward achievable phenomenon.

Lee, at the onset of his investigation was confused by his inability to obtain consistent data for sand spill in terms of amount and uniformity for a given puffback intensity, until he realized that the action of a successful puffback, with body movement of the sand, causes in general a loosening of the sand in respect to its fresh-filled packing condition. In principle (Lee et al., 1977), it appears that each puffback intensity is associated with a particular porosity of the sand, although the variation in this porosity does not appear to be very great over a range of puffback intensity of practical interest.

In order to obtain consistent data for sand spill and to achieve a reasonably uniform distribution of sand spill over the panel bed height, it is necessary to bring the sand into a loosened condition throughout the height of the panel bed. It was learned (Lee, 1975) that in order to reach more quickly the bed condition which would give consistent and uniform spills at a given puffback intensity, a stronger puffback may be applied before collecting data at moderate puffback intensities.

3.04.16 Practicable Upper Limit on Active Time

If the body movement of the second stage of puffback

lasts well into the third stage, during which sand is moving downward by gravity to make good sand losses occuring in the second stage, the loosening of sand in the upper part of the panel bed causes the body movement to be greater there than lower down. Thus, a puffback of too great intensity--i.e., too long active time--results in a non-uniform sand spill. Too much sand is lost near the top. A practicable upper limit on active time appears to be about 50 milliseconds, although times up to about 150 milliseconds may sometimes be useful if a non-uniform spill is acceptable and if the panel is not too tall (Lee et al., 1977).

At long active times, beyond about 150 milliseconds, the sand spill at first exhibits the body motion characteristic of puffback , but changes to the spill characteristic of blowback. That is to say, toward the end of the active time, a large amount of sand spills from the topmost few gas-entry surfaces, while little sand spills elsewhere. This large spill from the top may be far greater than the spill induced by the body movement of the sand bed in the early stages of the too intense puffback.

3.04.2 Room Temperature Filtration Data: Tests with a Laboratory Panel Bed Filter

Lee (1975) conducted exploratory filtration runs with a panel bed filter laboratory unit shown in Figure 3-8, and used coal fly ash of size distribution given by Figure 3-6.

Although Lee conducted filtration experiments with three different front louver designs, he concentrated his efforts in obtaining data with the preferred louvers arrangement at that time (Figure 3-10).

Figure 3-17 shows schematically the experimental set-up used for these filtration tests. Compressed air, after being filtered and dried, flows into a mixing pipe where dust is fed by a screw conveyor feeder. The not well dispersed mixture flows through a straight section of pipe until it reaches a critical orifice; this constriction produces a pressure drop of $\approx 10^5$ Pa, therefore promoting the dispersion of the dust. The now well-dispersed mixture finally enters the panel bed filter at the top of an 8^o tapered vertical inlet passage for dirty air.

As Figure 3-8 illustrates, there were three columns of louvers in the panel bed filter; the first column (front louvers) presented sand surfaces for filtering the dirty gas. A set of closely spaced louvers separated the fine filter sand from the coarse sand. Both the fine sand and the coarse sand beds were 2.54 cm across in the direction of gas flow, while the louver area was 7.62 cm wide and 30.48 cm high. Cleaned air left the bed of coarser sand across gas exit surfaces that rested upon horizontal louvers fitted with upturned "tabs" that retained the coarse sand. Isokinetic samples were taken at the outlet of the unit, with filter papers held at two different heights. Following the chamber that housed the two isokinetic sampling

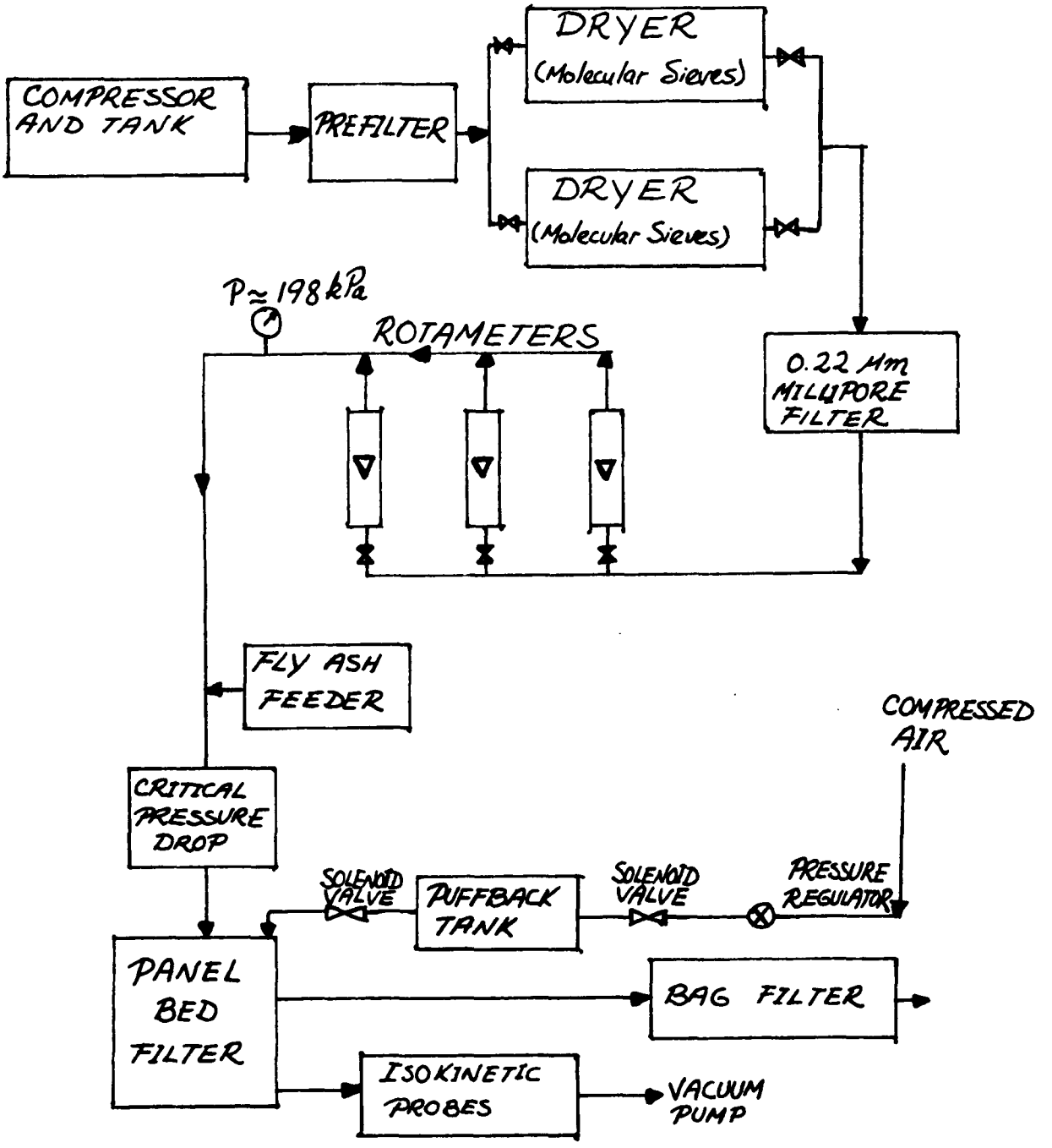

Figure 3-17 Schematic of Panel Bed Experimental Apparatus.

stations, the air entered a region of contracting section which terminated in an outlet for air that led to a three way valve (Lee, 1975).

During filtration, air flowed downward from the three-way valve and past a conventional isokinetic sampling station. At the end of a filtration cycle, the flow of air was interrupted, and the position of the three way valve was shifted so that the exit of the contracting region communicated to a puffback valve and gas reservoir fitted with air at a predetermined high pressure. The puffback solenoid valve was opened suddenly, allowing air to dump from the reservoir into the clean side of the panel bed. With proper adjustment of reservoir volume, gas pressure, and puffback valve area, a small amount of the finer sand was dislodged from each gas entry surface of the panel along with a filter cake that had formed on each surface. The resistance of the panel bed to air flow was restored substantially to its initial level, and the panel was ready for a succeeding filtration cycle.

The spent solid was collected from the bottom of the collection bin in the dirty side of the panel bed through a 2.54 cm ID hole. The spent solid was sieved to separate the ash from the sand, and weighed. The separated sand was recycled and used again as filter solid. The overall fly ash collection efficiency (weight percent) was calculated from the dust collected on the isokinetic sampling filter paper and the fly ash separated from the spent solid.

Tables 3-4 through 3-8 summarize the room temperature filtration data obtained by Lee (1975; 1976).

As can be observed in the tables there is a trend of increasing efficiency with decreasing size of sand, and a tendency of improving performance at higher velocities.

In operation with 40-50 mesh sand backed by 14-20 mesh sand, penetrations smaller than 0.01 Wt.% were obtained and therefore it was possible to estimate efficiencies at different particle diameters by passing the filtered air through a Royco particle counter having channels for four nominal particle sizes: 0.3 to 0.5; 0.5 to 1.0; 1.0 to 2.0; and over 2 micrometers. Figure 3-18 shows how the particle count per liter of air appearing on a Royco channel for particles "over 2 micrometers declines versus time during a filtration cycle." By extrapolating the size distribution given by Figure 3-6 and by assuming a weight of particle corresponding to one of the Royco channels and by taking the nominal sizes of the Royco channels literally, it was possible to estimate the collection efficiencies of the small particles present in the dust. The table below summarizes this information.

Channel	Particle Weight (mkg)	Percentage Penetration
0.3 to 0.5 micrometer	6.97×10^{-13}	0.3
0.5 to 1.0 micrometer	4.6×10^{-12}	0.4
1.0 to 2.0 micrometer	36.8×10^{-12}	0.5

TABLE 3-4 Lee's Room Temperature Filtration

Data with 20-30 Mesh Sand (V_s= 15.8 cm/s)

Superficial velocity	= 15.8 cm/sec
Puffback Tank Volume	= 206 cm^3
Puffback Pressure	= 239.2, 273.7, 342.6 kPa (This pressure was changed during the run to maintain a constant pressure drop after cleaning)
Panel Bed Pressure Drop	= 2.5 cm of water (clean bed) 2.8 cm of water (after cleaning steady value in 43 cycles) 6.8 cm of water (average before cleaning)
Fly ash inlet loading	= 3.6 g/m^3
Average time per cycle	= 17 minutes
Fly Ash/Sand from puffback	= 0.13
Penetration (Wt%) Cycle No. 1	= 0.33
Penetration (Wt% Cycle No. 2-43	= 0.032

TABLE 3-5 Lee's Room Temperature Filtration Data with 20-30 Mesh Sand (V_s= 21.3 cm/s)

Superficial velocity	=	21.3 cm/s
Puffback Tank Volume	=	206 cm^3
Puffback Pressure	=	308.2 kPa
Panel Bed Pressure Drop	=	3.6 cm H_2O (clean bed)
		7.6 cm H_2O (average before cleaning)
		4.7 cm H_2O (average after cleaning)
Fly Ash Inlet Loading	=	4.0 g/m^3
Average time per cycle	=	13.3 minutes
Fly Ash/Sand from puffback	=	0.15
Penetration (Wt%)		
Cycle No. 1	=	0.18
Cycle No. 2	=	0.06
Cycles 3-15	=	0.02

TABLE 3-6 Lee's Room Temperature Filtration Data with 40-50 Mesh Sand (V_s= 4.6 cm/s)

Superficial velocity	=	4.6 cm/s
Puffback Tank Volume	=	206 cm^3
Puffback Pressure	=	184.1 kPa
Panel Bed Pressure Drop	=	2.3 cm H_2O (clean bed)
		4.8 cm H_2O (before cleaning)
Fly Ash inlet loading	=	3.5 g/m^3
Average time per cycle	=	19 minutes
Fly Ash/Sand from puffback	=	0.75
Penetration (Wt%)		
Cycles 1-7	=	0.013

TABLE 3-7 Lee's Room Temperature Filtration Data with 40-50 Mesh Sand (V_s= 15.8 cm/s)

Superficial Velocity	=	15.8 cm/s
Puffback Tank Volume	=	206 cm^3
Puffback Pressure	=	204.8 - 239.2 kPa
Panel Bed Pressure Drop	=	7.2 cm H_2O (clean bed)
		8.9 cm H_2O (steady value after cleaning in 95 cycles)
		12. cm H_2O (average before cleaning)
Fly Ash Inlet Loading	=	4.8 g/m^3
Average time per cycle	=	5.3 minutes
Fly Ash/Sand from puffback	=	0.2
Penetration (Wt%)		
Cycles 1-5	=	0.026
Penetration (Wt%)		
Cycles 6-95	=	0.007

TABLE 3-8 Lee's Room Temperature Filtration Data with 40-50 Mesh Sand (V_s = 21.3 cm/s)

Superficial Velocity	=	21.3 cm/sec
Puffback Tank Volume	=	206 cm^3
Puffback Pressure	=	170.3 kPa
Panel Bed Pressure Drop	=	9.8 cm H_2O (clean bed)
		13.1 cm H_2O (before cleaning)
Fly Ash Inlet Loading	=	1.4 g/m^3
Average time per cycle	=	9.4 minutes
Fly Ash/Sand from puffback	=	0.3
Penetration (Wt%)		
Cycle No. 1	=	0.29
Penetration (Wt%)		
Cycles 2-9	=	0.009

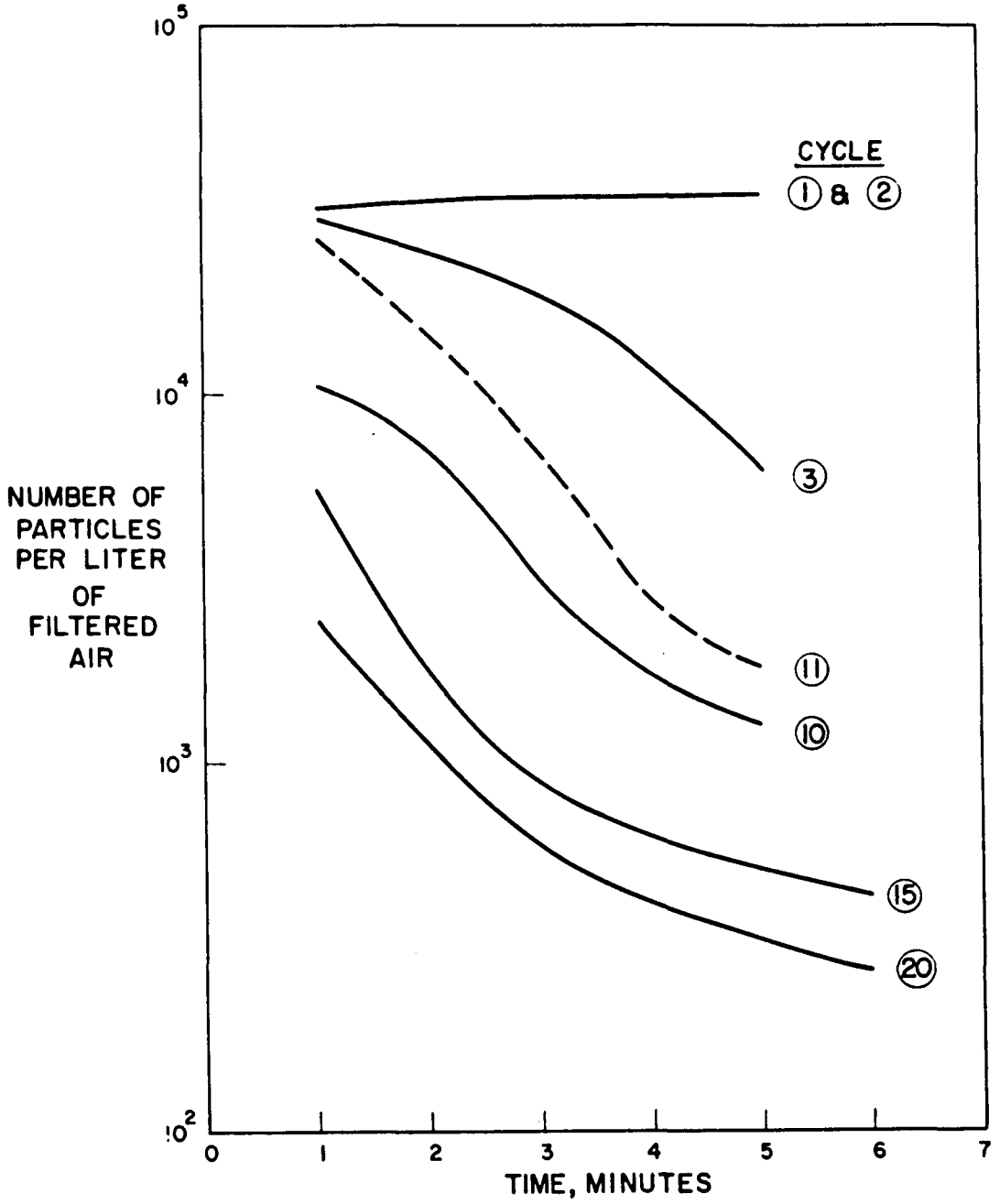

Figure 3-18 Number of particle counts at Royco channel for particles of nominal size "larger than 2 microns" versus elapsed time during several filtration cycles at atmospheric temperature with 40-50 mesh sand at 15.75 cm/sec (31 ft/min). The ordering of the cycles is given by numbers alongside the curves (Lee, 1975).

It was remarked that visual observation of the filter papers under a microscope disclosed only particles smaller than about 2 micrometers (Lee, 1975).

3.04.3 Lee's Panel Bed Filtration Analysis

Lee (1975) classified granular bed filtration process into three types--the clean bed filtration, the rooting cake filtration, and the surface cake filtration. Figure 3-19 illustrates Lee's view of gravel bed filtration. Clean bed filtration is the stage where the granules are basically clean, or have some dust particles adhering on their surface, but the dust is not heavy enough to form a thick layer over the surface. In the clean bed filtration process, the efficiency will be poor. In the rooting-cake filtration process, the front and rear of the granules will be filled with dust tending to form a continuous phase with the granules. The efficiency will increase markedly, yet the pressure drop will not change much. After the rooting cake step, the filter cake tends to grow and the efficiency will increase to such an extent that most of the dust will be stopped at the granular bed surface and will form a surface filter cake.

Lee pointed out (1975) that the characteristics of surface filter cakes could be quite different depending on the deposition velocity. The filter cakes formed at high velocities will be more dense, tending toward a higher pressure drop and higher efficiency. But due to the stronger drag forces, the formation of pin-holes will be

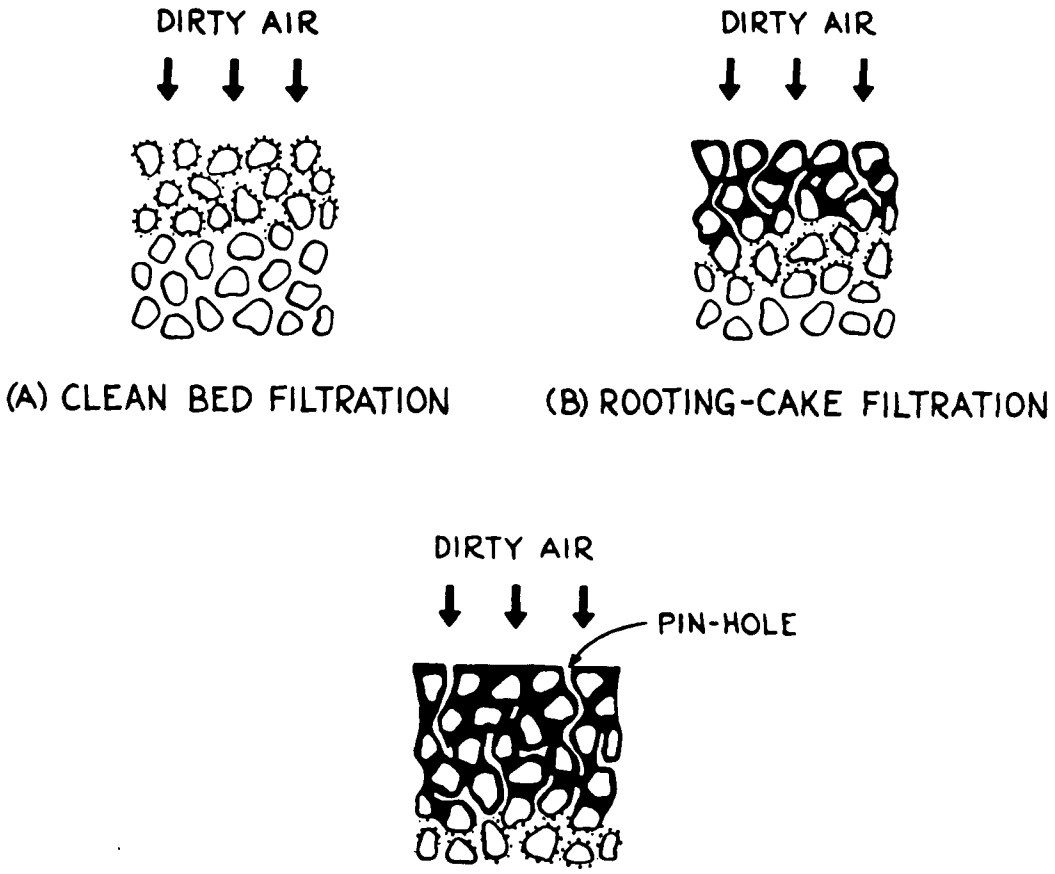

Figure 3-19 Three stages of filtration by a granular bed, with formation of a coherent surface deposit of dust.

favored. Thus, the net result of the combination of a dense filter cake and many pinholes is difficult to determine.

Lee concludes (1975) that in panel bed filtration puffback should be controlled in such a way as to avoid clean bed filtration. In other words, the panel bed filter should work under cake-filtration most of the time.

3.04.4 Macro-Mechanics of Puffback: Experiments with a Panel Bed 3.048 meters tall and 0.3048 meter wide

Downshot puffback appears to be the only practicable arrangement for a tall panel bed filter (Lee et al., 1977), and it was not obvious that the consistent, smooth operation of puffback in a 30.48 cm high laboratory panel bed could be scaled up without risk. Accordingly, a 3.048 meters tall and 0.3048 meter wide panel bed was designed and built. (Lee et al., 1977.)

3.04.41 Experimental Arrangements and Procedures

Figure 3-20 depicts schematically a tall panel bed built at The City College of New York to study puffback. The overall height of the unit is 5.182 m (17 feet); the louver area is 3.05 m high (10 feet) and 30.48 cm wide (1 foot), and at a louver spacing of 1.52 cm (0.6 inch), there is a total of 200 dirty-face louvers. The unit is built in three sections of aluminum, bolted together by flanges as indicated in the Figure. The top section is 1.83 m tall (6 feet) and provides a 91.6 cm high sand reservoir (3 feet) and a 1.83 m high dirty-air inlet

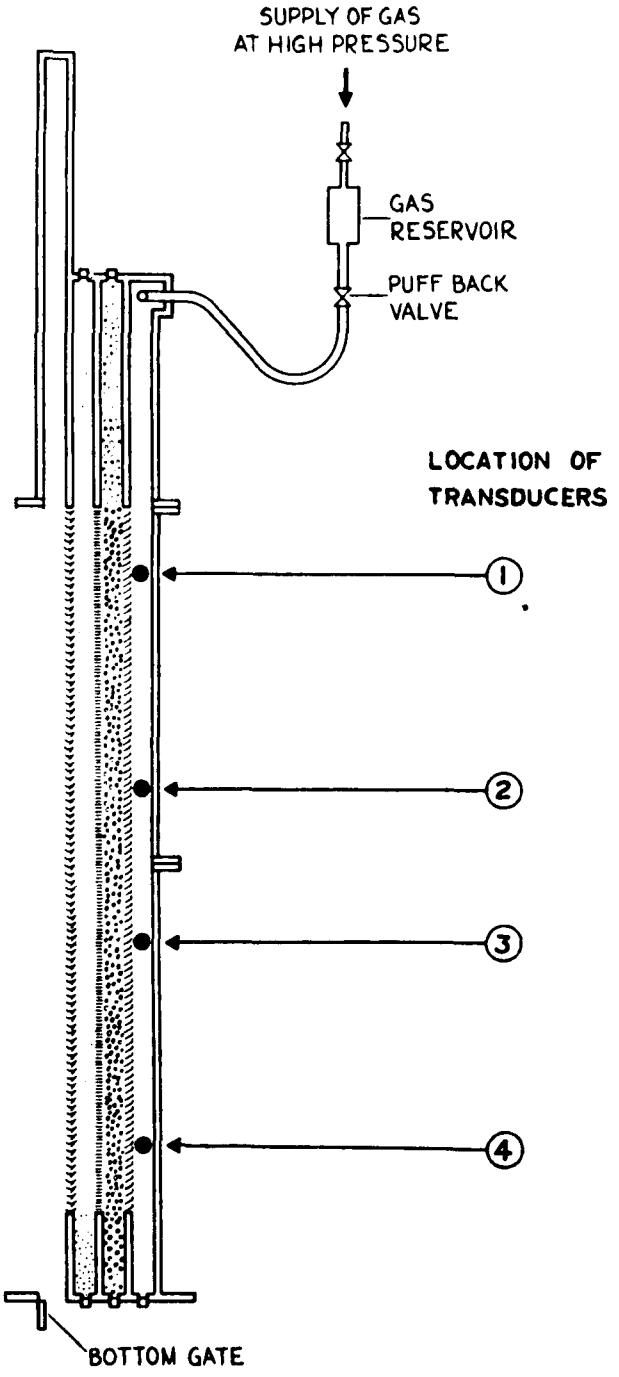

Figure 3-20 Schematic diagram of 3.048 m-tall panel bed filter

passage (6 feet) against the possibility that the unit may eventually be used for filtration studies. The second section is a filtration section fitted with louvers and is 1.52 m tall (5 feet). The third section is 1.83 m tall (6 feet), which includes a 1.52 m space (5 feet) for louvers and a 30.48 cm (1 foot) reservoir for sand at the bottom. The space on the clean side of the panel bed in Figure 3-20 is 3.81 cm across (1.5 inch), 38.1 cm wide (15 inch) and is 75.22×10^{-3} m^3 in volume (2.66 ft^3).

In some tests, the puffback valve and the clean side of the panel bed were connected by a 3.05 m length (10 feet) of flexible hose of 6.35 cm (2.5 inch) inside diameter. In other tests, the puffback valve was connected directly to the filter. The back plate enclosing the clean side of the unit was made of plexiglas to permit visual observation of the clean side. A plexiglas plate was also provided for enclosing the dirty side of the panel bed of Figure 3-20, but this plate was omitted in most of the tests, so that the dirty side was open to the atmosphere.

At the outset of this research a commercial valve with sufficient opening speeds at the required puffback pressures for effective puffback of the tall panel bed was not available, therefore, a valve was designed for this purpose. (Lee et al., 1977.) Figure 3-21 illustrates the details of this design. The valve designed, although useful, had serious practical disadvantages and it was replaced late in the work by a new valve which appeared

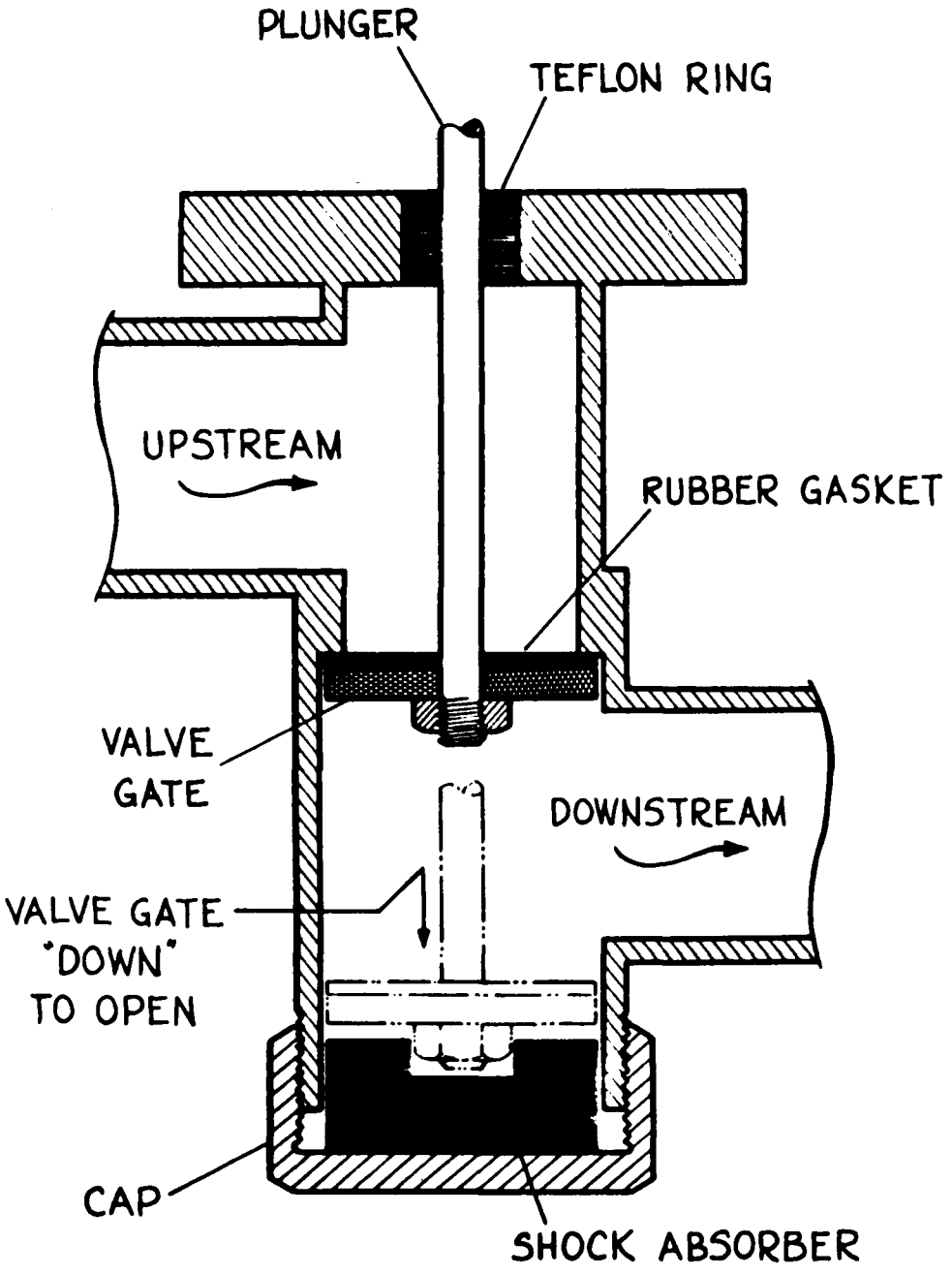

Figure 3-21 Construction of "City College" 5.08-cm puffback valve.

in the market under the name of "Big Blaster Air Cannon." This valve has a design similar to the one previously tested, but with the disadvantages removed. Figure 3-22 gives a schematic diagram of the Big Blaster Air Cannon and illustrates its operation. A Big Blaster Air Cannon having a 5.08 cm port was used in the final experiments with the tall unit of Figure 3-20. The air chamber of the Air Cannon was too large, and the volume of the chamber was reduced by partially filling it with water. Experiments were made with puffback reservoir volumes of 3780, 4780, 5780 and 8780 cm^3.

After having explored the louvers arrangement used by Lee (1975) in his small scale experiments (Figure 3-10) and having found it not suitable for consistent operation in the tall panel bed, the arrangement shown in Figure 3-3 was installed and used with success.

Only one grade of sand was tested in the tall panel bed, a commercially available grade designated No. 1/4 sand, whose particle size distribution is given in Table 3-9.

A sand spill from a puffback was caught in metal trays, resembling gutters, placed at the 34th, 64th, 104th, 134th, 164th, and 194th louver from the top. The spill from the bottom five gas-entry sand surfaces was caught at the bottom. Weights of sand were determined for each tray and at the bottom, giving data permitting assessment of the uniformity of the sand spill.

Four high-sensitivity, low impedance quartz transducers

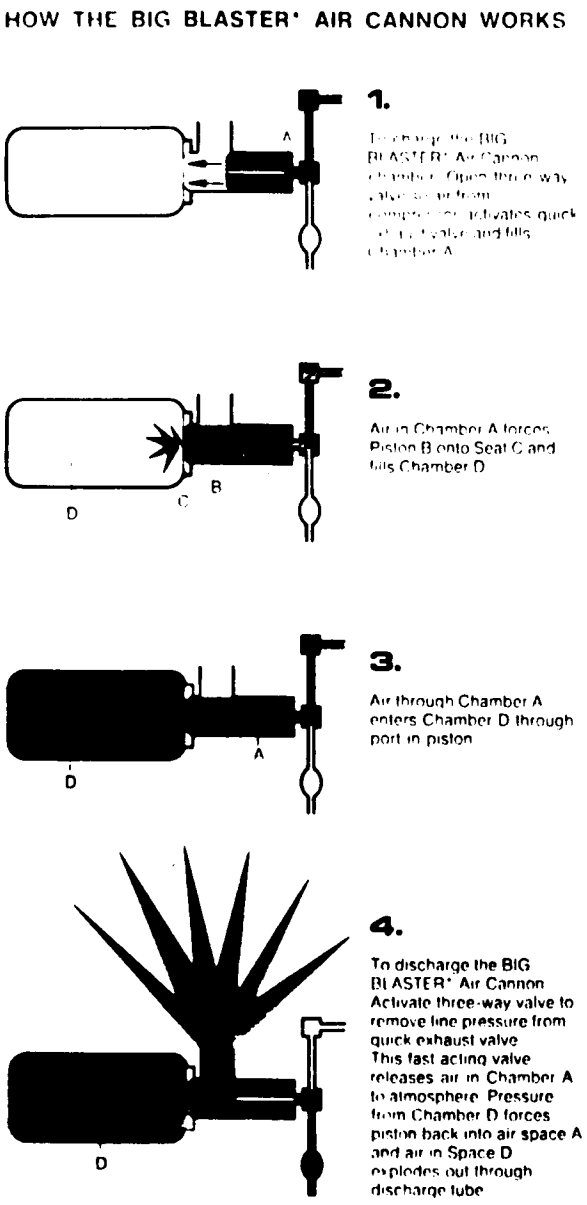

Figure 3-22 Diagrams illustrating operation of the "Big Blaster Air Cannon."

TABLE 3-9 Size Distribution of Test Sand Used in Tall Panel Bed

Size Cut U.S. Standard Mesh Number	Weight Percentage
+ 10	0.0
- 10 + 14	1.5
- 14 + 20	2.3
- 20 + 30	53.9
- 30 + 40	38.1
- 40 + 50	2.6
- 50 + 60	0.8
- 60	0.8
	100.0

(Kistler Model 206) were installed to follow the pressure transients on the clean side of the panel bed. They were placed as generally shown in Figure 3-20, at elevations 30.48, 121.92, 182.88 and 364.32 cm below the top of the louvers. The signals from the transducers were fed into a multi-channel oscilloscope fitted with a Polaroid camera.

3.04.42 Results and Discussion

In downshot puffback a packet of puffback air travels downward from top to bottom of the clean side, and as it moves, gas leaks forward through the panel bed and into the space on its dirty side. It was not at all obvious that the amount of air supplied to form the packet moving down the clean side could be adjusted, together with its initial peak pressure, to provide just sufficient leakage of gas forward at every point along the height of the panel bed to produce a uniform body movement of the sand and a uniform sand spill.

After several modifications, puffback in the tall panel bed could be controlled for achieving fairly uniform sand spills. Tables 3-10 and 3-11 show typical uniformity test data obtained while using The City College valve and the the Big Blaster Air Cannon.

It was gratifying that the active time principle, discovered from work at the 30.48 cm high scale (Subsection 3.04.1), appears also to govern the spill of sand from the 304.8 cm high unit.

It was concluded that:

Table 3-10

TALL PANEL BED FILTER PUFFBACK UNIFORMITY TEST DATA .
(CITY COLLEGE PUFFBACK VALVE)

Puffback Valve Orifice Size = 5.08 cm (City College)

Puffback Tank Size = 4.81 liters

Configuration = with hose

Louvers Arrangement = Wishbone Front Louver / Inclined Back Louver

	Sand Spill per Louver Space (grams) *					
Puffback Pressure (kPa)	239.2	308.2	377.1	446.	515.	583.9
Louver No.#						
1 - 34@	4.2	8.9	13.0	15.0	16.9	17.0
35 - 64@	3.5	8.2	12.0	14.7	17.3	18.5
65 - 104	2.4	6.3	10.5	13.8	18.5	20.9
105 - 134	1.7	5.5	10.5	14.7	19.0	22.2
135 - 164	1.3	5.4	10.4	14.7	20.0	23.7
165 - 194	1.7	6.3	11.6	16.2	21.4	24.9
195 - 199+	2.6	7.7	13.1	17.5	21.6	24.4

* Average value over the louver numbers indicated.

\# Louver number counted from the top of the panel.

@ At high puffback intensity some sand jumped over the collecting pan, and the number shown above is less than actual value.

\+ Not an accurate number, for reference purpose only.

Table 3-11

TALL PANEL BED FILTER PUFFBACK UNIFORMITY TEST DATA
(BIG BLASTER AIR CANNON)

Puffback Valve Orifice Size = 5.08 cm (Big Blaster Air Cannon)

Puffback Tank Size = 5.78 liters

Configuration = With Hose

Louvers Arrangement = Wishbone Front Louver / Inclined Back Louver

	Sand Spill per Louver Space (grams) *						
Puffback Pressure (kPa)	239.2	308.2	377.1	446.	515.	583.9	652.9
Louver No.#							
1 - 34@	3.3	6.3	8.5	13.1	14.0	16.8	18.8
35 - 64@	2.9	5.9	7.6	13.4	14.9	17.5	19.4
65 - 104	1.8	4.3	6.0	11.5	13.3	17.0	19.2
105 - 134	0.7	2.7	4.2	9.8	11.9	16.3	18.6
135 - 164	0.3	2.1	3.6	10.5	12.1	16.4	19.1
165 - 194	0.4	2.3	3.8	11.1	12.8	17.2	19.8
195 - 199+	0.5	3.5	5.9	12.5	14.1	18.9	21.5

* Average value over the louver numbers indicated.

\# Louver number counted from the top of the panel.

@ At high puffback intensity some sand jumped over the collecting pan, and the number shown above is less than actual value.

\+ Not an accurate number, for reference purposes only.

a) Active time governs the spill of sand in the tall panel bed.

b) Active time increases with increasing pressure in the puffback gas reservoir, but the increase is much more near the bottom of the panel bed than elsewhere. The increase in active time near the bottom can be attributed to conversion of gas velocity head into pressure head as the pulse of gas decelerates upon its arrival at the bottom of the clean space.

c) A relatively small puffback gas reservoir is preferable, in terms of sand spill uniformity, to a large reservoir.

d) The combination of wishbone and inclined louvers (Figure 3-3) gave a wider range of reasonably uniform sand spills than the combination of chevron and horizontal louvers (Figure 3-10).

e) An unexpected benefit of the inclined louvers was a marked increase in the puffback spill at a given puffback intensity. Also, they increased the range of sand spill for which the spill is reasonably uniform along the height of the panel bed.

f) The Big Blaster Air Cannon opens more quickly than the City College valve, and probably also with greater degree of reproducibility from one opening to another.

g) The dirty side of a panel bed undergoing puffback must be relatively unconfined in comparison with the clean side if uniformity of sand spill is required.

CHAPTER 4.0: LITERATURE REVIEW

4.01 Particle Size Distribution: Determination and Interpretation

The majority of natural and artificially produced particulates possess considerable polydispersity. The granular-form solids encountered in nature or produced in manufacturing and processing operations are seldom if ever, uniform in size. Crushing, grinding, precipitation, attrition, or any other particulate-forming processes result in granular products exhibiting a range of particle sizes. A final uniform size material is usually the result of further grading and size-separation steps.

In view of the strong dependence of the physical properties of particulates on particle size, a mean size is seldom sufficient for the specification of an aerodisperse system; the particle size distribution must be found.

When we deal with particles of regular shapes, we encounter no problem as to the meaning of size or size distribution. If the particle is spherical, we can use particle diameter; if it is cubical the length alone one edge is characteristic; and, for other shapes, we can use other equally appropriate dimensions. When particles are irregular, we must resort to an arbitrary definition as to what constitutes "size." It is generally considered that some average linear measure of the projection of many

particles in a fixed direction is statistically adequate for describing the size range or size distribution of particles. This assumes, of course, that the particles of the sample studied are randomly oriented and that the number of particles examined and measured is large enough to preclude additional measurements along any other selected direction from changing the distribution. Thus, a size distribution as determined by linear measurements is quite arbitrary.

Particles consisting of liquid droplets formed by condensation or by shearing action from a body of liquid are normally spherical. On the other hand, particles formed by fracture from a solid and particles formed by crystallization are usually nowhere near spherical in shape. It is for these particles that the concept of diameter requires modification. In order to facilitate the analysis a mean diameter is usually defined.

There are six different mean diameters for a collection of particles, which have different applications depending on which properties of the particles are to be calculated.

1. Measurement of length in a particular direction: "d_1"

To uniquely define length parallel to the reference direction and at the same time to provide an easily workable measurement process, length is measured through a point midway between the topmost and bottom-most points of the particle as it is oriented relative to the reference direction.

2. Average of measurement of length in several directions: "d_l,"

This should be done using an intersection point as near to the centroid of the particle as possible.

3. Surface area equivalent: "d_{Ae}"

A sphere having diameter d_{Ae} will have the same surface area as the particle in question.
Accordingly d_{Ae} is given by:

$$d_{Ae} = (A_s / \pi)^{1/2} \qquad (4\text{-}1)$$

where : A_s is the surface area of the particle.

4. Specific surface area equivalent: "d_{ae}"

A sphere of same density and having diameter d_{ae} will have the same specific area as the particle in question.
As a result d_{ae} is given by:

$$d_{ae} = 6\ V_p / A_s \qquad (4\text{-}2)$$

where V_p is the actual volume of the particle.

5. Volumetric equivalent: "d_{ve}"

A sphere with diameter d_{ve} will have the same volume as the particle in question and will have the same mass if the densities are equal. This results in:

$$d_{ve} = (6\ V_p / \pi)^{1/3} \qquad (4\text{-}3)$$

6. Aerodynamic equivalent diameter: "d_{st}"

This mean diameter is based on the free fall of the

particle in the laminar regime. A sphere having diameter d_{st} will have the same terminal velocity under the influence of gravity in a given fluid as will the particle in question. In this case the measured property of the particle will be its terminal settling velocity.

As a result d_{st} is given by:

$$d_{st} = \left(\frac{18 \mu V_{tp}}{\rho_p g} \right)^{1/2} \qquad (4\text{-}4)$$

Where μ is the viscosity of the fluid in which the terminal velocity of the particle V_{tp} is determined and ρ_p and g are the particle density and acceleration of gravity respectively. The equation for the terminal velocity in the laminar regime is valid for particle Reynolds number smaller than 2.

The particle Reynolds number is given by:

$$Re_p = \rho V_{tp} d_{st} / \mu \quad (\rho = \text{density of fluid}) \qquad (4\text{-}5)$$

4.01.1 Methods for Determination of Particle Size

The subject of particulates in air pollution control involves particles in the very wide range of sizes between 10^{-9} and 10^{-3} meters (0.001 and 1000 micrometers). It is not surprising that passage from the lower to the upper limit is accompanied by changes not only in nearly all the physical properties of particulates, but also in the nature of the laws governing them. Table 4-1 summarizes the current methods available for particle size determination, indicating the range for best application.

TABLE 4-1: Methods for Determination of Particle Sizes

Method	Particle Diameter (micrometers)
Sieves	44 and up
Hindered Settling	4-3000
Liquid Sedimentation	1-500
Gas Sedimentaion	2-200
Centrifugal Sedimentation	0.001-50
Impaction	0.2-100
Optical Microscope	0.3-300
Electron Microscope	0.001-10
Light Scattering and Transmission	0.1-30
X-ray scattering	0.01-0.1
Electrical Conductivity	2-200

A complete review of the different methods and their limitations can be found in Irani and Callis (1963), and Herdan (1960).

4.01.2 Particle Size Distributions

In most applications of Air Pollution Control Theory one encounters collection of particulates with a very large number of particles and in trying to determine the number of particles having diameter d we find that if d is specified to sufficiently many decimal places, there will be no particles having diameter d. There will be a certain number whose diameter is very close to d, however. More specifically, there will be a certain number of particles whose diameter lies in the range d to d+d(d). Since d(d) is arbitrary, though it must be small, the number of particles defined this way is an arbitrary number. To uniquely quantify the

number distribution, we can define N(d) as the total number of particles whose diameter are less than or equal to d. In this way $N = N(\infty)$ would be the total number of particles in the collection. Now, since N(d) is a continuous function of d, or at least almost so in a collection of very many particles, we may determine its derivative with respect to d:

$$n(d) = \frac{dN(d)}{d(d)} \qquad (4\text{-}6)$$ (Number distribution function)

And it is this function n(d) which is useful to characterize the particle size distribution in a collection.

The number of particles whose diameter is less than or equal to d is given by:

$$N(d) = \int_0^d n(d)\ d(d) \qquad (4\text{-}7)$$

and the total number of particles present is given by:

$$N = \int_0^\infty n(d)\ d(d) \qquad (4\text{-}8)$$

The limit of ∞ in Equation (4-8) causes no difficulty since n(d) approaches zero as d becomes large.

Since particle size distributions are commonly obtained on a number, weight or volume basis, it is useful to define distribution functions analogous to n(d) for the different possible ways of determination.

We can define M(d) as the sum of the masses of particles whose diameters are less than or equal to d. In this way $M = M(\infty)$ would be the total mass of the collection. And since

M(d) is a continuous function of d or at least almost so in a collection of very many particles, we may determine its derivative with respect to d.

$$m(d) = \frac{d\,M(d)}{d(d)} \qquad (4\text{-}9)$$ (Mass distribution function)

The mass of particles whose diameters are less than or equal to d would then be: $M(d) = \int_0^d m(d)\,d(d)$ (4-10)

The total mass of the collection is:

$$M = \int_0^\infty m(d)\ d(d) \qquad (4\text{-}11)$$

A relation between the two distribution functions given by equations (4-6) and (4-9) can be obtained by:

$$m(d) = m_d\ n(d) \qquad (4\text{-}12)$$

where m_d is the mass of a single particle of diameter d. The arithmetic mean of the masses of the particles in the collection is given by:

$$\bar{m}a = \frac{\int_0^\infty m_d\ n(d)\ d(d)}{\int_0^\infty n(d)\ d(d)} = \frac{M}{N} \qquad (4\text{-}13)$$

Since: $\bar{m}_a = \rho_p\ \bar{V}_a$ (4-14)

Where $\bar{V}_a$ is the arithmetic mean of the volumes of the particles, then for constant density ρ_p (collection of uniform composition and free from aggregates) the mass distribution function m(d) is identical to the volume distribution function:

$$v(d) = v_d\ n(d) \qquad (4\text{-}15)$$ (Volume distribution function)

where: v_d is the volume of a single particle. As a result we can define:

$$V(d) = \int_0^d v(d)\ d(d) \qquad (4\text{-}16)$$

and

$$V_o = \int_0^{\infty} v(d)\, d(d) \qquad (4\text{-}17)$$

where V(d) is the volume of particles whose diameters are less than or equal to d, and V_b is the total volume of the collection.

The usefulness of the cumulative distributions given by equations (4-7), (4-10) and 4-16) is that with them it is comparatively easy to smooth out random errors of measurement and fluctuations in the quantity measured in each fraction (Fuchs, 1964).

Similar distributions could also be defined on a surface area or specific surface area basis and be related to the ones defined above (Herdan, 1960).

A typical particle distribution curve is shown in Figure 4-1 indicating n(d) and N(d).

The formulas developed to this point are expressed in terms of integrals whose integrands involve the term n(d); therefore, all that is needed is to formulate a suitable mathematical equation describing this function. The question now arises whether particle size, like other variable quantities in nature, follows in its distribution certain well-defined mathematical forms or laws. Owing to the great complexity of the formation process of particulates, there exists, as yet no theoretical derivation of a distribution (excepting for the so called log-normal distribution); but there is a series of empirical formulas applicable mainly to particulates obtained by the mechanical disintegration of

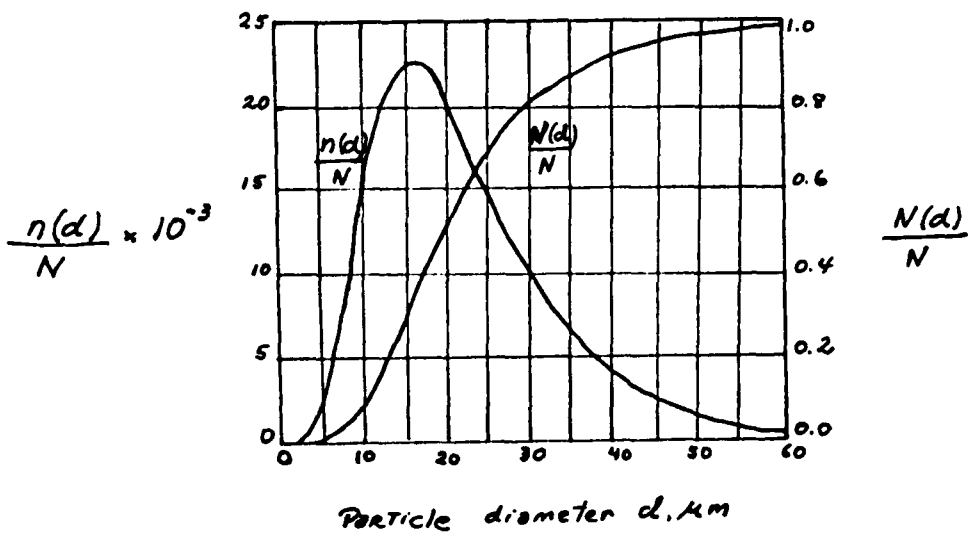

Figure 4-1 Typical Particle Size Distribution

solid and liquid bodies (Fuchs, 1964).

Some authors claim (Fuchs, 1964) that the formulas proposed by them are correct over the whole range and assign any deviations to experimental errors. The theoretical significance which can be attached to these formulas is doubtful, and the fact that each formula has been applied with success to several groups of particulates suggests that general significance is lacking. They are more or less successful empirical approximations to the actual distribution with undoubted practical value, because they make it possible to express the properties governed by particle size in terms of two parameters and so to compare one collection with another.

By employing a sufficiently large number of coefficients it would be possible to represent by a single formula all the distributions encountered in practice. However, the choice of coefficients would require a large effort and it would be difficult to assign any physical meaning to them; for this reason most formulas utilized in practice have two coefficients.

4.01.21 Normal Distribution Function

Since the differences in particle size in one and the same material are not accountable for by definite assignable causes, but only by the conflux of a multitude of small causes whose simultaneous presence or absence is governed by factors unknown to us, it suggests itself that a function of the type of the Normal or Gausian law of errors might be

suitable for describing particle size distributions (Herdan, 1960). It must however be admitted that normal distributions are less frequently found in the realm of small particles than in that of statistics proper and of statistical physics. Fuchs (1964) mentions that just in a very few aerosols, such as those formed by plant spores, the distribution curves are symmetrical and close to the shape of the Gaussian curve or Normal distribution which is given by:

$$n(d) = \frac{N \; e^{-(d-\bar{d})^2 \; / \; 2\sigma^2}}{(2\pi)^{1/2} \; \sigma} \qquad (4\text{-}18)$$

where:

$\bar{d}$ is the arithmetic mean diameter given by:

$$\bar{d} = \frac{\int_0^\infty n(d) \; d \; d(d)}{\int_0^\infty n(d) \; d \; (d)} = \frac{\int_0^\infty n(d) \; d \; d(d)}{N} \qquad (4\text{-}19)$$

and σ is the standard deviation or measure of the dispersion of the distribution around the average. Its square, the variance is given by:

$$\sigma^2 = (1/N) \int_0^\infty (d-\bar{d})^2 n(d) d(d) \qquad (4\text{-}20)$$

The cumulative particle diameter curve N(d) is obtained by integrating equation (4-18):

$$N(d) = (N/(2\pi)^{1/2}\sigma) \int_0^d e^{-(d-\bar{d})^2 \; / \; 2\sigma^2} \; d(d) \qquad (4\text{-}21)$$

The integral in equation (4-21) is not capable of evaluation in closed form. It is a standard form, however, known as

the error function, whose value can be obtained from a mathematical table.

In this way: $N(d) = (N/2)\ (1+\mathrm{erf}((d-\bar{d})/\ 2^{1/2}\ \sigma\ ))$ (4-22)

4.01.22 The Log-Normal Distribution Function

The overwhelming majority of condensation and dispersion aerosols possess frequency distributions which are skewed, rising relatively sharply at the lower end of the size spectrum and then tapering off as particle size increases (Fuchs, 1964).

Zenz and Othmer (1960) also indicate that an asymmetrical probability size distribution curve is characteristic of most naturally occurring or mass-produced particle grinds.

If the cumulative distribution given by equation (4-21) is plotted as a function of particle diameter in a "probability" coordinate system a straight line cutting the axis representing particle diameter at $d=\bar{d}$ (the arithmetic mean particle diameter) is obtained.

As we have already mentioned, almost no actual distribution gives a straight line in such a plot. On the other hand, if the logarithm of the particle diameter is used instead of the diameter itself, then the curves for actual distributions acquire a more symmetrical form and often approximate a Gaussian curve. In this case the distribution is log-normal.

Fuchs (1964) points out that the log-normal distribution may have theoretical significance. In particular Kolmogoroff.

(Fuchs, 1964) has shown that simple hypotheses about the process of grinding solid particles result in a particle size distribution which tends asymptotically to the log-normal distribution with progressive size reduction.

Epstein (1947) constructs a statistical model for breakage mechanisms and proves under certain hypotheses that the cumulative distribution function after n steps in the breakage process is asymptotically logarithmico-normal, a form of distribution frequently observed. He also mentions the inaccessible paper of the Russian mathematician Kolmogoroff (1941) as the first published attempt to construct theoretical breakage mechanisms based on the theory of probability which will lead to log-normal distributions.

Zenz and Othmer (1960) while discussing the concept of "powder viscosity" point out that the optimum size distribution of a multicomponent particulate system for best fluidity approaches that of a normal skewed-probability distribution. They mention that this is a possible explanation of the mechanism which leads naturally occurring grinds to exhibit a skewed particle-size distribution since it is certainly conceivable that in the grinding process there occurs sufficient particle motion for an analogy to fluidization. It also would seem rational to suppose that areas of maximum interparticle friction (orby analogy, bed viscosity), would suffer the greatest degree of attrition. Therefore, one could predicate the grinding mechanism as continually leading to a minimization of the "viscosity" of the particle mass being ground.

Zimon (1969) found that the particle size distributions obtained before and after the action of perpendicular air flows on dust-laden surfaces were log-normal. Analogous results were obtained for the distributions when dust-laden surfaces were subjected to the action of various vibrational forces.

Willeke and Whitby (1975) after having measured several thousand in situ aerosol particle size distributions in a variety of urban and non-urban surface locations throughout the United States, concluded that there is evidence now that atmospheric aerosols may be distributed log-normally in small size ranges notably the fine particle range below about 1 micrometer, but that they are not log-normally distributed over the entire particle size range.

In a log-normal distribution we can define a diameter parameter u as the logarithm of the diameter:

$$u = \ln d \tag{4-23}$$

The relation between n(u) and n(d) is obtained from the combination of equations (4-6) and (4-23)

$$n(d) = dN(d)/d(d) = (dN(u)/du)\ du/d(d) = n(u)/d \tag{4-24}$$

The curve for n(u) is a normal probability curve in u, centered about a value $\bar{u}$ and with a standard deviation σ_u The equation for this curve is:

$$n(u) = \frac{N\ e^{-(u - \bar{u})^2 / 2\sigma_u^2}}{(2\pi)^{1/2}\sigma_u} \tag{4-25}$$

The cumulative size distribution function N(u) is obtained

by integrating (4-25) and is given by:

$$N(u) = (N/2)(1 + \text{erf}((u-\bar{u})/2^{1/2}\,\sigma_u)) \qquad (4\text{-}26)$$

It is desirable to relate equations (4-25) and (4-26) to the corresponding equations involving diameter d. In transforming these equations, we need to define a new mean diameter d_m and a new standard deviation σ_m, which are related to the log-normal distribution as

$$\bar{u} = \ln d_m \qquad (4\text{-}27)$$

$$\sigma_u = \ln \sigma_m \qquad (4\text{-}28)$$

Combining equations (4-23), (4-24), (4-26) and (4-27) the distribution equations (4-25) and (4-28) become:

$$n(d) = \frac{N\, e^{-(\ln(d/d_m))^2/2(\ln \sigma_m)^2}}{(2\pi)^{1/2}\, d \ln \sigma_m} \qquad (4\text{-}29)$$

where $\ln d_m = \overline{\ln d}$, and consequently d_m is the geometrical mean of the particle diameters, and $(\ln \sigma_m)^2 = \overline{(\ln(d/d_m))^2}$ is the variance of the logarithms of the particle diameters. The standard deviation of the logarithm of the sizes, σ_m, is called the standard geometric deviation.

And:

$$N(d) = (N/2)\ (1 + \text{erf}\ (\ln(d/d_m)/2^{1/2}\ \ln \sigma_m) \qquad (4\text{-}30)$$

Combining equation (4-18) and (4-23) through (4-25) the arithmetic mean diameter is obtained:

$$\bar{d} = e^{\bar{u}}\, e^{\sigma_u^2/2} = d_m\, e^{(\ln \sigma_m)^2/2} \qquad (4\text{-}31)$$

In a similar way the equation for the standard deviation is developed (Crawford, 1976):

$$\sigma = (e^{2\bar{u}}\, e^{2\,\sigma_u^2} - 2\bar{d}e^{\bar{u}}\, e^{\sigma_u^2/2} + \bar{d}^{\,2})^{1/2} = \bar{d}(e^{(\ln \sigma_m)^2} - 1)^{1/2} \qquad (4\text{-}32)$$

As a rule, if the number distribution of a given variable obeys a certain distribution law (e.g., the normal law), the weight distribution does not, and viceversa. The case is different for the log-normal distribution. If the number distribution is log-normal, the weight and surface distributions are also log-normal and with the same geometric standard deviations (Herdan, 1960).

It can be shown (Herdan, 1960) that the relation between the geometric mean diameters is given by:

$$\ln d_m = \ln d_{mw} - 3\,(\ln \sigma_m)^2 \qquad (4\text{-}33)$$

where: d_{mw} is the geometric mean diameter by weight.
It can also be shown that:

$$\sigma_m = \frac{d_t}{dm} \qquad (4\text{-}34)$$

where: d_t is the diameter at $(N(d)/N) = 0.841$

4.02 Pollutant Concentrations and Collection Efficiencies

4.02.1 Pollutant Concentrations

In most areas of pollution control one encounters heterogeneous mixtures of a carrier fluid with solid or fluid pollutants, and as result different ways of expressing the amount of pollutant present in the carrier fluid have emerged. The most widely used can be defined as:

a) Mass Concentration

The mass concentration, C_M, is defined as the mass of

pollutant divided by the mass of mixture:

$$C_M = M_P / M_m \qquad (4\text{-}35)$$

where: M_P = mass of pollutant substance

M_m = mass of mixture

A similar expression to equation (4-35) is obtained if the concentration is expressed as a percentage and not as a fraction:

$$C_M \% = (M_P / M_m) \times 100 \qquad (4\text{-}36)$$

b) Volumetric Concentration

The volumetric concentration, C_V, is defined as the volume of pollutant divided by the volume of mixture :

$$C_V = V_P / V_m \qquad (4\text{-}37)$$

c) Mass-Volume Concentration

The mass-volume concentration, C_{MV}, is defined as the mass of pollutant divided by the volume of mixture

$$C_{MV} = M_P / V_m \qquad (4\text{-}38)$$

d) Parts Per Million Partial Volumetric Concentration

This concentration is defined as the partial volume of pollutant divided by the partial volume of carrier fluid:

$$C_{Vppm} = (V_P / V_C)\ 10^6 \qquad (4\text{-}39)$$

where V_C is the volume of carrier fluid. This concentration is usually utilized for expressing concentration of gaseous pollutants in gaseous carriers.

Useful relationships among these different concentrations can be obtained by combining their definitions with the densities of carrier ρ_C, and pollutant ρ_P

$$M_P = \rho_P \; V_P \tag{4-40}$$

$$M_C = \rho_C \; V_C \tag{4-41}$$

In this way we derive the following equations:

$$C_M = \frac{\rho_P C_V}{\rho_C(1-C_V)+\rho_P C_V} \tag{4-42}$$

$$C_{MV} = \rho_P \; C_V \tag{4-43}$$

$$C_V = \frac{C_{VppM}}{10^6+C_{VppM}} \tag{4-44}$$

For the usual range of pollutant concentrations and densities it is common to assume to a good approximation that:

$$C_V \approx V_P \; / \; V_C \tag{4-45}$$

$$C_M \approx (\rho_P C_V) \; / \; \rho_C \tag{4-46}$$

And as a result of this observation the following equation is obtained:

$$C_{MV} \approx \rho_C \; C_M \tag{4-47}$$

For mixtures of solid or liquid pollutants and fluid carriers the most widely used concentration is the mass-volume concentration C_{MV}, and this could be determined from the distribution functions defined by equations (4-6) and (4-9):

$$C_{MV} = \frac{M_P}{V_M} = \frac{\int_o^\infty m(d)\,d(d)}{V_M} = \frac{\int_o^\infty m_d \; n(d)\,d(d)}{V_M} \tag{4-48}$$

Or in terms of the volumetric equivalent diameter:

$$C_{MV} = \frac{(\pi/6) \; \rho_P \; \int_o^\infty n(d_{ve}) d_{ve}^{\;3} \; d(d_{ve})}{V_M} \tag{4-49}$$

4.02.2 Collection Efficiencies

Most collection devices are not absolute collectors and the effectiveness of their operation is expressed in terms of a collection efficiency.

Collection efficiency is defined as the ratio of the amount of pollutant collected to the total amount present. Several properties of the pollutant substance can be used in defining efficiency, and therefore it is important to distinguish among them.

a) Mass Collection Efficiency

This is the most commonly used for all types of pollutants and can be defined, for continuous flow operation of the collector as:

$$E_M = \frac{m_{pi} - m_{pe}}{m_{pi}} = \frac{\int_0^\infty m(d)_i d(d) - \int_0^\infty m(d)_e d(d)}{\int_0^\infty m(d)_i d(d)} \qquad (4\text{-}50)$$

where: m_{pi} = mass flow rate of pollutant at inlet of collector

m_{pe} = mass flow rate of pollutant at outlet of collector

$m(d)_i$ = mass distribution function at inlet of collector

$m(d)_e$ = mass distribution function at outlet of collector

For a constant volumetric flow rate through the collector equation (4-50) can then be written in terms of the mass volume concentrations:

$$E_M = \frac{C_{MV_i} - C_{MV_e}}{C_{MV_i}} \qquad (4\text{-}51)$$

This equation is usually valid for isothermal collectors operating at pressure drops which are a negligible fraction

of the operating pressure.

For solid and liquid pollutants showing a wide variation in particle diameters, it is important to distinguish between the overall collection efficiency given in this case by equations (4-54) and (4-55) and the efficiency at a particular particle diameter which could be defined as follows:

$$E_{M(d)} = \frac{m_{p(d)i} - m_{p(d)e}}{m_{p_{(d)_i}}} = \frac{m(d)_i - m(d)_e}{m_{(d)_i}} = \frac{n(d)_i - n(d)_e}{n_{(d)_i}} \qquad (4\text{-}52)$$

where: $m_{p(d)i}$ = mass flow rate of particles of diameter d at inlet of collector

$m_{p(d)_e}$ = mass flow rate of particles of diameter d at outlet of collector

For a constant volumetric flow rate through the collector equation (4-52) becomes:

$$E_{M(d)} = \frac{C_{MV(d)i} - C_{MV(d)e}}{C_{MV(d)i}} \qquad (4\text{-}53)$$

The overall collection efficiency can be related to the efficiency at a single diameter by means of the equation

$$E_M = \frac{\int_0^\infty m_d \left[n(d)_i - n(d)_e\right] \, d(d)}{\int_0^\infty n(d)_i \, m_d \, d(d)} = \frac{\int_0^\infty E_{M(d)} \, n(d)_i \, m_d \, d(d)}{\int_0^\infty n(d)_i \, m(d) \, d(d)} \qquad (4\text{-}54)$$

The use of the volumetric equivalent diameter allows us to write the overall efficiency in terms of the particle

diameter, inlet distribution function and efficiency at a particular particle diameter for a particle of any shape:

$$E_M = \frac{\int_0^\infty E_{M(d_{ve})}\ n(d_{ve})_i\ d_{ve}^3\ d(d_{ve})}{\int_0^\infty n(d_{ve})_i\ d_{ve}^3\ d(d_{ve})} \qquad (4\text{-}55)$$

If the inlet particle size distribution is log-normal, equation (4-55) could be combined with equation (4-29) to give

$$E_M = \frac{\int_0^\infty E_{M(d_{ve})} d_{ve}^2\ e^{-[\ln(d_{ve}/d_m)]^2/\ 2(\ln \sigma_m)^2}\ d(d_{ve})}{\int_0^\infty d_{ve}^2\ e^{-[\ln(d_{ve}/d_m)]^2/2(\ln \sigma_m)^2}\ d(d_{ve})} \qquad (4\text{-}56)$$

Equations (4-56) can be written in terms of the logarithm of the particle diameter by combining it with equations (4-23) through (4-25) (Crawford, 1976):

$$E_M = \frac{\int_{-\infty}^\infty E_{M(u)} e^{3u}\ e^{-(u-\bar{u}^2/2\sigma_u^2}\ du}{\sqrt{2\pi}\ \sigma_u\ e^{3\bar{u}}\ e^{9\sigma_u^2/2}} \qquad (4\text{-}57)$$

in which $u = \ln(d_{ve})$.

If the collection efficiency at a particular particle diameter as a function of particle diameter can be described by a log-normal function (Sundberg, 1974), equation (4-57) becomes:

$$E_M = \text{erf}\left\{ \frac{\ln\left(\frac{dmi}{dmc}\right)}{\left[(\ln \sigma_{mi})^2 + (\ln \sigma_{mc})^2\right]^{1/2}} \right\} \qquad (4\text{-}58)$$

where:

dmi= geometrical mean diameter or mass median diameter of the particle size distribution at inlet of collector

σ_{mi} = geometric standard deviation of the particle size distribution at inlet of collector

dmc = cut diameter (diameter of particles which are removed with a 50% efficiency)

σ_{mc} = geometric standard deviation of the distribution of efficiency at a particular particle diameter.

b) Number Collection Efficiency

If the number of particles is the property of interest in the determination of the performance of a collector, the efficiency is expressed as follows:

$$E_N = \frac{N_i - N_e}{N_i} = \frac{\int_0^\infty (n(d)_i - n(d)_e) d(d)}{\int_0^\infty n(d)_i d(d)} \qquad (4\text{-}59)$$

where:

N_i = number of particles entering collector per unit time

N_e = number of particles exiting collector per unit

If the volumetric flow rate remains constant in passing through the collector, (4-59) becomes:

$$E_N = \frac{C_{N_i} - C_{N_e}}{C_{N_i}} \qquad (4\text{-}60)$$

where:

C_{N_i} = number of particles per unit volume at inlet of collector

C_{N_e} = number of particles per unit volume at outlet of collector.

The number collection efficiency at a particular particle diameter is given by:

$$E_{N(d)} = \frac{N_{i(d)} - N_{e(d)}}{N_{i(d)}} = \frac{n(d)_i - n(d)_e}{n_{(d)_i}} \qquad (4\text{-}61)$$

A comparison of equation (4-52) with (4-61) illustrates the fact that for collection of particulates of uniform density the number and mass collection efficiencies at a particular particle diameter are the same.

Upon substitution of equation (4-61) into (4-59) a relation between overall and grade number efficiencies is obtained:

$$E_N = \frac{\int_0^\infty E_{N(d)}\ n(d)_i\ d(d)}{\int_0^\infty n(d)_i\ d(d)} \qquad (4\text{-}62)$$

If the inlet particle size distribution by number is log-normal, then the overall efficiency by number becomes:

$$E_N = \frac{\int_{-\infty}^{\infty} E_{N(u)}\ e^{-(u-\bar{u})/2\ \sigma_u^2}\ du}{(2\pi)^{1/2}\sigma_u} \qquad (4\text{-}63)$$

If the grade collection efficiency by mass of a collector follows a log-normal distribution, it will also follow it on a number basis (Herdan, 1960) and therefore an equation similar to (4-58) is obtained:

$$E_N = \text{erf}\left\{\frac{\ln\left(\frac{dn_i}{dn_c}\right)}{[(\ln \sigma_{ni})^2 + (\ln \sigma_{nc})^2]^{1/2}}\right\} \qquad (4\text{-}64)$$

where: dni = number median diameter of particle size distribution at inlet of collector

dnc= cut diameter by number or diameter at which the particles are collected with a 50% number efficiency

$\sigma_{ni}=\sigma_{mi}$= geometric standard deviation of particle size distribution at inlet of collector

$\sigma_{nc}=\sigma_{mc}$= geometric standard deviation of grade collection efficiency distribution

4.02.22 Penetration: A Better Indicator of Performance of Collecting Devices

Collection Efficiency as defined in the preceding sub-section is not a good indicator of the performance of a collecting device, since it does not reflect the amount of particulates which were not collected. As a result its definition does not permit rapid comparisons of performance at different operating conditions or between different collecting devices. Penetration, defined as the ratio of the amount of pollutant not collected to the total amount present, is given by:

$$P_M = \frac{m_{pe}}{m_{pi}} = 1 - E_M \qquad (4\text{-}65)$$

where: P_M = fractional mass penetration.

By analogy to equation (4-65), all the equations in the preceding sub-section could be written in terms of penetration.

The usefulness of the term can be illustrated by the

following example:

If two different collecting devices achieve 99.9 and 99.99 wt% overall collection efficiency while capturing the same dust at the same operating conditions, one might think that there is almost no difference between the performance of the two devices, while in reality the gas leaving the second collector is ten times cleaner than the one leaving the first. Thus, ratios of penetrations provide a more meaningful measure of separation performance.

4.03 Porous Bed Resistance to Gas Flow

4.03.1 Granular Bed Resistance

According to D'arcy's law the pressure drop across a granular bed will increase with gas velocity, and is given by equation (4-66)

$$dP/dx = -\mu V/K_d \qquad (4\text{-}66)$$

where:

P = gas pressure

x = direction of flow

V = approach velocity

μ = gas viscosity

K_d = D'arcy's permeability

If V, and K_d do not vary along x, equation (4-66) can be integrated to give:

$$-\Delta P = \mu VL/K_d \qquad (4\text{-}67)$$

where:

ΔP = pressure drop across the bed

L = thickness of the bed

The assumptions implicit in equation (4-67) are the following;

1) Fluid is incompressible (ΔP small compared to total pressure).

2) The regime is laminar (resistance to flow is controlled by viscous and not inertial forces).

3) There is no gas slip (particles are much bigger than mean free path of gas molecules).

In order to understand the applicability of equation (4-67) it is important to discuss the aforementioned assumptions.

1) The first assumption implies the constancy of gas velocity in the integration of equation (4-66); this is valid at small ratios of pressure drop to the total pressure. For the case in which the gas velocity cannot be assumed to be a constant the following treatment is valid:

Assuming isothermal flow and neglecting the effect of pressure upon gas viscosity, we can integrate equation (4-66) at low total pressures where the ideal gas law is applicable:

$$\rho = \frac{PM}{RT} \qquad (4\text{-}68)$$

Where:

ρ = density of the gas

R = universal gas constant

M = molecular weight of gas

T = absolute temperature

(For conditions where the ideal gas law is inapplicable, an appropriate equation of state should be used.)

From the continuity equation applied from entrance to exit

of a constant-area granular bed, we obtain:

$$V_i \rho_i = V_e \rho_e \qquad (4\text{-}69)$$

Where:

i stands for inlet

e stands for exit

Equation (4-69) can be written as follows:

$$V\rho = a \text{ (constant)} \qquad (4\text{-}70)$$

Substituting Equation (4-68) into (4-70) we obtain:

$$(V\ P\ M)\ /\ (R\ T) = a \qquad (4\text{-}71)$$

Or:

$$V = b/P \qquad (4\text{-}72)$$

Where:

b = aRT/M (A constant for a given gas and isothermal flow)

Substituting (4-71) into (4-66) and integrating, we obtain:

$$(P_e^2 - P_i^2)\ /\ 2 = -\mu bL\ /\ K_d \qquad (4\text{-}73)$$

But knowing that:

$$(P_e^2 - P_i^2)\ /\ 2 = (P_e - P_i)\ (P_e + P_i)/2 = \Delta P\ P_{av} \qquad (4\text{-}74)$$

Where:

P_{av} stands for arithmetic average pressure

Substituting (4-74) into (4-73) the following results:

$$-\Delta P = bL/P_{av}K_d \qquad (4\text{-}75)$$

But from (4-71) we know that :

$$b = VP = \text{constant} = V_iP_i$$

Then upon substitution into (4-75) we obtain:

$$-\Delta P = P_iV_iL/P_{av}K_d \qquad (4\text{-}76)$$

2) The assumption of laminar flow can be tested by calculating the particle Reynolds number:

$$Re_{p'} = VD_p\rho/\mu(1-\epsilon) \qquad (4\text{-}77)$$

Where:

$Re_{p'}$ = Reynolds number

ϵ = Void fraction or porosity of the bed

D_p = Diameter of a sphere whose volume/surface area ratio is the same as that of the particles

If the calculated Reynolds number is smaller than 1 the flow resistance is primarily viscous and D'arcy's law is valid. Other investigators (Leva, 1959; and Bird et al., 1960) extend the applicability of D'arcy's law up to $Re_{p'} = 10$. If the particle Reynolds number indicates that inertial effects are important, another term must be added to D'arcy's equation to correct for inertial effects:

$$- \Delta P = \mu LV/K_d + \rho LV^2/K_i \qquad (4\text{-}78)$$

Where:

K_i = constant which depends on the same parameters as D'arcy's permeability

An expression for D'arcy's permeability as a function of bed properties was obtained by Kozeny and modified by Carman and Ergun (Carman, 1937; and Ergun, 1952)

$$K_d = D_p^2 \epsilon^3 / s (1 - \epsilon)^2 \qquad (4\text{-}79)$$

Where:

s = constant = 150 from experimental data.

Substituting (4-79) into (4-67) D'arcy's equation becomes:

$$- \Delta P = 150 \mu L V (1 - \epsilon)^2 / (D_p^2 \epsilon^3) \qquad (4\text{-}80)$$

(This is called the Carman-Kozeny equation)

Burke and Plummer working in the turbulent flow regime found an expression for K_i, which later was modified by

Ergun (1952) and which is:

$$K_i = D_p \epsilon^3 / q (1 - \epsilon) \qquad (4\text{-}81)$$

Where:

q = constant = 1.75 from experimental data

Therefore equation (4-78) becomes:

$$-\Delta P = 150 \mu LV(1 - \epsilon)^2/(D_p^2 \epsilon^3) + 1.75 \rho LV^2 (1 - \epsilon)/ (\epsilon^3 D_p) \qquad (4\text{-}82)$$

Equation (4-82), although valid for both laminar and turbulent regimes is not applicable to compressible fluids.

The following treatment can be used for avoiding the above mentioned restriction:

If (4-82) is applied to a differential length dx of granular material, where the density of the fluid is assumed to be constant, the following results:

$$\frac{-dP}{\rho} = \left(\frac{A}{\rho^2} + \frac{B}{\rho^2}\right)dx = \frac{C dx}{\rho^2} = dF \qquad (4\text{-}83)$$

Where: $\frac{}{\rho} = \left(\frac{}{\rho^2} + \frac{}{\rho^2}\right)$

$$A = \frac{150 (1-\epsilon)^2 \mu G}{\epsilon^3 D_p^2} \qquad B = \frac{1.75 (1-\epsilon) G^2}{\epsilon^3 D_p}$$

$C = A + B$

$G = \rho V$ (Mass flux of fluid) and F = friction loss

Neglecting the effect of temperature and pressure upon viscosity of fluid, A, B, and C can be considered as constants for a given granular bed.

Disregarding any change in static head, Bernoulli's energy balance equation of a unit mass of fluid is:

$$\hat{v} dP + V dV + dF = 0 \qquad (4\text{-}84)$$

where $\hat{v} = 1/\rho$

then substituting equation (4-83) into (4-84) the following results:

$$\hat{v}dP + VdV + \frac{Cdx}{\rho^2} = \tilde{v}dP + G^2\tilde{v}\ d\tilde{v}\ + C\tilde{v}^2\ dx = 0 \tag{4-85}$$

But: $\hat{v} = \frac{ZRT}{MP}$ for a real fluid (4-86)

Where: Z is the compressibility factor

Dividing equation (4-85) by $\tilde{v}^2$ and substituting (4-86) into it the following results:

$$\frac{MPdP}{ZRT} + G^2\ \frac{d\tilde{v}}{\tilde{v}} + Cdx = 0 \tag{4-87}$$

Integration of equation (4-87) results in:

$$G^2\ \ln(\frac{\tilde{v}_e}{\tilde{v}_i}) + CL + \int_{P_i}^{P_e} \frac{MP}{ZRT}\ dP = 0 \tag{4-88}$$

If the compressibility factor is 1 (ideal gas behavior) or if it is properly averaged, integration of equation (4-87) gives:

$$G^2\ \ln\frac{\tilde{v}e}{\tilde{v}i} + CL + M\ \frac{(Pe^2 - Pi^2)}{2\ ZRT} = 0 \tag{4-89}$$

Substituting the expression for C given in equation (4-83) into (4-89) results in:

$$P_i^2 - P_e^2 = \frac{2\ ZRG^2\ T}{M}\left[\ \ln(\frac{\tilde{v}_e}{\tilde{v}_i}) + \frac{150\ (1-\epsilon)^2\ \mu\ L}{\epsilon^3 D_p^2\ G} + \frac{1.75\ (1-\epsilon)L}{\epsilon^3\ D_p}\right] \tag{4-90}$$

3) The validity of assuming no gas slip depends on the size of the particles relative to the mean free path of the gas molecules; when they are of the same order of magnitude equation (4-67) is no longer applicable.

According to kinetic theory of gases the mean free path

can be calculated by:

$$\lambda = RT / ((2 \pi^{1/2} N_o \sigma_g^2 P) \quad (4\text{-}91)$$

Where:

λ = mean free path

N_o = Avogadro's number

σ_g = diameter of gas molecule

4.03.2 Filter Cake Resistance to Gas Flow

a) General Correlations

As far back as 1940 researchers (Williams et al., 1940) were using a Kozeny type of equation for the prediction of the resistance of filter cakes deposited on cloth filters. First et al. (1963) indicated that the depth of the filter cake on a cloth could be expressed in terms of the weight of dust per unit of cloth area and the density and porosity of the dust as follows:

$$L_c = w/(\rho_t (1- \epsilon_e) \quad (4\text{-}92)$$

Where:

L_c = thickness of filter cake

w = weight of dust on the filter per unit area (areal density)

ρ_t = true density of the dust

ϵ_c = porosity of the cake

This expression may be further modified to include the time factor by substituting for w the following:

$$w = C_{MV_i} t V \quad (4\text{-}93)$$

Where:

t = elapsed time of operation

V = approach gas velocity

(Equation (4-93) assumes that the filter is behaving as an absolute filter, with 100% Efficiency.)

Substituting equations (4-93) and (4-92) into (4-80) gives:

$$-\Delta P = s \mu (1 - \epsilon_c) C_{MV_i} V^2 t / (D_p^2 \epsilon_c^3 \rho_t) \quad (4\text{-}94)$$

Equation (4-94) predicts that at constant inlet conditions (gas velocity, gas viscosity, and dust loading) the filter cake resistance (for a given dust) should vary linearly with time (or areal density) as long as the porosity of the filter cake remains constant (i.e., no compaction effects are present). It also predicts the pressure drop to vary as the square of the superficial gas velocity, after the same time period, for equal loadings and bulk density of the filter cake.

b) Compaction Effects

Snyder et al. (1955) investigated the time dependance of filter cake resistance, and found that certain dusts conform to the theory of no cake compaction (constant porosity during filtration). However, they indicated that few dusts behave in this manner and that exponential curves are more apt to be found, especially for extremely fine materials. Generally speaking, the linear curve was seen for relatively coarse materials. First and Silverman (1963) while studying high velocity filtration on bag filters, have considered the compaction of filter cakes and its implications. They recognized that Kozeny's equation yields excellent results for

powders which are compressed to a specified porosity provided the particles are isometric.

Compaction of the cake is a complicated phenomenon, and is probably due to the increased drag exerted by the gas on the cake. Although the dust on the surface of the cake is under negligible mechanical stress due to this drag, the dust below the surface must support the drag experienced by the dust layer above it. At the bottom of the cake (i.e., at the dust-granular material interface), the compressive stress is the greatest and equals the total pressure drop across the cake plus the stress due to the landing of new particles.

Orr indicates (1966) that compaction of the cake can take place by three mechanisms: 1) sliding; 2) elastic and plastic deformation; and 3) fragmentation. The latter is unlikely except for extremely fragile particles, since the compressive stresses are relative small. The most likely mechanism is sliding which is opposed by frictional and cohesion forces between particles in the cake. Compaction effects are generally expressed as follows:

$$\epsilon_{c_f} = \epsilon_{c_o} e^{-a'F_c} \qquad (4\text{-}95)$$

Where:

ϵ_{c_f} = final porosity of compressed cake

ϵ_{c_o} = initial cake porosity

F_c = compressive stress

a' = constant

4.04 Adhesion of Solid Particles

In most particulate control devices the adherence of the particles to a collector or to previously deposited particles is of great importance in the separation. The great majority of filtration models assume that once a particle strikes a collector it adheres and it is not re-entrained.

Davies (1973) indicated that although at that time no experimental work on the redispersion of deposited particles in commercial filters had been reported, several papers on air filtration had suggested that this may take place.

Recent studies (Leith et al., 1977) in a commercial bag filter have shown that after the initial filtration period (cake formation step), the principal means of penetration becomes the delayed release of collected particles rather than the passage of particles through the filter.

4.04.1 State of the Art

Dusts apparently adhere with great tenacity to solid surfaces. Atmospheric dust clings to leaves, walls, fabrics and automobile surfaces. Inversion of solid surfaces with adhering dust indicates that the gravitational force fails to overcome the adhesion force of most particles; similarly, vigorous blowing of the surface dislodges only a few particles.

Corn (1961a, 1961b, 1966) has done systematic reviews of the findings relative to the factors which affect the adhesion of solid particles to solid surfaces in air, and he indicates that it is not yet possible to accurately predict

the forces of adhesion between a specified population of particles and a substrate.

Fuchs (1964) points out that the quantitative aspects of adhesion of small solid particles to solid surfaces in air are not well defined and the adhesion mechanism is not well understood.

Zimon (1969) presents the first systematic treatment of the subject of particle adhesion (interaction particle-surface) and autohesion (interaction particle-particle).

After establishing the theoretical basis of the subject and reviewing the experimental data available, he encounters the need for subsequent investigations in the direction of a deeper and more systematic understanding of the problem.

Gregg et al. (1976) point out that impressive advances in the field of surface forces have been made in recent years, although these are in the nature of refinements rather than fundamental revisions of the basic ideas. Since perforce the advances refer to idealized systems, we are still far from the state where accurate prediction of surface forces can be made from molecular parameters.

4.04.2 Variables Which Influence the Adhesion Mechanism

Adhesion usually refers to the interaction of particles with a solid surface, while autohesion is commonly used to describe the interaction of particles among themselves.

Cohesion is a phenomenon akin to adhesion and autohesion and is used to describe the attraction between the molecules within the bounds of a single body.

The adhesion of dust particles and powders generally constitutes the interaction of microscopic particles with a solid surface due to forces which depend both on the properties of the bodies in contact and on those of the surrounding medium.

4.04.21 Adhesion as a Function of Surrounding Medium

The forces of adhesion are to a great extent determined by the properties of the surrounding medium. Thus, in order to detach 50% of spherical glass particles 5-10 mm in diameter from a steel surface in air, it is necessary to apply a force of the order of 10^{-7} Newtons whereas, in water less than 10^{-11} Newtons suffices (Zimon, 1969). Thus, in a liquid medium the adhesion of particles is much smaller than in a gaseous medium.

In a gaseous medium, microscopic particles adhere to a solid surface not only as a result of molecular forces, but also under the influence of capillary forces in the liquid condensing in the space between contiguous particles, the double electric layer formed in the zone of contact, and also Coulomb interaction and other like causes.

The adhesive forces of microscopic particles in a liquid medium are made up of the molecular attraction of contiguous bodies and the repulsive forces of the thin layer of liquid in the contact zone. Capillary and electrical forces which act in gaseous media hardly appear at all in liquids. In view of this it is practically convenient and theoretically justifiable to distinguish adhesion in gas and liquid media (Zimon, 1969).

4.04.22 Molecular forces

All molecular and atomic forces ultimately find their root in the mutual behavior of the constituent parts of the atoms; it is still convenient to treat the various forms of mutual interactions of atoms as different forces acting independently (Corn, 1966).

Molecular interaction is characterized by Van der Waals forces appearing between the molecules at a distance equal to between one and several hundred molecular diameters. The gap between the contiguous bodies is no greater than a few molecular diameters in either the adhesion of particles (in the absence of layers of liquid between these) or the adhesion of films. Hence, molecular interaction exerts an appreciable influence on the development of adhesive forces (Zimon, 1969).

Dispersion forces, whose existence was first recognized by London (Gregg et al., 1976) derive their name from the connection between their origin and the cause of optical dispersion; they arise from the rapid fluctuations in electron density within a given atom, which induce an electrical moment in a near neighbor and thus lead to attraction between the atoms.

London, making use of quantum-mechanical perturbation theory, worked out an expression for the potential energy $\epsilon_D(r)$ of two isolated atoms separated by a distance r; developed by later workers (Hirschfelder et al., 1954) it reads:

$$\epsilon_D(r) = - A_1 r^{-6} - A_2 r^{-8} - A_3 r^{-10} \qquad (4\text{-}96)$$

and is valid provided the atoms are not too far apart. In this expression A_1, A_2 and A_3 are the dispersion constants associated with instantaneous dipole-dipole, dipole-quadrupole, and quadrupole-quadrupole interactions respectively.

In view of the secondary importance of the last two terms in equation (4-96) they are usually omitted. As a result equation (4-96) simplifies to:

$$\epsilon_D (r) = - A_1 r^{-6} \qquad (4\text{-}97)$$

In addition, there is a force of repulsion (arising from the interpenetration of the electronic cloud of the constituent atoms), which may be represented by the empirical equation:

$$\epsilon_R (r) = B r^{-j} \qquad (4\text{-}98)$$

where B and j are empirical constants, the latter usually being assigned the value j = 12.

The total potential between the two molecules thus becomes:

$$\epsilon_{(r)} = - A_1 r^{-6} + Br^{-12} \qquad (4\text{-}99)$$

often designated as the Lennard Jones 6-12 potential.

Muller (1936) derived an equation for the dispersion constant A_1, as a function of atomic properties, while the empirical constant B cannot be evaluated. Until recently (Ricca et al., 1973) the general practice has been to assess $\epsilon_R(r)$ empirically as 40% of the total potential $\epsilon(r)$.
A characteristic feature of the dispersion (London) forces is their additivity. A molecule induces periodic dipoles in several neighboring molecules. The induced dipole is

attracted to the original dipole. In view of this, the energy of attraction between the two bodies may be regarded as the sum of the energies of attraction between the corresponding pairs of molecules forming the bodies in question.

Strictly speaking (Zimon, 1969), London interaction is valid for two very rarefied systems, i.e., gases. The extension of the additivity of the forces to condensed systems not constituting a simple sum of free molecules has not yet been given a firm theoretical basis.

However, Bradley (1936) experimentally determined the force of interaction between two quartz and borate spheres; the result was close to the calculated value obtained on the principle of additive molecular interaction. Hence, since at present time there are no other methods of estimating the molecular interaction of solid bodies when they are separated by a small gap, the additivity of London interaction is accepted and extended to condensed systems (Zimon, 1969). The London Van der Waals attractive force F between two molecules at distance H apart is given by equation (4-100):

$$F = \frac{d \epsilon_D (r)}{dH} = \lambda_v H^{-7} \qquad (4\text{-}100)$$

Where λ_v is the Van der Waals constant for attraction. Hamaker (Corn, 1966) extended the calculations of dispersive forces to macroscopic bodies. Equation (4-101) was derived to describe the London-Van der Waals attractive force F, in dynes between two ideally smooth spheres of diameters d_1 and d_2 separated by a distance H in vacuo.

$$F = \frac{\pi^2 q_o^2}{12 H^2} \left(\frac{d_1 d_2}{d_1 + d_2} \right) \qquad (4\text{-}101)$$

where:

q_o is the number of atoms per cm^3, and d_1, d_2 and H are in cm.

If d_2 is allowed to approach infinite size, the following expression for the attractive force between a sphere of diameter d_1 at a distance H from a flat plate is obtained:

$$F = \frac{\pi^2 q_o^2 \lambda_v d_1}{12 H^2} \qquad (4\text{-}102)$$

Unfortunately the utilization of equation (4-101) is limited in practice, because in order to apply it to the adhesion of real particles it is necessary to make assumptions about the distance of approach or separation of the surfaces "H", and the effective diameters of surface asperities making contact or approaching contact. At the same time the dispersion constant can just be roughly estimated.

Moreover, because of the dependence of the Van der Waals forces on particle shape, it is extremely difficult to make quantitative calculations for particles of irregular shape.

Under conditions of interest to industrial hygiene and air pollution, the presence of adsorbed gases or condensed moisture on the solid surfaces as well as surface roughness would probably result in London-Van der Waals forces between the solids having little influence on any observed adhesion.

4.04.23 Electrical Forces Depending on the Properties of the Bodies in Contact

When particles come into contact with a substrate, the

electrical charges situated on the surface of the particles attract equal and opposite charges on the substrate. This leads to the appearance of excess charges on the surface (Zimon, 1969).

In order to study the effect of electrical forces on adhesion, it is convenient to consider two types of contact process: those occurring between a semiconductor (dust particles) and a metal (substrate) and those occurring between a semiconductor (dust particles) and another semiconductor. Thus, we may expect that the potential difference arising when particles come into contact with a semiconductor is greater than on coming with contact with a metal for the same charge density. An increase in the potential difference inevitably involves an increase in the adhesive forces. The electrical forces arising on formation of a charge at the instant of contact between the particles and the surface may be measured in two ways (Zimon, 1969). First, from the magnitude of the charges observed on detaching the dust particles from the substrate, and secondly by superimposing potentials on the substrate in order to neutralize the double-layer charge.

As Loeb (Corn, 1966) states in his review of literature on electrification in solid-solid contact, "...assuming that the measurements are conducted under controlled conditions designed to avoid all unnecessary complicating factors, when one regards the electrification on contact of the whole gamut of inorganic, organic insulating and conducting solids known

and used, the various possible interchanges of charged carriers leads to such an extensive range of interactions that it is virtually impossible to derive any basic understanding of the mechanisms at work..."

4.04.24 Electric Forces Arising Under the Influence of the Charge on the Particles

Most particulate clouds are charged to some extent. Even if the cloud is initially uncharged, a charge distribution will result from diffusion to the particles of ions present in the atmosphere.

The determination of adhesive forces of charged particles to an uncharged surface may be reduced to a consideration of the Coulomb interaction between particles situated on both sides of the surface at equal distances from the latter. The charged dust particles induce equal and opposite charges on the surface (Zimon, 1969). Image forces are thus set-up.

The adhesive force resulting from the image interaction between the particle charges and the induced charge may be expressed as follows:

$$F_{im} = k \frac{Q_2}{l^2} \qquad (4\text{-}103)$$

where Q is the charge on the particles, and l is the distance between the centers of the charges.

$$l = 2(r_p + H - \Delta - \xi) \qquad (4\text{-}104)$$

where: r_p is the radius of a particle, H is the gap between the particles and the substrate, Δ is the reduction in particle radius resulting from the deformation at the contact zone, ξ is the displacement of the center of the charge on

the particle under the influence of F_{im}.

If the particle touches the metallic substrate:

$r_p \gg H \quad f = o, \quad \Delta = o$ and

$$F_{im} = k \frac{Q^2}{(2r)_p^2} \tag{4-105}$$

The precise determination of the displacement f is a rather difficult problem. Balabanov (Zimon, 1969) showed that for

$$H = \alpha^2 r_p \tag{4-106}$$

and for $\alpha \ll 1$ (α = coefficient)

$$f = \alpha r_p \sqrt{3} \tag{4-107}$$

Combining equations (4-106), (4-107), (4-103) and (4-104) we obtain:

$$F_{im} = \frac{k Q^2}{12 r_p H} \tag{4-108}$$

The charge on the particles covering a grounded surface is not constant. This charge falls as the time spent by the particle on the surface increases. The reduction in the charge leads to a fall in Coulomb interaction.

Zimon (1969) concludes that in the absence of particle charging, the image forces need only be considered for strongly charged conducting particles at the first instant of their contact with a grounded surface. For particles possessing insulating or semiconducting properties, the time of action of the image forces depends on the state of the medium (humidity, temperature) and the presence of adsorbed layers on the surface of the bodies in contact. If the surface is nonconducting and nongrounded, and if other means

of charge leakage such as ionization of the gas are improbable, then Coulomb forces may produce adhesion of the particles for a considerable time.

4.04.25 Capillary Forces

Condensation of water vapor takes place in the gap between bodies in contact. The meniscus so formed first draws on the particle by way of surface tension and secondly, reduces the pressure of the liquid by virtue of its concave shape.

Zimon (1969) shows that the interaction of two spherical particles associated with capillary forces is given by:

$$F_c = 2\pi \sigma_s r_p \qquad (4\text{-}109)$$

Where σ_s is the surface tension of the film, and r_p is the radius of the particles. If one of the contiguous surfaces is a plane, the height of the intermediate layer will be twice as small. Then,

$$F_c = 4\pi \sigma_s r_p \qquad (4\text{-}110)$$

Equations (4-109) and (4-110) are applicable to perfectly smooth surfaces and under conditions ensuring the total wetting of the surface. For unwetted surfaces the right-hand sides of equations (4-109) and (4-110) must be multiplied by cos θ where θ is the wetting angle.

It is generally accepted that an increase in gas humidity increases the adhesive forces between solid particles immersed in the gas. Discrepancies, however, in the strength of this functionality are frequently encountered. Corn (1961) found that the adhesion of microscopic particles increases

uniformly as the relative humidity of the air rises.

Zimon (1969) found that capillary condensation starts influencing adhesion at relative humidities above 65%. He concludes that under conditions of capillary condensation, the adhesive forces are determined entirely by the capillary forces, which exceed all other adhesive components. Thus the capillary forces producing the adhesion of particles are the larger, the greater the surface tension of the liquid, the vapor of which surrounds the dust-laden surface, the greater the particle dimensions, and the better the wettability of the surface in contact. A liquid interlayer between the particles and the surface eliminates or greatly reduces the effect of electrical forces. The simultaneous action of capillary and electrical forces is practically excluded (Zimon, 1969).

4.04.26 Effect of Contact Area on Adhesion

The adhesion forces depend on the area of contact of the particle with the substrate, since the force of molecular interaction and the electrical component of the adhesive forces are directly proportional to the area of the actual contact zone.

a) Particle Shape

Real particles are seldom perfect spheres, and even rounded particles have irregular surfaces which cause variation in the area of contact, and hence the adhesion of the particles. For particles which do not deviate much from the spherical shape, a "sphericity factor" is used for characterizing the

shape of the particles. This sphericity factor is usually defined as the ratio of the surface area of a sphere whose volume equals that of the particle to the surface area of the particle. Adhesion of close to spherical shape particles increases as the sphericity of the particles decreases. (Zimon, 1969). Thus, the minimum adhesive force occurs for particles of isometric shape, approaching that of a sphere or regular polypon.

The adhesive forces of plane particles (i.e., particles with lengths and widths much greater than their thickness) is greater than that of isometric particles.

In addition to the shapes already mentioned, there are also particles of fibrous or acicular form having one dimension greatly exceeding the others. For these particles the adhesive force is greater than for plane and isometric ones, owing to the greater area of contact of the particles with the surface.

b) Particle Size

Adhesion forces should according to theory increase with particle size, in absence of electrical components. Corn (1961) mentions several experimental determinations which indicate that in fact adhesive forces increase with particle size. However, in most experiments the adhesive force is measured from the force necessary for detaching the particles from the substrates. Centrifugal force or airjets are commonly used to effect particle removal, mechanisms dependent on the cube and square of particle diameter respectively. Therefore larger particles are easier to remove, in general,

than smaller particles retained on the surface by lower adhesion forces.

Zimon (1969) found a great scatter in adhesive forces for microscopic particles. (Those for which the forces of interaction with a plane surface are smaller than their weight) while for macroscopic particlesthis was not observed. Even for particles of uniform size, a great difference between the maximum and minimum force of adhesion was observed. It was hypothesized that this spread in adhesive forces could be caused by electrical effects which arise as the result of contact between the surfaces and/or by reference to the energy inhomogeneity of the surface and the presence of active surface centers. One of the reasons for the spread in adhesive forces may well be the inadequate "purity" of the experimental conditions.

Zimon (1969) concludes that for macroscopic particles the forces of interaction are proportional to the size of the particles and that for microscopic particles experimentation suggests that the adhesive forces are either inversely proportional or independent of particle size.

c) Surface Roughness

We may distinguish three cases characterizing the effect of surface roughness on the adhesion of particles.

As Figure 4-2a illustrates, the first case is possible when the contiguous surfaces are ideally smooth or that there is no surface roughness effect.

Figure 4-2b shows the second case, which is possible if

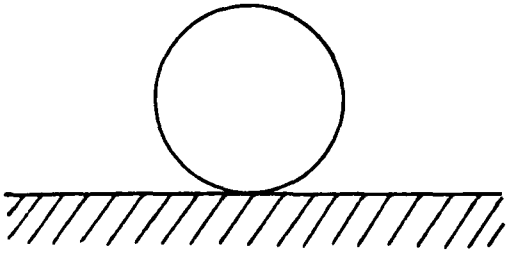

(a)

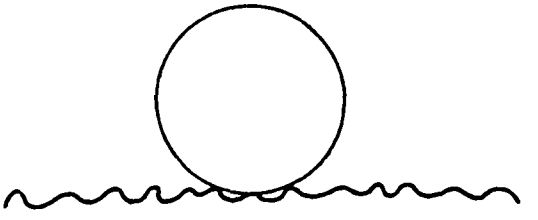

(b)

(c)

Figure 4-2 Effect of Particle Surface Roughness upon Adhesion.

the substrate possesses microscopic asperities, i.e., if the height of the projections is an order smaller than the particle dimensions. Here the true particle surface area is smaller, and the adhesive force accordingly falls. In the third case, shown in Figure 4-2c, an increase in adhesive force takes place as a result of the macroscopic roughness of the surface, when the heights of the projections are comparable to the size of the dust particles. The true contact area rises and this leads to an increase in the adhesive forces.

Zimon (1969) concludes from experimental data that adhesion to a microscopically rough surface is smaller than to smooth or macroscopically rough surfaces. The surface roughness of the dust particles also affects the adhesive forces. Thus, the adhesive force between particles possessing microscopic surface roughness and a plane surface is smaller than that of smooth spherical particles of the same material.

d) State of particle agglomeration

Even when information is not available we can expect that the forces of adhesion between a surface and an agglomerate are different from the forces of adhesion between the surface and individual particles of the same material. An agglomerate will contact the surface differently than an individual particle of the same size.

In terms of the ease of particle removal from the surface one can only note that the apparent density of an agglomerate can differ by an order of magnitude from that of the particle material if the agglomerate is composed of heterogeneous particles.

e) Nature of particle and surface material

Besides the effect on molecular, electrical and capillary forces, the nature of particle and surface material will affect the adhesive forces due to differences in true contact area. After contact is made, the viscoelastic behavior of the solids will influence the deformation of surface peaks and therefore will affect the true area of contact and hence adhesion. The nature of the adhering surfaces also affects adhesion as a result of its effect on the extent of adsorption of vapor films on the surfaces.

4.04.27 Effect on External Medium

Restricting ourselves to gaseous media, factors on which adhesive forces depend include the temperature of the external medium, the presence of certain vapors in the atmosphere and the period of contact between the particle and the surface.

a) Temperature

The temperature of the surrounding medium can affect the adhesivity of particles in several ways:

1) Modification of Surface Properties

An increase in the temperature of the gas medium can in some cases affect adhesivity through modification of surface properties.

A rise in adhesive force with increasing temperature on glass and painted surfaces has been observed (Zimon, 1969). The stronger rise in adhesive force for painted surfaces is explained by the development of surface tackiness, which increases with temperature.

A temperature change can alter the viscoelastic bond between solid surface high spots in contact.

2) Effect on capillary forces

An increase in temperature decreases the surface tension of most liquids, therefore if capillary forces are present an increase in temperature will decrease the adhesive forces.

b) Presence of vapors in the atmosphere

If gases or vapors surrounding the dust-laden surface interact with the latter in the course of adsorption the adhesion of the particles may change. Analogous processes take place in the autohesion of particles.

Zimon (1969) studied the effect of adding ammonia and sulphur dioxide to dry air upon the adhesion of spherical glass particles to glass of the same type. While the presence of sulphur dioxide did not alter the adhesive force, a rise in adhesion in an ammonia atmosphere was observed. It was concluded that by virtue of hydrogen bonding, the ammonia was able to combine with the condensed and adsorbed moisture on the surface and thus influenced the adhesive force.

c) Time of Contact

It has been found (Corn, 1961; Zimon, 1969) that the adhesive forces also increase with the time of contact. However, the result of different authors differ in respect of the period after which adhesion reaches a maximum. Due to contradiction found in the explanation of different researchers, no clear picture of this phenomenon has emerged.

4.04.28 Effect of Surface Contamination

The presence of foreign adsorbed matter such as surface active substances, moisture, or any other substances can affect the adhesive forces drastically.

It is well known that layers of substances adsorbed on a surface may change the molecular interaction. Although adsorbed layers have no great influence on the electrical forces arising as a result of the charge of the double layer, nevertheless, if these layers engender a surface conductivity, we may expect a reduction in Coulomb interaction as the time of contact increases. Moisture on the surface promotes capillary condensation in the gap between the contiguous bodies and enhance adhesion (Zimon, 1969).

The presence of oil contamination on the surface increases the adhesion of particles as a result of the corresponding tackiness. Although published data regarding the mechanism underlying the behavior of a tacky layer in the capture of dust are not available it should be noted that the property of tackiness is used for the trapping of dust particles in self-cleaning oil filters, rough-cleaning automobile antidust filters, settling plates in konimeters, impactors and similar apparatus (Zimon, 1969).

4.04.3 Detachment of Particles By an Air Flow

In the detachment of an adhering dust layer by an air flow, the following processes may occur: the removal of the top particle, i.e., the overcoming of autohesion, the detachment of a layer of dust, i.e, the overcoming of the

adhesive force in the layer, and the detachment of individual particles remaining after the removal of the layer.

The autohesive process of dust-layer detachment is called erosion and it is possible when Fad > Faut. In this case, the dust is raised to a comparatively short distance above the original surface.

When the autohesive forces exceed the adhesive forces, detachment occurs at the boundary between the surface and the dust layer. This process is called denudation. In denudation, detachment of the dust starts at the leading edge of the dust deposit and a dust cloud rapidly fills the whole channel.

4.04.4 Adhesion During Filtration of Dust-Laden Gases

During cleaning of dust-laden gases in porous filters, adhesion appears at two stages of the filtration process:

a) In holding the particles when those strike the filtering element; and

b) In preventing them from being carried away on subsequent passage of the gas.

In filters with intermittent cleaning, adhesion also appears as a force opposing the regeneration of a spent filter.

Adhesivity and autohesivity should therefore be determined before designing a filter in order to optimize the performance of the device.

Autohesion Properties of Some Industrial Dusts

The operating efficiency of many gas-purifying systems depends on the nature and particle size of the dust trapped.

Very often poor operation of dust traps is due to the fact that no proper allowance has been made for the characteristics of the dusts, especially their particle size and their capacity to adhere to each other and to other surfaces, i.e., their autohesion and adhesion. The autohesive and adhesive properties of dusts have not yet been studied and applied sufficiently (Zimon, 1969).

Industrial dusts are separated into four classes:

1) Non-Autohesive (Alumina and slag dust)

2) Weakly Autohesive (coal ash, slate dust, dry dust of the magnesite, blast furnace dust, and apatite dust types

3) Moderately autohesive (ash, peat dust, cement dust, dust from the concentrates of nonferrous metallurgy, soot and also dust of the previous second class after wetting)

4) Strongly Autohesive (wet cement, gypsum, alabaster dust, flour and dust from fibrous materials).

The division of dusts into classes is quite arbitrary and subjective. Thus ashes may give particles and dust layers with different autohesive properties, depending on the properties of the fuel and the conditions of combustion (Zimon, 1969).

4.05 Deep Bed Filtration

Deep bed filtration is characterized by cylindrical granular beds of sand arranged in layers of increasing fineness in the direction of flow. This concept was proposed for the filtration of very dilute suspensions of aerosols at high efficiency and for low velocity operation, providing relatively

low pressure drops and long operating interval between cleaning or renewal.

The first systematic study of deep bed filtration goes back to 1956 when Thomas and Yoder (1956a) studied the penetration of beds of sand and lead shot by monodispersed solid and liquid aerosols. This work established for the first time the existence of a size of maximum penetration (at constant face velocity and for a given filtration system).

After this pioneering work in the field, several researchers have tried to explore deep bed filtration using horizontal beds of granular materials. (Thomas and Yoder, 1956b; Strauss et al., 1960; Jackson, 1974; Taub, 1970; Paretsky et al., 1971; Paretsky, 1972; Yu, 1972; Bohm et al., 1974a, 1974b; Lee, 1975; Bohm et al., 1976; Gutfinger and Tardos, 1977).

All these investigations have been conducted at ambient conditions.

4.05.1 Mechanisms of Filtration of Dilute Aerosols

The primary mechanisms involved in the filtration of aerosols are:

a) Inertial Impaction

b) Brownian diffusion

c) Gravitational settling

d) Direct interception

e) Electrical Deposition

f) Thermophoresis

Since electrical and thermal effects are generally induced externally to the filtration process they are not

considered here.

Two important assumptions are generally made in classical filtration theory:

1) The collecting obstacles are sufficiently far apart so that the fluid flow in the vicinity of an obstacle approaches the flow around an isolated obstacle.

2) The particles adhere on contact and they do not bounce, migrate or become resuspended.

Figure 4-3 shows the four basic mechanisms that we are going to discuss.

a) Inertial Impaction

The mechanism of removal by inertial impaction occurs when the size or velocity of the particle is so large that the particle does not follow the streamline of the fluid but resists the directional change imposed by the collector and strikes it. An increase in velocity and mass of the impinging particle increases the effect of this mechanism. In analyzing deposition by inertial impaction the particles are considered to be point masses in the calculation of the collection efficiency. Their size, however, is accounted for in the evaluation of the fluid's resistance to the particles' motion. The characteristic parameter for this mechanism is:

$$N_I = \frac{\text{Force necessary to stop particle in distance = radius of collector}}{\text{Fluid resistive force to particle}}$$

$$N_I = \frac{4/3\,\pi r_p^3\ \rho_p\ U_o^2\ /\ 2r_c}{6\pi\, r_p \mu\, U_o\ /C_u} = \frac{1/9\ \rho_p\ r_p^2\ U_o\ C_u}{\mu\ r_c} \qquad (4\text{-}111)$$

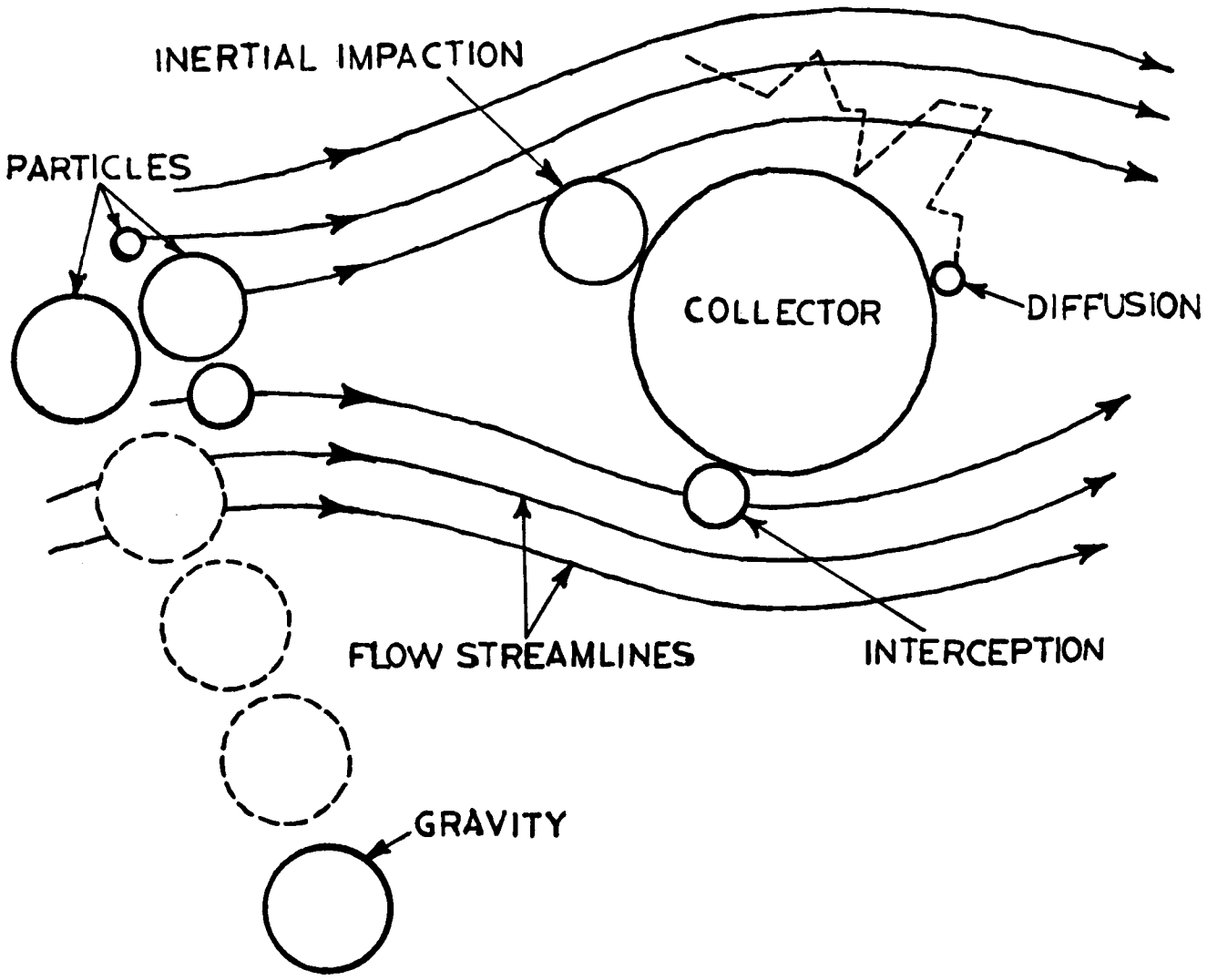

Figure 4-3 Basic Collection Mechanisms

Where: r_p = radius of particle to be collected

ρ_p = real density of particle to be collected

U_o = superficial velocity of gas

r_c = radius of collector

μ = viscosity of gas

C_u = Cunningham correction factor

Equation (4-111) assumes that the particles are spheres and that Stoke's law for fluid resistance is applicable. From equation (4-111) it can be predicted that an increase in velocity of gas or size and density of the dust will increase the efficiency of collection by this mechanism, while an increase of the gas viscosity or size of collector will decrease it.

b) Brownian Diffusion

Deposition by diffusion is caused by the Brownian motion of the aerosol particle which results in a deviation from its normal flow and subsequent deposition and adherence to the filter media. This effect is prevalent at low velocities and for small particles. In analyzing collection by this mechanism it is customary to consider the particles as points with no mass or size. The aerosol particle velocity upon which the Brownian velocity is superimposed is assumed to be equal to the fluid velocity.

The characteristic parameter for this mechanism is:

$$1/Pe = \frac{\text{Diffusional forces}}{\text{Inertial forces}}$$

Or:

$$1/Pe = \frac{\mathcal{D}\, U_o \,/\, (2r_c)^2}{U_o^2 \,/\, 2r_c} = \frac{\mathcal{D}}{2r_c\, U_o} \qquad (4\text{-}112)$$

Where:

Pe = Peclet number

$\mathcal{D}$ = Diffusion coefficient

c) Gravitational Settling

Deposition by gravity can be considered as a removal mechanism superimposed on any of the others. It is most prevalent at lower velocities and for larger and denser particles.

The characteristic parameter is:

$$N_G = \frac{\text{Force of gravity}}{\text{Fluid resistive force}}$$

or:

$$N_G = \frac{4/3\ \pi r_p^3\ \rho_p\ g}{6\pi r_p\ \mu\ U_o\ /C_u} = \frac{2/9\ \rho_p\ r_p^2\ g\ C_u}{\mu\ U_o} = \frac{2g\ r_c^2}{U_o^2} N_I \qquad (4\text{-}113)$$

N_G is also equal to:

$$N_G = \frac{\text{Settling velocity of particle}}{\text{Free Sream Velocity}} \qquad (4\text{-}114)$$

or:

$$N_G = \frac{2\ g\ \rho_p\ r_p^2\ C_u\ /\ 9\mu}{U_o}$$

d) Direct Interception

Deposition by direct interception occurs when the particles moving along streamlines of a fluid approach the collector within a distance equal to the radius of the impinging particle. This mechanism is independent of the fluid velocity in the laminar regime, but increases with the size of the aerosol particle, and decreases as the size of the collector increases. In analyzing filtration by this

mechanism the particles are considered to have size but no mass. The characteristic parameter for this mechanism is:

$$R = \frac{r_p}{r_c} \tag{4-115}$$

It is important to indicate that these mechanisms usually are superimposed upon on another; therefore the analytical prediction of filtration efficiencies demands a high degree of mathematical skill even for idealized simple models. Aerosol filtration theory as applied to single particle targets is fairly well established; and the limiting factor is a thorough knowledge of the fluid dynamics around the target. Obviously, as the targets become more numerous and the voidage becomes smaller, the hydrodynamic problem becomes more complicated. The problem is usually approached by modifying a single-collector filtration model to one which will fit multiple target filtration data, as in a fibrous filter or a gravel bed.

4.05.2 Clean Granular Bed Filtration Models

The literature on filtration of dusts by granular beds is meager, and most of the filtration models which have been developed are semi-empirical in nature and lack generality.

An excellent monograph summarizing the work done on granular bed dust filters was presented by Gutfinger and Tardos (1977).

In the analysis of the filtration process, the granular bed filter is usually assumed to be a homogeneous bed of uniformly sized spherical particles. Filtration of the

particulates is due to their adhesion to the filter elements. It is assumed that a particle which approaches the collector, to a distance comparable to its radius, will collide with it and stick to it.

In practice the process in which a dust particle is attached to the collector is much more involved, and depends on several different short range forces whose nature to this day is a topic of some controversial investigations. Thus, the assumption of the sticking particle usually employed in the classical filtration theory, is at best an oversimplification (Gutfinger and Tardos, 1977). It is further assumed that the dust particle concentration in the gas stream is low enough as not to influence the flow field around the collectors.

Recognizing the limited applicability of the clean bed filtration models which have been developed to the present investigation, we shall refer them as valuable scientific information which will provide insight for modeling the mechanisms involved in cake filtration.

The models of Paretsky et al. (1971), Paretsky (1972), Tardos et al. (1974, 1976), Spielman and Fitzpatrick (1973), Payatakes et al. (1974), Prieve and Ruckenstein (1974), Gutfinger et al. (1975), Nielson and Hill (1976), and Rajagopalan and Tien (1976) constitute the most important developments in this area.

4.06 Dust Cake Filtration

An important characteristic of clean gravel filters is

that the void spaces surrounding individual collectors are larger than most of the dust particles to be captured and sieving or straining is of no importance in the collection of fine particles by clean filters.

Sieving is a significant factor in particle collection when a dust layer accumulates on a gravel filter surface and becomes closely packed. This situation leads to "cake filtration," which differs in several important characteristics from "media filtration." Particle deposition in the pores and on the surface of the filter greatly modifies its performance characteristics. Particles retained on the superficial granules act as secondary particle collectors and are effective for this purpose as they present targets of approximately the same size as the particles to be collected. Next, dust which accumulates as a thick layer, or cake, on the surface of the filter will retain most small particles by straining or by acting as deposition targets.

Filter resistance rises rapidly when particle straining occurs, because of blockage of pore spaces.

Therefore, it is usual practice to clean the filters periodically in such a manner that only the surface dust layer is removed. Dust accumulations in the interstices of the filter are quasi-permanent. They increase the resistance of the filter even after cleaning, and eventually the cleaned filter resistance ceases to increase and reaches equilibrium and the filter is considered to be loaded.

4.06.1 Miyamoto's Work

Miyamoto et al. (1974, 1975) developed the first semi-

empirical model for a gravel bed filter operating under cake filtration conditions. This model was developed based on the data obtained from ammonium chloride fume removal from dry air at room temperature by sieved gravel fractions.

River gravel was water washed, dried, and sieved into 1 to 2, 2 to 4, 4 to 6.35, and 6.35 to 8 mm screen fractions. Ammonium chloride fume was used as the particulate matter because it is easy to generate reproducibly and because its reported diameter, 0.1 to 3 μm, is suited for gravel or fiber filtrations. The particle density of ammonium chloride is 1.53 g/cm^3. Dry air (relative humidity $\leq$ 5%) was used as a carrier with the superficial velocities ranging from 1.5 to 4.0 cm/sec and with ammonium chloride concentrations between 1.5 to 2.0 g/m^3. The temperature of the air was $23^{\circ} \pm 1^{\circ}$ C.

Filtration was carried out in a horizontal bed of gravel contained in the sample holder (5 cm ID). A fine glass fiber filter paper (fiber diameter less than 1μm) protected by two sheets of regular filter paper was attached to the end of the sample holder. The collection efficiency of this filter paper is more than 99% for similar particulates.

The "downshot" collection efficiency was determined from measurements of the concentration of ammonium cloride fume with and without the gravel by the weight gain on the sampling filter papers.

The gravels were packed into the filtration column with a vibrator to obtain a desired porosity, ϵ=0.4 for all sizes of gravel in this experiment.

Filtration was carried out at constant velocity and concentration measurements were taken every 5 or 10 minutes. It was reported (Miyamoto et al., 1974) that the flow system and procedures used were generally adequate and the reproducibility of the collection efficiency in duplicate runs was mostly within $\pm$ 2%.

a) Initial Collection Efficiency of a Gravel Layer

The formulation of the initial collection efficiency as a function of the size of the gravel, the thickness of the gravel layer, and the airflow velocity is based on Friedlander's work (Friedlander, 1957). Friedlander analyzed rates of mass and heat transfer from flowing fluids to single spheres under conditions where the Stoke's stream function is assumed to apply (Particle Reynolds number $<$ 5) and found a relationship between the Nusselt number and the Peclet number. For Pe $\geq 10^3$ the relation was:

$$N_u = a\ Pe^{1/3} \qquad (4\text{-}116)$$

Where a is a constant determined theoretically for a perfect sphere in the steady flow without interference from force fields, and ranges from 0.89 to 0.97 depending on the analytical methods used.

$Nu = \frac{D_p k}{\mathcal{D}}$ where k is a mass transfer coefficient.

Since the Peclet number is a measure of the ratio of transport by convective forces to transport by particulate diffusion, a large Pe corresponds to convection as the predominant mode of transfer. Miyamoto et al. were interested in high velocity

filtration where Pe is generally large, but Re does not exceed approximately 5.

Friedlander (1957) also showed that the initial collection efficiency of a single sphere E_o', i.e., the fraction of the air volume from which a sphere removes all the particulates is:

$$E_o' = \frac{4\ Nu}{Pe} \qquad (4\text{-}117)$$

Miyamoto et al. applied equation (4-117) to a gravel filter of thickness L, of unit cross-sectional area normal to flow direction and uniform spheres of diameter D_p and under steady-state flow conditions obtained:

$$\ln\ (1 - Eo) = -\ 6\ \frac{(1-\epsilon)L}{D_p}\ \frac{Nu}{Pe} \qquad (4\text{-}118)$$

Equation (4-116) was modified for the conditions in the gravel layer and upon substitution in (4-118) the following equation was derived:

$$\ln\ (1\text{-}Eo) = -\ (\alpha'\ \lambda_t^{8/3}\ Da^{-2/3})\ \ (1-\epsilon)\ \epsilon^{4/3}\ D_p^{-5/3} V_s^{-2/3}$$

Where:

$$\alpha' = 6a\ (\phi\ RT/3\ N_o \mu)^{-2/3} \qquad (4\text{-}119)$$

Where: Da is the aerosol particle diameter

λ_t is the tuortuosity factor

ϕ is the relative force field

V_s is the superficial velocity of gas

N_o is the Avogadro's number

Since ϕ is unknown and the several assumptions may be

unrealistic, α' should be determined empirically. For simpler applications, $-\alpha' \lambda_t^{8/3} Da^{-2/3}$ can be treated as an empirical constant α'' because λ_t and Da are difficult to determine. Equation (4-119) does not apply to filtration carried out by direct screening of particulate matter by the micropores. Miyamoto et al. verified equation (4-119) experimentally by obtaining efficiency data at different filtration velocities, gravel particle sizes and gravel layer lengths, for constant inlet fume loading rates and initial bed porosities.

In order to obtain the initial collection efficiencies Miyamoto et al. measured the cumulative collection efficiencies at different fume areal densities (grs of fume collected per unit area of gravel bed) and extrapolated the curves to zero areal density. As Figure 4-4 illustrates Eo was obtained from the intercept of the extrapolated curves with the ordinate. Figure 4-4 also illustrates the definite trend of increasing efficiency with areal density typical of cake filtration. (The cumulative efficiency at zero areal density equals the instantaneous efficiency used in equation (4-119) The experimental data obtained from ammonium chloride fume removal, generally supported equation (4-119) except that the effect of the mean gravel size was represented by the -1.43 power of the average diameter. Miyamoto et al. indicated that this discrepancy may be due to the non-uniform size and irregular shape of the river gravels used in the experiments. The value of α'' depends primarily upon the original properties of gravel and particulates, but is also

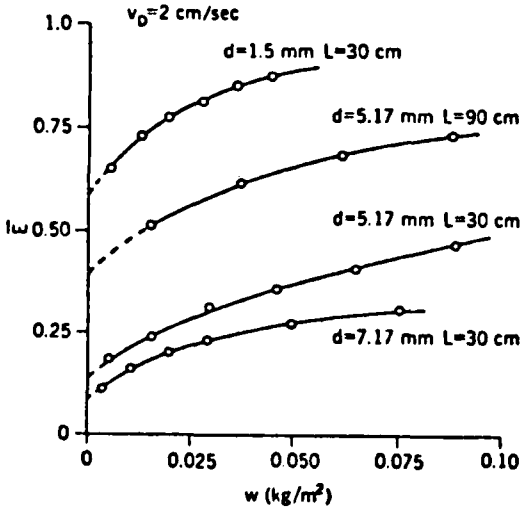

Figure 4-4 Effect of Particulate Load W on the Cumulative Collection Efficiency $\bar{E}$.

influenced by several other external properties and must be determined separately for different particulates and gravels.

b) Cake Filtration: Efficiency and Pressure Drop

Miyamoto et al. (1975) studied the effect of cake areal density on collection efficiency and pressure drop over a range of gravel sizes, layer thicknesses and air velocities in removing ammonium chloride fume from a dry air stream. In these experiments the measured collection efficiency was necessarily the cumulative value $\bar{E}$:

$$\bar{E} = \frac{Min - Mout}{Min} = \frac{Mcollected}{Min} = \frac{W}{Win} \qquad (4\text{-}120)$$

Where:

$\bar{E}$ = cumulative overall collection efficiency (mass fraction)

Min = mass of particulates which was fed to the filter in time t

Mout= mass of particulates which penetrated the filter in time t

W = areal density of particulates deposited on the filter surface in time t

Win = mass of particulates which was fed to the filter in time t per unit surface area of bed

(For constant filtration velocity and inlet dust loading rate, Win is directly proportional to time)

The instantaneous collection efficiency (mass fraction) could be expressed as:

$$E = \frac{dW}{dWin} = \frac{1}{(1+ dWout/dW)} \qquad (4\text{-}121)$$

In order to convert $\bar{E}$ to E analytically, the relationship between $\bar{E}$ and W must be known. Miyamoto et al. found the following equation to be suitable at $\bar{E} < 1$:

$$\ln \frac{(1-Eo)}{(1-\bar{E})} = \beta W^{\gamma} \qquad (4\text{-}122)$$

Where β and γ are empirical constants, which can be determined graphically by plotting the measured quantities $\ln\left[\frac{(1-Eo)}{1-\bar{E}}\right]$ vs W on log-log scales.

Combining equations (4-120) and (4-122) the following is obtained:

$$Wout = \frac{W\ (1-Eo)\ \exp\ (-\beta W^{\gamma})}{1\ -\ (1-Eo)\ \exp\ (-\beta W^{\gamma})} \qquad (4\text{-}123)$$

Differentiating equation (4-123) with respect to W, then substituting into (4-121) gives:

$$E = \bar{E} \Big/ \left\{\bar{E} + (1-\bar{E})\left[1 - \frac{\gamma}{\bar{E}} \ln \frac{(1-Eo)}{(1-\bar{E})}\right]\right\} \qquad (4\text{-}124)$$

Figure 4-5a shows how the collection efficiency increased with areal density. The collected particulates act as a filter and contribute to this increase. The smaller the gravel size the higher the collection efficiency and the sharper the increase of E with W.

As Figure 4-5b shows, thicker gravel layers had higher initial collection efficiencies but little influence on E at higher W, because the collection is primarily due to the collected particulates rather than the filter media itself at higher W. As shown in Figure 4-5c, higher flow velocities markedly decreased the rate of increase in E with W, probably

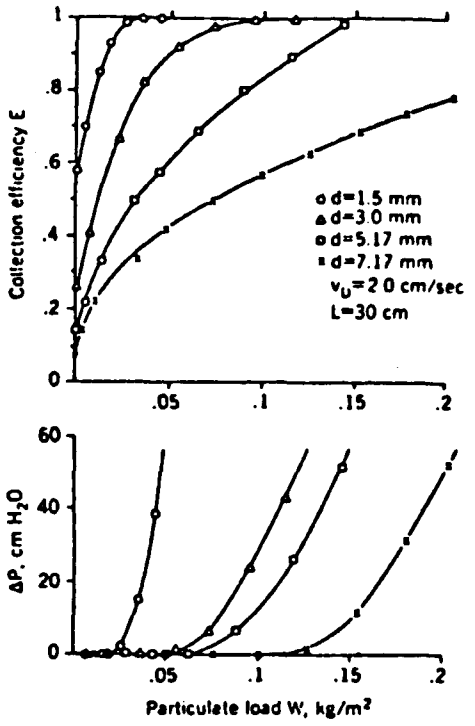

Figure 4-5a Effect of Mean Gravel Size d and Particulate Load W on Collection Efficiency E and Pressure Drop ΔP. Darcy Flow Velocity V_D=2 cm/sec and Gravel Thickness L=30 cm.

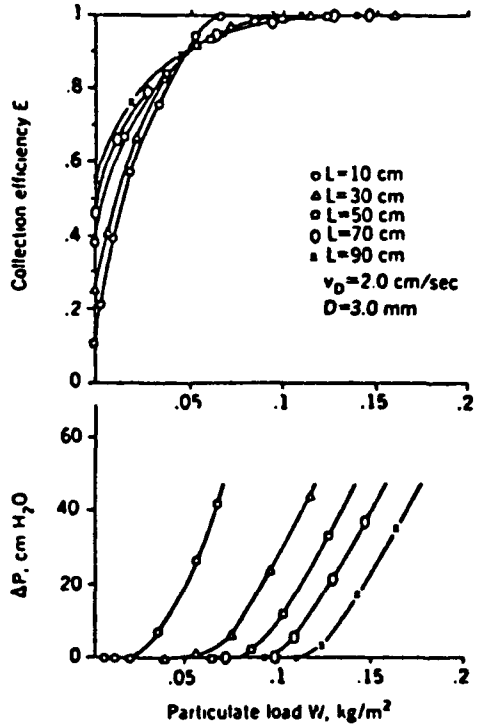

Figure 4-5b Effect of Gravel Layer Thickness L and Particulate Load W on Collection Efficiency E and Pressure Drop ΔP. Mean Gravel Diameter d=3.0 mm and Darcy flow Velocity V_D=2 cm/sec

Figure 4-5 Effect of Gravel Size, Bed Thickness, Velocity and Areal Density upon Collection Efficiency and Pressure Drop. (Miyamoto et al., 1975)

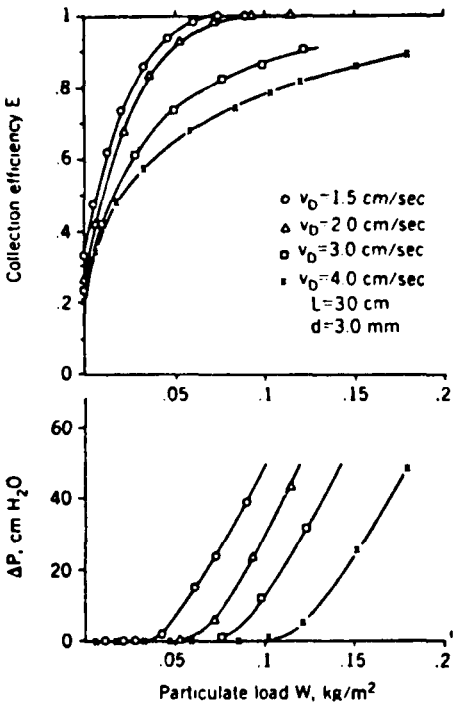

Figure 4-5c Effect of Darcy Air Flow Velocity V_D and Particulate Load W Upon Collection Efficiency E and Pressure Drop ΔP. Mean Gravel Diameter d=3.0 mm and Layer thickness L=30 cm.

because the "surface dust cake" formed on and in the surface of the layer is less stable at higher velocities.

Figure 4-5c also shows the pressure drop increase as a function of areal density. Miyamoto et al. observed that the pressure drop increased very little until the particulate areal density reached a threshold load at which the pressure drop began to increase rapidly. This rapid increase of ΔP fluctuated irregularly, probably due to the irregular flaking off the "surface dust cake." The degree of fluctuation increased with the particulate load, gravel size and flow velocity, and it reached as much of 20% of the peak values. Figure 4-5c shows only the smoothed curves connecting the peak values.

4.06.2 Leith's Work

Leith (1975), recognizing the ability of fabric filters for achieving high particle collection efficiency over the entire spectrum of particle sizes, and their inability to compete, in some air pollution control areas, with more compact, less expensive collectors, undertook research leading to the optimization of commercial fabric filters for high-velocity filtration. At the onset of his investigation there was little knowledge of a fabric filter's collection efficiency as a function of its primary operational variables, and even less information was available concerning the mechanisms by which particles collect in or pass through a fabric filter.

The inadequacies of classical filtration theory in describing the performance of fabric filter was soon discovered, and it was necessary to understand how and why fabric filters

perform as they do before an increase in filtration velocity can be expected to succeed.

A) Trends of Fly Ash Penetration in Bag Filters

Leith (1975) tested a pulse-jet-cleaned filter with two polyester felt bags at ambient conditions.

Electrostatically precipitated fine coal fly ash (0.3-5.1 μm in diameter) was redispersed in ambient air and fed to a commercial, two bag filter, which had been previously conditioned by operating with about 1 g/m^3 dust concentration for several hundred hours, before experimental measurements were made.

The filters were two polyester, needled-felt cylinders, each 11.4 cm in diameter and 240 cm long, made from 16 μm diameter fibers. Each filter had an effective area of 1.72 m^2. Face velocities from 5 to 15 cm/s were explored, while working at a constant inlet dust loading of about 0.6 g/m^3. The filters were always cleaned after a sixteen-minute interval, independently of the operating conditions. At the highest velocity tested, 15 cm/s, pressure drops exceeded 100 cm of water.

Efficiency was measured against face velocity, deposit thickness (cake pressure drop) and particle diameter by collecting isokinetic samples on membrane filters upstream and downstream of the fabric collector. The size distributions of upstream and downstream dust were determined after observing slides, prepared from the membrane filters, under an optical microscope.

The following trends in penetration were found:

1) Penetration decreases with increasing time since cleaning.

2) Penetration increases with increasing face velocity.

3) Penetration increases with increasing logarithm of particle diameter.

1) Penetration as a function of time since cleaning

As Figure 4-6 illustrates, an initial sharp decrease in penetration with increasing filtration time (cake thickness or pressure drop) was obtained. As deposit thickness increased further, penetration leveled off. This phenomenon was expected from field experience and laboratory data (Leith, 1975).

2) Penetration as a function of face velocity

Figures 4-7 and 4-8 illustrate the probable explanation for the lack of commercial high-velocity bag filters. As shown in Figure 4-7, an increase in filtration velocity causes a faster increase in cake pressure drops, implying that the savings in initial cost originating from a reduction in filter size (higher velocities) is always followed by an increase in operating costs (higher pressure drops), if relatively high efficiency is demanded (thick cakes).

Figure 4-8 illustrates what could be the factor which determines that the economic optimum lies in the region of low-velocity filtration: "No matter how thick the cake is, an increase in velocity causes a sharp increase in penetration, these two factors, combined with problems originated with bag stability,

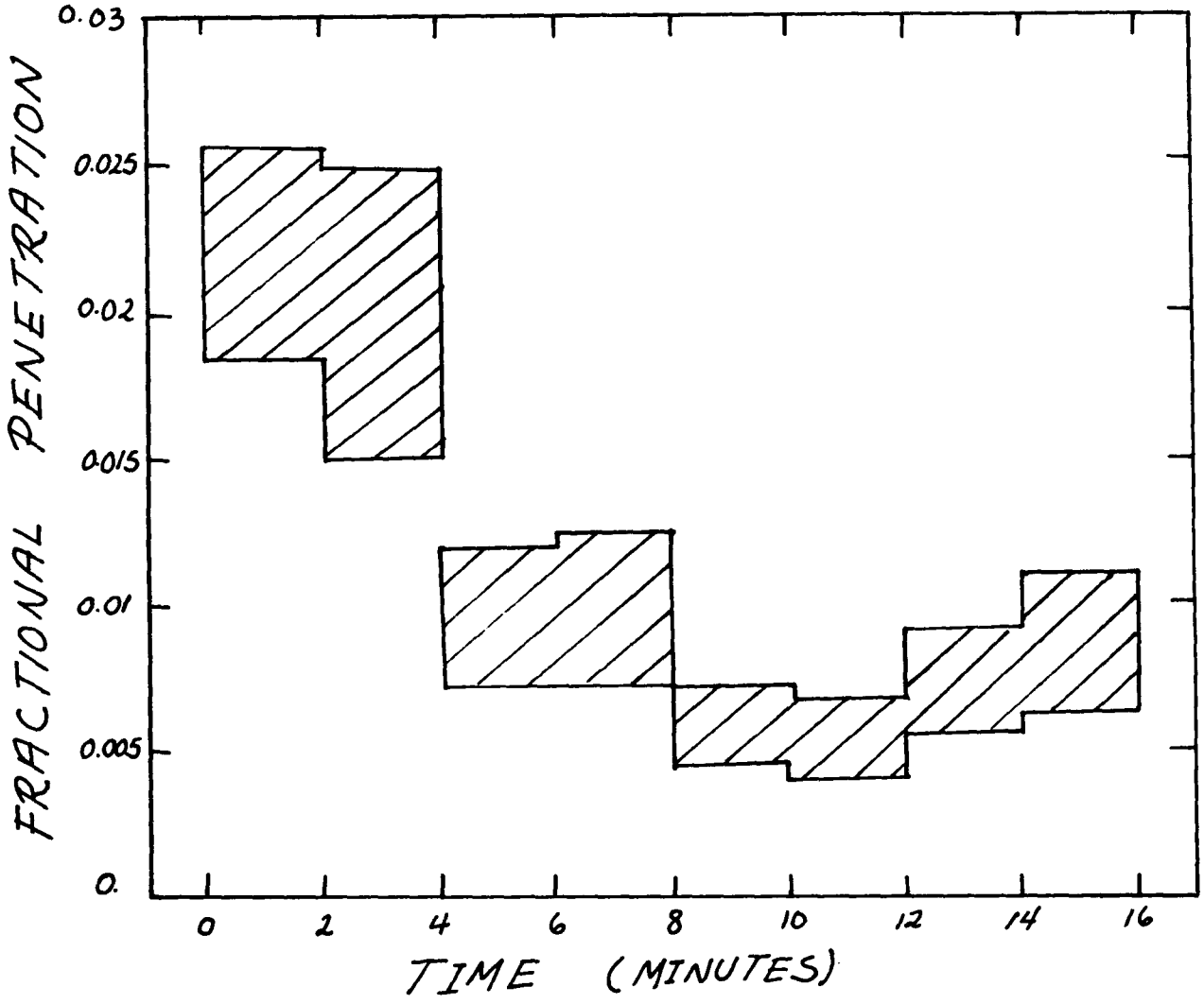

Figure 4-6 Fractional Penetration versus Time

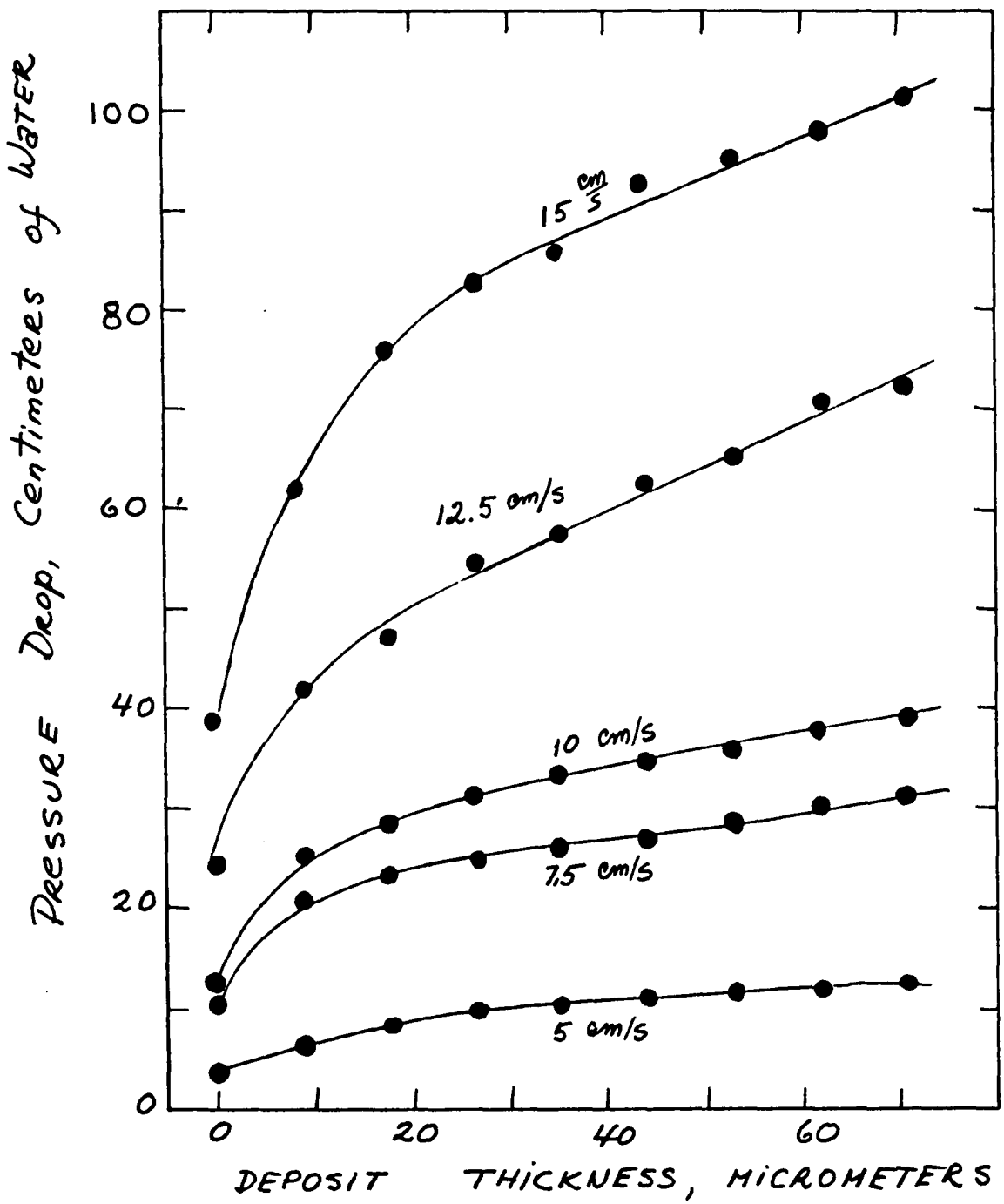

Figure 4-7 Pressure Drop versus Deposit Thickness, Velocity as Parameter.

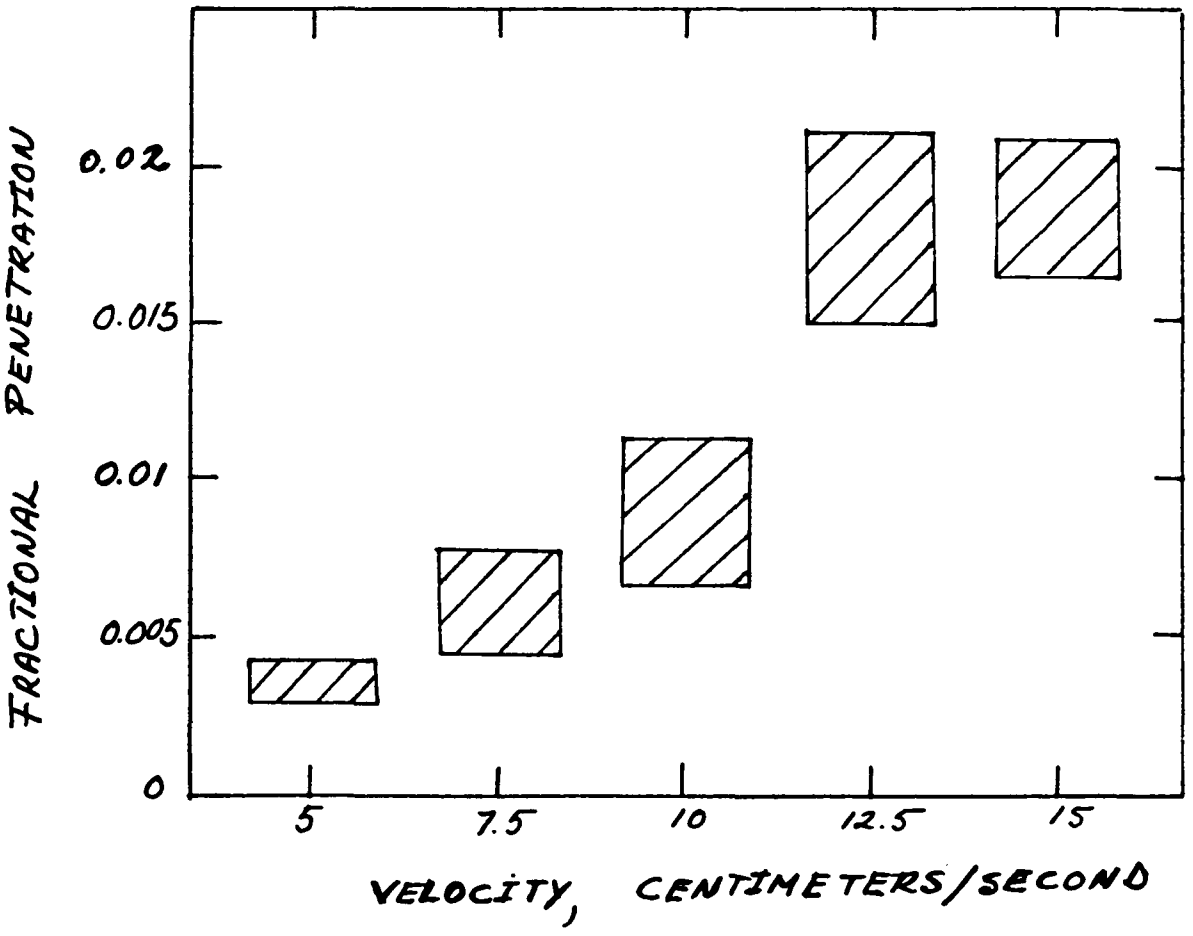

Figure 4-8 Fractional Penetration versus Face Velocity.

have probably caused the absence of commercial high-velocity bag filters.

3) Penetration as a function of particle diameter

As Figure 4-9 illustrates, penetration increased only slightly with particle diameter.

As a result of this trend, Leith concluded that "overall penetration," i.e., the weighted average for all particle sizes, is a good indicator of fabric filter collection capabilities. The fact that Leith used such a fine fly ash and with such a small size range, limits the above conclusion to his experimental conditions, and the conclusion may not reflect typical commercial operation (unless an efficient collector preceeds the bag-house).

Leith concluded that the penetration trends shown in Figures 4-6, 4-7, 4-8 and 4-9, cannot be explained by classical filtration theory and that therefore a search for the penetration mechanisms present in cake-filtration in bag filters was needed.

B) Penetration Mechanism Experiments

Leith concluded that the only explanation to the penetration trends found, must be dust reentrainment (previously collected particles which penetrate after being reentrained in the gas flow).

As a result of his investigation, Leith defined three penetration mechanisms which operate simultaneously during cake filtration in bag filters:

a) Straight Through Penetration

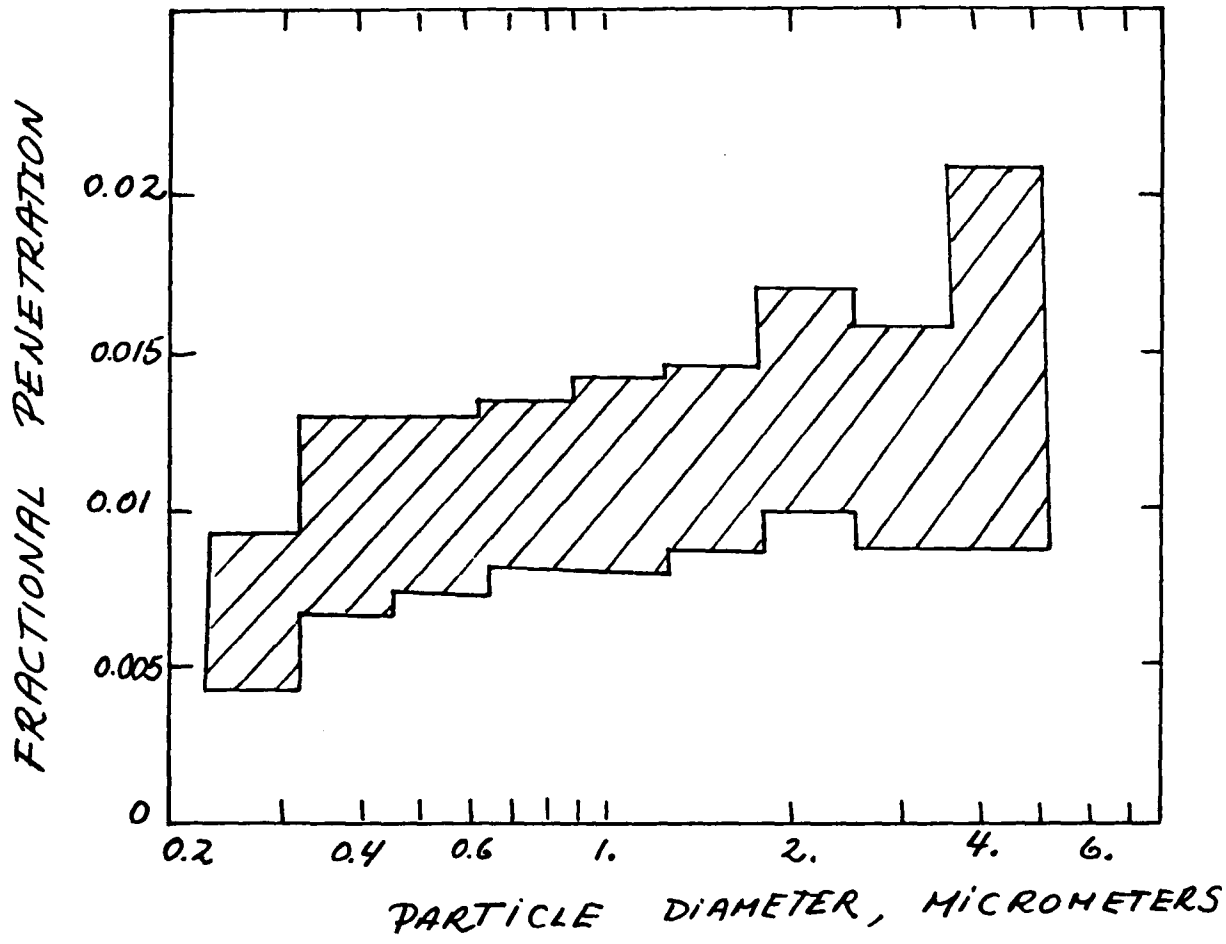

Figure 4-9 Fractional Penetration versus Particle Diameter

b) Seepage or Bleeding Penetration

c) Pinhole Plug Penetration

a) Straight Through Penetration

In straight through penetration particles pass through the filter without stopping. The size distribution of particles passing through the filter by this mechanism should reflect a dependence on the forces causing the particles to be collected there: inertial impaction, direct interception, diffusion, gravity, electrostatic forces, etc. This is a very important mechanism for clean bed filtration and an important one immediately after cleaning the filter.

b) Seepage or Bleeding Penetration

Once a particle lands on or between collectors, it need not necessarily remain at its point of initial impact. As the dust deposit builds up, the pressure drop can increase to several times its initial value, allowing eventually some previously collected particles to work through.

Penetration of dust of this sort is called "seepage." Accordingly, the size distribution of the particles which pass through by seepage should be the same as the size distribution of the deposited dust, which is very close to the size distribution of the dust fed to the filter.

Williams et al. in 1940 mentioned this mechanism as an important one in cloth filtration. They interpreted it as follows: "When the resistance becomes too great, the dust deposit which forms the actual filter breaks and allows dust particles to pass through."

Dennis (1974) mentions this mechanism of dust penetration, indicating: "Dust that migrates through the filter by successive deposition and reentrainment under the combined effects of aerodynamic and mechanical (vibrational) forces." He also indicates that it may be more pronounced in the case of spherical or smooth surfaced regular particles and in the absence of electrostatic or other forces enhancing adhesion.

c) Pinhole Plug Penetration

Small diameter pinholes have been found at the surface of a dust deposit on fabrics and gravel bed filters (Leith, 1976; Lee, 1975). In pinhole plug penetration, a plug of deposited particles may dislodge from the dust deposit and pass through the filter all at once.

As in the seepage penetration the size distribution of the dust which pass through the pinhole plugs should be the same as the size distribution of the deposited dust, which is very close to the size distribution of the dust fed to the filter.

The pinhole plug penetration is assumed to be caused by the effect of velocity and/or pressure drop on relatively weak regions in the filter cake.

These penetration mechanisms illustrated in Figure 4-10 are probably present in any collection device which operates under cake filtration conditions (i.e., the panel bed filter).

To determine the importance of these three emission mechanisms, three types of chemically tagged fly ash were aerolized and fed to the filter in the sequence given in

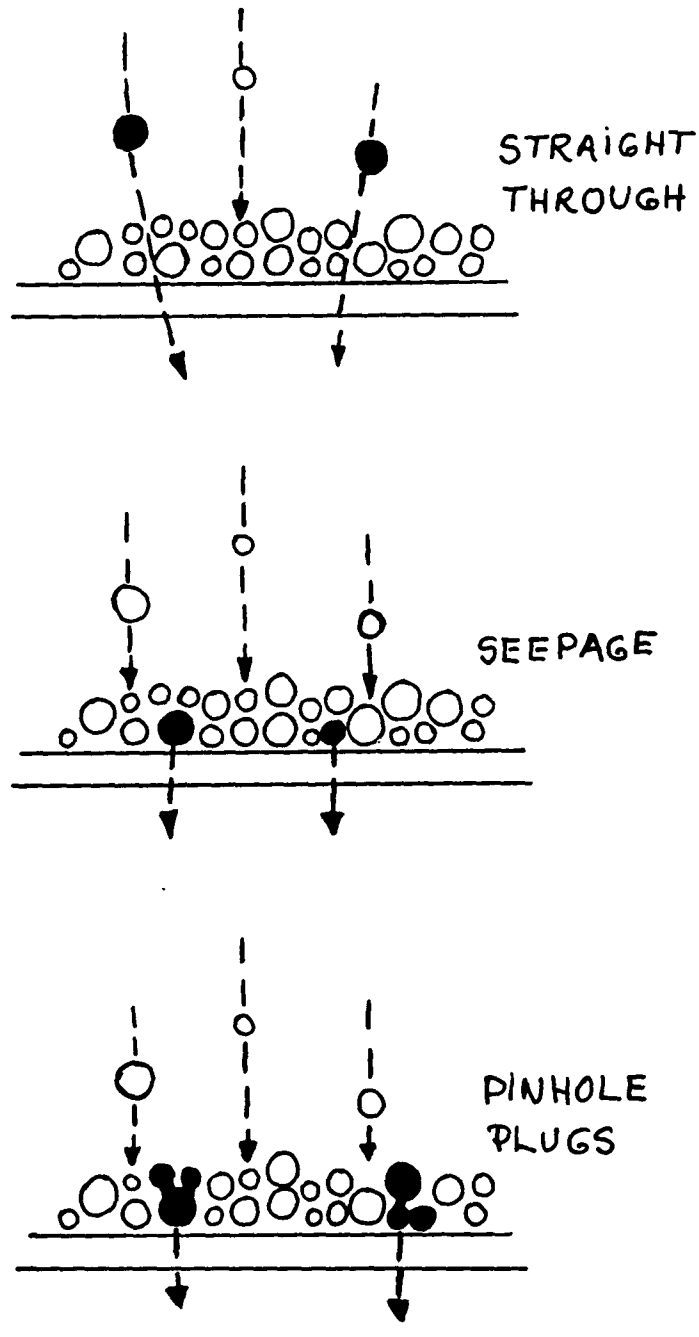

Figure 4-10 Leith's Penetration Mechanisms.

Table 4-2. The proportion of each tag in the total fly ash collected downstream of the filter depended upon which of the emission mechanisms was operating at the time. "Straight-through" dust should carry the same tag as the dust fed to the filter at the time. "Seepage" dust should be tagged the same as the dust initially fed. "Pinhole-plug dust" should be tagged in the same tag proportion as the dust fed up until the time the plug breaks away and slips through.

Dust samples taken during eight two-minute intervals were analyzed to find the amount of each of the three tracer metals present. The total dust emission was found by adding the amounts of each tagged dust present, so that the proportion of this total represented by each tag could be found. These experiments were carried out at different face velocities and at the same operating conditions as those at which the penetration trends were found.

It was observed that the time interaction was highly significant. As time increases and the dust deposit thickens the mechanisms change by which dust is emitted. The velocity mechanism interaction, however, was not significant; at any fixed time, the fraction of dust emitted by each mechanism is fairly constant from velocity to velocity.

Figure 4-11 gives the results expressed as the fraction of the total fly ash emitted which is accountable to each of the three emission mechanisms. Immediately after cleaning, most dust comes from the filter by the straight-through mechanism. Pinhole plugs rise quickly, and fall. Seepage

Table 4-2

Sequence in which Tagged Dusts were Fed

Time	Tagged Fly Ash Injected
0-1 minutes	magnesium
1-1.5 minutes	manganese
1.5-4 minutes	lithium
4-8 minutes	manganese
8-14 minutes	lithium
14-16 minutes	manganese

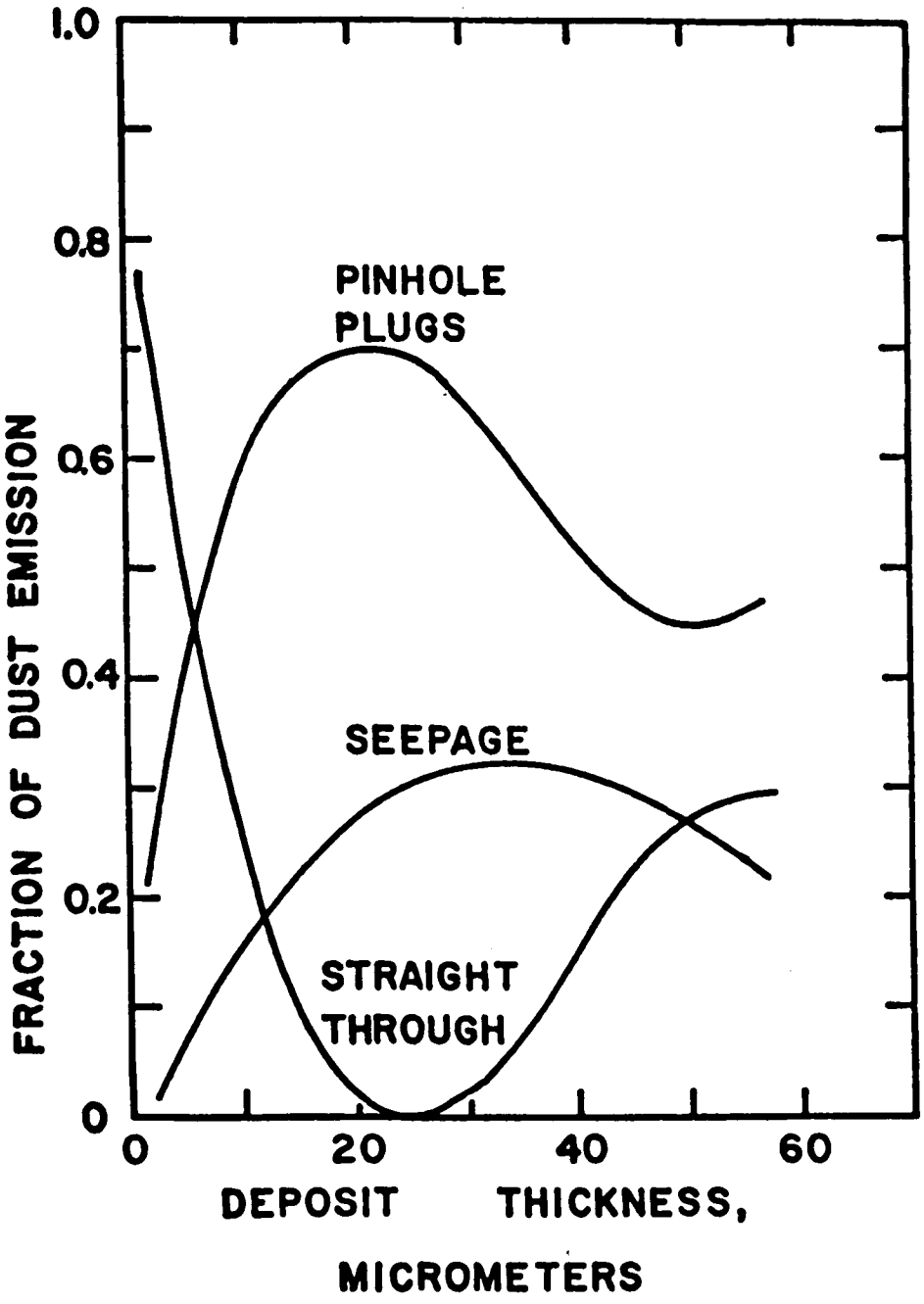

Figure 4-11 Results by Leith et al. (1976) showing fraction of total fly ash emitted from rear of fabric filter, working at high velocity, which is accountable to each of three emission mechanisms, plotted versus "theoretical" thickness of fly ash deposit.

rises and falls a bit more slowly. The straight-through mechanism declines to zero as the filter cake becomes coherent, but rises again as pinhole plugs offer avenues bypassing the cake.

The penetration data trends were then examined in light of the emission mechanism data. The sharp decrease in penetration immediately after cleaning, shown in Figure 4-7, is contemporary with a decline in the importance of the straight through emission mechanism. Thereafter, seepage and pinhole plug mechanisms gain in importance, causing penetration to level off. The seepage and pinhole plug mechanisms should pass deposited particles of all sizes with equal facility. Because these mechanisms dominate emissions from shortly after cleaning through to the end of the filtration cycle, penetration for particles of all sizes should be roughly equal as is shown in Figure 4-9. Emissions due to seepage and pinhole plugs may increase with increasing velocity, thereby explaining the increase in penetration with velocity shown in Figure 4-8.

c) Leith's Model for Cake Filtration in Bag Filters

Leith developed a semi-empirical model for cake filtration in bag filters, isolating the different penetration mechanisms as a function of the operating variables. Leith used a "theoretical cake thickness" (Williams et al., 1940; First et al., 1963) as a basis for expressing his filtration results. Leith simplified the concept by assuming that the bulk density of the cake on the fabrics were independent of the operating

conditions and equal to the bulk density of the dust as measured in the laboratory before the filtration experiments.

Combining equations (4-92) and (4-93) the theoretical cake thickness is obtained:

$$X = L_c = \frac{C_{MV_i}\ t\ V}{\rho_b} \qquad (4\text{-}125)$$

Where: ρ_b = bulk density of cake (1.2 g/cm^3)

Leith from his penetration mechanism experiments concluded that in a fabric filter, when the primary means of emission is the delayed release of collected particles rather than the passage of particles straight through the filter, outlet mass flux, the mass emerging per unit filter area per unit time, is a better indicator of fabric filter behavior than is penetration with its implied proportionality to inlet concentration.

Outlet mass flux M_{F_e} is related to outlet dust concentration C_{MV_e} and face velocity V by equation (4-126):

$$M_{F_e} = C_{MV_e}\ V \qquad (4\text{-}126)$$

The outlet mass flux attributable to any one of the straight-through, seepage, or pinhole plug mechanisms, $M_{F_{ei}}$, can be calculated multiplying total outlet mass flux by the proportion, f_i, of total emissions attributable to that mechanism.

$$M_{F_{ei}} = C_{MV_e}\ V\ f_i \qquad (4\text{-}127)$$

Mass flux due to the straight through penetration mechanism, $M_{F_{est}}$, should decrease as the dust layer builds up, for as

this layer increases, a particle passing straight through would have to penetrate by a longer and more tortuous path.

Leith (1975) derived the following equation for the outlet mass flux attributable to the straight-through mechanism:

$$M_{F_{est}} = M_{F_i} \exp\left(-(k_1 X)^{k_2}\right) \qquad (4\text{-}128)$$

Where:

M_{F_i} = mass flux of dust entering the filter

k_1, k_2 = constants which may depend upon dust, collector characteristics, and operational variables.

The mass flux due to the seepage mechanism should depend upon the drag force exerted by the gas flowing past deposited particles. This force should increase with increasing velocity, but not with deposit thickness. At constant velocity, seepage mass flux should be constant at all thicknesses:

$$M_{F_{es}} = k_3 \qquad (4\text{-}129)$$

Mass flux from pinhole plug penetration will depend upon both the thickness of the dust deposit and the probability of plug break off. Plug thickness should be proportional to plug mass, and therefore also to outlet mass flux accountable to this mechanism.

$$M_{Fep} \propto X \qquad (4\text{-}130)$$

However, as the deposit becomes thicker, the additional interparticle bonds which form should make the generation of a pinhole plug increasingly difficult, although increasing pressure drop could act against this trend. This relationship

might be described by equation (4-131):

$$M_{Fep} \propto \exp\ (-k_4 X) \qquad (4\text{-}131)$$

The combination of equations (4-130) and (4-131) gives an expression for the mass flux due to pinhole plug penetration where k_5 is a proportionality constant.

$$M_{Fep} = k_5 X \exp\ (-k_4 X) \qquad (4\text{-}132)$$

The total mass flux from the fabric filter, M_{Fe}, can be found by adding the contributions of the straight through, seepage, and pinhole emission fluxes.

$$M_{Fe} = M_{Fest} + M_{Fes} + M_{Fep} =$$

$$M_{F_i} \exp\ (-(k_1 X)^{k_2}) + k_3 + k_5 X \exp\ (-k_4 X) \qquad (4\text{-}133)$$

Leith, after correlating his experimental data and theoretical equations and having found good correlation, concluded that the postulated forms of the mass flux equations for each mechanism may be suitable, and the assumptions made in establishing their form may be realistic.

In industrial operation one may be interested in the total mass of dust released to the atmosphere over many filtration cycles, as well as the proportion of small particles in that release. By finding the fraction of total mass released which is accountable to each emission mechanism, the relative importance of each mechanism can be evaluated.

The fraction, y, of total mass released due to any single mechanism can be found from equation (4-134) for a filtration cycle with cleaning at dust deposit thickness X.

$$y = \frac{\int_0^X M_{Fe_i}\, dX}{\int_0^X M_{Fe}\, dX} \qquad (4\text{-}134)$$

The mass flux due to any one mechanism, M_{Fei}, and the total mass flux, M_{Fe}, depend upon deposit thickness, X, and velocity as described by equations (4-128) through (4-133). Leith (1975) numerically integrated equation (4-134) to find the fraction of total mass emitted by each mechanism as a function of deposit thickness at cleaning. Figures 4-12 and 4-13 show the results of the integrations for velocities of 5 and 15 cm/s.

At low velocity, as shown by Figure 4-12, the proportion of all dust emitted which is accountable to the straight-through mechanism is large compared to the proportions accountable to the other mechanisms, no matter when cleaning takes place. However, at higher velocity, as shown by Figure 4-13, the proportion of all dust emitted which is accountable to the pinhole plug mechanism is largest, if cleaning does not occur until the deposit thickness reaches at least 15 μm, as would normally be the case. The overall importance of the straight-through mechanism decreases with increasing velocity, whereas that of pinhole plug generation increases.

4.06.3 Dust Filter Cakes on Horizontal Sand Surfaces

Horizontal beds of granules have been operated under conditions which promote the establishment of a filter cake of the dust being filtered on the surface of the fixed granular beds. Experiments have been conducted to study the stability and filtration performance of these surface filter cakes.

4.06.31 Paretsky's Work

Based on Squires' idea (Squires, 1967) that a filter

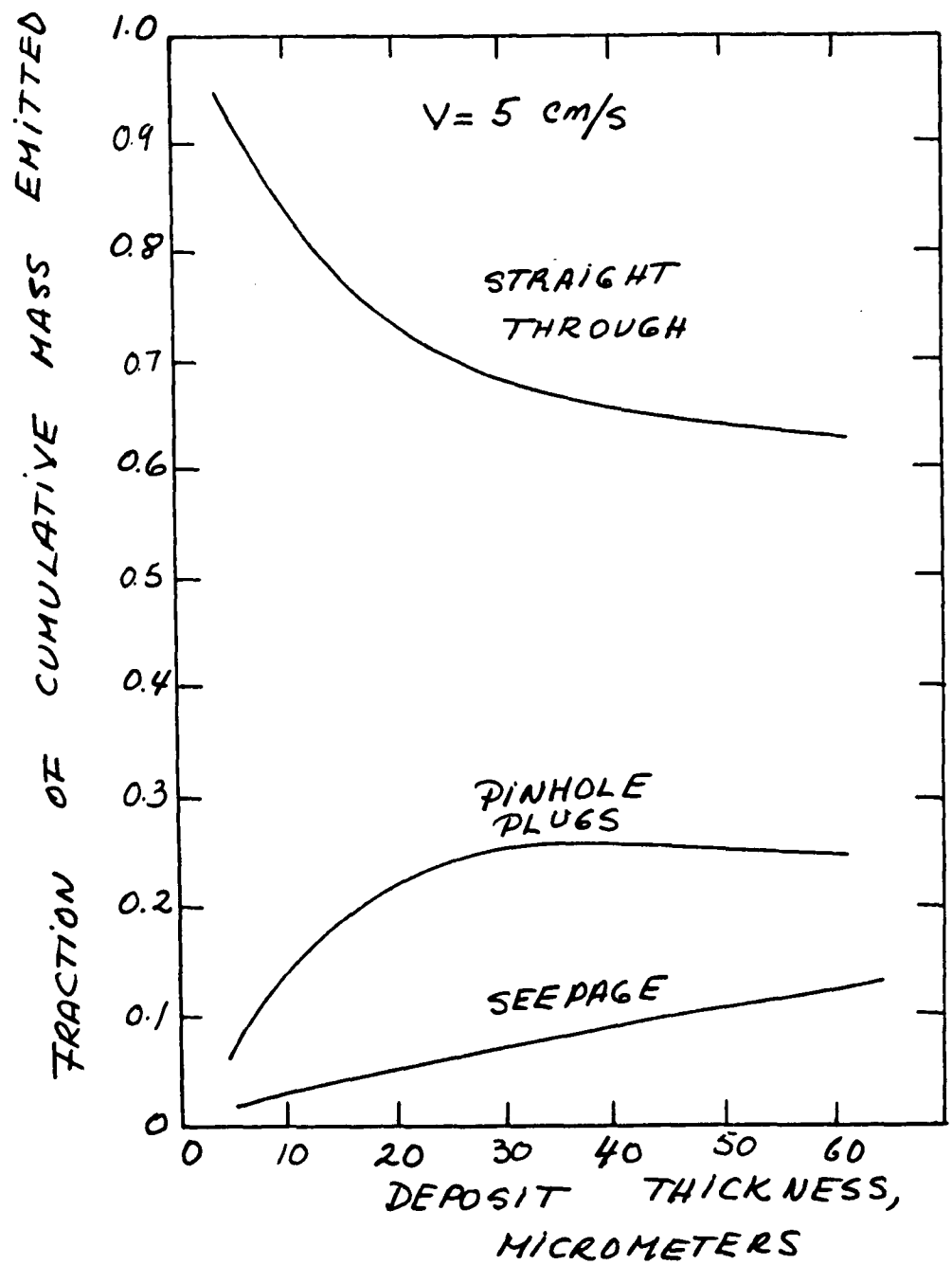

Figure 4-12 Fraction of Cumulative Mass Emitted Over Many Cleaning Cycles versus Deposit Thickness at Cleaning with Mechanism as Parameter, Velocity of 5 cm/s.

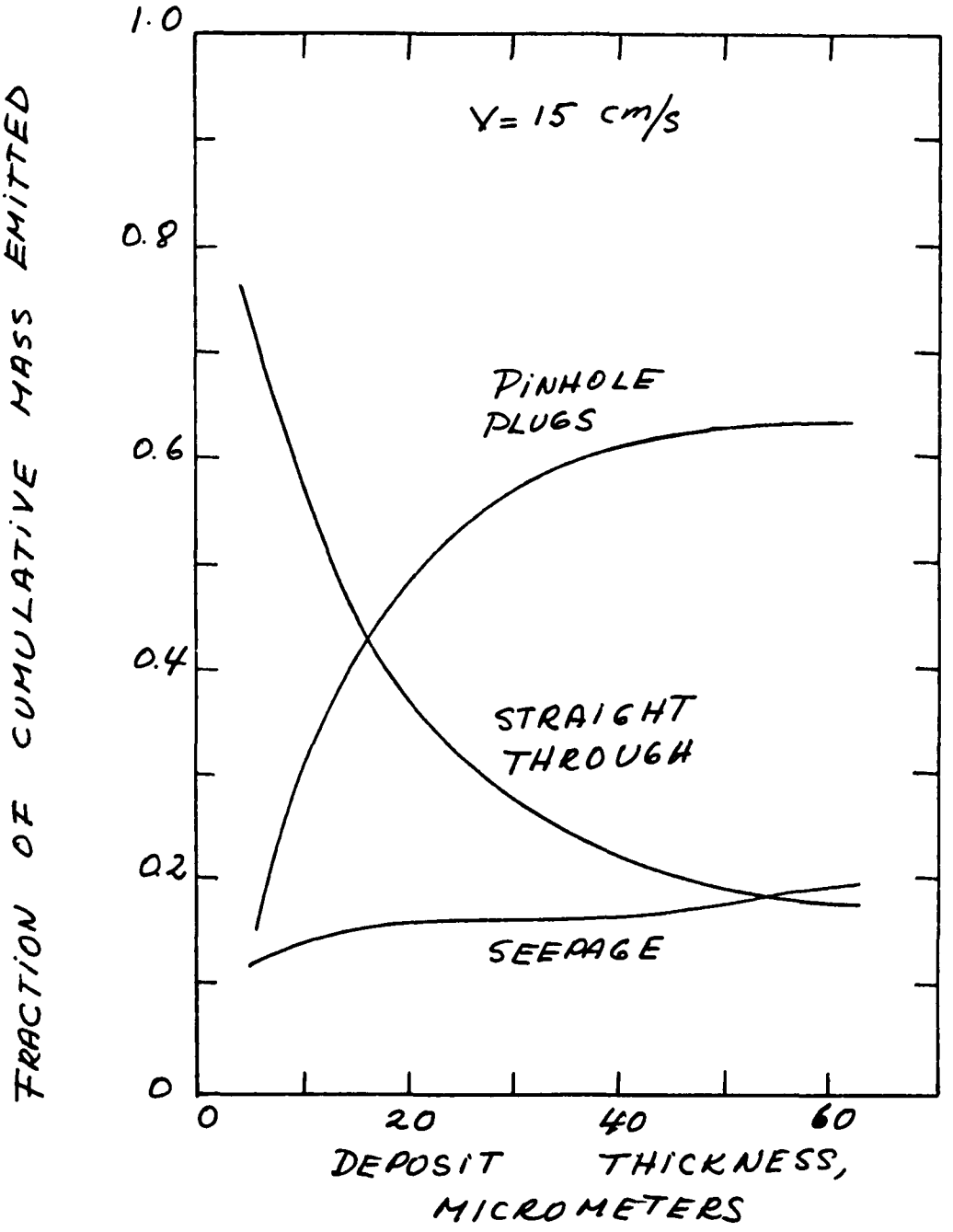

Figure 4-13 Fraction of Cumulative Mass Emitted Over Many Cleaning Cycles versus Deposit Thickness at Cleaning with Mechanism as Parameter, Velocity of 15 cm/s.

cake deposited on a sand surface can produce extremely high filtration efficiencies, Paretsky (1972) studied the penetration of 1.1 μm polystyrene aerosols in fly ash filter cakes deposited on fixed sand beds contained in a 5.08 cm diameter plexiglass cylinder.

Paretsky first deposited fly ash, whose size distribution is given by Figure 3-6, upon a horizontal bed of 20-30 mesh sand, and after having formed a fly ash surface filter cake, passed a dilute suspension of the above mentioned aerosol (10^{-5} g/m^3 or about 50 particles/cm^3) in ambient air through the combination of filter cake and sand bed. A Royco counter Model 220-4 sensor with a Model 263 digital display was used for monitoring the aerosol concentration.

Figure 4-14 shows Paretsky's results for a bed height of 7.9 cm of 20-30 mesh sand. The fractional number penetration of the 1.1 μm aerosol through the filter cake is plotted as a function of the fly ash areal density and as a function of the cake pressure drop/superficial velocity ratio. The data presented in Figure 4-14 was obtained by slowly depositing the fly ash cake while passing ambient air at 3.2 cm/s superficial velocity and by filtering the aerosol particles from air flowing at 2.3 cm/s. The initial pressure drop for the clean bed (just sand) at the aerosol test velocity was 1.83 cm of H_2O.

The Figure clearly shows the filtration performance of a surface cake. At fly ash areal densities of about 0.14 g/cm^2 the efficiency of collection of the 1.1 μm aerosol is

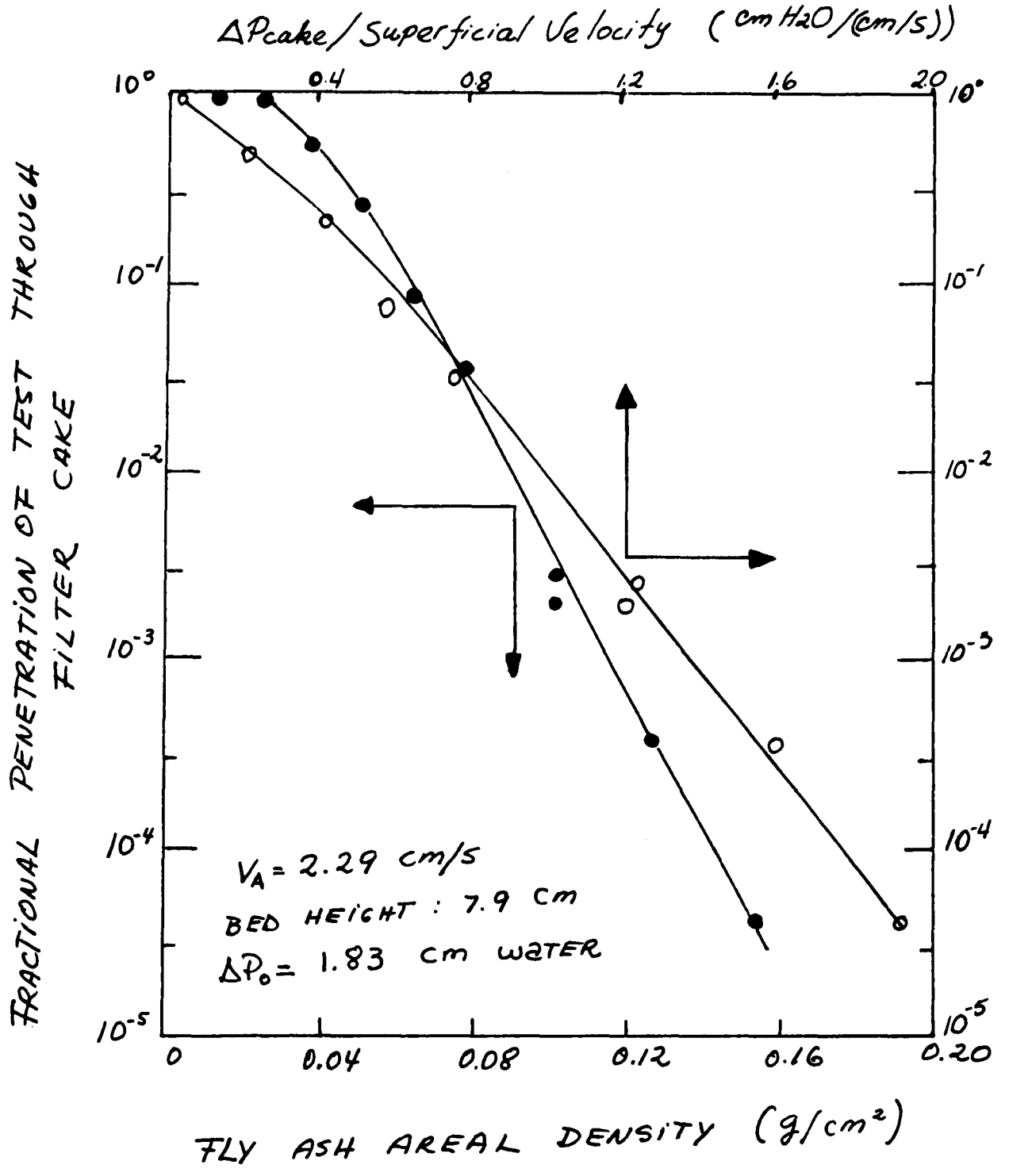

Figure 4-14 Effect of amount of fly ash deposited on fractional penetration of test aerosol through fly ash filter cake deposited on horizontal sand bed.

higher than 99.99 number % (or weight %, if the particles are perfect spheres, as in this case). Paretsky estimated that at this areal density the highly efficient surface cake was just 0.23 cm thick, which is about three sand grains in thickness. (The bulk density of fly ash was about 0.6 g/cm^3, and 20-30 mesh sand has an average grain size of 0.071 cm).

Paretsky indicated that the performance of the filter cake on horizontal beds of sand strongly depended on the intensity of deposition of the fly ash filter cake and upon the air velocity during deposition. He also indicated that the fracture of the cakes and/or formation of big pinholes in their surfaces deteriorated the efficiency of the filter cake in capturing the 1.1 μm aerosol particles.

4.06.32 Lee's Work

Lee (1975), in order to study the mechanics governing the formation and retention of a filter cake on a free surface of a granular solid, conducted experiments whereby a layer of different powders was deposited on a horizontal surface of a sand bed. Lee then used a 1.1 μm monodispersed aerosol of polystyrene microspheres as a probe to explore the nature of a deposit of filter cake at different thicknesses upon free surfaces of sand. Lee used a horizontal bed similar to the one used by Paretsky, but he conducted the aerosol tests at the same velocity at which the cakes had been deposited (5.54 cm/s). Lee also learned how to avoid cake cracking as a result of variations in operating conditions.

The dusts were deposited onto the sand surface of 20.3

cm^2 in small increments. After each incremental addition of dust, the pressure drop across the unit and the penetration of the test aerosol through the filter cake and sand bed were measured. Lee used the same aerosol generation system utilized by Paretsky and also the same concentration (10^{-5} g/m^3 or 50 particles/cm^3). The same particle counter was utilized (Royco 220-4). Lee used fly ash whose size distribution is given in Figure 3-6, two grades of Perlite with 4.2 μm and 15 μm average particle diameter, and Teflon powder with a particle size range between 3 to 8 μm.

The three powders were fed to the unit after vibrating a conical dust feeder provided with a 100 mesh screen. Figure 4-15 shows the penetration of the 1.1 μm aerosol through a filter cake of fly ash resting upon 7.5 cm height sand beds of different particle size. As can be seen in the Figure, penetration declines with decreasing sand particle size, indicating that the structure of the surface cake improved with decreasing sand size. The filter cake formed upon 40-50 mesh sand can be almost considered as an absolute filter for the 1.1 μm aerosols at the highest cake pressure drops utilized ($\approx$ 5.6 cm of H_2O).

The cake formed on the coarsest sand (10-14 mesh) was full of big pinholes on its surface, and therefore did not perform well in the filtration of the 1.1 μm aerosol. Its efficiency did not change much with increasing amount of fly ash. When the sand size was decreased to 20-30 mesh the cake looked much better but still had a few pinholes. These

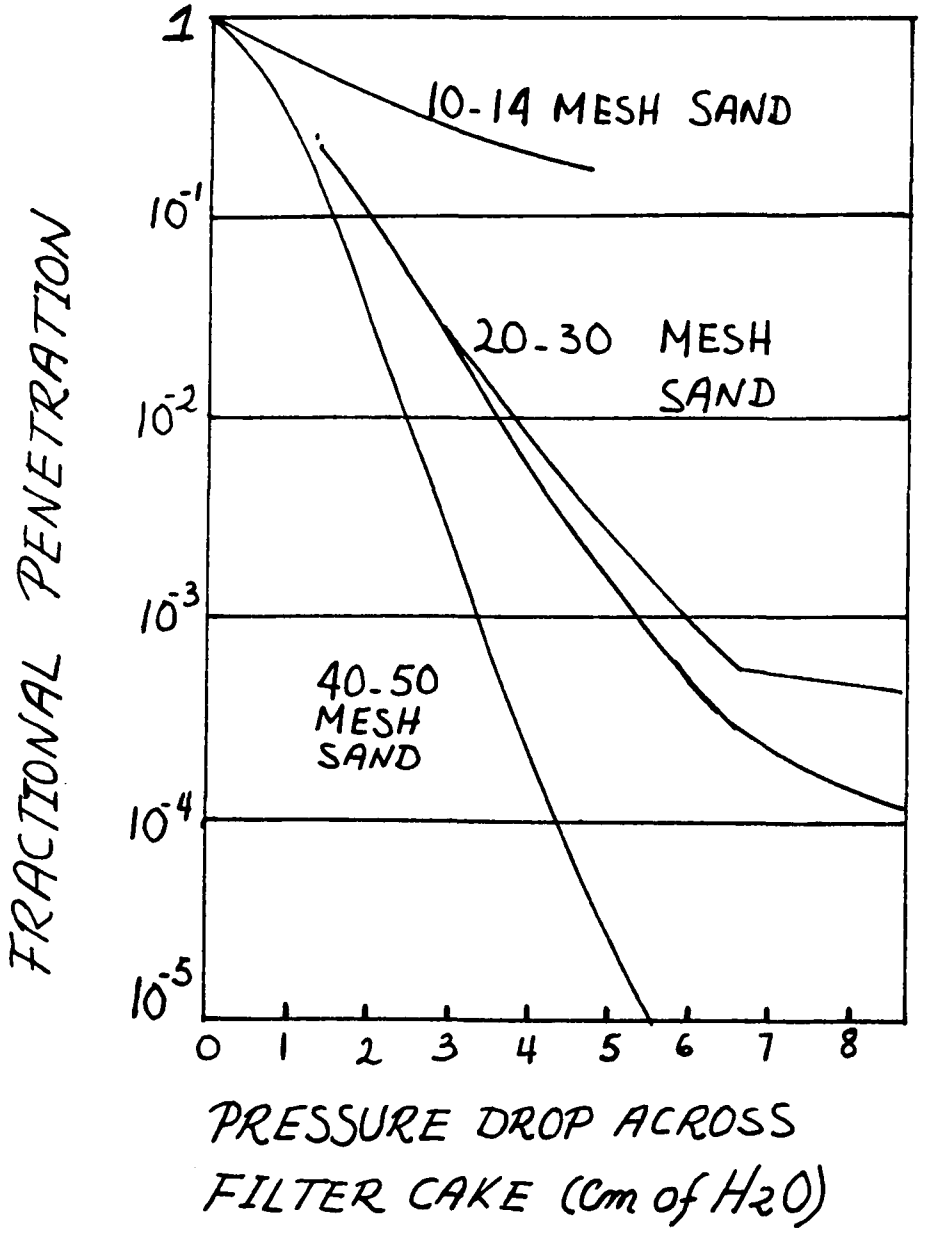

Figure 4-15 Penetration of 1.1 μm polystyrene microspheres in a filter cake of coal fly ash resting upon a sand surface. Atmospheric air at a superficial velocity of 5.54 cm/s.

pinholes tended to produce a leveling off of the filtration efficiency at thicker cakes. Due to the change in the number of pinholes, different curves were observed for higher pressure drops or thicker filter cakes (Figure 4-15).

Figure 4-16 shows Lee's data for the penetration of different dust cakes deposited on 20-30 mesh sand, by the 1.1 μm polystereneaerosol. The Figure includes the data on fly ash shown in the preceeding Figure. Teflon powder did not form a dense, stable filter cake, and the aerosol could easily penetrate it; its behavior resembles the one of fly ash deposited on 10-14 mesh sand. Lee concluded that Teflon powder must have weaker adhesive and autohesive properties than the other two dusts.

The Perlite cakes performed even better than fly ash although high cake pressure drops were not explored.

4.06.33 Wu's Work

Wu (Lee et al., 1977) studied the micro-mechanics of fly ash deposits upon granular media over a range of temperature. Figure 4-17 is a schematic diagram of the sand bed holder developed by Wu and Lee (Lee et al., 1977) for work at temperatures to 315.6^{o} C. The tapered sections for gas inlet and exit are drilled from solid pieces of brass cylinder. The sand bed rests inside a glass tube and upon 100-mesh screen. The tube sits inside a metal sleeve in which there are two rectangular windows for viewing the bed and fly ash deposits on the bed. The sleeve forms a continuous metal structure together with the tapered inlet and exit sections.

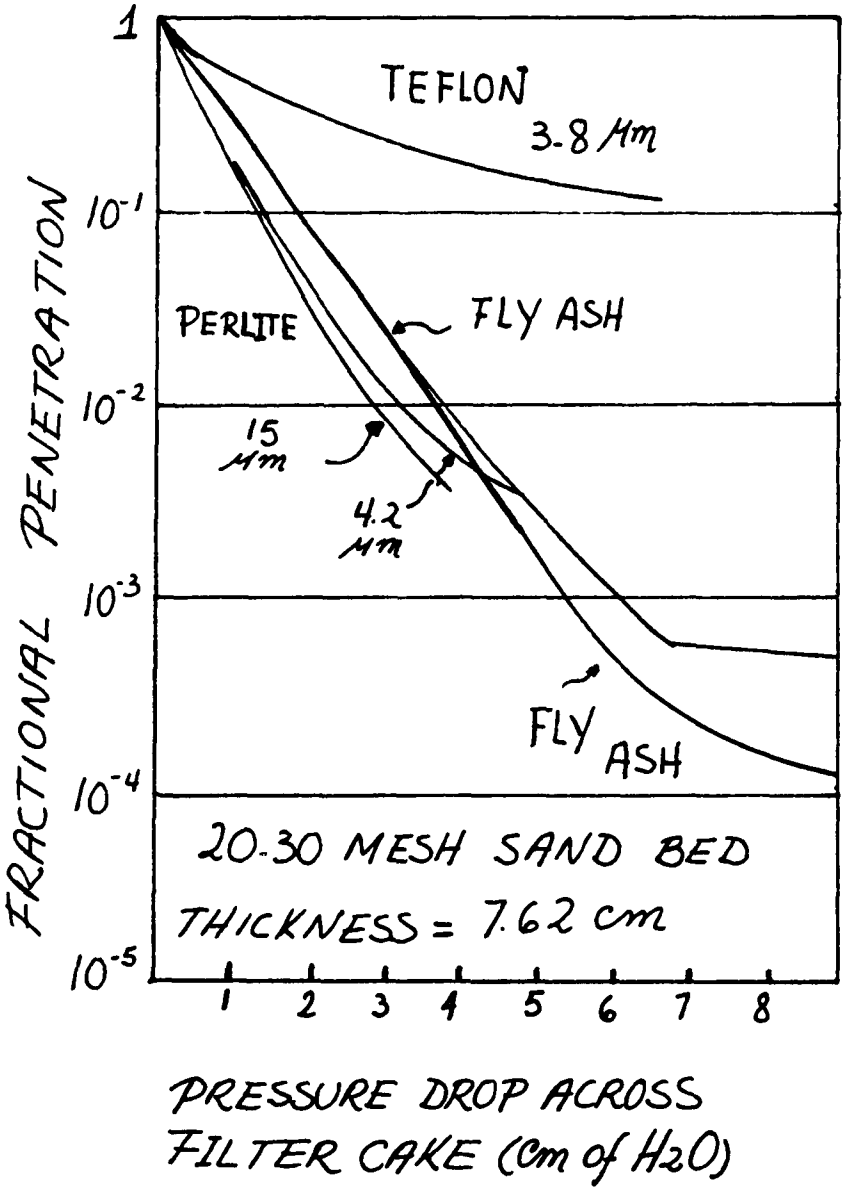

Figure 4-16 Penetration of 1.1 μm polystyrene microspheres in a filter cake of a fine dust resting upon a surface of 20-30 mesh sand. Atmospheric air at a superficial velocity of 5.54 cm/s.

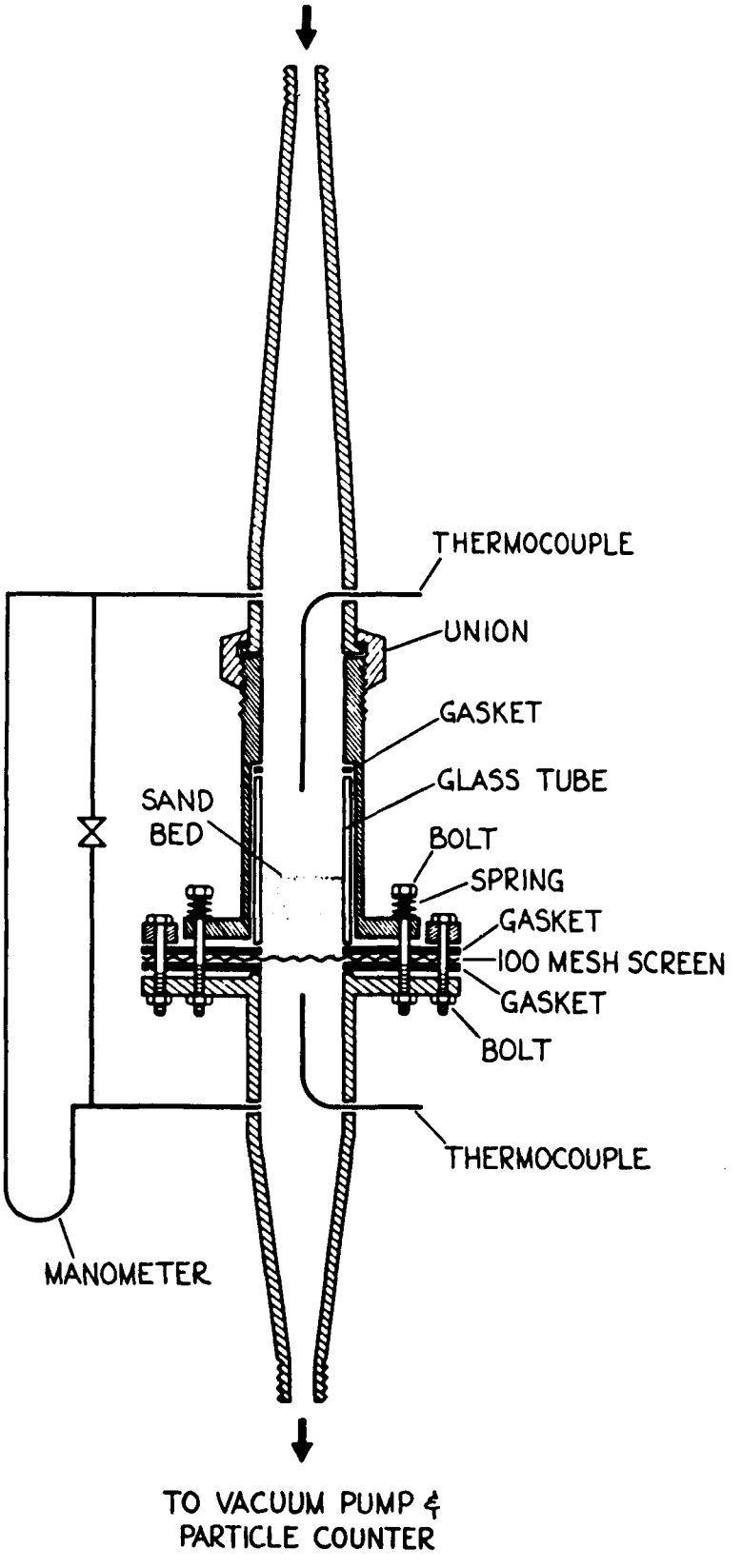

Figure 4-17 Horizontal Bed for Tests at Elevated Temperature.

The glass tube is held in place by gasket material (Union Carbide high-temperature graphite sheet and cord), which allows for the difference in thermal expansion of glass and metal. The diameter of the sand bed is 5.84 cm (horizontal area = 26.79 cm^2).

Fly ash of particle size distribution given by Figure 3-6 was screened through 120-mesh and dried at 110° C for a day, before being deposited upon the sand by sifting the ash through a 100-mesh screen placed above the top opening of Figure 4-17. The sifting of the ash was assisted by an electric vibrator. As ash was deposited on the sand bed, air was pulled downward across the bed at a flow rate to be used in later experiments, i.e., in measurements of the pressure drop across combination of fly ash deposit and sand bed or in determination of the penetration of 1.1 μm aerosol across this combination.

Wu, after finding a reproducible procedure for establishing the sand bed, deposited fly ash cakes upon 40-50 mesh angular sand, 40-50 mesh silicon carbide, and 40-60 mesh copper shot. (A few experiments were made with other sizes of sand.) These experiments were conducted at three different temperatures: 21.1, 150, and 315.6° C, and at three different superficial velocities: 15.24, 30.5 and 45.7 cm/s. The height of the horizontal beds was about 6.3 cm for all runs.

Wu, after having deposited fly ash cakes at different temperatures and velocities, measured the penetration of 1.1 μm polystyrene aerosol at 21.1° C and at the same

velocity at which the high-temperature cakes had been formed. (The unit was cooled to 21.1° C before conducting the penetration tests.)

Wu used the same aerosol-generator, aerosol concentration and aerosol particle counter that Paretsky (1972) and Lee (1975) had utilized.

Figure 4-18 gives pressure drops across fly ash deposits on sand at three air velocities and at 150°C

Run (a) in Figure 4-18 is for a deposit on 20-30 mesh sand. No coherent surface deposit formed, the surface remaining pitted through the run. The low pressure drop at the end of the run reflects the fact that most of the fly ash penetrated deep within the sand bed. From a comparison of run (a) in Figure 4-18 and earlier data for 20-30 mesh sand with the same fly ash but at ambient temperature (Lee, 1975; Lee et al., 1977), it was concluded that the autohesivity of fly ash and/or its adhesivity toward sand is less at 150° C than at 21.1° C. This change was primarily attributed to absence at the higher temperature of the capillary forces that arise because of presence of moisture at the lower temperature.

Run (b) in Figure 4-18 was for half-and-half mixture of 20-30 mesh and 40-50 mesh sand. As in run (a), deep penetration of fly ash was observed. Pinholes were large, and closed up only one by one after large additions of fly ash had been made.

The remaining runs of Figure 4-18 were for 40-50 mesh sand. The surface deposits of fly ash at 150° C were fully

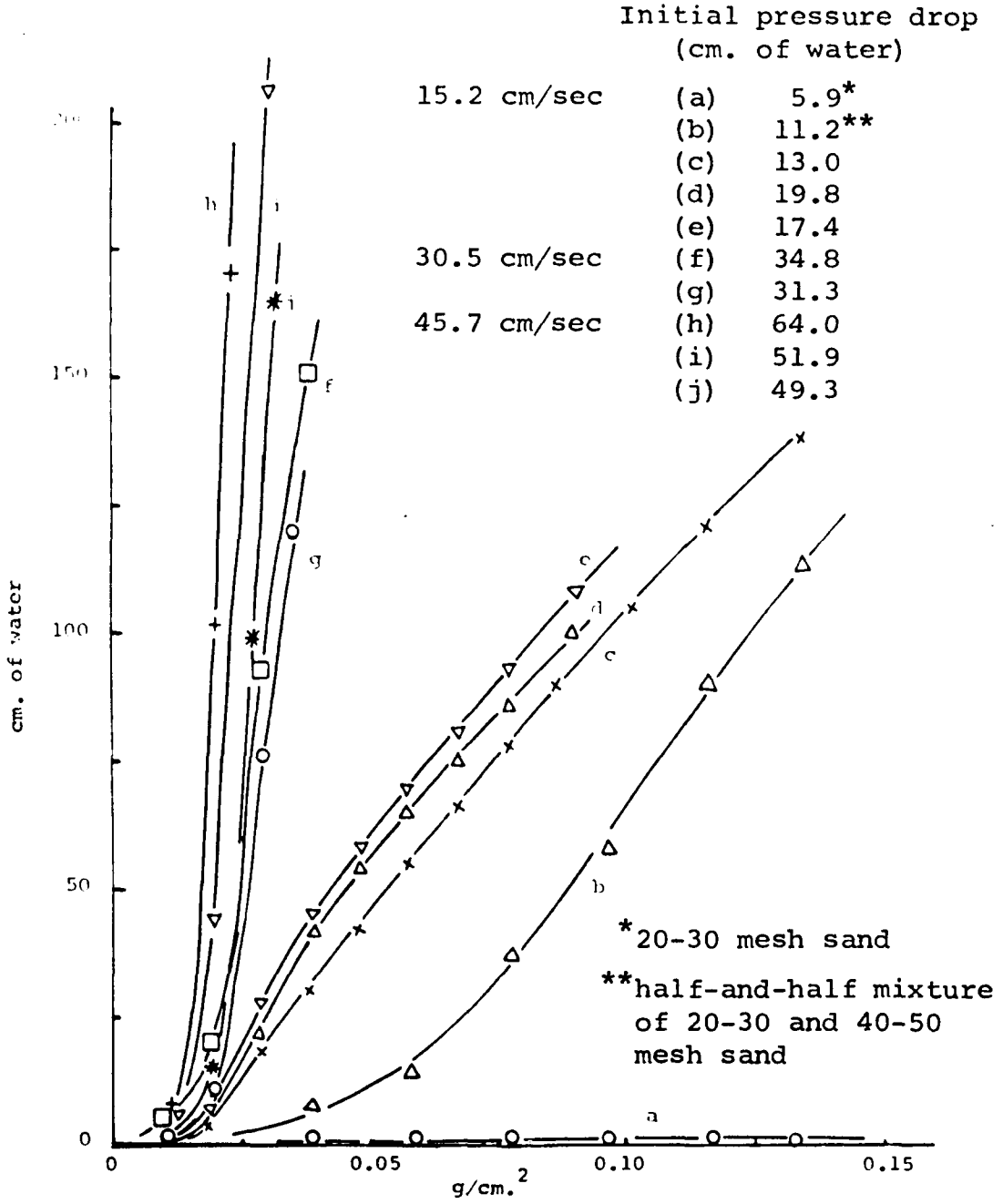

Figure 4-18 Pressure drop across fly ash deposit on sand versus specific weight of the deposit. Air at 150°C and three velocities. Sand = 40-50 mesh, except as noted.

as coherent as deposits at 21.1° C. Pinholes closed up nicely, although Wu had the impression this occurred only after somewhat more fly ash had been deposited. However, pressure drops at a given amount of fly ash were a bit higher at 150° C than at 21.1° C, indicating just the opposite to Wu's observation. Wu hypothesized that this may be because less fly ash appeared to adhere to the walls of the test bed holder of Figure 4-17 at the higher temperature. (Wu did not take into consideration wall losses in the calculation of fly ash areal densities.)

Figure 4-19 gives 1.1 μm aerosol penetration data across the combination of sand bed and fly ash deposits put down at 150° C. The penetration measurements were taken at 21.1° C. Each point in Figure 4-19 represents a single run commencing from a clean, fresh sand bed. The decrease in penetration with increase in velocity, is clearly seen in the data at relatively low fly ash areal densities. At the three velocities tested, penetration decreases with first additions of fly ash, but bottoms out and increases with later additions of fly ash; this phenomenon accurred sooner as velocity increased. Wu believes that this effect was caused by development of pinhole defects in the fly ash deposit, or perhaps also by reentrainment of fly ash particles by the air stream. (Some of the fly ash particles are of a size to produce counts on the Royco counter that would mimic counts produced by the 1.1 μm aerosol particles.)

Figure 4-20 summarizes Wu's penetration data for fly

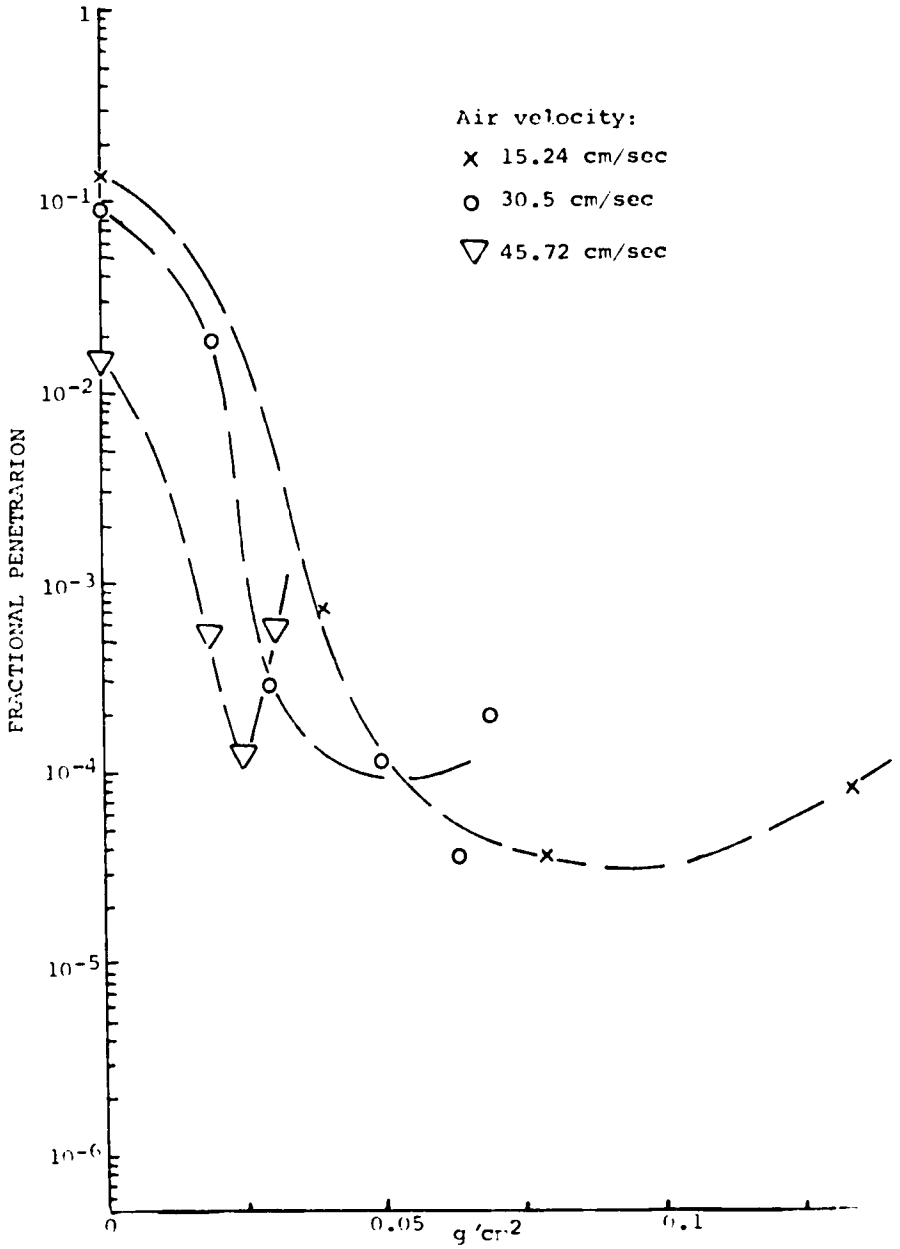

Figure 4-19 Fractional penetration of 1.1 micron monodisperse aerosol through 6.3 cm of 40-50 mesh sand with fly ash deposit versus specific weight of the deposit. Air at three velocities during penetration tests and at 21°C. Fly ash deposits put down at 150°C and at the three respective air velocities.

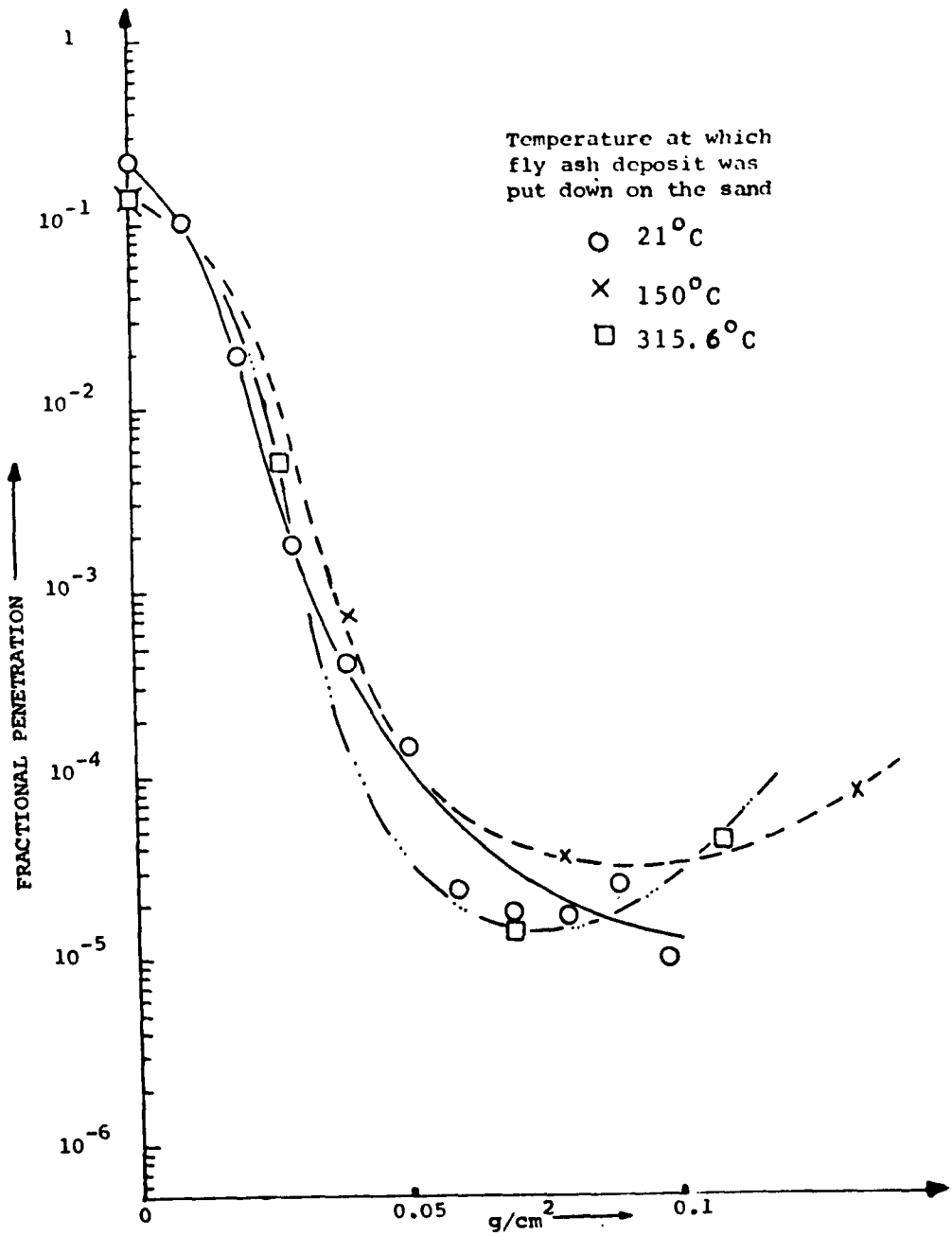

Figure 4-20 Fractional Penetration of 1.1 micron monodispersed aerosol through 6.3 cm of 40-50 mesh sand with fly ash deposit versus specific weight of the deposit. Air at 15.24 cm/s and 21°C during penetration tests. Fly ash deposits put down at three temperatures.

ash deposits put down at the lowest velocity used (15.24 cm/sec) and at three temperatures. It can be seeing in Figure 4-20 that the filtration behavior of the fly ash deposits toward the 1.1 μm aerosol test varies very little with the temperature at which they were put down. It was concluded (Lee et al., 1977) that if a cake forms, as it does upon 40-50 mesh sand at all temperatures, the cake appears to have reasonably consistent mechanical properties vis-a-vis aerosol filtration.

Wu (Lee et al., 1977) found little difference in filtration behavior of fly ash deposits put down at three different temperatures (21.1, 150, 315.6^{o} C) upon horizontal beds of sand and silicon carbide of about same particle size.

CHAPTER 5.0: EXPERIMENTAL ARRANGEMENTS AND PROCEDURES

In this Chapter 5.0 we shall describe the equipment and procedures utilized to perform experiments in which redispersed dusts were filtered by a small laboratory panel bed filter at 150° C. We shall also discuss the equipment and procedures for tests conducted in a horizontal bed of sand at 150° C. All collateral techniques and methods of calculation will be outlined.

5.01 Laboratory Panel Bed Filtration at 150° C

a) Description of Apparatus

A simulation of the removal of dusts from gaseous industrial streams has been studied. This entailed the use of a panel bed 7.6 cm wide and 30.5 cm tall operating at 150° C. Our panel bed is a modification of equipment developed by Lee (1975) for studies at atmospheric temperature.

Figure 5-1 is a schematic cross-sectional view, and Figure 5-2 gives details of the louvers used in most of the work.

The panel bed filter has three parallel set of louvers which hold two beds of granular material of different particle size. The fine solids that form the filtration bed are placed between the filtering face louvers and the middle louvers, which are horizontal and spaced at a distance to prevent the coarser solids from participating in the body movement of the fine solids during cleaning (puffback).

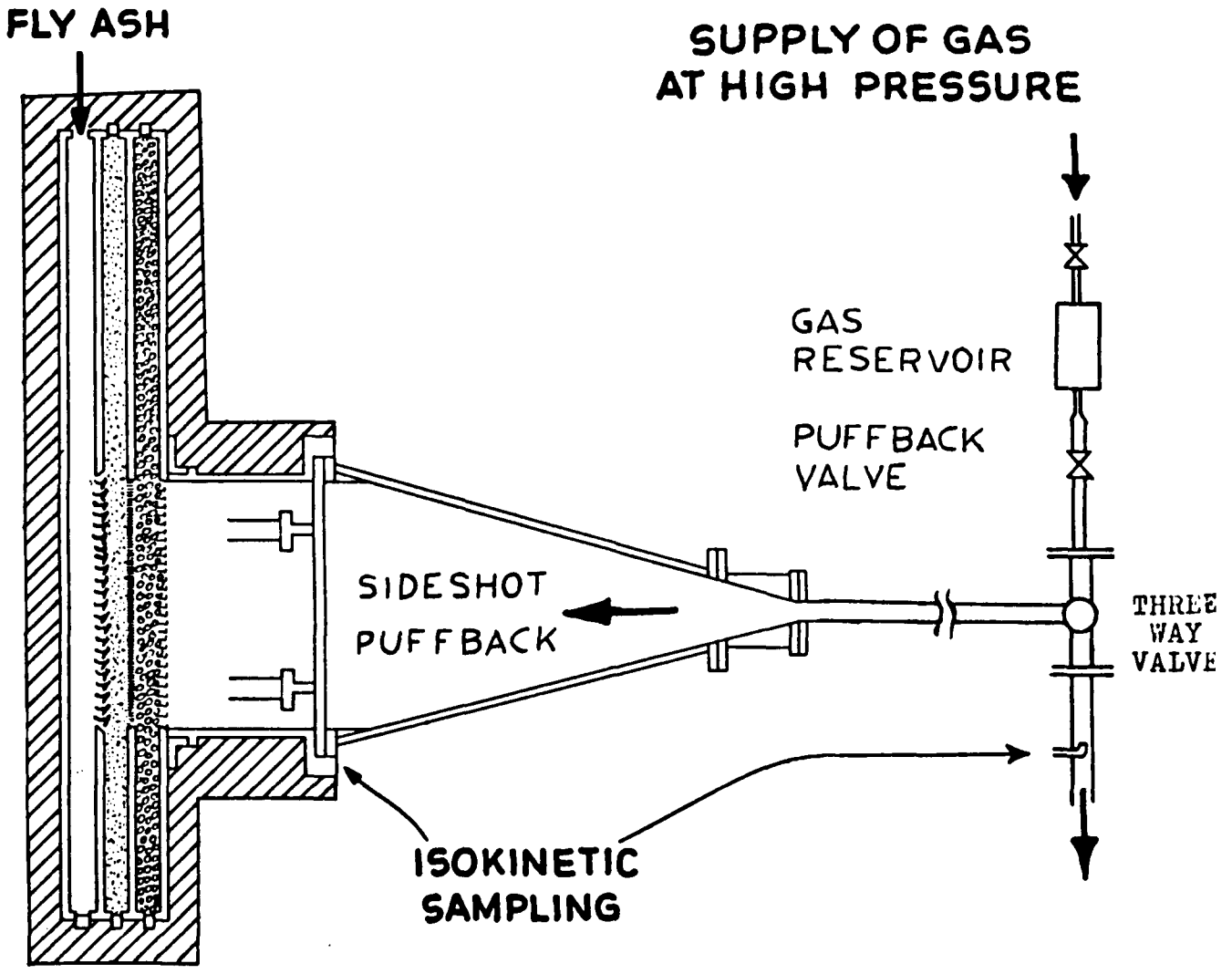

Figure 5-1 Schematic cross-sectional view of apparatus for test of panel bed filter. Notice that two isokinetic samples are taken directly downstream of the filter bed, one near the top and another near the bottom.

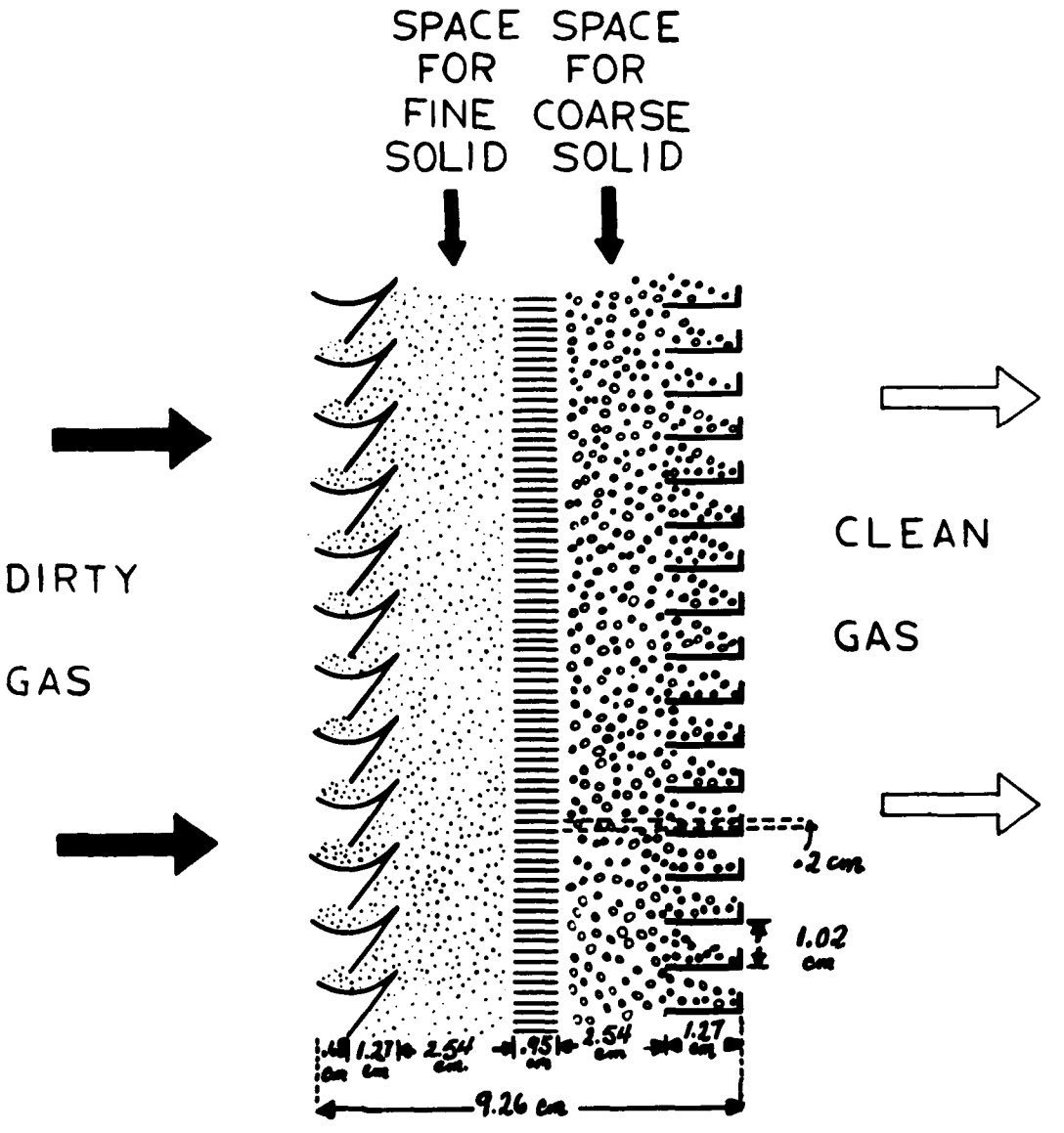

Figure 5-2 Arrangement of louvers for tests of dust filtration at 150°C. The louvers at the dirty face are the "wishbone" design.

A coarser grade of solids is provided behind the filtering bed merely to prevent its being blown away from the clean side of the panel; this arrangement enables us to operate the filter at high velocities. Both the fine sand and the coarse sand beds were 2.54 cm wide.

Angular sand 14-20 mesh in particle size was used as the coarse solid throughout this investigation.

The filtering face of the panel bed, seen at the left in Figures 5-1 and 5-2, has 19 louvers of a design which we called "wishbone." The structure in Figure 5-1 is made of aluminum, and is insulated and fitted with heating tapes governed by variable transformers.

Figure 5-3 is a schematic block diagram of our apparatus. Compressed air, available at 791 kPa, is filtered and dried to a dew point of ca. -73° C over molecular sieves (Davidson Chemical Grade 514, 8-12 mesh, regenerated at 370° C). The air flows through pressure regulator and rotameter and to a 6-kilowatt electric heater with temperature control, capable of heating the air to about 250° C.

Our dust feeder, seen in Figure 5-4, is a modification of a device developed by the U. S. Bureau of Mines (Lucas and Smith, 1974). We feed dust into a chamber supplied with heated air at ca. 200 kPa absolute and the dust is redispersed by allowing dust-laden air to pass through a critical orifice into the space on the dirty side of the panel bed. The feeder shown in Figure 5-4 contains a screw conveyor that is driven by a motor with variable speed control. The dust is supplied

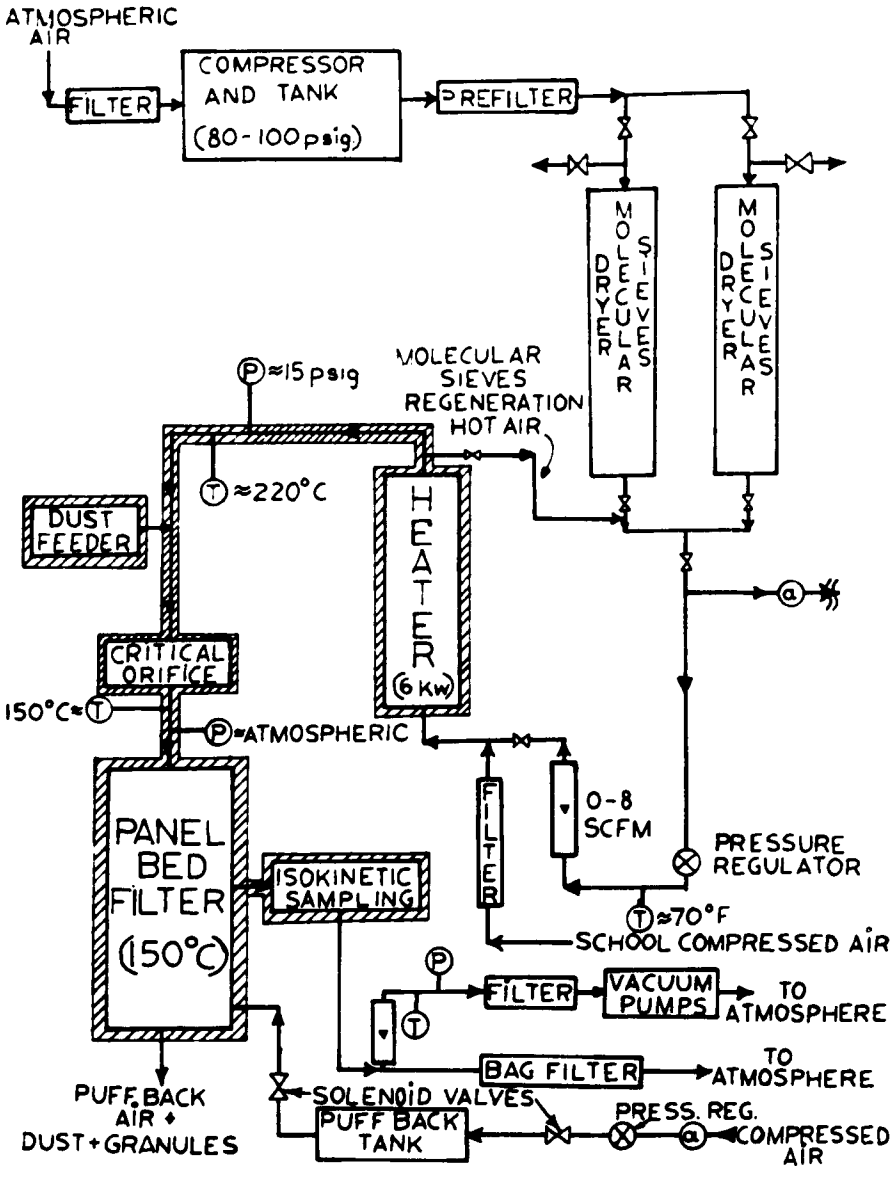

Figure 5-3 Schematic of Panel Bed Experimental Apparatus

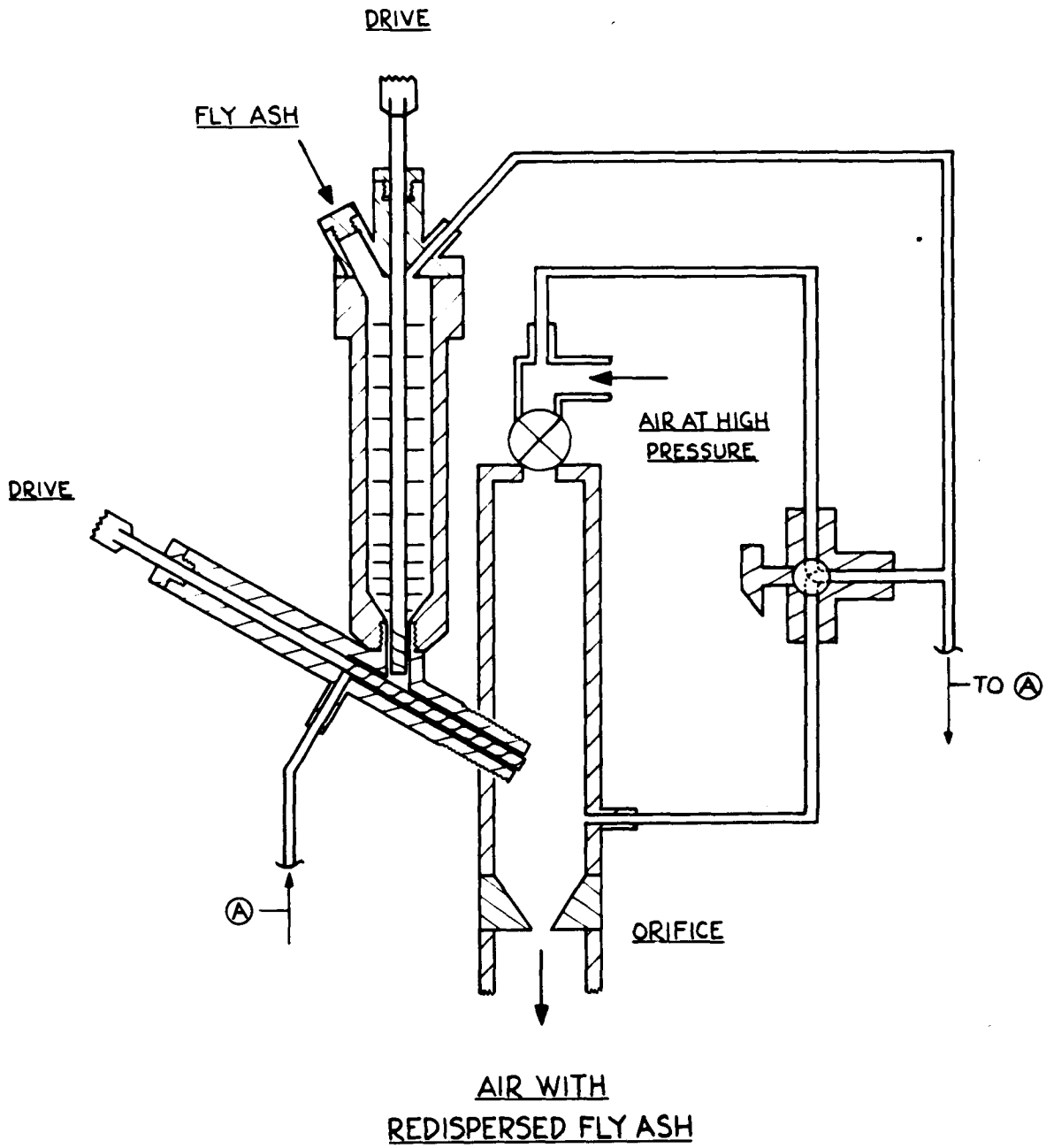

Figure 5-4 Feeder for Redispersion of Dust in Air at Atmospheric Pressure and at 150°C

to the screw conveyor from a cylinder that is stirred by paddles on a shaft driven by a second motor. The purpose of the paddles is to prevent bridging and consolidation of dust particles in the cylinder.

The feeder was used for feeding dusts of different physical properties into an air stream at high pressure and temperature. We wanted to achieve approximately constant dust concentration in the air stream independently of filtration velocity. This implied wide variations in the feeder's outlet mass flow rate of dust, anytime that the velocity of filtration was varied. In some occasions a variation of the speed of the shafts was not enough for the required change in dust mass flow rate, and therefore an additional driving force was needed. This was obtained by provoking a pressure difference in between the cylinder-screw conveyor system and the air chamber at the feeder's outlet. As shown in Figure 5-4, a three-way high temperature valve allowed us to connect the air inlet tube, where the pressure was kept slightly higher than the air in the chamber by a gate valve, to the cylinder-screw conveyor system.

The use of a critical orifice upstream of the filter provoked the redispersion of the dust being fed into a cloud of individual particles. In work at atmospheric temperature, we sampled air downstream from the orifice. Dust particles collected on a filter paper viewed through a microscope appear fully redispersed. Orifice size and upstream air pressure are the controls on air flow rate to the panel bed.

We have provided a glass section before the critical orifice and close to the feeder to allow visual observation of the feeding.

An unrealistic feature of our experiment is that our redispersed dust particles are charged electrically. We recognize that this feature may give us an assist in filtration.

During a filtration step, we monitor the pressure difference across the panel bed with a micromanometer. When this difference reaches a pre-determined level, we stop the flow of dust-laden air and shift the position of a three-way valve, seen in Figure 5-1. We then create a reverse surge flow of room temperature air across the panel by quickly opening a valve that releases air at high pressure from a gas reservoir now connected to the clean side of the panel bed. The puffback causes a body movement of all of the fine granules in the panel bed toward the gas-entry face, causing dust filter cake and a small quantity of sand to spill from each gas-entry surface of the sand bed. Parameters governing the puffback (Lee, 1975) are selected so that the spills from the various gas-entry surfaces are nearly uniform. Puffback reduces flow resistance across the panel, which is then ready for a succeeding filtration step. We term this step and a subsequent puffback a "filtration cycle."

The puffback valve is a quick-opening solenoid valve nominally 0.8 cm in diameter supplied by Valcor Engineering Corp. of Kenilworth, New Jersey. The orifice area is 0.495 cm^2; Cv = 3.4. The time for opening is about 15 to 20 milliseconds.

The puffback gas reservoir is 206 cm^3. Air is supplied to the reservoir at room temperature, the pressure is adjusted to a desired level, and the reservoir is then isolated from the supply.

There are two isokinetic sampling stations on the clean side of the panel bed. Each sampling station was comprised of a holder for a filter paper, a duct to draw air through the filter paper, and a gas collecting "chimney" facing the gas stream. The dust collecting chimney used was 3.175 cm in inside diameter and 6.99 cm long. The rate at which gas is pulled through the filter paper was governed so that a sample of gas entered the chimney at the same velocity as the main gas flow past the chimney (isokinetic sampling).

Each station has a glass fiber filter paper (Gelman Type A-E) good for work up to 400° C and affording 99.7% collection efficiency by the dioctyl phthalate penetration test. At our face velocities, air would deposit dust if it were caused to turn a corner or to negotiate a sharp contraction. We have found that air negotiates the converging section seen in Figure 5-1 without losing dust. Data from an isokinetic sampling station of the usual type in the pipe downstream from the three-way valve agree with data from the two earlier sampling stations, working at lower air velocity. After we established this agreement, we obtained all of our data from the two earlier stations.

Most tests were extended to a series of 10 filtration cycles. It was not possible to execute more cycles in a

single day's work, and it was not felt advisable to hold the unit at temperature overnight.

b) Experimental Procedure and Calculations

The experimental determination of the penetration (cumulative, overall and on a weight basis) of a given dust in the panel bed filter was done according to the following procedure:

1. Both coarse and fine solids were thoroughly cleaned in a fluidized bed elutriator and fed to the panel.

2. The air compressor was turned on and later drained.

3. The air heater was turned on, and controller set at predetermined temperature.

4. The heating tapes around the filter and feeder were activated by turning on the variable transformers.

5. From a knowledge of the frontal area of the panel bed and a prefixed superficial velocity at the inlet of the filter (150^{o} C and atmospheric pressure) a critical orifice was designed and installed.

6. For a given critical orifice, the rotameter reading was adjusted at a volumetric flow rate, at room temperature, which proportions the mass flow rate needed at the entrance of the filter.

7. In approximately three hours (depending on filtration velocity) steady state was reached and the unit was ready for doing the final adjustments needed for a filtration run. (At this time the air pressure upstream the orifice was about 200 kPa.)

8. With the unit at 150° C, the air flow was stopped for a short period of time and dust, which had been previously dried for three days at 315° C, is charged to the feeder.

9. Several puffbacks, at a higher pressure than the one planned to be used during the experiments, are applied. The granular material spilled from those puffbacks is caught at the bottom of the unit in a tray and after closing the hole with a plug, and disconnecting the puffback system, the air flow is restored.

10. In approximately half an hour, steady state is reached again and at this moment the converging section on the clean side of the panel bed is removed, permitting us to mount two previously weighted filter papers in the sampling station.

11. After attaching the converging section to the filter, the sampling velocity is adjusted by turning on two vacuum pumps which are connected to two rotameters, which in turn communicate with the filter holders. (Isokinetic sampling.)

12. After steady state is reached again (constant temperature at inlet and outlet of the filter), the clean bed pressure drop is recorded.

13. With the unit ready to begin operation, the two motors of the feeding system are started (the dust feeding rate had been previously determined in a trial and error run) and dust begins to be filtered.

14. The pressure drop through the bed is recorded as a

function of time and when the preselected cake pressure drop is reached the motors are stopped and the flow is suspended.

15. The plug at the bottom is removed, the position of the three-way valve is shifted to communicate the clean side of the panel with the puffback tank, and at a preselected regulated pressure the puffback tank is charged. (This is done by activating a switch which at this moment opens the inlet solenoid valve and closes the one at the outlet of the puffback tank simultaneously.)

16. Once the puffback pressure has been adjusted, puffback is applied by closing the inlet solenoid valve and opening the one at the outlet of the tank. This is done by activating the puffback switch while holding a tray against the bottom of the panel where dust and granules are captured.

17. After shifting the position of the three-way valve and closing the unit, the flow is restored and the pressure drop is recorded.

18. While waiting for temperature uniformity, the dust and granules are separated by sifting in a 80-mesh screen.

19. The weight of dust which fell to the bottom of the unit before cleaning is recorded besides the weights of dust and granules spilled from puffback.

20. Steps 12 through 19 are repeated three times (3 filtration cycles) before the filter papers are removed from the sampling stations and new ones are mounted. (All filter papers needed for one day's work had been previously weighted and kept in sealed containers.)

21. Steps 12 through 19 are repeated for cycles 4 through 10 before the unit is taken out of service.

22. The "dirty" filter papers are weighted in an automatic balance with a precision of $\pm$ 0.1 x 10^{-3} g.

23. The cumulative overall penetrations by weight for cycles 1-3 and cycles 4-10 are calculated as follows:

a. Outlet mass-volume concentration C_{MVe} :

$$C_{MVe} = \frac{Mds}{Asc\ Vs\ tc} \qquad (5\text{-}1)$$

Where:

Mds = Average weight gain of the two sampling filter papers in one filtration cycle (arithmetic average of n cycles)

Asc = Area of sampling chimney (Dirty area of sampling filter paper)

Vs = Superficial air velocity (based on panel bed flow area)

tc = time elapsed in one filtration cycle (arithmetic average of n cycles)

b. Inlet mass-volume concentration C_{MVi} :

$$C_{MV_i} = \frac{Mdsd + (Mds\ Apb/Asc)}{Apb\ Vs\ t_c} \qquad (5\text{-}2)$$

Where:

Mdsd = Total mass of both drained and spilled dust during one filtration cycle (arithmetic average of n cycles)

Apb = Panel bed flow area (panel bed without louvers and granules)

c. Penetration % = 100 - Efficiency % (cumulative, overall and on a weight basis)

$$\text{Pov } \% = \frac{C_{MV_e}}{C_{MV_i}} \times 100 = \frac{\text{Mds Apb}}{\text{Mdsd Asc + Mds Apb}} \times 100 \qquad (5\text{-}3)$$

Where:

Pov % = Cumulative, overall, penetration percentage on a weight basis (arithmetic average of n cycles)

24. The estimation of the superficial and "filtration" velocities was done as follows:

a. Superficial Velocity:

The superficial air velocity (face velocity) was estimated by dividing the volumetric flow rate at filter inlet conditions (150^{o} C and about 10^{2}kPa) by the panel bed filter flow area Apb. This is the velocity of air at the inlet and outlet of the filter.

b. "Filtration" velocity:

The "filtration" velocity is the velocity of air at the surface of the granular material. (Note that this is not the intersticial velocity.) This velocity is difficult to calculate precisely in the panel bed filter.

As Figure 5-5a illustrates, there is a reduction in area as air penetrates the louvers' frame; moreover, the louvers themselves block the passage of air and the flow area is again reduced. As figure 5-5b illustrates the free sand

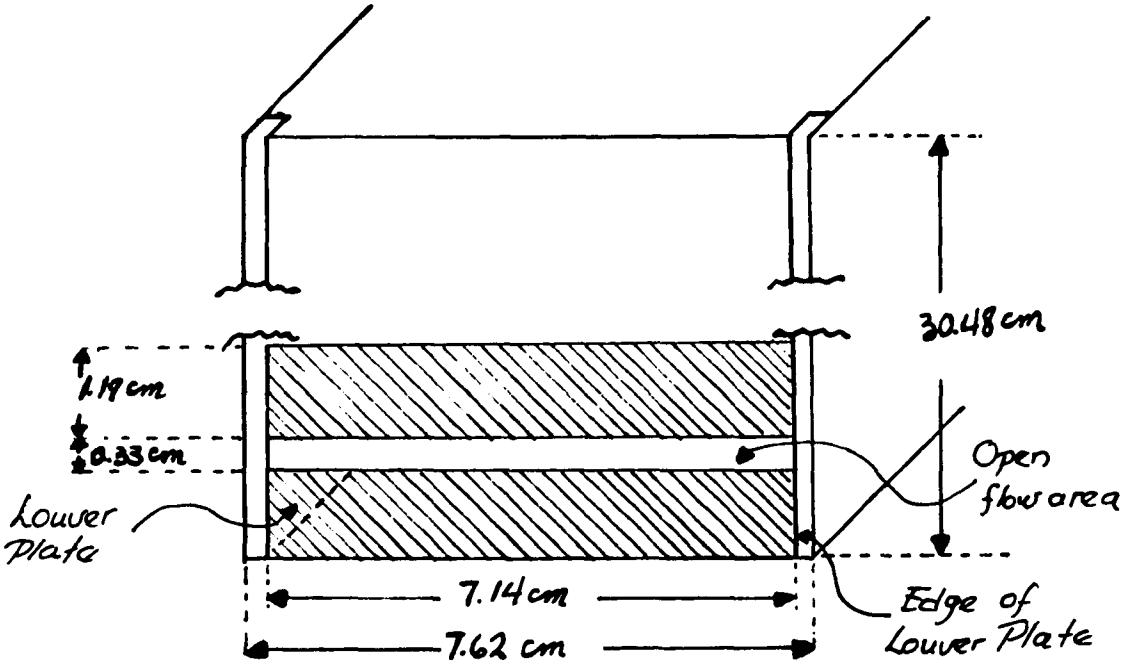

Figure 5-5a Filtration Face of Panel Bed Filter

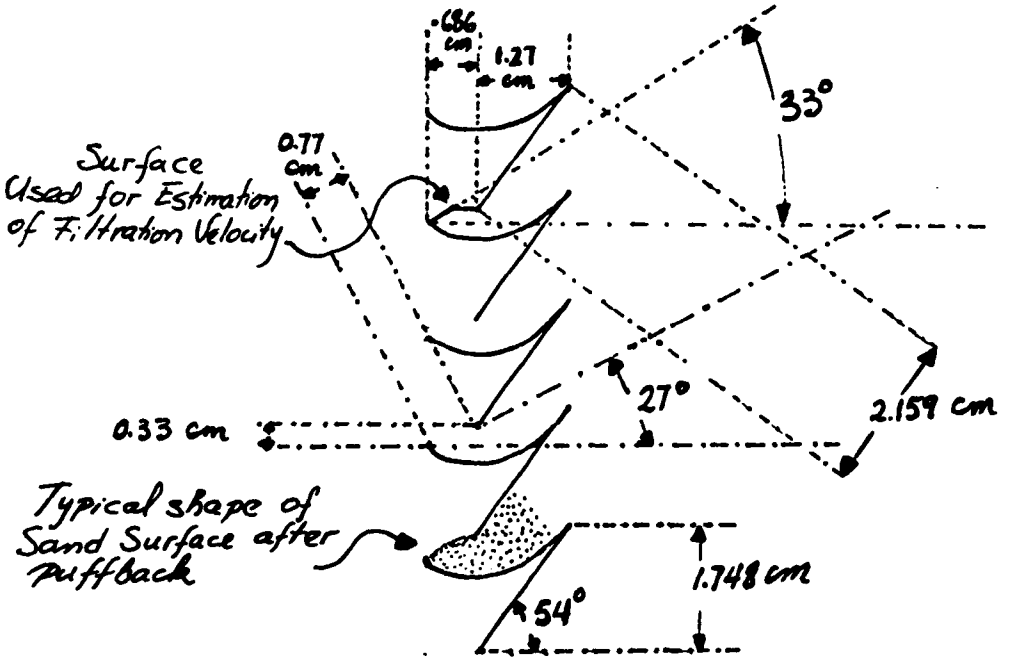

Figure 5-5b Geometric Details Needed for Estimation of Free Sand Surface in Panel Bed Filter

Figure 5-5 Estimation of Filtration Velocity

surfaces exposed to the flow, acquire a curved shape after puffback is applied. As a result the bed's surface area was estimated from averaging the typical curved surfaces observed after puffback. The two above mentioned velocities were then calculated as follows:

$$Vs = \frac{Qpb}{Apb} \qquad (5\text{-}4)$$

Where: Qpb = air volumetric flow rate at inlet of panel bed filter (150° C, 100 kPa)

$$V_f = \frac{Qpb}{A_{fs}} \qquad (5\text{-}5)$$

Where: A_{fs} = estimated free sand surface

The following results were obtained from calculations made based on the dimensions shown in Figure 5-5:

Apb = 232.26 cm^2

A_{fs} = 107.21 cm^2

This implies that the estimated filtration velocity is about 2.17 times the superficial velocity.

5.02 Horizontal Bed of Sand at 150° C

a) Description of Apparatus

A horizontal bed of sand at 150° C was used for depositing cakes of different dusts at different velocities. The pressure drop through the cakes was recorded as a function of the amount of dust deposited. Visual observation of the cakes formed upon fixed beds of sand of different particle size and

at different velocities provided useful information which was then translated into panel bed filter parameters.

Figure 4-17 is a schematic diagram of the sand bed holder which was developed by Lee et al. (1977) for work at temperatures to 315.6° C. A detailed description of the bed holder was given in Chapter 4.0 (4.06.23) of this dissertation. Figure 5-6 is a schematic block diagram of the apparatus. Dusts which had been previously dried at 315.6° C, were deposited upon horizontal beds of sand at 150° C, by sifting them through a 100-mesh screen placed above the top opening of Figure 5-6. The sifting of the dusts was assisted by an electric vibrator. As dust was deposited on the sand bed, air at 150° C was pulled downward across the bed at constant velocity. This was done by using a vacuum pump, connected through a rotameter, to the bed holder. As the pressure downstream of the cake-sand bed combination decreased, the volumetric flow rate was increased in order to keep a constant mass flow rate or constant deposition velocity. (This was done at small pressure drop intervals.)

b) Experimental Procedure

The detailed procedure for these experiments can be described as follows:

1. A fixed mass of clean and dry sand of a predetermined size was fed to the bed holder. (The bed holder had been previously removed from the set-up.)

2. The bed holder with the sand is threaded to the

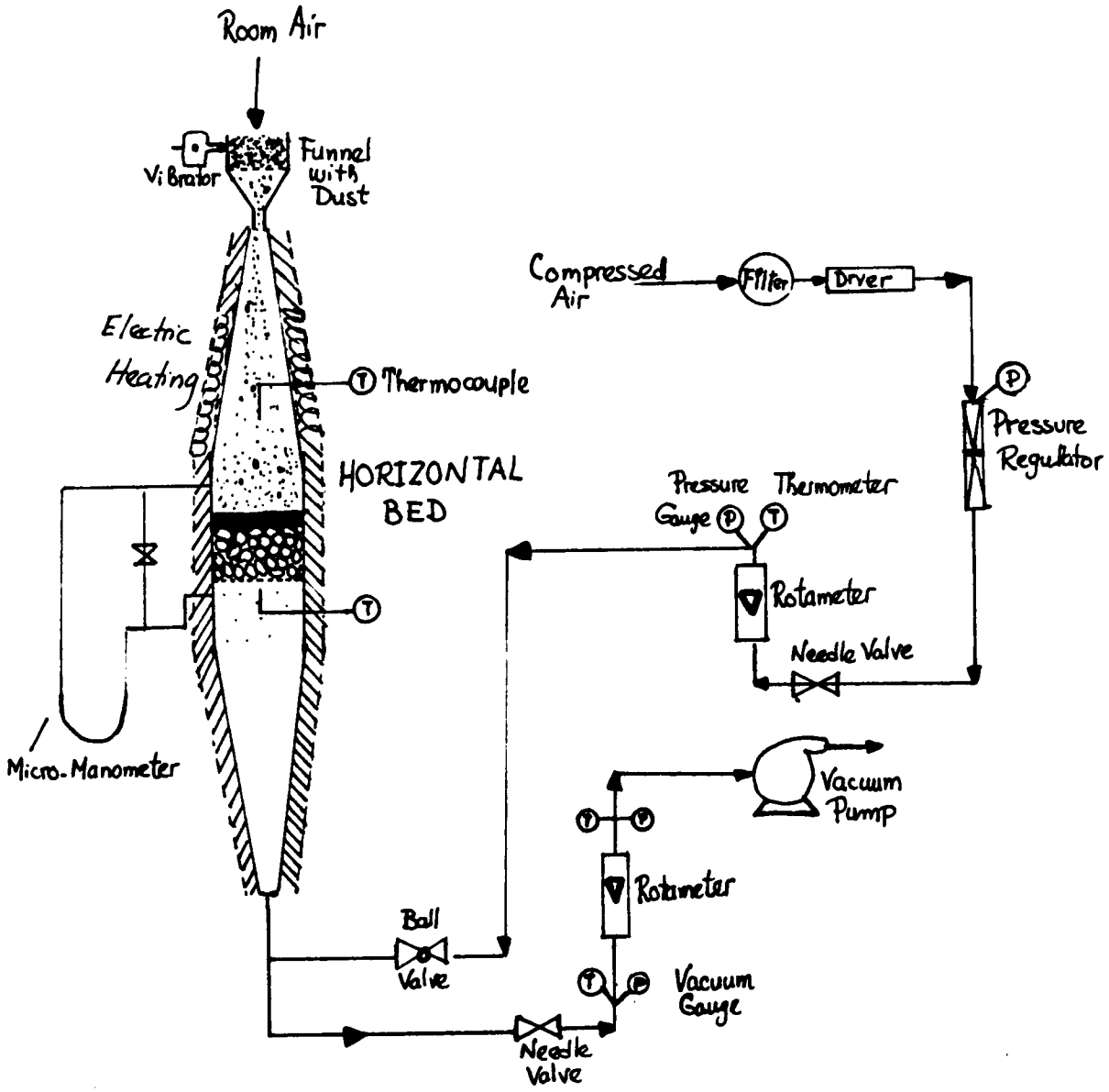

Figure 5-6 Schematic of Horizontal Bed Apparatus.

pipe-line system and the unit is levelled.

3. The following procedure was used for establishing the sand bed:

a. We directed a jet of dry air upon the inner wall of the upper part of the bed housing of Figure 5-6 to remove any dust that had clung to the wall during the previous deposition experiment.

b. The sand was fluidized at a velocity much higher than the minimum fluidization velocity, until no trace of dust could be seen from the gases leaving the holder at the top (this was done with a powerful light and after removing a hose which connected the bed holder to a bag filter).

c. The velocity is decreased and fixed as closely as possible to the minimum fluidizing-gas velocity for a short period of time, while tapping the glass around its circumference.

d. When the surface of the bed is thoroughly levelled, the flow is suddenly stopped by closing a ball valve.

This procedure, although somewhat arbitrary, was a reproducible one for establishing the sand bed.

4. Once the sand bed is ready for the deposition experiments, the electrical heaters and vacuum pump are turned on.

5. Temperature is measured before and after the sand bed with thermocouples, which lead to a temperature controller connected to variable transformers.

6. For a preselected superficial velocity, the mass flow

rate is adjusted with a rotameter until steady state is reached (uniform temperature).

7. With the bed holder at 150° C, and with air flowing through it at a given velocity the initial pressure drop is recorded.

8. At this moment a previously weighed batch of the dust is charged to a metalic funnel provided with a 100-mesh screen, and depositing the dust was begun with the help of an electrical vibrator. The rate of feeding was difficult to control, and was usually somewhat greater in the earlier part of a step putting down an increment in dust. In general, we tried to feed the dust at a rate of about 0.5 gram per minute.

9. Pressure drops were determined by a micromanometer and water, oil or mercury manometers, as appropriate. For small pressure drop intervals the volumetric flow rate was adjusted in order to keep a constant-velocity deposition.

10. The amount of dust fed is recorded as a function of air pressure drop until a surface cake is formed.

11. At this moment the flow is reduced very slowly until no air enters the system.

12. The insulation is removed and the cake is visually examined. Emphasis is given to a) cake's surface roughness; b) size and number of pinholes; c) cracks or fissures at the cake's surface.

13. After waiting until the unit is at ambient temperature, the bed holder is carefully removed and the

sand-dust mixture is separated after sifting in a 80-mesh screen.

14. By substracting the total amount of dust deposited from the total amount fed, the wall losses are estimated.

15. For calculating the areal density of dust (grams of dust deposited per unit surface area of sand bed) as a function of cake pressure drop, the wall losses were distributed proportionally to amount of dust fed.

16. Some tests were repeated for studying the stability of the cakes formed. After depositing the cakes, air was introduced from the bottom until the cake collapsed.

5.03 Particle Counting in Optical Microscope

While working with the laboratory panel bed filter at 150^{o} C, we undertook limited studies to determine the distribution of particle size in the filtered air, in order to obtain an estimate of the efficiency of capture of sub-micron particles. We took the glass fiber filter papers from selected runs and made them transparent after pouring a few drops of a high-viscosity Cargille's Immersion Oil on their surfaces. The filter papers were then mounted on pre-cleaned Kimble Exax Micro Slides and covered with Corning Glass Cover No 0 to protect the microscope's lenses. Using an optical microscope with 1000X magnification (100X objective, and 10X eye-piece) and using an oil immersion technique, we were able to detect particles as small as 0.4 microns under white light. A filter paper is 47 mm in diameter, and the circle of collected dust is 31.79 mm. We divided the dust circle

into two rings of equal area, and we focused our microscope upon four counting fields at the center of each ring, to obtain eight counting fields altogether, as illustrated in Figure 5-7. The microscope was calibrated with a 0.01 mm scale, with which we used a micrometer for which, at 1000X magnification, one division = one micron. The area of the viewing field was 25,450 square microns, while the area covered by the scale of the micrometer was 7,854 square microns (diameter = 100 microns). We used this last area as a counting field.

5.04 Dust and Granules General Characteristics

a) Granules

a-1 Angular Sand

Commercially available angular silica sand of different particle sizes was obtained from a local distributor in the Bronx. The true density of these granules was estimated as 2.61 gr/cm^3. The sphericity (as defined in Section (4.04.26) of angular sands is reported to be 0.73 (Perry and Chilton, page 5-73, 1973). For this value of sphericity experience indicates that the range of bed porosities would be between 0.42 and 0.52 (Figure B-12, p.537, Foust et al, 1960).

a-2 Silicon Carbide

Silicon Carbide with a plate-like shape was supplied by Norton Company of Worcester, Massachusetts. It is specified as "Crystolon Abrasive Grain." For particles of this shape the concept of sphericity cannot be applied and therefore equivalent spherical diameters cannot be propery defined.

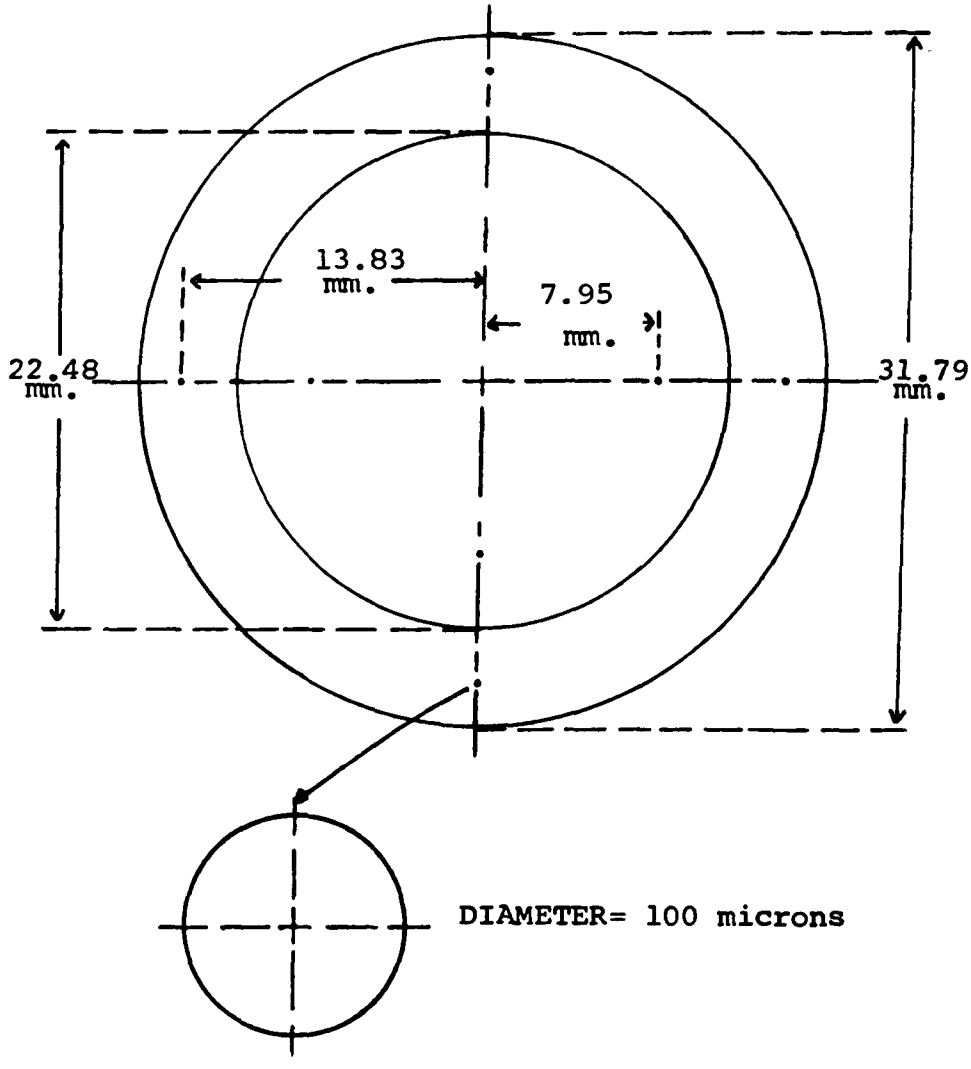

Figure 5-7 Location of microscopic counting fields used for determination of particle size distribution on glass fiber filter papers.

From experience, however, the porosity of beds formed with granules of this shape tend to be smaller than the ones obtained in beds of particles with a close to spherical shape.

b) Dusts

b-1 Consolidated Edison Coal Fly Ash

Coal fly ash furnished by Consolidated Edison Company of New York from a station with an electrostatic precipitator working at beyond 99% efficiency (overall and on a weight basis) was the first dust tested in our 150° C panel bed filter. This ash was also used by Paretsky (1972) and Lee (1975) in their room temperature panel bed filtration experiments. Its particle size distribution as determined by Paretsky and Con Edison (Paretsky, 1972) was given in Figure 3-6 of this dissertation.

In early 1977, we arranged for Coulter Electronics Laboratory to obtain a particle size distribution of this ash in a Model TA II Coulter Counter. This distribution shown in Figure 5-8 is a typical log-normal distribution with a mass median diameter of 15.8 micrometers and a geometric standard deviation of about 3.1.

b-2 Commonwealth Edison Coal Fly Ash

Coal fly ash, collected in an electrostatic precipitator working at efficiencies beyond 99% (overall and on a weight basis) in the stack of a coal-fired power plant owned by Commonwealth Edison Company of Chicago was the second dust tested in our 150° C laboratory panel bed filter. Its particle size distribution, as determined by Coulter Electronics Laboratory in a Model TA II Coulter Counter is given in Figure 5-9.

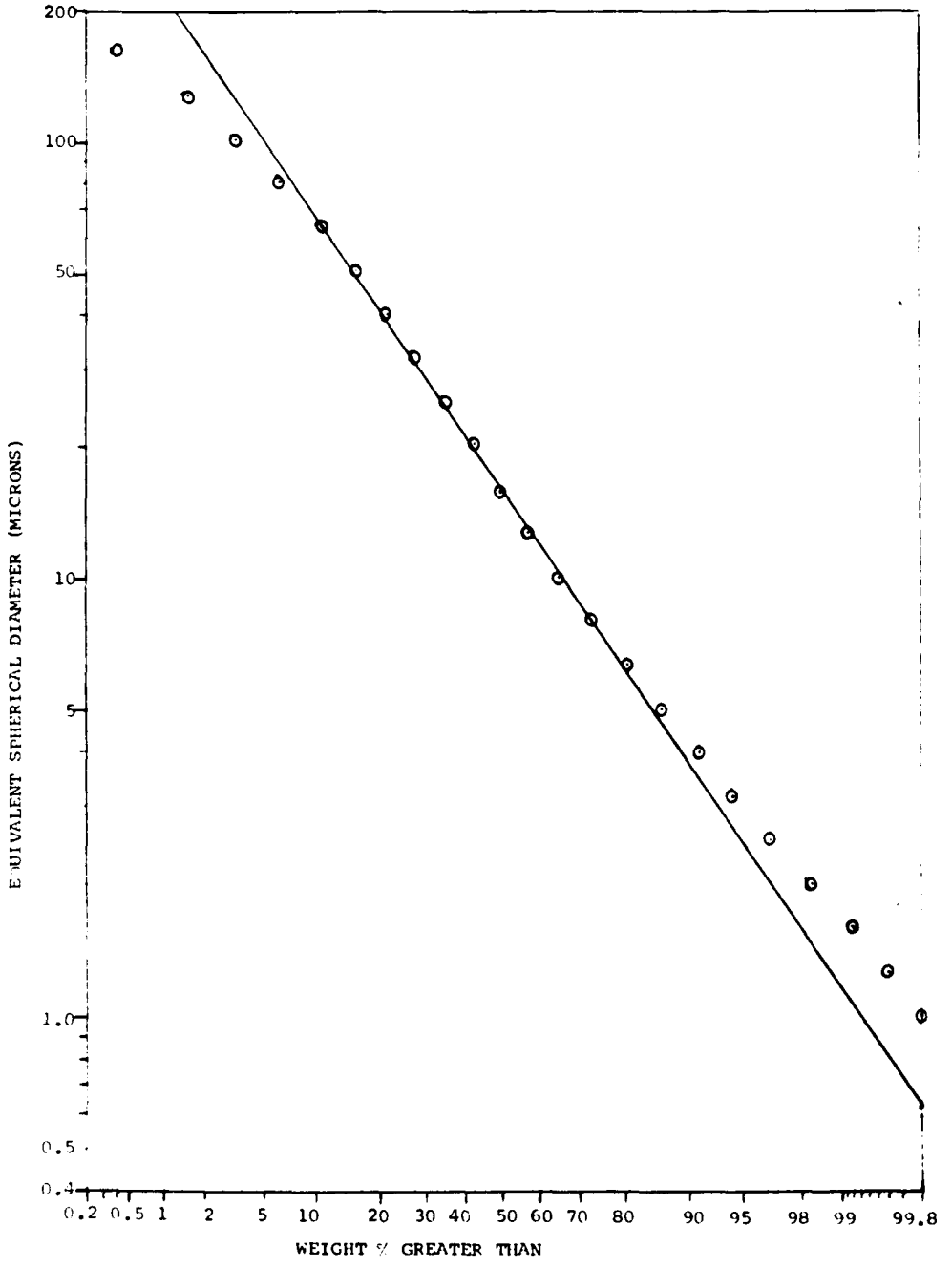

Figure 5-8 Distribution of particle size in fly ash determined by a Model TA-II Coulter Counter. (Consolidated Edison Coal Fly Ash)

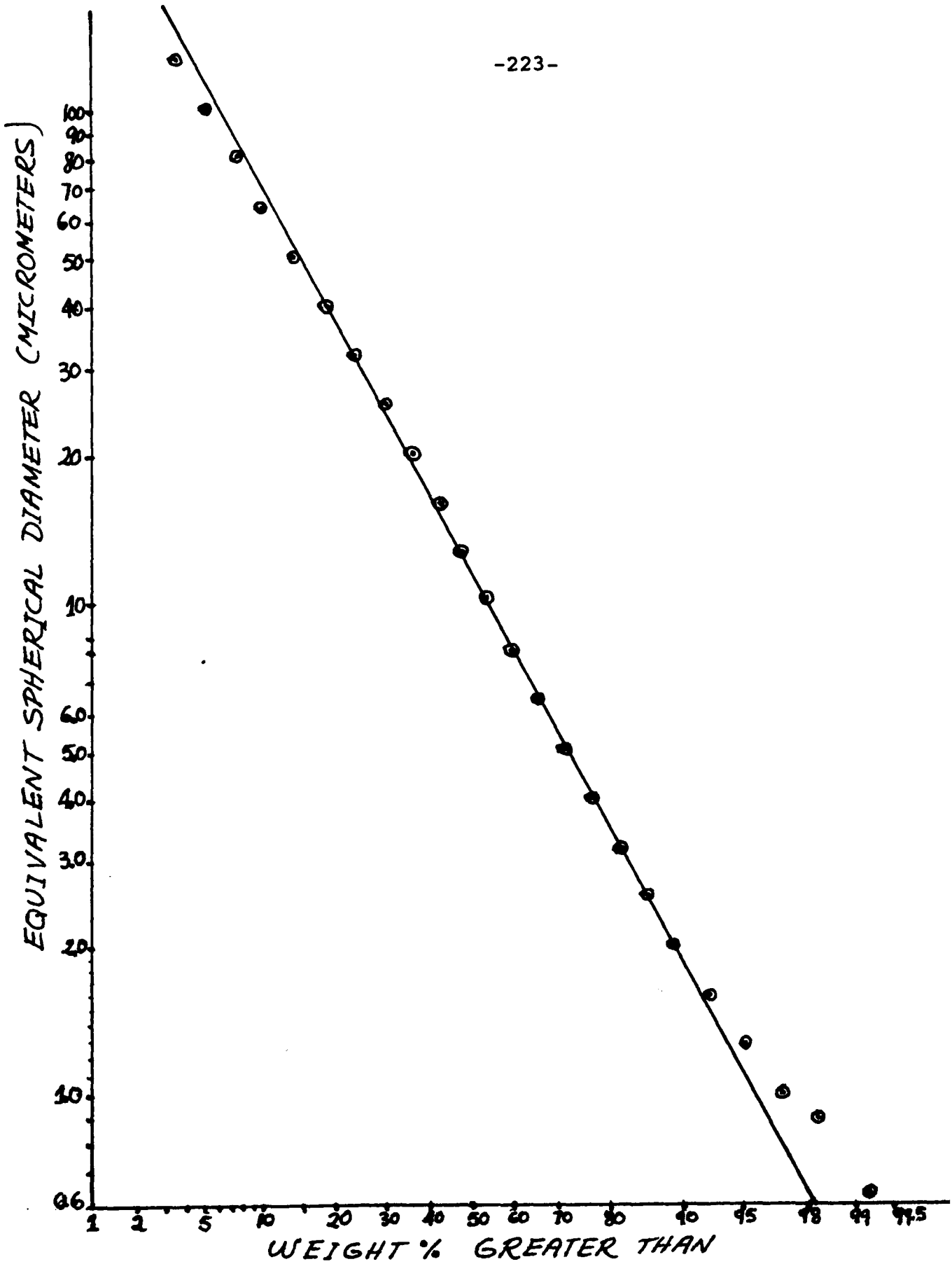

Figure 5-9 Distribution of Particle Size in Fly Ash Determined by a Model TA II Coulter Counter (Commonwealth Edison Coal Fly Ash).

This log-normal distribution has a mass median diameter of 11.4 micrometers and a geometric standard deviation of about 4.1.

b-3 Clinker Cooler Cement Dust

A sample of Portland cement, collected in a bag filter working at efficiencies beyond 99.9% (overall, on a weight basis) at the outlet of a clinker cooler of a cement plant owned by Lehigh Portland Cement Company, was the third dust used in our filtration experiments.

Its particle size distribution as determined by Coulter Electronics Laboratory in a Model TA II Coulter Counter is given in Figure 5-10. This distribution deviates considerably from a log-normal distribution. It has a mass median diameter of 38.2 micrometers and a standard deviation of about 3.1.

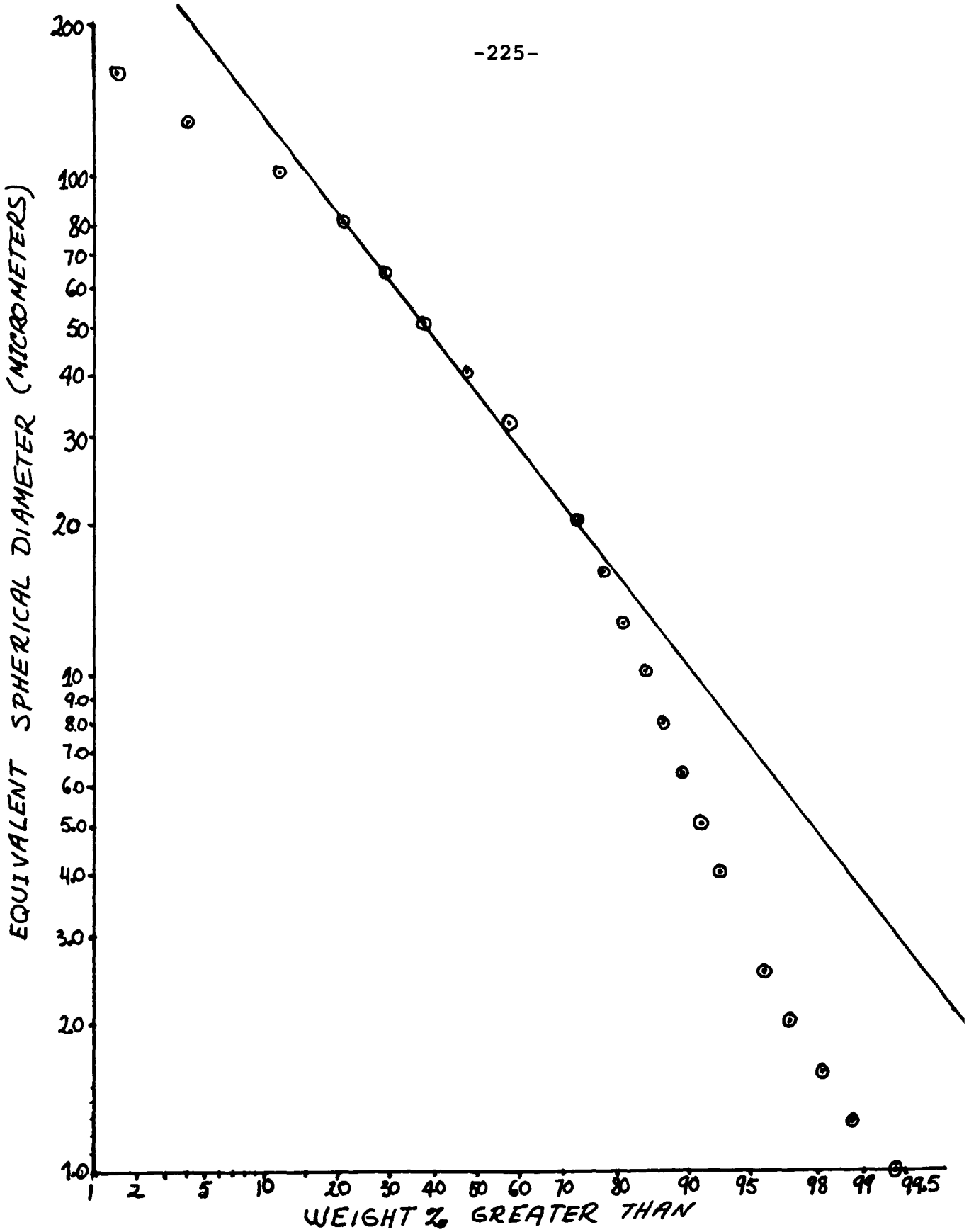

Figure 5-10 Distribution of Particle Size in Cement Determined by a Model TA II Coulter Counter (Clinker Cooler Cement Dust).

CHAPTER 6.0: 150° C PANEL BED FILTRATION DATA

This Chapter 6.0 presents the filtration performance of a small laboratory panel bed filter operated at 150° C and atmospheric pressure. The effect of filtration velocity, filtration cycle time and intensity of cleaning, upon the penetration of three different dusts in the 150° C panel bed were explored. Most experiments were performed using angular sand as the filtration foundation medium, but a few experiments have been conducted with silicon carbide.

Exploratory runs, using the arrangement of louvers shown in Figure 3-10 were conducted before we realized the advantages that the wishbone louvers (Figure 5-2) have for dust filtration. Thereafter, most of the work was done with this later arrangement.

6.01 Consolidated Edison Coal Fly Ash

Coal Fly Ash captured in an electrostatic precipitator working at beyond 99% by weight collection efficiency was supplied by Consolidated Edison Company of New York. This ash was previously used by Paretsky (1972) and Lee (1975) for room-temperature laboratory panel bed filtration experiments. Figure 3-6 gives the distribution of particle sizes in the ash as reported by Con Edison and also as determined by Paretsky (1972). Figure 5-9 gives the distribution, obtained with a Model TA II Coutler Counter in early 1977.

6.01.1 Exploratory Tests in Panel Bed fitted with Chevron Louvers

The louvers arrangement shown in Figure 3-10 was the one used and recommended by Lee (1975) for panel bed filtration. At the outset of this research those louvers were installed and tested in our laboratory panel bed at 150^{o} C.

The very first experiments, after smooth operation was achieved, were conducted with 20-30 mesh angular sand at superficial velocities ranging from 11.2 to 20.3 cm/s. Visual observation of the free sand surfaces indicated that the formation of an efficient, dense, stable filter cake was not favoured by this sand particle size. The cumulative overall penetrations varied from about 0.1 to 0.3 Wt%, and always increased with superficial velocity.

With this sand particle size, fly ash penetrated deep into the bed and high puffback intensities were required for effective cleaning of the unit. Even with strong puffbacks the ash penetrated deeper at the bottom of the filter, provoking non-uniformity in the dust concentration on the clean side of the panel, higher penetrations being indicated by the lower of our two sampling stations.

It was soon recognized that the advantages of this coarse sand (small pressure drops) implied a drastic loss in filtration performance. As a result the sand size was reduced to 40-50 mesh and exploratory runs were conducted.

Table 6-1 gives a summary of the filtration data ob-

tained with the chevron louvers and 40-50 mesh sand.

TABLE 6-1: Panel Bed with Chevron Louvers: Filtration with 40-50 Mesh Sand at 150° C

Vs (cm/s	Pov (Wt%)	ΔP cake (cm H_2O)	(Fly Ash/Sand) Puffback
11.12	0.037	1.3	0.08
17.2	0.062	3.1	0.12
20.05	0.32	3.1	0.05
26.9	0.23	4.6	0.08

where:

Vs: stands for superficial velocity of air

Pov: stands for cumulative, overall penetration on a weight basis

ΔP cake: stands for gas pressure drop across the cake

(Fly Ash/Sand) puffback = Weight Ratio of solids spilled during puffback

One filtration run at 11.12 cm/s was extended to 20 filtration cycles and no deterioration in the condition of the unit or the fly ash deposit was observed.

In most of these filtration runs deeper penetration of dust at the bottom of the unit was observed, a clear indication that some of the dirty sand close to the filter's surface was descending behind the louver plates during puffback.

After recognizing the advantages that the wishbone louvers have for dust filtration, the chevron louver tests

were stopped, and a systematic study of filtration performance was undertaken with the new louver's design.

6.01.2 Tests with Panel Bed Fitted with Wishbone Louvers

As Figure 6-1 illustrates, the wishbone louvers guarantee that if dust penetration does not go beyond the louver's plate, no "dirty" sand descends into the bed as puffback is applied.

Lee et al. (1977), while studying puffback in a 3.048 m-tall panel bed, concluded that the wishbone design afforded uniform sand spills across the height of the filter for a wider range of puffback parameters than the chevron design. More importantly, the wishbone design did not display a defect of the chevron design when used in a tall panel, viz., a massive descent of solid from upon the upper most louvers into the interior of the column of fine solid in the last stages of puffback.

The wishbone louver design allowed us to explore the effect of higher cake pressure drops upon filtration performance without risk of an eventual saturation of the bed.

6.01.21 Tests with 40-50 Mesh Sand

The experience gained with the exploratory runs conducted with 20-30 mesh sand and the chevron louvers indicated us that if high efficiency at 150^{o} C is required, a smaller sand size must be used. Without exploring intermediate sizes, 40-50 mesh sand was selected.

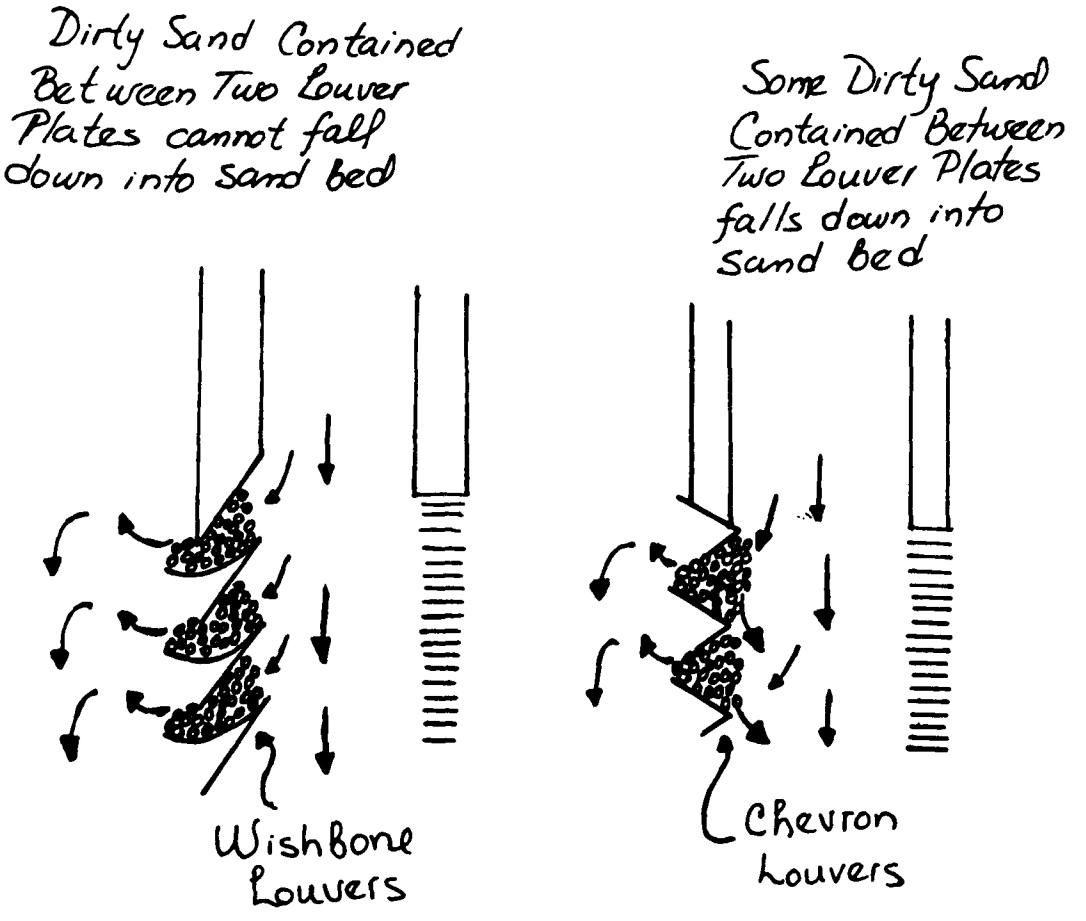

Figure 6-I Comparison Between "Wishbone" and "Chevron" Louver Designs

6.01.21.1 Tests with 40-50 Mesh Sand at 7.75 cm/s and 150° C

This was the lowest velocity that we explored. Commercial applications at still lower velocities seem unlikely. Preliminary tests, not reported here, showed relatively little effect of puffback intensity upon penetration of fly ash at a face velocity of 7.75 cm/sec, so long as the pressure in the puffback gas reservoir was at least 170.3 kPa (10 psig). We standardized upon this pressure thereafter.

Figure 6-2 shows the measured penetrations of fly ash for operation at 7.75 cm/s and 150° C at four densities of fly ash cake. Table 6-2 summarizes the performance of the panel bed at this velocity. Tables 6a-1 through 6a-4 of the Appendix to Chapter 6.0 give the data.

TABLE 6-2: Summary of Panel Bed Performance at 7.75 cm/s and 150° C

Puffback Tank: Volume = 206 cm^3 Pressure = 170.3 kPa (10 psig)

ΔPc (cm H_2O)	ΔPi (cm H_2O)	DPB_{4-10} (grs)	DD_{4-10} (grs)	GPB_{4-10} (grs)	$(DPB/GPB)_{4-10}$	Pov_{1-3} (Wt%)	Pov_{4-10} (Wt%)
3.81	6.5	8.14	1.74	49.2	0.17	.022	0.025
7.62	6.7	12.9	2.78	65.5	0.20	0.0127	0.011
11.4	7.7	16.93	3.51	135.7	0.12	0.018	0.0143
15.2	7.9	18.99	4.24	137.84	0.14	0.0085	0.009

where:

ΔPi = Initial, "clean bed" pressure drop

DPB_{4-10} = Average weight of dust spilled during one puffback (Arithmetic average for filtration cycles 4 through 10)

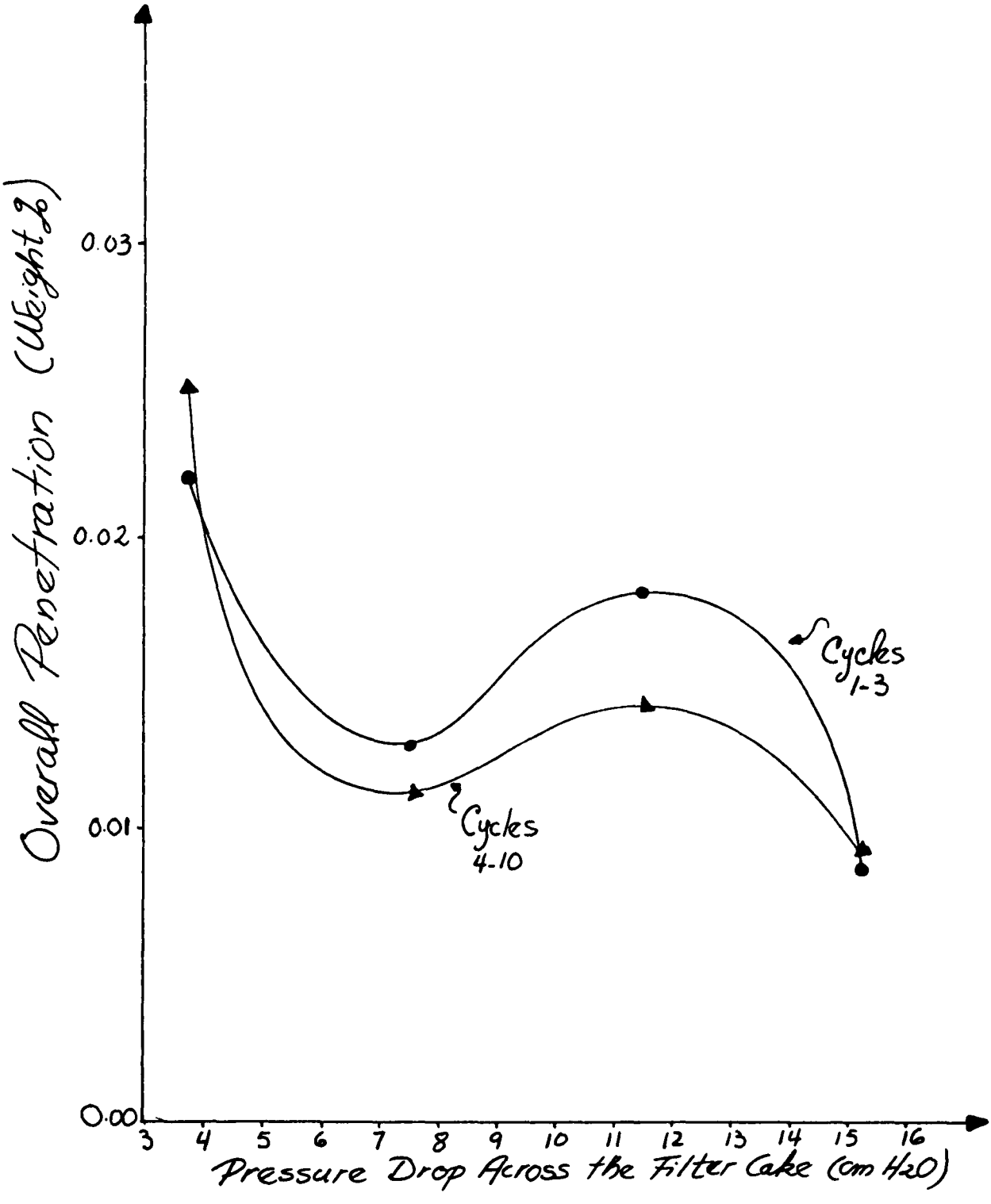

Figure 6-2 Penetration versus buildup in pressure drop due to filter cake for 7.75 cm/s (15.2 ft/min) at 150°C.
ANGULAR SAND (40-50 Mesh)-CON EDISON FLY ASH

DD_{4-10} = Average weight of dust drained before cleaning (Arithmetic average for filtration cycles 4 through 10)

GPB_{4-10} = Average weight of granules spilled during one puffback (Arithmetic average for filtration cycles 4 through 10)

Pov_{1-3}, Pov_{4-10} = Cumulative, overall penetration on a weight basis for cycles 1-3 and 4-10 respectively

It will be seen from the tables that the weight gain on filter papers was small, and therefore no attempt was made to determine a value of the penetration for a single filtration step. Experience of Lee (1975) at room temperature had shown higher penetrations in the initial cycle, with penetration falling to a reasonably steady value by about the third cycle. Accordingly, we measured the combined penetration for the first through the third cycles, and also for the fourth through subsequent cycles.

Notice the trend toward larger spills of sand in Table 6-2, although the puffback intensity was held constant. This trend is typical for increasing density of the fly ash filter cake achieved prior to puffback, and is caused, we believe, by increased resistance to movement of puffback gas across the panel bed and a resulting increase in active time.

6.01.21.2 Tests with 40-50 Mesh Sand at 11.12 cm/s and 150° C

A series of runs, at a constant cake density before cleaning and at puffback pressures of 170.3, 204.7 and 239 kPa (10,15 and 20 psig) showed little effect of this variable upon penetration at 11.12 cm/s and 150° C. Table 6-3

summarizes the data given in Tables 6a-5 through 6a-7 of the Appendix.

TABLE 6-3: Puffback Intensity Effect at 11.12 cm/s and 150° C

Puffback Tank: Volume = 206 cm^3

Pressure Drop due to Filter Cake before cleaning = 7.62 cm H_2O

PBP kPa	ΔPi cm H_2O	DPB_{4-10} grs	DD_{4-10} grs	GPB_{4-10} grs	$(DPB/GPB)_{4-10}$	Pov_{1-10} Wt%
170.3	6.5	12.03	3.43	62.16	0.19	0.026
204.7	8.4	11.64	2.64	134.29	0.09	0.027
239	7.7	12.63	3.73	142.67	0.09	0.023

We then conducted another series of runs, each at a puffback pressure of 170.3 kPa, to explore the effect of the density of filter cake achieved prior to puffback cleaning. Figure 6-3 gives the penetration versus cake pressure drop and Table 6-4 summarizes the data given in Tables 6a-8 through 6a-11 of the Appendix.

TABLE 6-4: Effect of Density of Cake at 11.12 cm/s and 150° C

Puffback Tank: Volume = 206 cm^3 Pressure = 170.3 kPa (10 psig)

ΔPc cm H_2O	ΔPi cm H_2O	DPD_{4-10} grs	DD_{4-10} grs	GPB_{4-10} grs	$(DPB/GPB)_{4-10}$	Pov_{1-3} Wt%	Pov_{4-10} Wt%
3.81	8.4	6.61	0.53	46.86	0.14	0.055	0.023
7.62	10.8	11.67	0.66	91.89	0.13	0.033	0.03
11.43	9.4	14.3	0.78	106.94	0.13	0.012	0.0104
15.24	9.1	18.06	1.86	108.41	0.17	0.02	0.023

Notice that tables 6a-5 and 6a-9 give data for duplicate runs. Penetrations are substantially identical, but the run of Table 6a-9 experienced appreciably larger spills of sand for

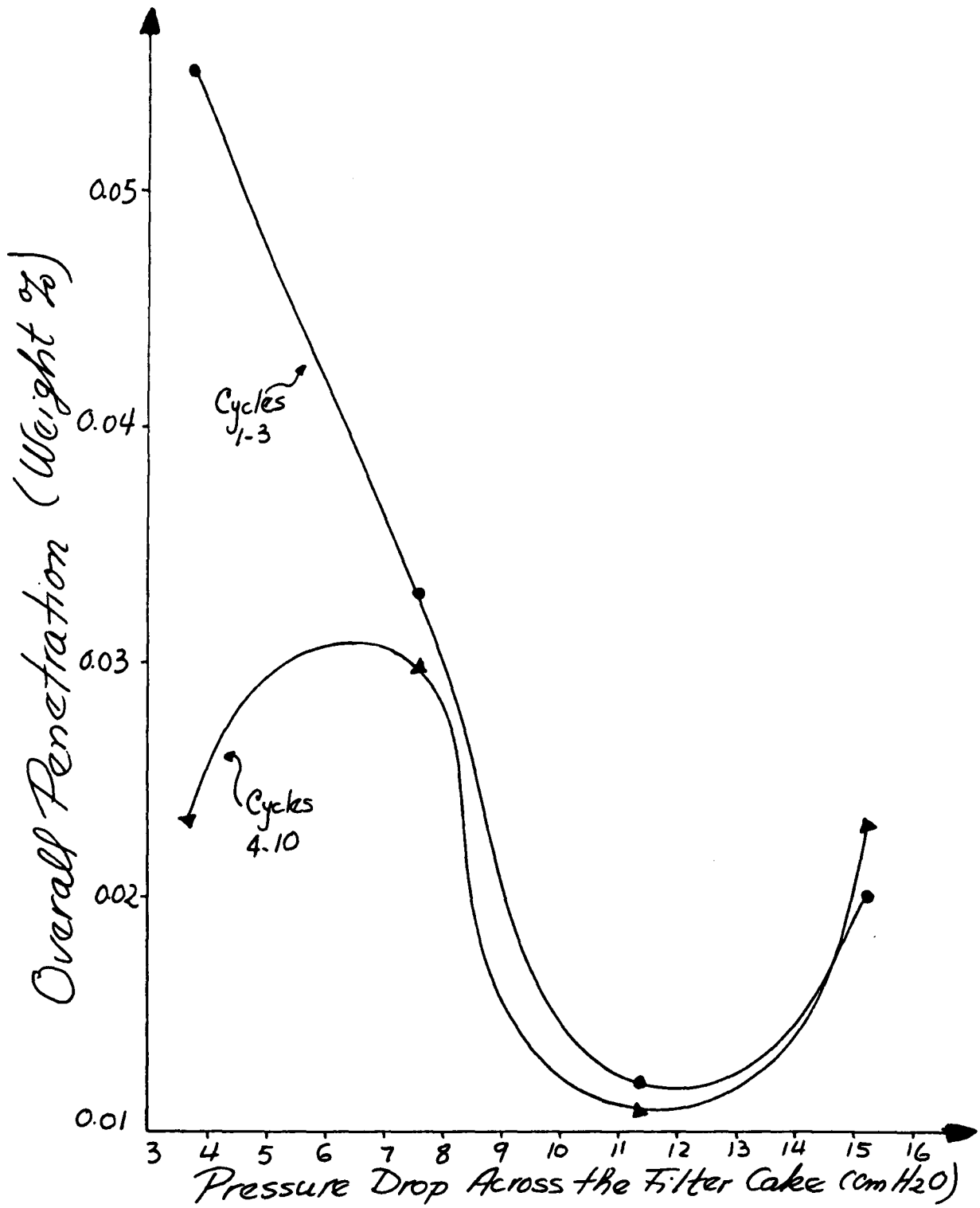

Figure 6-3 Pemetration versus buildup in pressure drop due to filter cake for 11.12 cm/s (21.9 ft/min) at 150°C. ANGULAR SAND (40-50 Mesh)-CON EDISON FLY ASH.

an identical puffback intensity. The run of Table 6a-9 was conducted nine months later than the run of Table 6a-5, and we attribute the difference in spills to a change in the working of our set-up for puffback. (Our earlier practice was to tighten bolts by hand, connecting the tapered section in Figure 5-2 to the panel bed. In later work, the bolts were tightened using a wrench.) Another difference to notice in the tables is that the sand bed was looser at the outset of the run in table 6a-5, giving a lower pressure drop in the first few filtration cycles.

6.01.21.3 Tests with 40-50 Mesh Sand at 17.2 cm/sec and 150° C

A series of runs exploring effect of puffback pressure produced a major surprise, and indicated to us that the situation at 17.2 cm/sec was markedly different from anything we had seen before. As Figure 6-4 illustrates, the penetration was relatively high, beyond 0.2%, at puffback pressure of 170.3 kPa used in work at the lower velocities. Penetration declined drastically, however, with increase in puffback pressure to 239 kPa. Moreover, at 170.3 and 204.7 kPa, the penetration in cycles 4 through 10 was markedly higher than in cycles 1 through 3.

Table 6-5 summarizes the data given in Tables 6a-12 through 6a-14 of the Appendix. All these runs were conducted at a constant density of dirt deposit before cleaning, equivalent to a pressure drop due to the filter cake of 7.62 cm of H_2O.

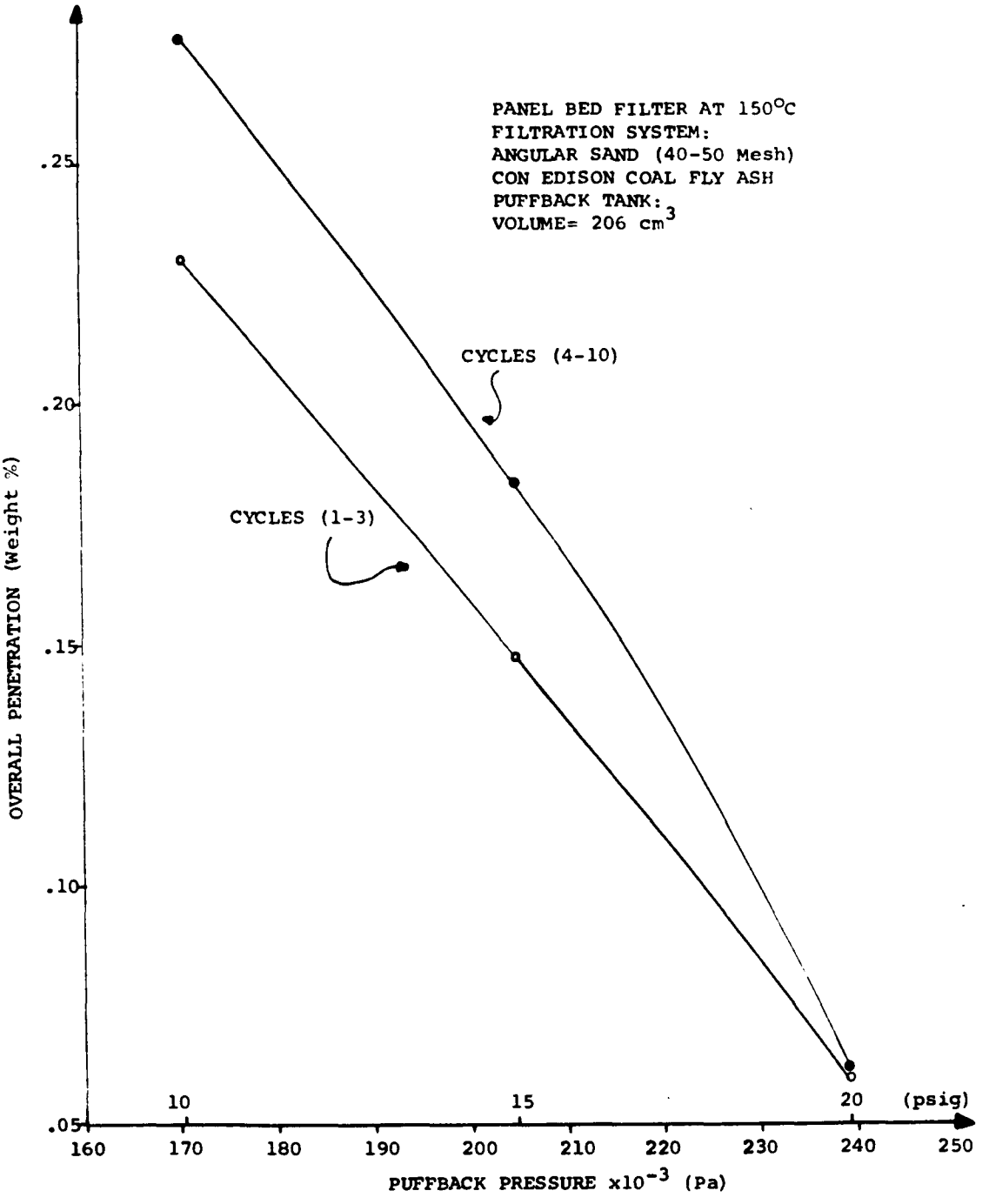

Figure 6-4 Penetration versus puffback pressure for 17.2 cm/s (33.8 ft/min) at 150°C, with buildup of pressure drop due to filter cake of 7.62 cm of H_2O.

TABLE 6-5: Puffback Intensity Effect at 17.2 cm/s and 150° C

Puffback Tank: Volume = 206 cm^3

Pressure Drop due to filter cake = 7.62 cm of H_2O

PBP kPa	ΔPi cm H_2O	DPB_{4-10} grs	DD_{4-10} grs	GPB_{4-10} grs	$(DBP/GPB)_{4-10}$	Pov_{1-3} Wt%	Pov_{4-10} Wt%
170.3	11.5	6.96	1.04	52.0	0.13	0.23	0.276
204.7	10.1	7.67	1.16	88.66	0.09	0.148	0.184
239	13.2	7.76	1.51	123.67	0.06	0.06	0.061

Lee (1975), working at room temperature, had developed a view of panel bed filtration stressing the importance of the "roots" of the filter cake for good filtration efficiency. In his view, puffback intensity should not be so high as to remove all of the roots, which play a role in reestablishing a new filter cake quickly at the beginning of a subsequent filtration step.

In the context of the data of Figure 6-4, however, we should remark that Lee's fly ash deposits were alway comparatively "thin." Their pressure drop was usually less than 3 cm of water. They did not need to be thick to achieve good filtration efficiency, because of the good auto- and adhesivity of fly ash at room temperature. With thick cakes, an intensive puffback would remove the roots and lead to poor efficiency in a subsequent filtration step, as Lee observed.

Figure 6-4 reveals a new effect. It is evident that fly ash is penetrating fairly deep within the bed at 17.2 cm/sec. An intense puffback, as at 239.2 kPa, can concentrate the ash toward the surface of the sand, and thereby lead to

better efficiency. A weaker puffback, as at 170.3 or 204.7 kPa, is less effective in dislodging fly ash within the sand bed and moving it toward the gas-entry surfaces of the bed. Accordingly, penetration is greater because a new filter cake builds more slowly, and penetration values deteriorate with successive filtration cycles as fly ash works its way across the bed. In the terminology of Leith et al. (1976), straight-through penetration is worse at the beginning of a new cycle, and penetration by seepage and/or pinhole plug mechanisms develops gradually with time and hurts performance.

Other experimental evidence is consistent with this picture. Large pinholes appeared in the filter cake in runs at 17.2 cm/sec and lower puffback intensities. Large fly ash particles appeared on the filter papers of our isokinetic samples downstream from the panel bed, something not seen in work at lower velocities. The filter paper near the bottom of the panel bed experienced larger weight gains than the filter near the top, reflecting larger penetrations of fly ash across the bed at the bottom. This, too, is something not seen in work at lower velocities at 150^{o} C, although Lee (1975) had seen such behavior in tests at room temperature with 10-14 mesh sand at a face velocity of 5.6 cm/sec (11 ft/min), for which penetrations ranged from 1.2% during a first cycle downward to 0.3% in fourth and fifth cycles.

The new behavior seen in Figure 6-4 was not evident from runs exploring effect of puffback pressure at our two lower

velocities, 7.75 and 11.12 cm/sec. It does not appear necessary, therefore, to abandon Lee's view of the role of filter cake roots in panel bed filtration if the penetration of fly ash into the bed is not "too deep." Lee's picture may be somewhat over-simple, and it would be good to know, the relative importance of Leith et al.'s three penetration mechanisms in determining the efficiency of a panel bed. The behavior exemplified in Figure 6-4 has taught us that one role of puffback may be to dislodge fly ash that has penetrated "too far" within the sand bed, and to move it toward gas-entry surfaces. Even at our lower velocities, we know that the pressure drop across the panel bed builds steadily if the puffback is too weak.

Figure 6-5 gives results of runs exploring effect of the thickness of the filter cake at 17.2 cm/s and 150° C, with puffback pressure held constant at 204.7 kPa. Table 6-6 summarizes these data given in detail in Table 6a-15 through 6a-18 of the Appendix.

TABLE 6-6: Effect of Density of Cake at 17.2 cm/s and 150° C

Puffback Tank: Volume = 206 cm^3 Pressure = 204.7 kPa

ΔPc cm H_2O	ΔPi cm H_2O	DPB_{4-10} grs	DD_{4-10} grs	GPB_{4-10} grs	$(DPB/GPB)_{4.10}$	Pov_{1-3} Wt%	Pov_{4-10} Wt%
7.62	12.7	7.94	0.57	162.74	0.05	0.068	0.032
11.43	14.0	11.39	1.31	169.0	0.07	0.03	0.044
15.24	13.0	13.66	1.23	190.81	0.07	0.031	0.03
19.05	13.9	16.27	1.59	185.29	0.09	0.022	0.014

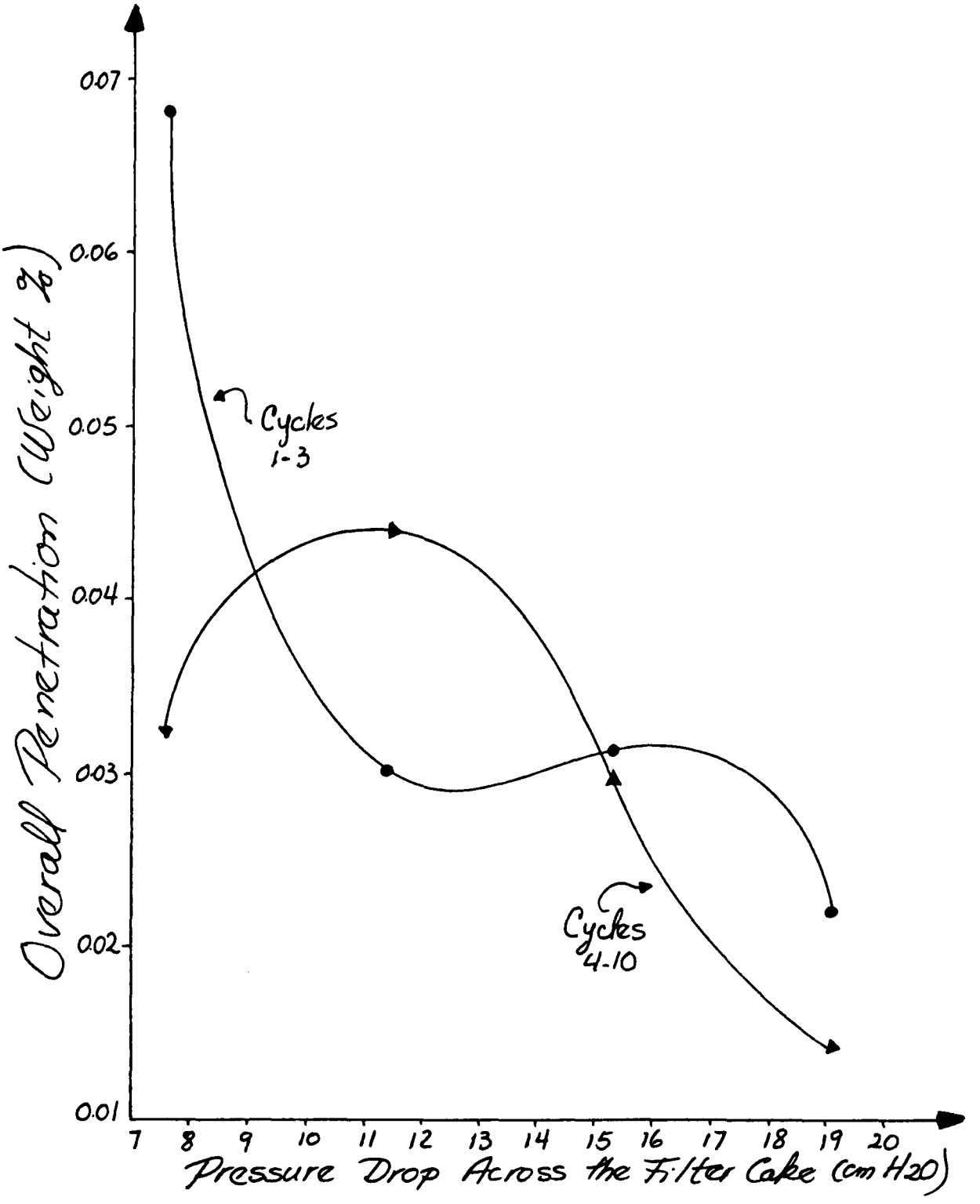

Figure 6-5 Penetration versus buildup in pressure drop due to filter cake for 17.2 cm/s (33.8 ft/min) at 150°C. ANGULAR SAND (40-50 Mesh)-CON EDISON FLY ASH.

Notice that tables 6a-13 and 6a-15 give data for duplicate runs, but the run of Table 6a-15 experienced appreciably larger spills of sand for an identical puffback intensity. The run of Table 6a-15 was conducted nine months later than the run of Table 6a-13. The same problem with our set-up for puffback, discussed in 6.01.21.2 was present here. In total there are six runs reported in this dissertation which we believe were conducted with a leak of puffback air. The presence of this problem is indicated by footnotes at the bottom of tables 6a-5 through 6a-7 and 6a-12 through 6a-14.

The exploration of the effect of the thickness of the filter cake at 17.2 cm/s was conducted at a puffback pressure of 204.7 kPa merely because the sand spills obtained at 239.2 kPa were believed to be too high for panel bed commercial application; nevertheless, one run was made under these conditions. Table 6-7 summarizes the data obtained at this too-strong puffback intensity and Table 6a-19 gives the details of this run.

TABLE 6-7: Performance of Panel Bed at 17.2 cm/s, with a too-strong Puffback Intensity

Puffback Tank: Volume = 206 cm^3

Pressure drop due to filter cake = 11.43 cm H_2O

PBP kPa	ΔPi cm H_2O	DPB_{4-7} grs	DD_{4-7}	GPB_{4-7}	$(DPB/GPB)_{4-7}$	Pov_{1-3}	Pov_{4-7}
239.2	13.68	12.7	1.5	228.58	0.06	0.02	0.01

A comparison between Tables 6-6 and 6-7 discloses that at 11.43 cm of H_2O of cake pressure drop, an increase in puffback

pressure from 204.7 to 239.2 kPa increases the filtration performance of the panel bed. This indicates that even at a puffback pressure of 204.7 kPa the main source of dust penetration is re-entrainment of previously captured particles. Apparently at this filtration velocity, what is really important is to be able to remove dust which penetrates deep into the bed.

6.01.21.4 Exploratory Tests with 40-50 Mesh Sand at 20.3 cm/sec

One series of runs was conducted at 20.3 cm/sec and 150° C to probe further the effect of puffback intensity upon performance at high velocity. Table 6-8 summarizes the data given in Tables 6a-20 through 6a-22 of the Appendix.

TABLE 6-8: Summary of Exploratory Tests with 40-50 Mesh Sand at 20.3 cm/sec

Puffback Tank: Volume = 206 cm^3

Pressure drop due to filter cake = 7.62 cm H_2O

PBP kPa	ΔPi cm H_2O	DPB_{4-10} grs	DD_{4-10} grs	GPB_{4-10} grs	$(DPB/GPB)_{4-10}$	Pov_{1-3} Wt%	Pov_{4-10} Wt%
170.3	17.8	4.14	0.91	27.43	0.15	0.083	0.101
204.7	17.5	5.19	0.83	57.89	0.09	0.069	0.108
239.2	15.8	7.04	1.16	113.11	0.06	0.15	0.089

At the two lower puffback intensities, penetration increased with number of cycles. At the highest intensity, penetration improved with cycling. These effects are consistent with the effects observed at 17.2 cm/s and summarized in Figure 6-4.

It is a puzzle, however, why the penetrations at the two lower intensities are markedly better for the runs at 20.3 cm/s than for those at 17.2 cm/s. Perhaps inertial effects arising from the higher velocity are helping, and indeed may tend to reduce the penetration of fly ash deep within the sand bed. It might also be that the denser cake formed at this high velocity is more stable than the ones formed at the lower velocities and that there is a related reduction in dust penetration by the pinhole-plug mechanism (4.06.2). On the other hand, the penetration at the highest intensity is markedly worse for the run at 20.3 cm/sec than for that at 17.2 cm/s. To understand these curious effects, we may need to know more about the relative importance of Leith's three penetration mechanisms (4.06.2) at each run condition.

6.01.22 Tests with 40-50 Mesh Silicon Carbide at 150^{o} C

The thought occurred to us that a plate-like granule might provide a better foundation for a filter cake than angular sand. Accordingly, we tested 40-50 mesh silicon carbide in the panel bed. Silicon carbide is electrically conducting, and so we were changing two factors at the same time, reducing our chance of drawing a definitive conclusion from comparisons between sand and silicon carbide.

Figures 6-6 through 6-8 give results for runs at 7.75, 11.12, and 17.2 cm/s respectively. Tables 6-9 through 6-11 summarize the data given in detail in Tables 6a-23 through 6a-33 of the Appendix.

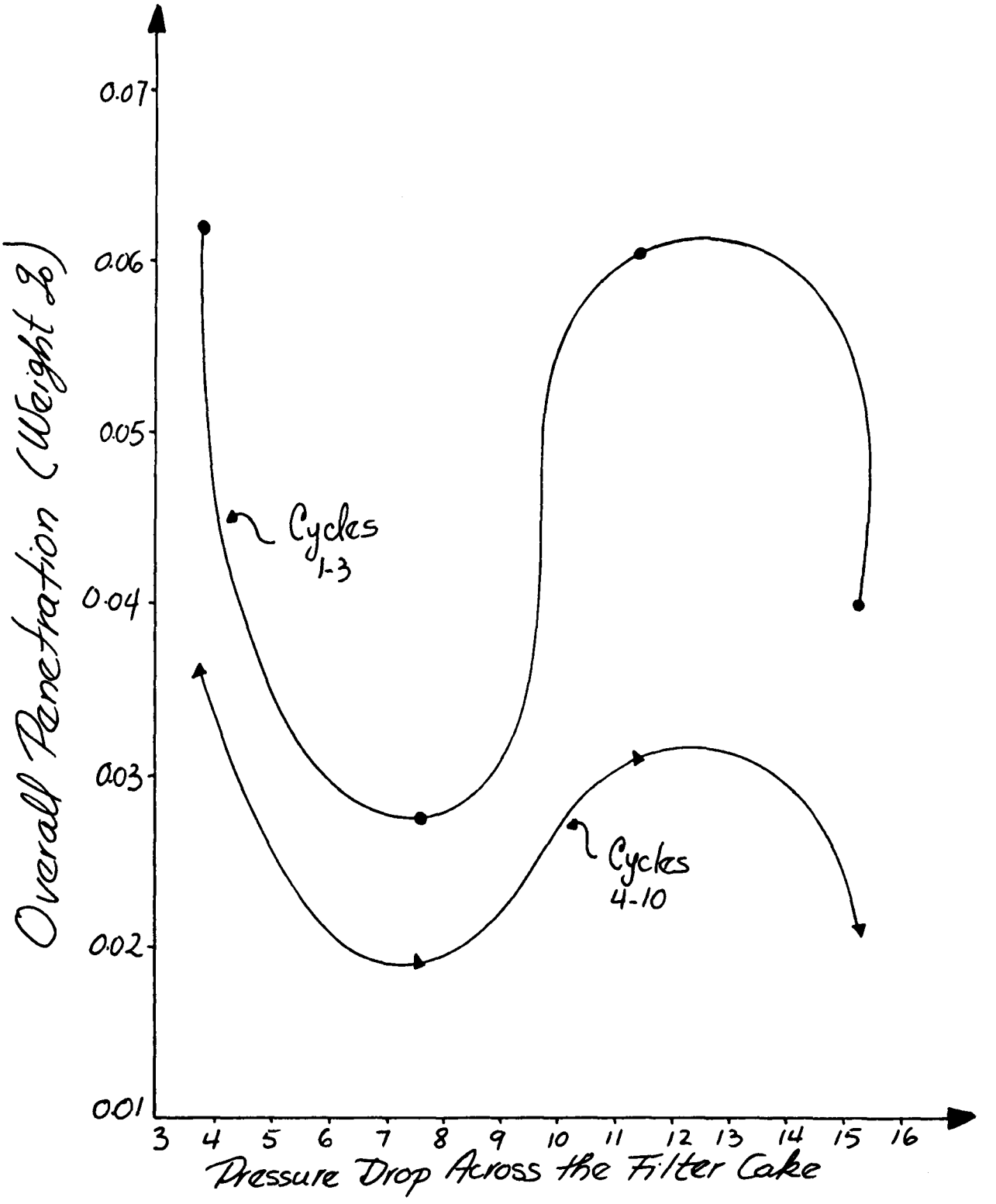

Figure 6-6 Penetration versus buildup in pressure drop due to filter cake for 7.75 cm/s (15.2 ft/min) at 150°C. SILICON CARBIDE (40-50 Mesh)-CON EDISON FLY ASH.

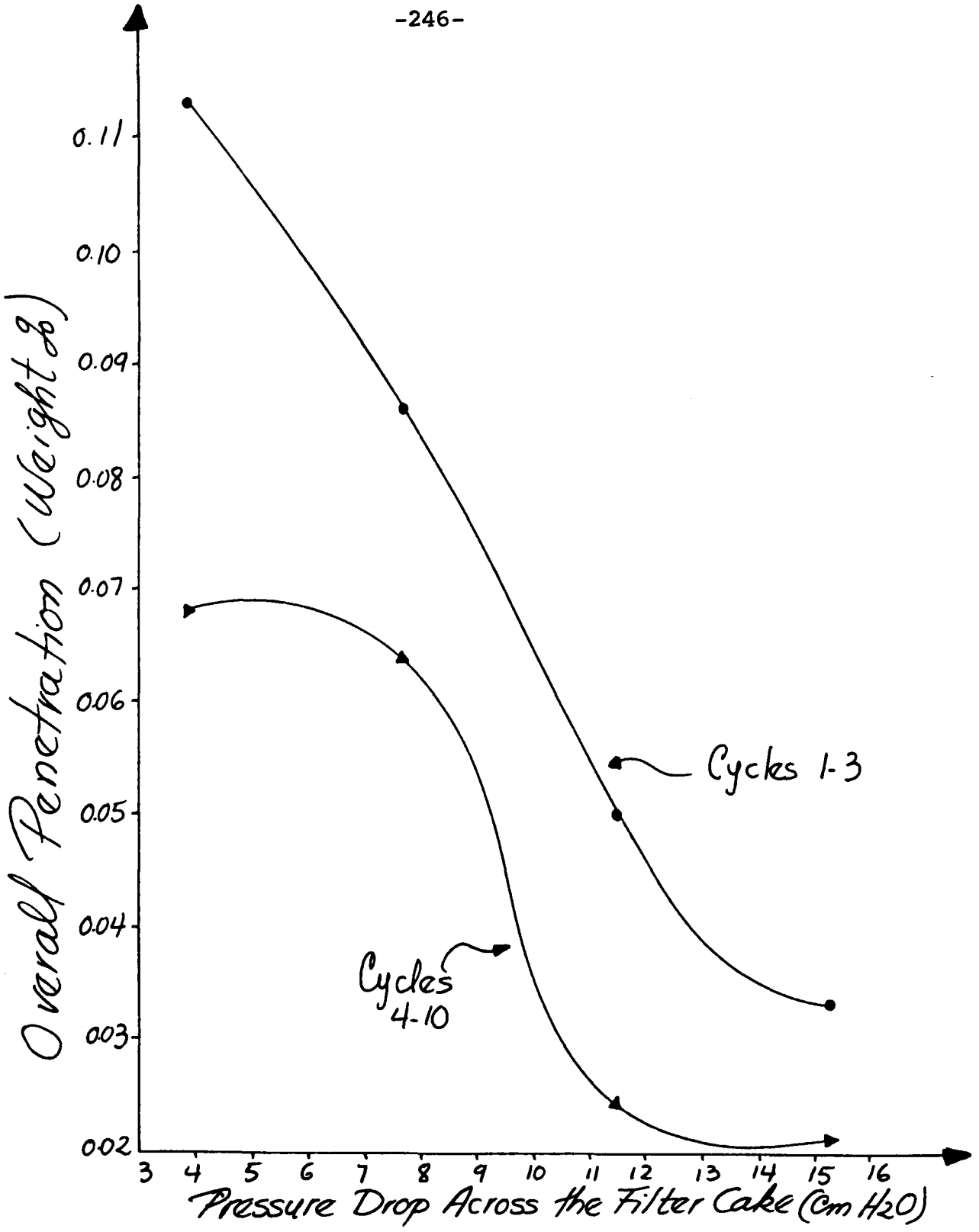

Figure 6-7 Penetration versus buildup in pressure drop due to filter cake for 11.12 cm/s (21.9 ft/min) at 150°C.
SILICON CARBIDE (40-50 Mesh)-CON EDISON FLY ASH.

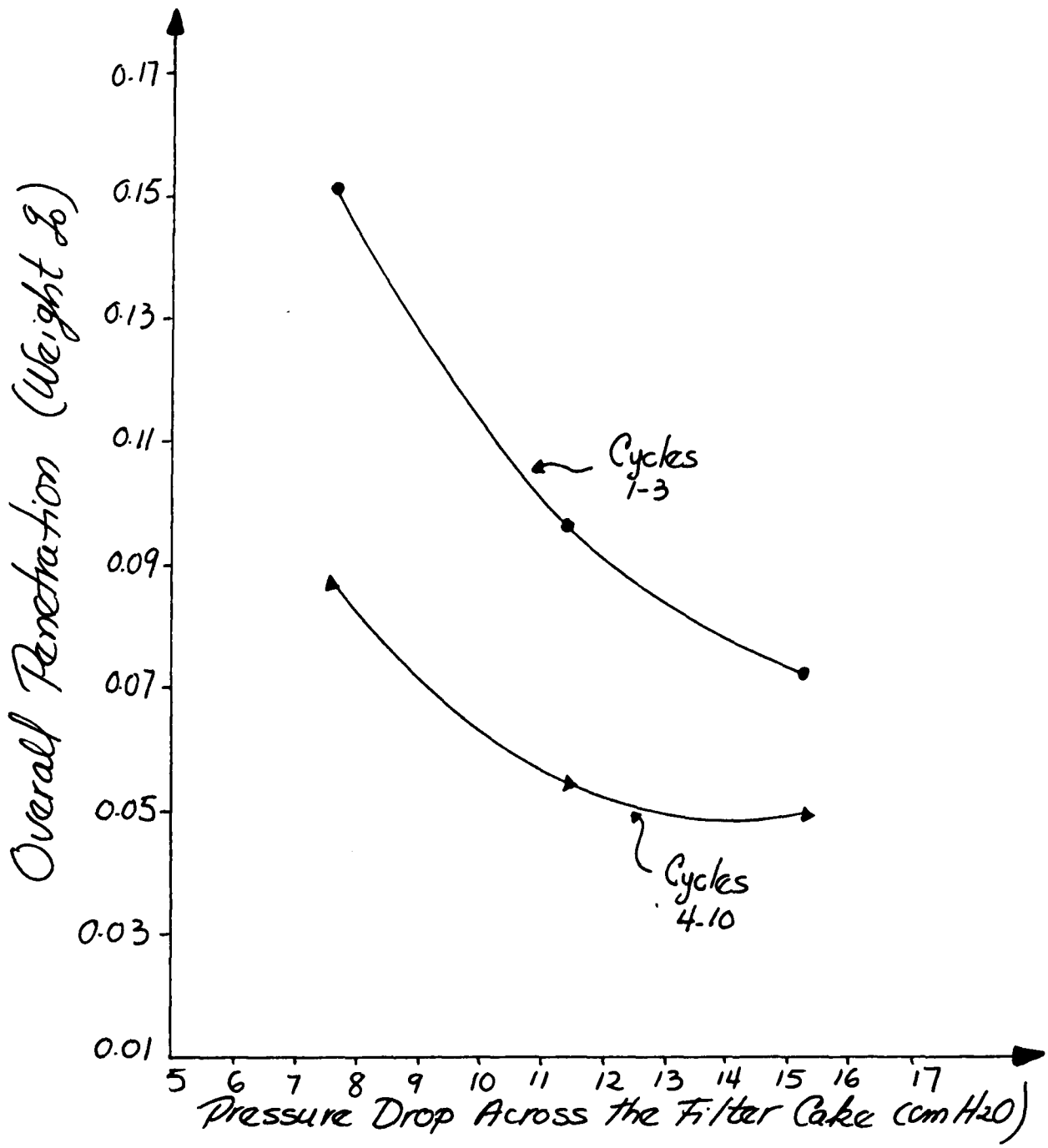

Figure 6-8 Penetration versus buildup in pressure drop due to dilter cake for 17.2 cm/s (33.8 ft/min) at 150°C.
SILICON CARBIDE (40-50 Mesh)-CON EDISON FLY ASH.

TABLE 6-9: Effect of Density of Cake: Tests of Silicon Carbide at 7.75 cm/s and 150° C

Puffback Tank: Volume = 206 cm^3 Pressure = 170.3 kPa

ΔPc cm H_2O	ΔPi cm H_2O	DPB_{4-10} grs	DD_{4-10} grs	GPB_{4-10} grs	$(DPB/GPB)_{4-10}$	Pov_{1-3} Wt%	Pov_{4-10} Wt%
3.81	6.7	5.39	0.43	48.56	0.11	0.062	0.036
7.62	7.0	9.90	2.06	61.29	0.16	0.0273	0.019
11.43	7.0	14.46	1.81	84.04	0.17	0.06	0.031
15.24	7.4	20.34	3.41	108.19	0.19	0.04	0.021

TABLE 6-10: Effect of Density of Cake: Tests of Silicon Carbide at 11.12 c/s and 150° C

Puffback Tank: Volume = 206 cm^3 Pressure = 170.3 kPa

ΔPc cm H_2O	ΔPi cm H_2O	DPB_{4-10} grs	DD_{4-10} grs	GPB_{4-10} grs	$(DPB/GPB)_{4-10}$	Pov_{1-3} Wt%	Pov_{4-10} Wt%
3.81	9.1	7.96	1.43	75.47	0.11	0.1131	0.068
7.62	8.4	8.36	1.79	38.56	0.22	0.0865	0.064
11.43	11.8	10.86	1.26	58.81	0.18	0.05	0.0242
15.24	11.5	12.37	1.27	45.81	0.27	0.033	0.0215

TABLE 6-11: Effect of Density of Cake: Tests of Silicon Carbide at 17.2 cm/s and 150° C

Puffback Tank: Volume = 206 cm^3 Pressure = 204.7 kPa

ΔPc cm H_2O	ΔPi cm H_2O	DPB_{4-10} grs	DD_{4-10} grs	GPB_{4-10} grs	$(DPB/GPB)_{4-10}$	Pov_{1-3} Wt%	Pov_{4-10} Wt%
7.62	14.6	9.47	1.20	163.17	0.06	0.15	0.086
11.43	15.1	13.23	1.55	187.13	0.07	0.096	0.054
15.24	14.4	15.96	1.89	196.87	0.08	0.072	0.049

6.01.3 Estimation of Penetration of Sub-Micron-Size Particles

Figure 5-8 gave a particle size distribution in our fly ash as determined by a Coulter counter. Figure 6-9 gives the extrapolation of this size distribution that we have used to obtain an estimate of penetration of sub-micron-size particles. Table 6-12 gives the particle counts determined by microscopic examination of the top filter paper from cycles 4 through 10 of a run at 150° C at a velocity 11.12 cm/sec and with a buildup of cake pressure drop amounting to 7.62 cm of water. The overall penetration for this series of cycles, given in Table 6-4 was 0.03%.

Table 6-13 gives particle counts for the bottom filter paper from cycles 4 through 9 of a run at 150° C at a velocity of 11.12 cm/sec and with a cake pressure drop of 11.43 cm of water. The overall penetration, seen in Table 6-4, was 0.01%.

Figures 6-10 and 6-11 give plots of the number size distribution of particles on the two filter papers of Tables 6-12 and 6-13 respectively. The figures also translate the number size distributions into weight size distributions with the assumption of log-normality.

Comparison of the weight size distributions in Figure 6-10 and 6-11 with that shown in Figure 6-9 allows us, taking into account the overall weight percentage penetrations that we measured in the two runs, to determine the following very rough estimates of percentage penetrations of particles in various size ranges:

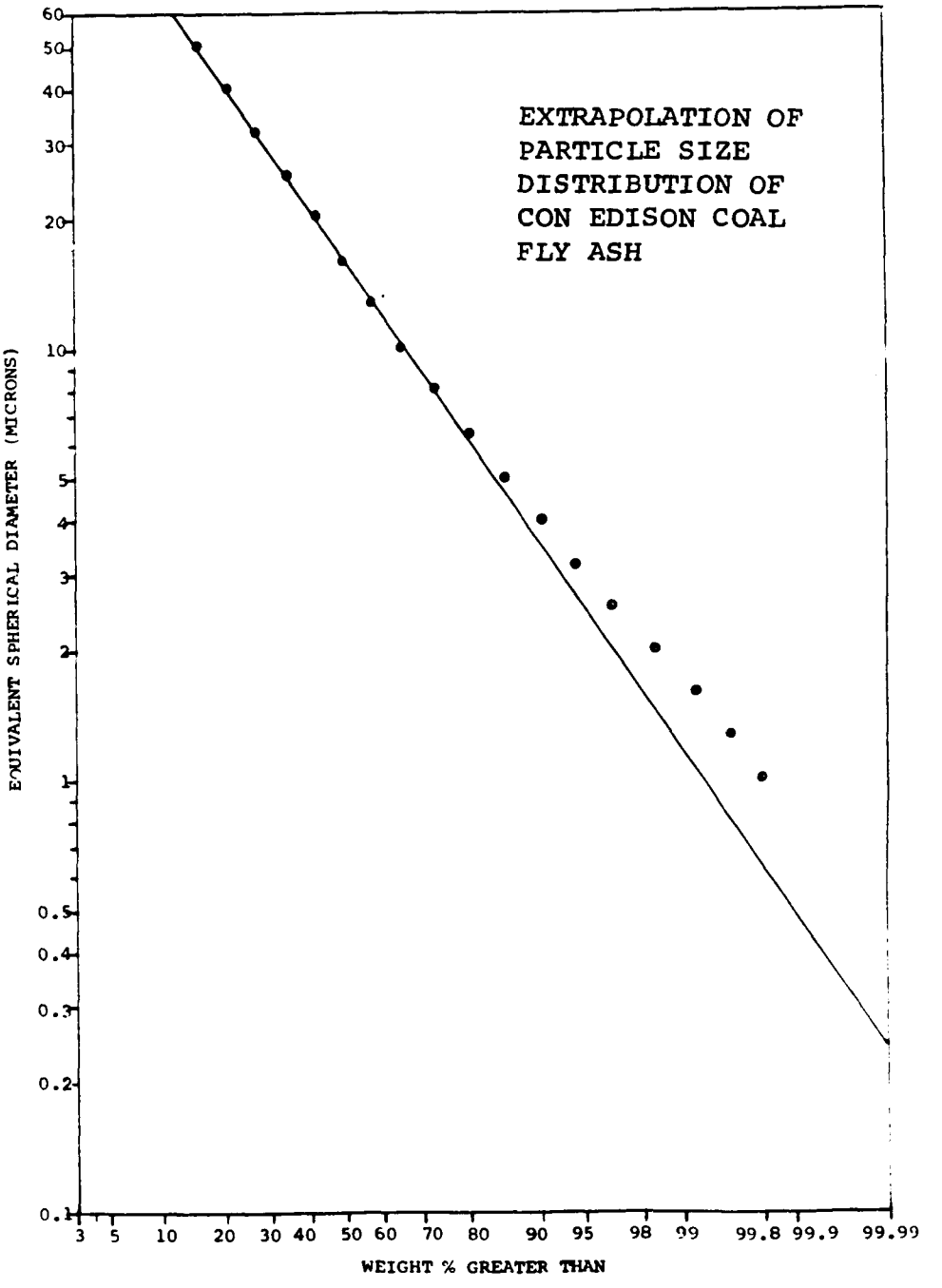

Figure 6-9 Extrapolation of fly ash particle size distribution (Con Edison) used in estimate of penetration of sub-micron-size particles.

Table 6-12

DETERMINATION OF FLY ASH PARTICLE SIZE DISTRIBUTION AT OUTLET OF PANEL BED FILTER

SOURCE: OPTICAL MICROSCOPE MAGNIFICATION: 1000X

PANEL BED FILTER AT 150°C (300°F)
FILTRATION SYSTEM:
ANGULAR SAND (40-50 Mesh) -CON EDISON COAL FLY ASH
SUPERFICIAL VELOCITY - 11.12 cm sec ΔP_{cake} 7.62 cm H_2O
PUTTBACK TANK: VOLUME 206 cm^3
PRESSURE 170.3×10^3 Pa (10 psig)
SAMPLE: TOP FILTER PAPER CYCLES 4-10

Field #	0.3-1.0 microns	1.0-1.5 microns	1.5-2.5 microns	2.5-3.5 microns	3.5-4.5 microns	4.5-5.5 microns	5.5-6.5 microns	6.5-7.5 microns	7.5-8.5 microns
I	546	23	3	3	0	0	0	0	0
II	403	18	5	1	0	0	0	0	0
III	1050	54	8	1	0	0	0	0	0
IV	1056	35	5	1	0	0	0	0	0
V	1035	28	9	1	0	0	0	0	0
VI	823	17	0	1	0	1	0	0	0
VII	759	17	1	0	0	0	0	0	0
VIII	608	17	1	0	0	0	0	0	0
	6280	209	32	8	0	1	0	0	0

Table 6-13

DETERMINATION OF FLY ASH PARTICLE SIZE DISTRIBUTION AT OUTLET OF PANEL BED FILTER

SOURCE: OPTICAL MICROSCOPE MAGNIFICATION: 1000X

PANEL BED FILTER AT 150°C (300°F)
FILTRATION SYSTEM:
ANGULAR SAND (40-50 Mesh) -CON EDISON COAL FLY ASH
SUPERFICIAL VELOCITY= 11.12 cm/sec ΔP_{cake}= 11.43 cm H_2O
PUFFBACK TANK: VOLUME= 206 cm^3
PRESSURE= 170.3×10^3 Pa (10 psig)
SAMPLE: BOTTOM FILTER PAPER CYCLES 4-9

Field #	0.3-1.0 microns	1.0-1.5 microns	1.5-2.5 microns	2.5-3.5 microns	3.5-4.5 microns	4.5-5.5 microns	5.5-6.5 microns	6.5-7.5 microns	7.5-8.5 microns
I	283	74	14	2	0	0	0	0	0
II	392	47	8	0	0	0	0	0	0
III	226	19	8	1	2	0	0	0	0
IV	424	79	20	3	2	0	0	0	1
V	547	49	11	2	1	0	0	1	0
VI	276	27	4	0	0	0	0	0	0
VII	459	34	9	0	0	0	0	0	0
VIII	294	19	1	0	0	0	0	0	0
	2901	348	75	8	5	0	0	1	1

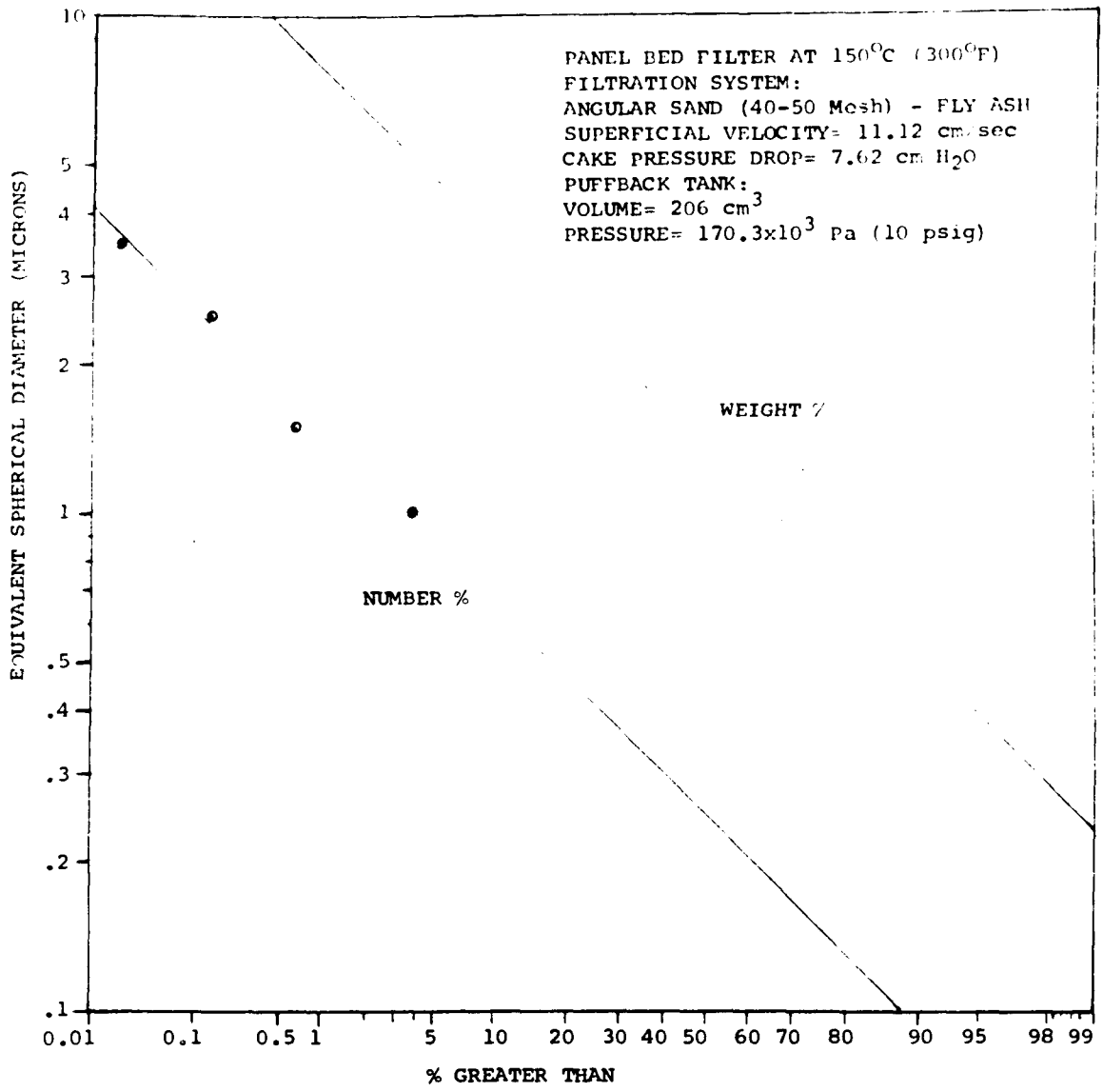

Figure 6-10 Distribution of particle size in Con Edison Fly Ash emitted from rear of panel bed filter operating at 150°C. Source: Optical Microscope Magnification: 1000X

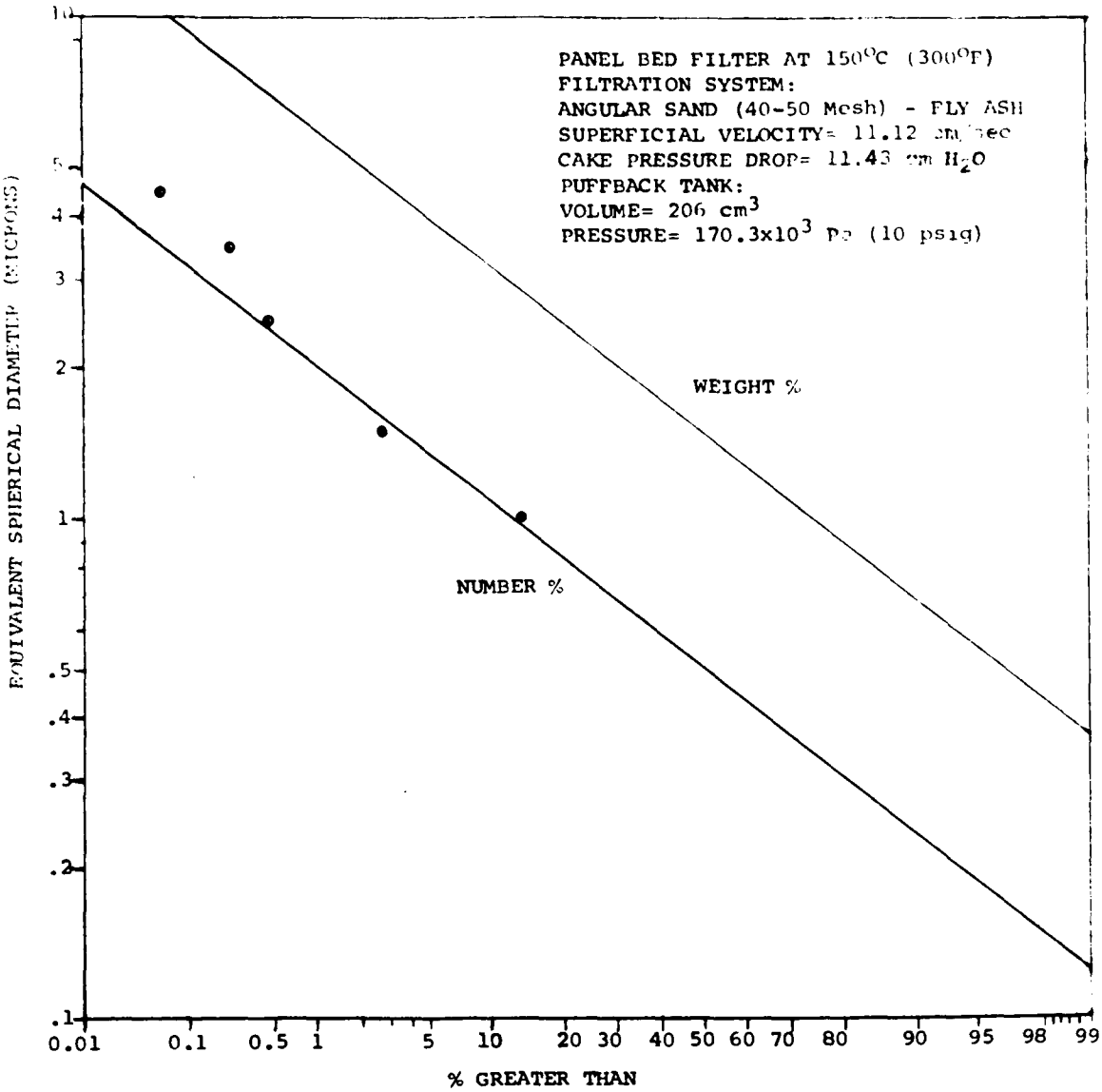

Figure 6-11 Distribution of particle size in Con Edison Fly Ash emitted from rear of panel bed filter operating at 150°C. Source: Optical Microscope Magnification: 1000X

Size range, micrometers	0.3-1.0	1.0-1.5	1.5-2.5	2.5-3.5
Table 6-12, Figure 6-10	1.20%	0.48%	0.17%	0.056%
Table 6-13, Figure 6-11	0.37%	0.24%	0.10%	0.033%

Figure 6-12 gives the cumulative grade efficiency curves for filtration of this specific coal fly ash in the panel bed filter at 11.12 cm/s and 150°C. Tables 6-14 and 6-15 summarize the calculations from which the data plotted in Figure 6-12 were obtained.

6.01.4 Discussion of Sand and Silicon Carbide Data at 150°C

Comparison of Figures 6-2,6-3, and 6-5 for sand with the comparable figures for silicon carbide,Figures 6-6 through 6-8 respectively, reveals gratifying consistencies in general behavior, increasing our confidence in the data.

We shall analyze the data obtained in the laboratory panel bed in terms of penetration trends rather than toward specific numerical values. The analysis will be concentrated to the filtration of fly ash with 40-50 mesh angular sand.

General trends which can be identified from the response of the panel bed to this filtration system could be summarized as follows:

1. There exists strong experimental evidence which makes us believe that dust re-entrainment is present as an important penetration mechanism in panel bed filtration at 150°C. It was generally observed that an increase in cake density would eventually reach a density of minimum dust penetration. In some instances the results suggested that

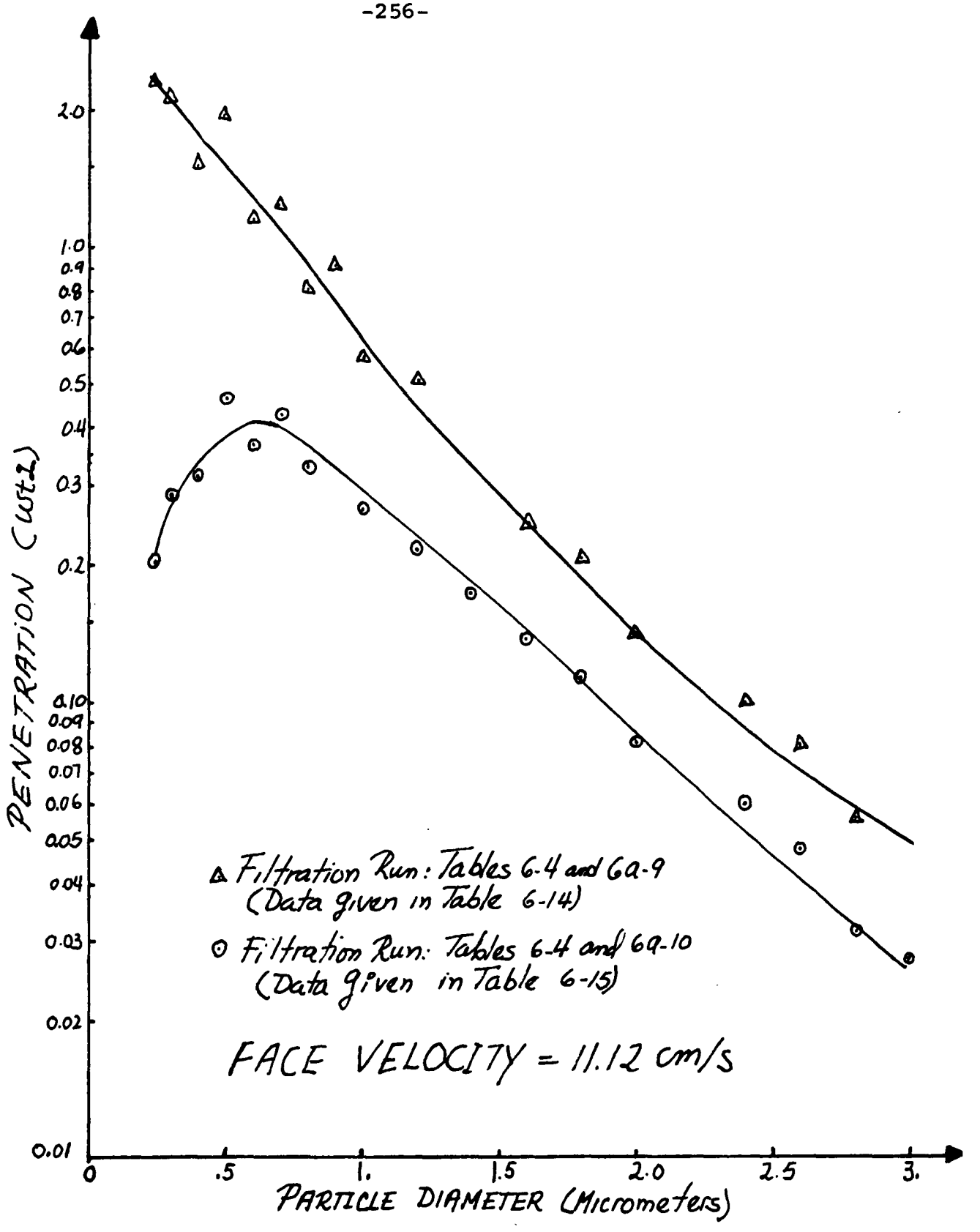

Figure 6-12 Rough Estimate of Grade Efficiencies in 150°C Panel Bed Filtration.
Solid: 40-50 Mesh Sand
Dust: Con Edison Fly Ash

Table 6-14

CUMULATIVE GRADE EFFICIENCY OF PANEL BED FILTER FILTRATION RUN : CORRESPONDS TO DATA GIVEN IN TABLES 6-4 and 6a-9

INLET DISTRIBUTION				OUTLET DISTRIBUTION				
D_p	Wt%	$D_{pav.}$	Wt%	D_p	Wt%	D_{pav}	Wt%	PENETRATION Wt%
0.24	99.990	0.27	0.012	0.24	99.00	0.27	1.20	2.333
0.30	99.978	0.35	0.033	0.30	97.80	0.35	3.10	2.192
0.40	99.945	0.45	0.065	0.40	94.70	0.45	4.30	1.544
0.50	99.880	0.55	0.060	0.50	90.40	0.55	5.10	1.983
0.60	99.820	0.65	0.110	0.60	85.30	0.65	5.50	1.167
0.70	99.710	0.75	0.110	0.70	79.80	0.75	5.80	1.230
0.80	99.600	0.85	0.150	0.80	74.00	0.85	5.20	0.809
0.90	99.450	0.95	0.150	0.90	68.80	0.95	5.80	0.902
1.00	99.300	1.10	0.400	1.00	63.00	1.10	9.80	0.572
1.20	98.900	1.30	0.480	1.20	53.20	1.30	10.40	0.506
1.40	98.420	1.50	0.520	1.40	42.80	1.50	5.00	0.224
1.60	97.900	1.70	0.600	1.60	37.80	1.70	6.30	0.245
1.80	97.300	1.90	0.600	1.80	31.50	1.90	5.30	0.206
2.00	96.700	2.10	0.700	2.00	26.20	2.10	4.20	0.140
2.20	96.000	2.30	0.700	2.20	22.00	2.30	3.30	0.110
2.40	95.300	2.50	0.700	2.40	18.70	2.50	2.90	0.100
2.60	94.600	2.70	0.700	2.60	15.80	2.70	2.40	0.080
2.80	93.900	2.90	0.800	2.80	13.40	2.90	1.90	0.055
3.00	93.100	3.10	0.800	3.00	11.50	3.10	1.70	0.050
3.20	92.300	3.30	0.800	3.20	9.80	3.30	1.30	0.038
3.40	91.500	3.50	0.900	3.40	8.50	3.50	1.20	0.031
3.60	90.600	3.70	0.700	3.60	7.30	3.70	1.10	0.037
3.80	89.900	3.90	0.800	3.80	6.20	3.90	0.80	0.023
4.00	89.100			4.00	5.40			

Table 6-15

CUMULATIVE GRADE EFFICIENCY OF PANEL BED FILTER FILTRATION RUN : CORRESPONDS TO DATA GIVEN IN TABLES 6-4 and 6a-10

INLET DISTRIPUTION				OUTLET DISTRIBUTION				
D_p	Wt%	$D_{pav.}$	Wt%	D_p	Wt%	$D_{pav.}$	Wt%	PENETRATION Wt%
0.24	99.990	0.27	0.012	0.24	99.90	0.27	0.24	0.208
0.30	99.978	0.35	0.033	0.30	99.66	0.35	0.97	0.287
0.40	99.945	0.45	0.065	0.40	98.75	0.45	1.95	0.312
0.50	99.880	0.55	0.060	0.50	96.80	0.55	2.70	0.468
0.60	99.820	0.65	0.110	0.60	94.10	0.65	3.90	0.369
0.70	99.710	0.75	0.110	0.70	90.20	0.75	4.50	0.426
0.80	99.600	0.85	0.150	0.80	85.70	0.85	4.70	0.326
0.90	99.450	0.95	0.150	0.90	81.00	0.95	5.20	0.361
1.00	99.300	1.10	0.400	1.00	75.80	1.10	10.10	0.263
1.20	98.900	1.30	0.480	1.20	65.70	1.30	10.00	0.217
1.40	98.420	1.50	0.520	1.40	55.70	1.50	8.70	0.174
1.60	97.900	1.70	0.600	1.60	47.00	1.70	8.00	0.139
1.80	97.300	1.90	0.600	1.80	39.00	1.90	6.50	0.113
2.00	96.700	2.10	0.700	2.00	32.50	2.10	5.50	0.082
2.20	96.000	2.30	0.700	2.20	27.00	2.30	4.50	0.067
2.40	95.300	2.50	0.700	2.40	22.50	2.50	4.00	0.059
2.60	94.600	2.70	0.700	2.60	18.50	2.70	3.20	0.048
2.80	93.900	2.90	0.800	2.80	15.30	2.90	2.40	0.031
3.00	93.100	3.10	0.800	3.00	12.90	3.10	2.10	0.027
3.20	92.300	3.30	0.800	3.20	10.80	3.30	1.80	0.023
3.40	91.500	3.50	0.900	3.40	9.00	3.50	1.40	0.016
3.60	90.600	3.70	0.700	3.60	7.60	3.70	1.30	0.019
3.80	89.900	3.90	0.800	3.80	6.30	3.90	1.00	0.013
4.00	89.100			4.00	5.30			

unstable cakes could gain stability with further deposition of dust, although at some point a maximum thickness of filter cake, beyond which it would not be prudent to go, will be reached.

2. A comparison of our data with the room temperature data obtained by Lee (1975) with the same ash and sand suggests that the adhesivity and authohesivity of the dust being filtered is important in determining the conditions at which the panel bed filter must be operated if high-efficiency cake filtration is required.

3. Our data suggests that for a given filtration system there exists a critical size of granules beyond which cake filtration disappears from the operational scene of a panel bed. A change in any variable which affects adhesivity or autohesivity of the dust being filtered could modify the aforementioned critical particle size.

4. For the filtration system studied and for the operating conditions used, the results suggest a trend of increasing penetration with increasing filtration velocity. The data also suggests the existence of a critical velocity beyond which performance sharply deteriorates.

5. The exploration of the cleaning intensity effect shows that in panel bed filtration there exists a minimum puffback intensity below which subsequent penetration of previously collected dust cannot be detained. The results also show that if the filter is operated at velocities lower than the critical velocity at which a sharp deterioration of

performance occurs, a cleaning intensity higher than the minimum does not produce a striking change in performance. If the filter is operated at velocities beyond the critical, the minimum cleaning intensity increases substantially. The fact that stronger cleaning intensities allow efficient operation at velocities beyond the critical suggests that penetration of re-entrained dust is a gradual phenomenon.

6. Our estimation of the penetration of sub-micron-size particles, suggests that cake filtration in the panel bed filter at 150^{o} C can provide high collection efficiency of very fine particulates.

6.02 Commonwealth Edison Coal Fly Ash

It is generally accepted that performance in any collecting device depends fundamentally on the physical and chemical properties of the gas and particulates treated. In a coal-fired power plant, these properties are governed by the nature and pre-processing of the coal burned, the combustion chamber design and the overall operation of the boiler.

Coal fly ash collected by an electrostatic precipitator operating at efficiencies beyond 99% by weight was provided by Commonwealth Edison Company of Chicago. Its particle size distribution given, in Figure 5-9, shows the presence of larger proportions of fine particles than in the previously tested Con Edison fly ash. Visual observation suggested that this new ash has a stronger agglomerating tendency than the Con Edison Fly Ash.

Following the pattern of our tests with the previous ash, we tested the new finer dust in our laboratory panel bed at 150° C.

6.02.1 Tests with 40-50 Mesh Sand at 11.12 cm/s

We had the impression that this fly ash was going to be more difficult to filter than Con Edison's fly ash. Consequently, we began our tests with 40-50 Mesh angular sand and at a superficial velocity which had proved best while filtering the previous ash.

Table 6-16 summarizes the data obtained at a fixed cake density and at two puffback intensities. Details of these runs are given in Tables 6a-34 and 6a-35 of the Appendix. Figure 6-13 and Table 6-17 summarize the data obtained while exploring the effect of the cake's density upon penetration at a fixed puffback intensity. Tables 6a-35 through 6a-38 of the Appendix give the details of these runs.

TABLE 6-16: Puffback Intensity Effect at 11.12 cm/s and 150° C

Puffback Tank: Volume = 206 cm^3

Pressure Drop due to filter cake = 15.24 cm H_2O

PBP kPa	ΔPi cm H_2O	DPB_{4-10} grs	DD_{4-10} grs	GPB_{4-10} grs	$(DPB/GPB)_{4-10}$	Pov_{1-3} Wt%	Pov_{4-10} Wt%
170.3	8.88	5.21	0.79	59.54	0.09	0.0689	0.0418
204.7	9.6	5.30	0.47	115.97	0.05	0.2066	0.1812

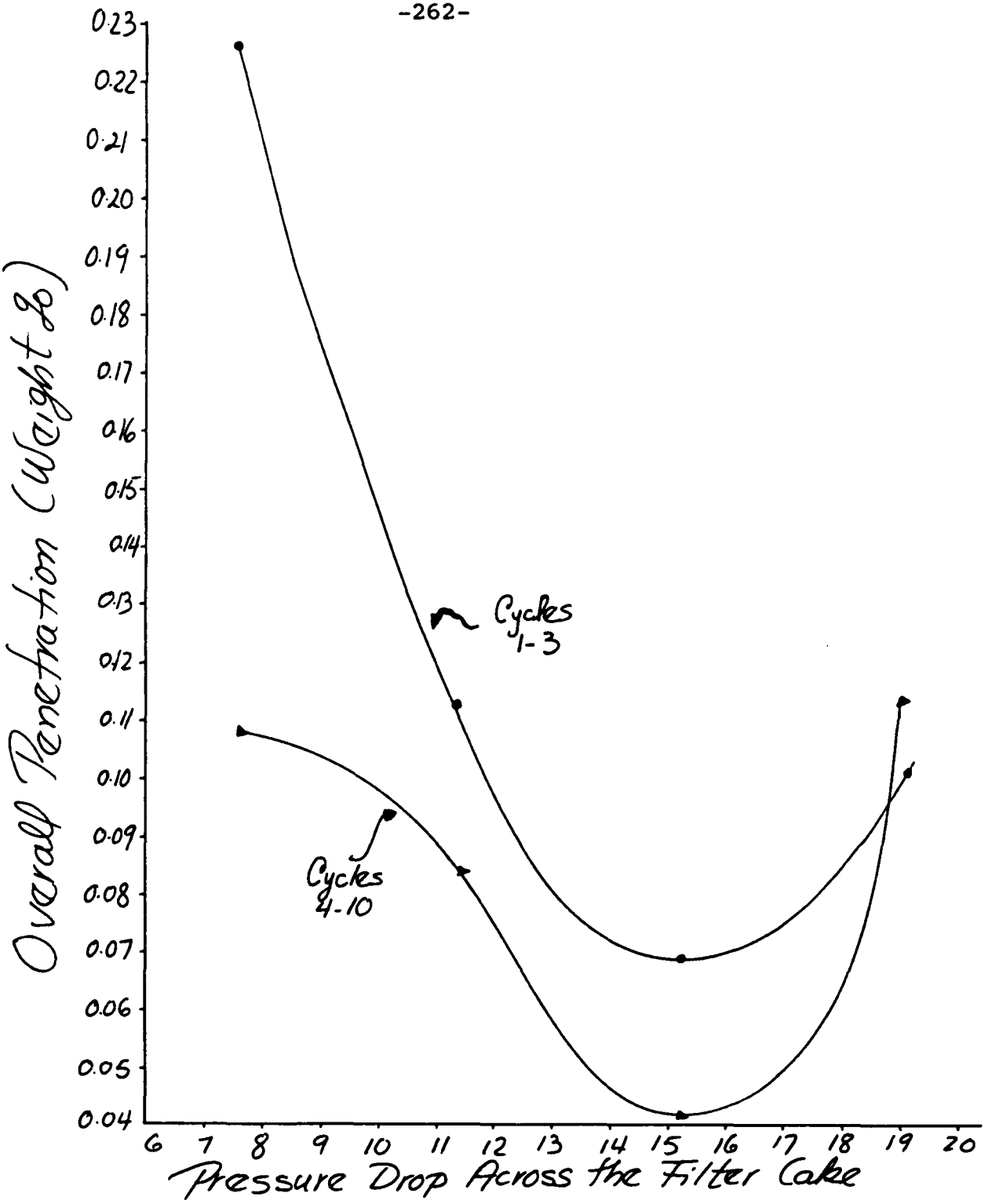

Figure 6-13 Penetration versus buildup in pressure drop due to filter cake for 11.12 cm/s (15.2 ft/min) at 150 °C. ANGULAR SAND (40-50 Mesh)-COMMONWEALTH EDISON FLY ASH.

TABLE 6-17: Cake Density Effect at 11.12 cm/s and 150° C

Puffback Tank: Volume = 206 cm^3 Pressure = 170.3 kPa

ΔPc cm H_2O	ΔPi cm H_2O	DPB_{4-10} grs	DD_{4-10} grs	GPB_{4-10} grs	$(DPB/GPB)_{4-10}$	Pov_{1-3} Wt%	Pov_{4-10} Wt%
7.62	9.36	2.99	0.33	59.93	0.05	0.226	0.1072
11.43	8.64	4.27	0.73	56.1	0.08	0.1126	0.0835
15.24	8.88	5.21	0.79	59.54	0.09	0.0689	0.0418
19.05	9.6	6.29	0.67	75.14	0.08	0.1003	0.1113

It can be seen in Table 6-16 that at this velocity an increase in puffback pressure of 34.4 kPa caused sharp deterioration in the performance of the panel bed (air at outlet of panel bed is about four times dirtier at the higher puffback intensity). As a result of this phenomenon, the exploration of the cake's density effect was conducted at the lower puffback intensity (170.3 kPa).

Table 6-17 shows that penetration decreases with increasing cake density up to a cake pressure drop at 15.24 cm H_2O; a further increase to 19.05 cm of H_2O caused a substantial increase in penetration. Table 6-17 also shows that an increase in cake density up to 15.24 cm H_2O did not affect the amount of sand spilled; however, a further increase in cake density provoked a considerable increase in sand spill.

6.02.2 Tests with 40-50 Mesh Sand at 17.2 cm/s and 150° C

After having tested the panel bed at 11.12 cm/s, the superficial velocity was increased to 17.2 cm/s. This was the velocity at which a sharp deterioration in performance

occurred while testing Con Ed's fly ash.

Table 6-18 summarizes the data obtained at a fixed cake density and two puffback intensities. Tables 6a-39 and 6a-40 of the Appendix show the details of these runs. Figure 6-14 and Table 6-19 show a summary of the runs conducted for studying the effect of the cake density upon penetration. Tables 6a-39 through 6a-42 of the Appendix give details of these tests.

TABLE 6-18: Puffback Intensity Effect at 17.2 cm/s and 150° C

Puffback Tank: Volume = 206 cm^3

Pressure Drop Due to Filter Cake = 11.43 cm H_2O

PBP kPA	ΔPi cm H_2O	DPB_{4-10} grs	DD_{4-10} grs	GPB_{4-10} grs	$(DPB/GPB)_{4-10}$	Pov_{1-3} Wt%	Pov_{4-10} Wt%
170.3	14.88	3.9	0.4	62.14	0.06	0.0977	0.0633
204.7	14.16	4.1	0.4	103.2	0.04	0.0451	0.0651

As shown in Table 6-18 an increase in puffback pressure of 34.4 kPa did not much affect the performance of the filter, and as a result the tests shown in Table 6-19 were conducted at the lower pressure.

TABLE 6-19: Cake Density Effect at 17.2 cm/s and 150° C

Puffback Tank: Volume = 206 cm^3 Pressure = 170.3 kPa

ΔPc cm H_2O	ΔPi cm H_2O	DPB_{4-10} grs	DD_{4-10} grs	GPB_{4-10} grs	$(DPB/GPB)_{4-10}$	Pov_{1-3} Wt%	Pov_{4-10} Wt%
11.43	14.88	3.9	0.4	62.14	0.06	0.0977	0.0633
15.24	14.64	4.86	0.39	62.83	0.08	0.0772	0.0639
19.05	13.92	5.31	0.53	63.3	0.08	0.0794	0.0717

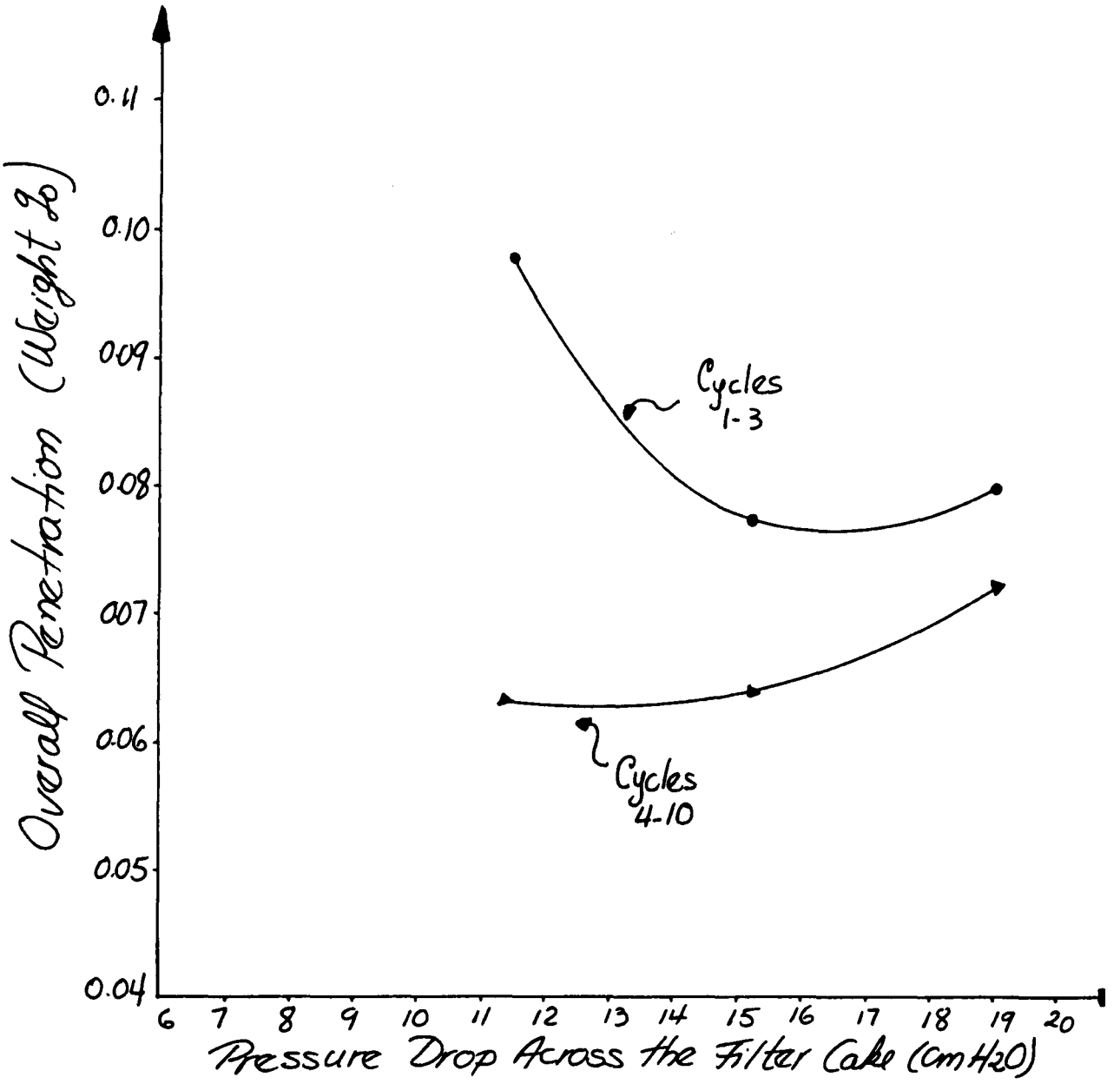

Figure 6-14 Penetration versus buildup in pressure drop due to dilter cake for 17.2 cm/s (33.8 ft/min) at 150 °C. ANGULAR SAND(40-50 Mesh)-COMMONWEALTH EDISON FLY ASH.

It can be seen in Table 6-19 that an increase in cake density from 11.43 to 19.05 cm of H_2O slightly increases the penetration of dust in the filter. It can also be observed that denser cakes did not alter the amount of sand spilled at a fixed puffback intensity.

6.02.3 Exploratory run with 40-50 Mesh Sand at 7.75 cm/s and 150° C

One run of ten filtration cycles was conducted at the lowest velocity used with the previous ash. Table 6-20 summarizes the data obtained at this velocity. Table 6a-43 of the Appendix shows the details of this run.

TABLE 6-20: Exploratory test with 40-50 Mesh Sand at 7.75 cm/s and 150° C

Puffback Tank: Volume = 206 cm^3 Pressure = 170.3 kPa

ΔPc cm H_2O	ΔPi cm H_2O	DPB_{4-10} grs	DD_{4-10} grs	GPB_{4-10} grs	$(DPB/GPB)_{4-10}$	Pov_{1-3} Wt%	Pov_{4-10} Wt%
11.43	7.08	4.31	0.6	63.59	0.07	0.2214	0.1193

Table 6-20 suggests that decreasing the superficial velocity to 7.75 cm/s would result in a substantial decrease in filtration efficiency.

6.02.4 Discussion of Sand Data at 150° C

It was gratifying to be able to filter this finer fly ash at high efficiencies without having to alter the operating conditions of the panel bed.

The discussion of the data obtained with Commonwealth Edison fly ash will be directed toward trends in penetration of the filtration system tested. A comparison of the panel

bed responses to different filtration systems will be made in Chapter 8.0.

General trends which can be identified from the reaction of the unit to this filtration system can be summarized as follows:

1. The presence of dust reentrainment as a penetration mechanism can be identified after observing the filter's response to increasing cake densities. At relative low velocities there is an increase in performance with denser cakes, until a point is reached at which further dust deposition causes a drastic reduction in collection efficiency. At high velocity dust reentrainment appears to be proportional to cake density; as a result thicker cakes did not seem to improve the filter's collection capability. Penetration was almost constant in the range of cake densities explored.

2. Although we did not test sand of different particle sizes, the reaction of the unit to 40-50 mesh sand suggests that bigger particle sizes could not be used for high-efficiency operation.

3. The exploration of the effect of puffback intensity produced major surprises. At relative low velocity (11.12 cm/s) an increase in puffback intensity sharply deteriorated the filter's performance. This phenomenon is a clear indication that for this filtration system it is important to leave dust roots at the filters surface after cleaning. These roots will accelerate the formation of a highly efficient filter cake in the subsequent filtration

cycle. At higher velocities (17.2 cm/s) an increase in puffback intensity of 34.4 kPa did not produce the drastic increase in penetration observed at the lower velocity. Penetration decreased substantially during the initial filtration cycles and remained almost constant for the rest of the run. This behavior reflects the fact that at higher velocity dust penetrates deeper into the bed and does so gradually. Apparently the higher puffback intensity was not high enough to stop this gradual dust reentrainment. A higher puffback intensity could eventually avoid this gradual penetration of dust deep into the bed; however, it might also remove all the roots at the cake's surface and result in a decrease in performance.

4. For the filtration system studied and for the range of operating conditions tested, the data suggest a trend of decreasing penetration with increasing filtration velocity. The lack of sufficient data at the lowest velocity tested does not permit a definite conclusion about the trend, yet the results suggest that there is a substantial improvement in performance when the superficial velocity is increased from 7.75 to 11.12 cm/s. A further increase to 17.2 cm/s showed a slight increase in performance, although phenomena appear which indicate that we are approaching a velocity level at which performance will begin to deteriorate.

5. The exploration of the effect of cake density upon penetration with this filtration system showed almost no variation in the amount of sand spilled (at a fixed puffback

pressure) with different cake densities. Apparently, the increase in soil strength as a result of the binding of sand grains by the fly ash deposit was contravened by the decrease in permeability provoked by the presence of the cake. A combination of these opposing effects resulted in constant sand spills. The only run which showed a substantial change in the amount of sand spilled was the one conducted at 11.12 cm/s and at the highest cake pressure drop tested (19.05 cm of H_2O). Here we observed an increase in sand spill with increasing cake density; the reduction in permeability was not accompanied by a sufficient offsetting in soil strength.

6.03 Clinker Cooler Cement Dust

Recognizing the importance of the nature of the filtration system in determining the limits of performance of a collecting device, we decided to test our laboratory panel bed filter with a dust whose composition and physical properties differ from the previously tested coal fly ashes. Raw cement, an important air pollutant was selected for this purpose. A sample of Portland cement dust collected at the outlet of a clinker cooler, by a bag filter operating at efficiencies beyond 99.9 Wt%, was supplied to us by Lehigh Portland Cement Co. from their New York plant. Its particle size distribution as determined in a Coulter counter model TAII and given in Figure 5-10 shows a dust with larger proportions of coarse particles than in the previously tested coal fly ashes. Visual observation of the cement sample suggested the presence

of strong agglomerating tendencies. This fact is confirmed by the results of Frederick (1961).

At the outset of these tests, it was believed that the operating conditions utilized for high-efficiency filtration of the coal fly ashes should afford comparable or better efficiencies with this coarser dust. Consequently, tests were conducted using 40-50 mesh angular sand.

6.03.1 Tests with 40-50 Mesh Sand at 11.12 cm/s

Two runs, conducted at a constant cake density before cleaning and at puffback pressures of 170.3 and 204.7 kPa showed a strong increase in penetration with increasing puffback intensity. Table 6-21 summarizes these data which is given in detail in Tables 6a-44 and 6a-45 of the Appendix. Figure 6-15 and Table 6-22 summarize the data obtained while studying the effect of cake density upon penetration at a fixed puffback intensity. Tables 6a-45 through 6a-47 of the Appendix give details of these runs.

TABLE 6-21: Puffback Intensity Effect at 11.12 cm/s and 150° C

Puffback Tank: Volume = 206 cm^3

Pressure Drop due to Filter Cake = 11.43 cm H_2O

PBP kPa	ΔPi cm H_2O	DPB_{4-10} grs	DD_{4-10} grs	GPB_{4-10} grs	$(DPB/GPB)_{4-10}$	Pov_{1-3} Wt%	Pov_{4-10} Wt%
170.3	8.64	5.47	0.26	63.63	0.09	0.1125	0.0328
204.7	9.12	5.11	0.47	108.8	0.05	0.0488	0.0711

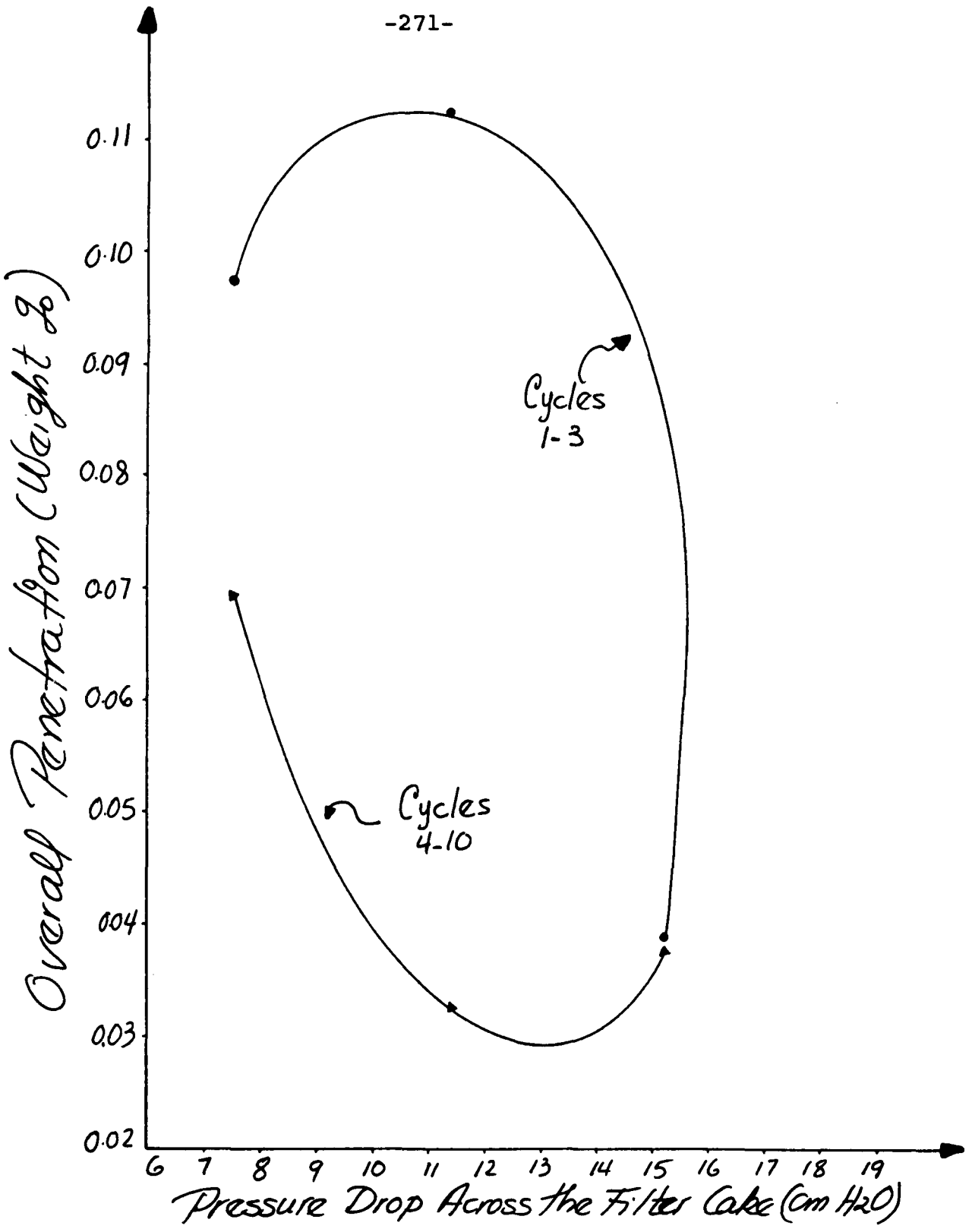

Figure 6-15 Penetration versus buildup in pressure drop due to filter cake for 11.12 cm/s (21.9 ft/min) at 150°C.
ANGULAR SAND (40-50 Mesh)-CLINKER COOLER CEMENT.

TABLE 6-22: Cake Density Effect at 11.12 cm/s and 150° C

Puffback Tank: Volume = 206 cm^3 Pressure = 170.3 kPa

ΔPc cm H_2O	ΔPi cm H_2O	DPB_{4-10} grs	DD_{4-10} grs	GPB_{4-10} grs	$(DPB/GPB)_{4-10}$	Pov_{1-3} Wt%	Pov_{4-10} Wt%
7.62	9.12	3.84	0.2	65.63	0.06	0.0976	0.0698
11.43	8.64	5.47	0.26	63.63	0.09	0.1125	0.0328
15.24	8.88	7.35	0.39	74.87	0.10	0.0389	0.0379

It can be seen in Table 6-21 that an increase in puffback intensity of 34.4 kPa decreases penetration substantially at the beginning of the filtration run; however, a substantial increase in penetration was observed for the rest of the filtration cycles. It was then decided to conduct tests at different cake densities at the lower puffback intensity. As Table 6-22 shows an increase in cake density caused a decrease in penetration until a point was reached at which the start of deterioration was observed.

6.03.2 Tests with 40-50 Mesh Sand at 17.2 cm/s and 150° C

Exploratory runs at a superficial velocity of 17.2 cm/s were conducted. Table 6-23 summarizes two filtration runs carried out at a fixed cake density before cleaning and at 170.3 and 204.7 kPa puffback pressures. Tables 6a-48 and 6a-49 of the Appendix show details of these tests. Table 6-24 summarizes the data obtained at two different cake densities and at a fixed puffback pressure. Tables 6a-49 and 6a-50 of the Appendix give details of these runs.

TABLE 6-23: Puffback Intensity Effect at 17.2 cm/s and 150° C

Puffback Tank: Volume = 206 cm^3

Pressure Drop due to Filter Cake = 11.43 cm H_2O

PBP kPa	ΔPi cm H_2O	DPB_{4-10} grs	DD_{4-10} grs	GPB_{4-10} grs	$(DPB/GPB)_{4-10}$	Pov_{1-3} Wt%	Pov_{4-10} Wt%
170.3	12.72	4.57	0.3	61.2	0.07	0.0964	0.06
204.7	12.72	5.49	0.21	108.76	0.05	0.1002	0.0587

TABLE 6-24: Cake Density Effect at 17.2 cm/s and 150° C

Puffback Tank: Volume = 206 cm^3 Pressure = 170.3 kPa

ΔPc cm H_2O	ΔPi cm H_2O	DPB_{4-10} grs	DD_{4-10} grs	GPB_{4-10} grs	$(DPB/GPB)_{4-10}$	Pov_{1-3} Wt%	Pov_{4-10} Wt%
11.43	12.72	4.57	0.3	61.2	0.07	0.0964	0.06
15.24	13.68	4.54	0.23	50.11	0.09	0.0323	0.0219

Table 6-23 shows that at this velocity a puffback pressure increase of 34.4 kPa does not much affect the filtration performance of the banel bed filter. Table 6-24 shows a drastic reduction in dust penetration when the cake pressure drop was increased from 11.43 to 15.24 cm of H_2O. This increase in cake density caused a decrease in sandspill at the same puffback intensity.

6.03.3 Exploratory Runs at 7.75 cm/s and 150° C

Two filtration runs with 40-50 mesh angular sand and the lowest velocity tested are summarized in Table 6-25. Details of these runs are shown in Tables 6a-51 and 6a-52 of the Appendix.

TABLE 6-25: Exploratory runs at 7.75 cm/s and 150° C

Puffback Tank: Volume = 206 cm^3 Pressure = 170.3 kPa

ΔPc cm H_2O	ΔPi cm H_2O	DPB_{4-10} grs	DD_{4-10} grs	GPB_{4-10} grs	$(DPB/GPB)_{4-10}$	Pov_{1-3} Wt%	Pov_{4-10} Wt%
7.62	6.24	3.51	0.34	63.29	0.06	0.15	0.1191
11.43	6.24	5.03	0.66	68.11	0.07	0.0712	0.0589

Table 6-25 shows a sharp decline in penetration for an increase in cake pressure drop before cleaning of 3.81 cm of H_2O. The amount of sand spilled did not vary substantially.

6.03.4 Discussion of Sand Data at 150° C

The exploratory runs conducted with cement do not permit a complete definition of penetration trends in wide ranges of operating conditions; nevertheless, the following observations can be made:

1. Even when just one sand particle size was used, the results indicate that if high efficiency at 150° C is required, the sand size cannot be larger than 40-50 mesh.

2. Filtration of cement dust in the panel bed seems to be favoured by an increase in superficial velocity and by the use of denser cakes.

3. For the range of cake densities tested no indication of sharp deterioration was observed. In general denser cakes were much more efficient at all velocities tested.

4. At low velocity an increase in puffback intensity of 34.4 kPa caused a decline in filtration performance whereas at relative high velocity the same increase in puffback intensity did not affect dust penetration.

5. At low velocities, the effect of cake deposits on amount of sand spilled during puffback was negligible, excepting at very high cake pressure drops, where an increase in sand spill was observed. At high velocity, a small reduction in sand spills occurred.

CHAPTER 7.0: DUST DEPOSITION ON HORIZONTAL BED OF SAND AT 150° C

This Chapter 7.0 gives results of experiments in which dusts were put down upon horizontal surfaces of sand at 150° C.

Even after we recognized that the operation of a horizontal bed filter differs from panel bed filtration, we believed that useful information could be obtained if we could visualize the process of dust deposition and cake formation upon high-temperature horizontal sand surfaces.

Three dusts were deposited at different velocities upon sand beds of different particle size. While filtering at constant velocity the air pressure drop was monitored as a function of time (cake thickness). After the cakes were deposited, visual observation provided a better understanding of the cake's structure.

7.01 Experimental Arrangements and Procedures

The sand bed holder, used in these experiments, was described in Chapter 5.0 (Section 5.02) where we also pointed out the details of the experimental procedure.

Con Edison and Commonwealth Edison coal fly ashes, and clinker cooler cement dust, from the same batches used in panel bed filtration, were deposited on the horizontal beds. Their particle size distributions were given by Figures 5-8 through 5-10.

Angular sand from the same bags used in the panel bed

filter was screened, cleaned and dried. Four different particle sizes were utilized: 20-30, 30-40, 40-50 and 50-60 mesh, with average particles diameters of 718 μm, 507.5 μm, 358.5 μm and 273.5 μm respectively (arithmetic averages of the screen openings).

Two gas velocities, close to the ones explored in panel bed filtration, were tested. These filtration velocities correspond to 18.57 and 28.67 cm/s superficial velocities (average velocity of air in absence of sand bed).

7.02 Consolidated Edison Coal Fly Ash Deposited on Sand Beds of Different Particle Size at 150° C

Figure 7-1 shows the effect of areal density (mass of deposited dust per unit surface area of sand bed) upon the pressure drop across the dust deposit (total pressure drop at a given instant minus the initial, "clean bed" pressure drop) at 18.57 cm/s superficial velocity.

By using the least squares linear regression analysis, the following equations were obtained for the close-to-straight line regions of the curves. It was assumed that all the error was made in the determination of the areal density.

"30-40 Mesh Angular Sand," Superficial Velocity = 18.57 cm/s

$$\Delta P_{(\text{cm of } H_2O)} = 1742.3\ W_{(\text{grs/cm}^2)} - 141.9 \qquad (7\text{-}1)$$

Correlation coefficient = 0.9962

Points included: Last five points

"40-50 Mesh Angular Sand," Superficial Velocity = 18.57 cm/s

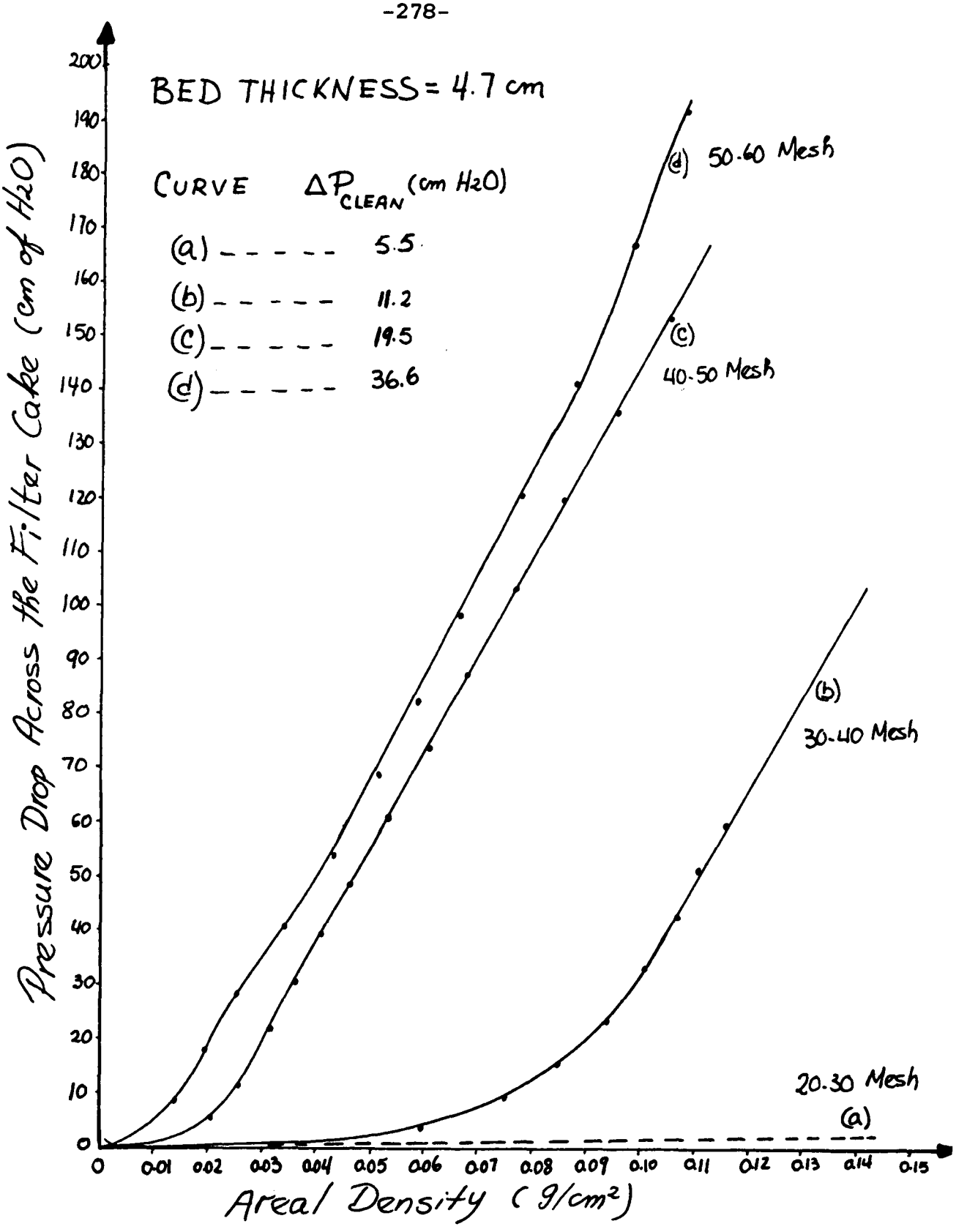

Figure 7-1 Pressure drop versus areal density of Con Edison fly ash deposit on four sizes of sand. Air at 150°C and 18.57 cm/s .

$$\Delta P_{(cm\ H_2O)} = 1780.08\ W_{(grs/cm^2)} - 32.54 \qquad (7\text{-}2)$$

Correlation Coefficient = 0.9996

Points Included: All data points

"50-60 Mesh Angular Sand," Superficial Velocity = 18.57 cm/s

$$\Delta P_{(cm\ H_2O)} = 1897.95\ W_{(grs/cm^2)} - 25.96 \qquad (7\text{-}3)$$

Correlation Coefficient = 0.996

Points Included: Seven points which preceed the last two

Figure 7-2 shows the same plot but at a superficial velocity of 28.67 cm/s.

The regression lines obtained at this higher velocity are:

"30-40 Mesh Angular Sand," Superficial Velocity = 28.67 cm/s

$$\Delta P_{(cm\ H_2O)} = 2856.6\ W_{(grs/cm^2)} - 201.96 \qquad (7\text{-}4)$$

Correlation Coefficient = 0.9807

Points Included: Last four

"40-50 Mesh Angular Sand," Superficial Velocity = 28.67 cm/s

$$\Delta P_{(cm\ H_2O)} = 4202.73\ W_{(grs/cm^2)} - 41.82 \qquad (7\text{-}5)$$

Correlation Coefficient = 0.9972

Points Included: Last nine

"50-60 Mesh Angular Sand," Superficial Velocity = 28.67 cm/s

$$\Delta P_{(cm\ H_2O)} = 4040.0\ W_{(grs/cm^2)} - 8.77 \qquad (7\text{-}6)$$

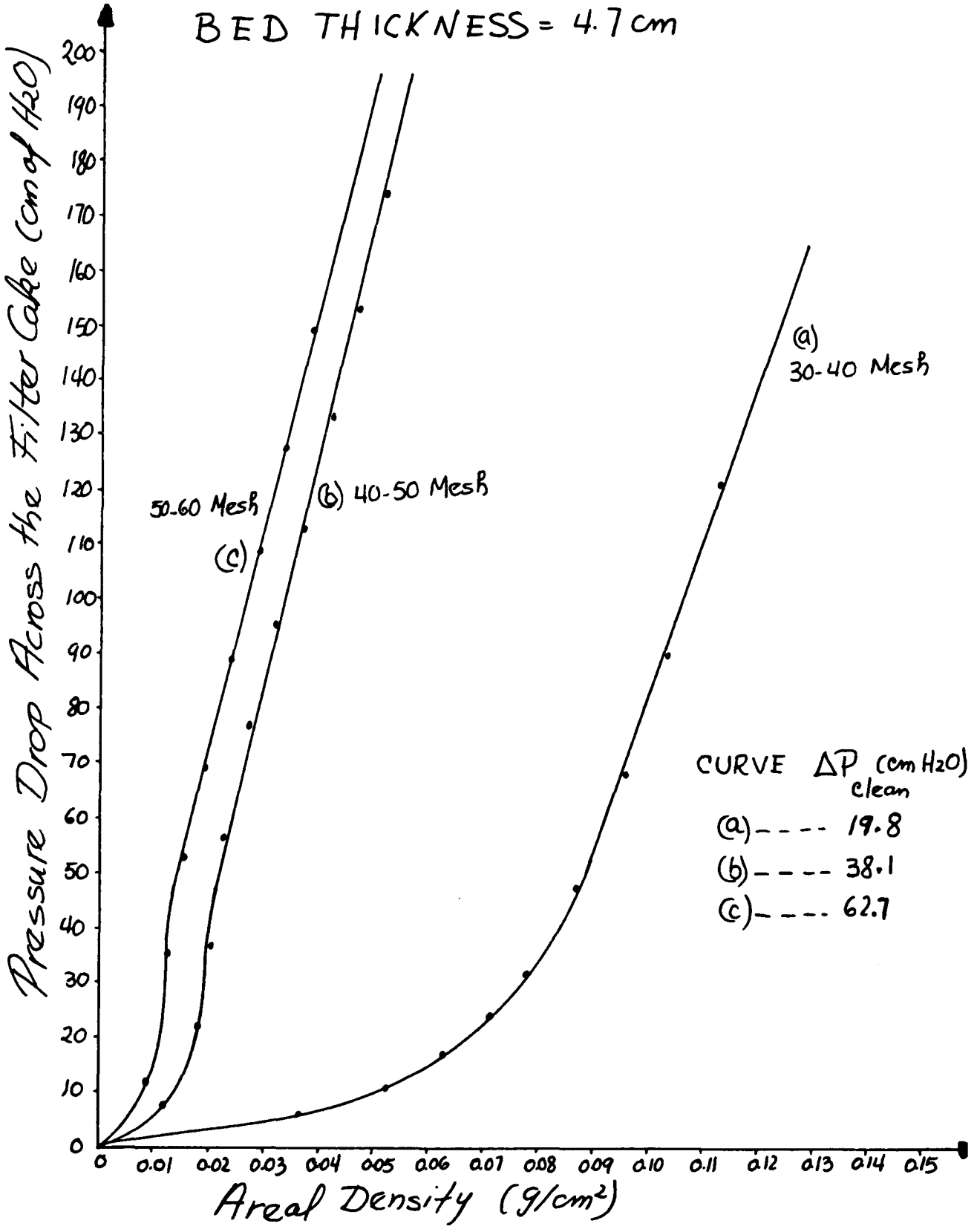

Figure 7-2 Pressure drop versus areal density of Con Edison fly ash deposit on three sizes of sand. Air at 150°C and 28.67 cm/s .

Correlation Coefficient = 0.9988

Points Included: Last seven

Run (a) in Figure 7-1 is for a dust deposit on 20-30 mesh sand. No coherent surface deposit formed, the surface remaining pitted through the run. The low pressure drop at the end of the run reflects the fact that most of the fly ash penetrated deep within the sand bed. As in Taub (1970), fly ash eventually broke through the rear of the bed, and at the end of the run, the float of a rotameter downstream from the bed had become coated with fly ash.

The data suggest the existence of two clearly separated sand size ranges between which a sharp acceleration in the formation of the cake occurs. In other words, between these two sand sizes there is a sharp decrease in the "threshold" areal density of dust at which the pressure drop begins to increase rapidly with further additions of dust. This effect is more pronounced at higher velocity. It can be observed in Figures 7-1 and 7-2 that with 30-40 mesh sand, the cake formed after a considerable amount of dust had been deposited. The difference in "speed of cake formation" between 40-50 and 50-60 mesh sand is negligible if compared to the one which exists in between these two sand sizes and 30-40 mesh sand.

Visual observation of the cakes formed was consistent with the pressure drop data. On 30-40 mesh sand at 18.57 cm/s the roots of the cake extended to about 10 sand grains into the bed and the cake's surface was full of big pinholes

(craters). At 28.67 cm/s the roots extended to 15 grains into the bed and the surface also had pinholes. In general, the cakes formed at 28.67 cm/s looked more coherent than the ones formed at 18.57 cm/s.

Upon 40-50 mesh sand the cakes were unblemished, their surfaces were perfect, with no detectable pinholes. Penetration of dust was restricted to 1 or 2 grains of sand into the bed. The cakes formed at higher velocity looked denser than the ones formed at 18.57 cm/s.

On 50-60 mesh sand the cakes were again unblemished, no pinholes could be seen on the surfaces, and no detectable penetration of dust into the bed was observed.

Tests were conducted with 40-50 and 50-60 mesh sand in which the beds were subjected to an upward air flow entering the bed holder at the bottom. By increasing the upflow of air, a point was reached at which the cakes were fully separated from the sand bed. This ascending plug of dust usually had sand grains attached to its bottom. A further increase in air velocity caused the cake to collapse and the dust particles were entrained in the gas stream. When using 30-40 mesh sand the cakes collapsed upon fluidization without having been separated from the sand surface.

Our pressure drop data confirm Lee's and Wu's earlier finding (Lee, 1975; Lee et al., 1977) that fly ash deposits put down at higher velocities can be appreciably denser than deposits put down at lower velocity. The slopes of the straight portions of the curves in Figures 7-1 and 7-2 given

in Equations 7-1 through 7-6 are summarized in Table 7-1.

TABLE 7-1: Slopes of Straight-Line-Sections of Pressure Drop Curves: Con Edison Fly Ash

Sand Size Mesh No.	Superficial Velocity, cm/s	Slope, (cm of water) (g/cm^2)
30-40	18.57	1742.3
	28.67	2856.6
40-50	18.57	1780.1
	28.67	4202.7
50-60	18.57	1897.9
	28.67	4040.0

According to Equation 4-93, if the fly ash deposits were all of the same porosity, the slopes should have values just proportional to velocity. The slopes for 40-50 and 50-60 mesh sand increase at about the square of the velocity ratios, indicating the marked effect of velocity upon the density of the deposits. The effect with 30-40 mesh sand is not so pronounced.

7.03 Commonwealth Edison Coal Fly Ash Deposited on Horizontal Beds of Sand of Different Particle Size at 150° C

Figure 7-3 illustrates the effect of areal density upon cake pressure drop, at 18.57 cm/s for three sand sizes. Figure 7-4 shows the same plot but at 28.67 cm/s.

The regression lines obtained for this finer ash can be expressed as:

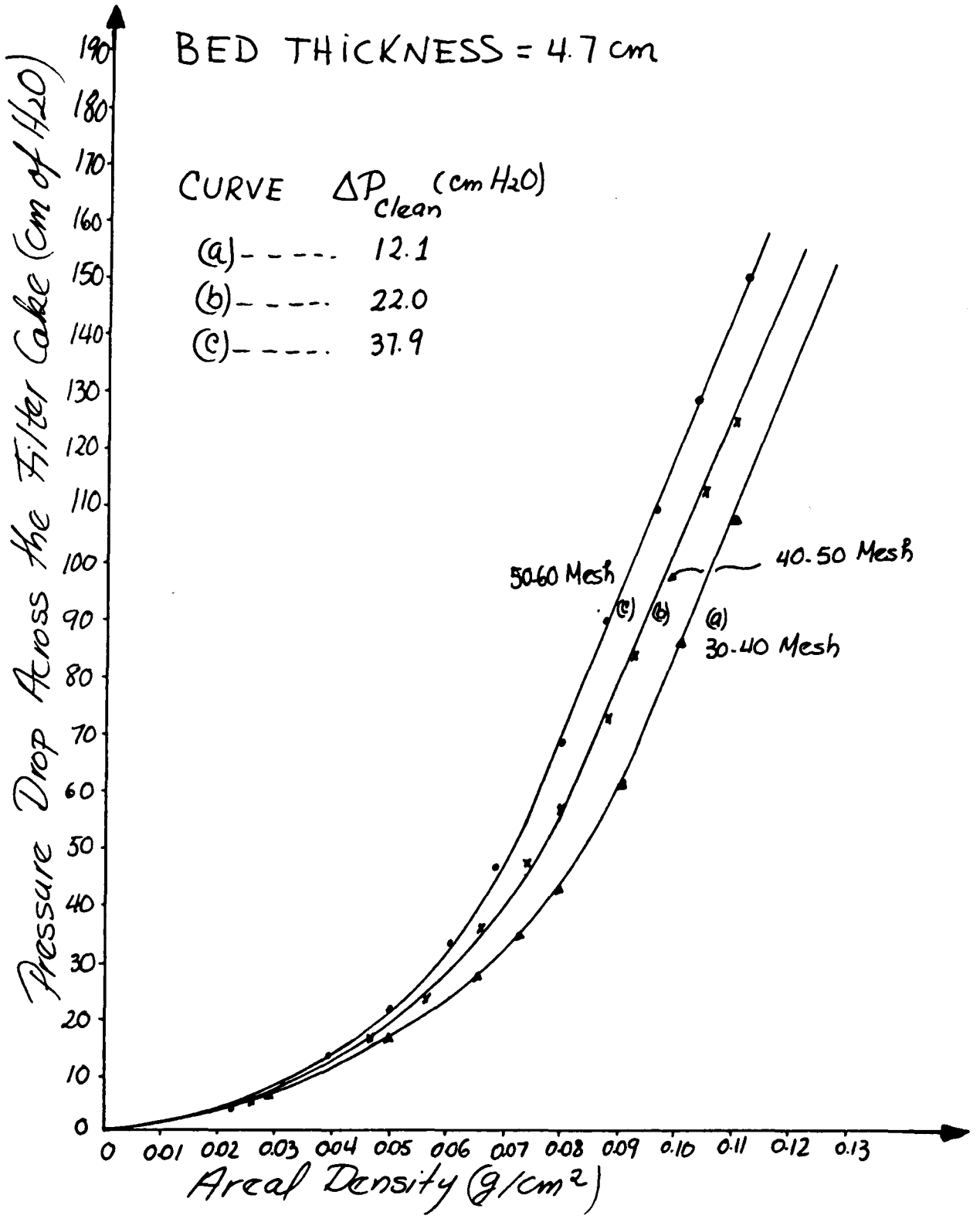

Figure 7-3 Pressure drop versus areal density of Commonwealth Edison fly ash deposit on three sizes of sand. Air at 150°C and 18.57 cm/s .

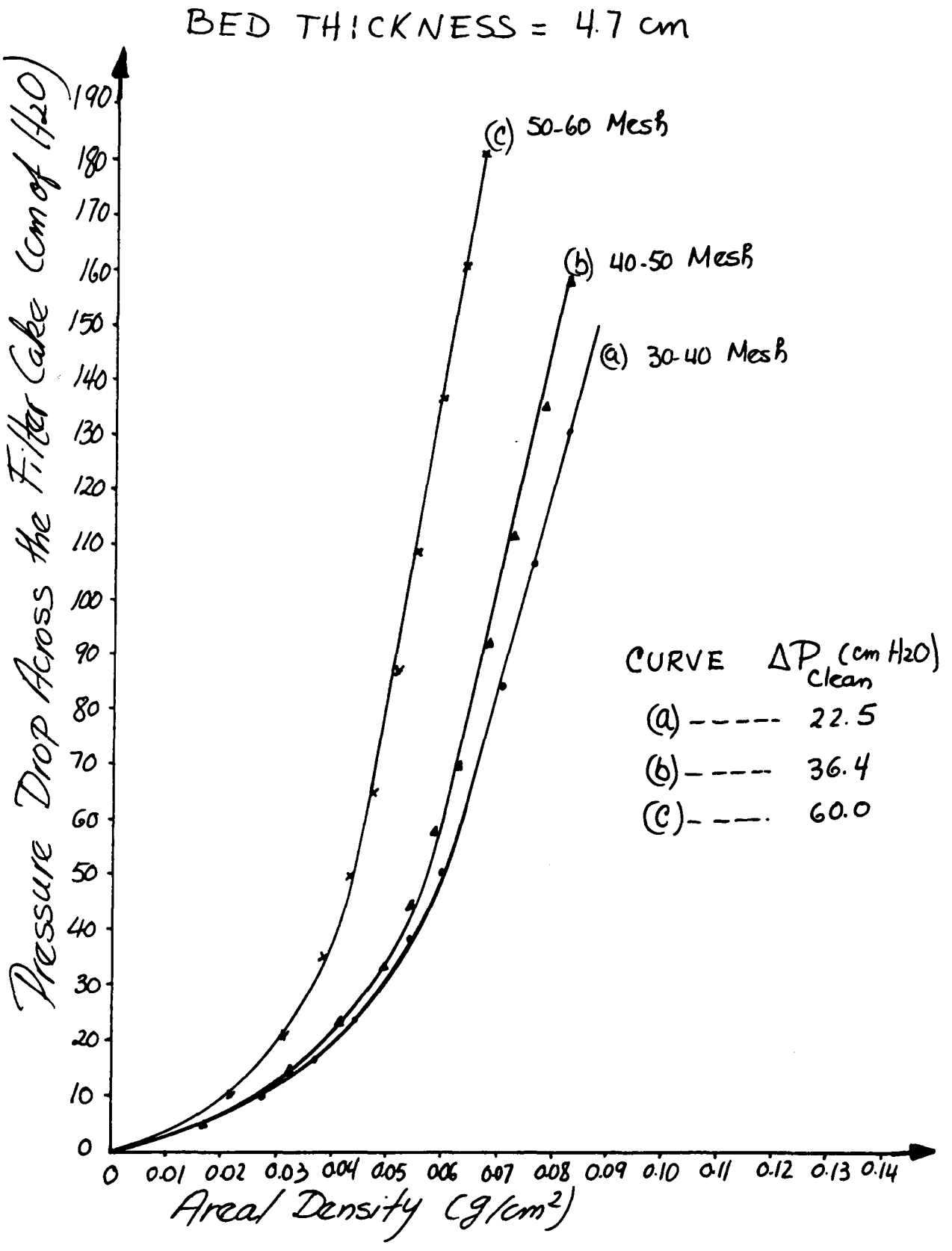

Figure 7-4 Pressure drop versus areal density of Commonwealth Edison fly ash deposit on three sizes of sand. Air at 150°C and 28.67 cm/s .

"30-40 Mesh Sand," Superficial Velocity = 18.57 cm/s

$$\Delta P_{(cm\ H_2O)} = 2456.3\ W_{(grs/cm^2)} - 159.95 \qquad (7\text{-}7)$$

Correlation Coefficient = 0.9974

Points Included: Last three

"40-50 Mesh Sand," Superficial Velocity = 18.57 cm/s

$$\Delta P_{(cm\ H_2O)} = 2360.55\ W_{(grs/cm^2)} - 132.29 \qquad (7\text{-}8)$$

Correlation Coefficient = 0.9994

Points Included: Last six

"50-60 Mesh Sand," Superficial Velocity = 18.57 cm/s

$$\Delta P_{(cm\ H_2O)} = 2444.3\ W_{(grs/cm^2)} - 123.02 \qquad (7\text{-}9)$$

Correlation Coefficient = 0.9967

Points Included: 6 points preceding last

"30-40 Mesh Sand," Superficial Velocity = 28.67 cm/s

$$\Delta P_{(cm\ H_2O)} = 4017.4\ W_{(grs/cm^2)} - 199.3 \qquad (7\text{-}10)$$

Correlation Coefficient = 0.9963

Points Included: Last four

"40-50 Mesh Sand," Superficial Velocity = 28.67 cm/s

$$\Delta P_{(cm\ H_2O)} = 4504.4\ W_{(grs/cm^2)} - 212.2 \qquad (7\text{-}11)$$

Correlation Coefficient = 0.9906

Points Included: Last six

"50-60 Mesh Sand," Superficial Velocity = 28.67 cm/s

$$\Delta P_{(cm\ H_2O)} = 6104.9\ W_{(gr/cm^2)} - 222.72 \qquad (7\text{-}12)$$

Correlation Coefficient = 0.9892

Points Included: Last six

The data shown in Figures 7-3 and 7-4 suggest that the

finer the sand the quicker the cake is formed; the "acceleration" in cake formation with this dust is not a great as before. In other words, the "threshold" areal density at which the pressure drop turns sharply upward does not undergo a drastic drop between two sand sizes, as it did in the data for Con Edison fly ash. At higher velocities (28.67 cm/s) a small effect of this kind is seen when the sand size is reduced to 50-60 mesh.

Visual observation of the cakes formed with this dust brought to light the following phenomena:

The cakes formed on 30-40 mesh sand had a highly irregular surface full of pinholes and extended about 7 to 8 sand grains into the bed. Cakes formed at the higher velocity looked somehow denser and more coherent than the ones formed at lower velocity. Upon fluidization the cakes were slightly separated from the sand bed as plugs until a velocity was reached at which the cakes collapsed. Cake fracture always started at points in the cake where the pinholes were located.

Decreasing the sand size to 40-50 mesh improved the appearance of the cake. The cakes surfaces although still rough were not as irregular as the ones formed on 30-40 mesh sand. Lots of pinholes were present and the roots of the cakes extended to about 4 to 6 sand grains into the bed. The cakes formed at 28.67 cm/s looked denser than the ones formed at 18.57 cm/s. Upon fluidization the cakes were separated from the sand beds and collapsed from fractures originating at pinholes on the surface.

A further decrease in sand size to 50-60 mesh apparently provided a major change in cake structure. The surface looked flatter and the size of pinholes was greatly reduced. The roots now penetrated to about 2 grains of sand into the bed and seemed to be denser than the ones seen with the coarser sands. The cakes formed at 28.67 cm/s showed a denser structure than the ones formed at 18.57 cm/s. The cakes deposited on this finer sand were clearly separated from the bed upon fluidization, and did not collapse as easily as the ones formed on coarser sands.

As Table 7-2 illustrates, an increase in deposition velocity provoked the formation of denser cakes. This effect was more pronounced in cakes formed upon 50-60 mesh sand.

TABLE 7-2: Slopes of Straight-Line-Sections of Pressure Drop Curves: Commonwealth Edison Fly Ash

Sand Size Mesh No.	Superficial velocity, cm/s	Slope (cm of water) (grs/cm^2)
30-40	18.57	2456.3
	28.67	4017.4
40-50	18.57	2360.5
	28.67	4504.4
50-60	18.57	2444.3
	28.67	6104.9

7.04 Clinker Cooler Cement Dust Deposited on Horizontal Beds of Sand of Different Particle Size at 150^{o} C

Figures 7-5 and 7-6 show the effect of increasing cake

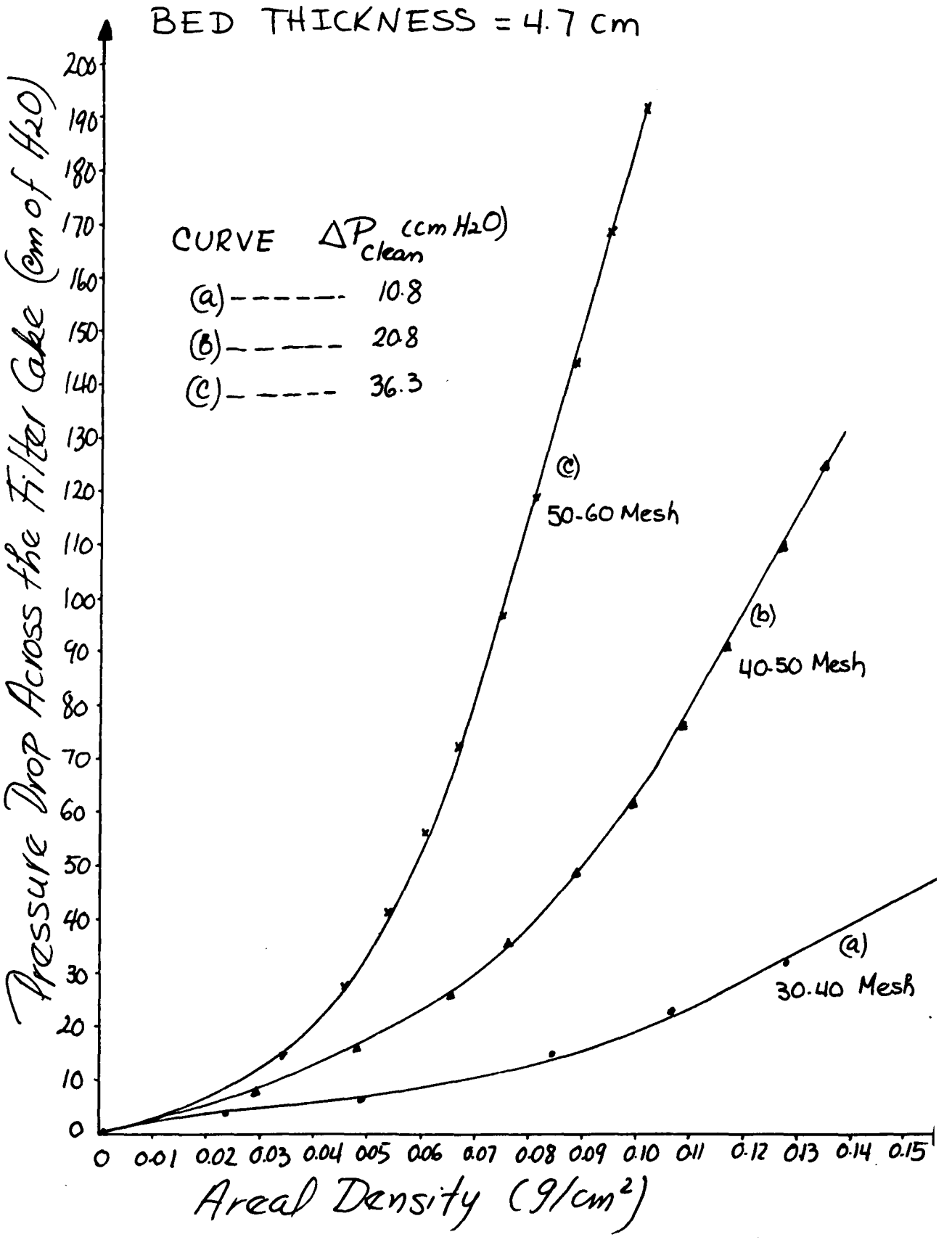

Figure 7-5 Pressure drop versus areal density of Clinker Cooler cement dust deposit on three sizes of sand. Air at 150°C and 18.57 cm/s .

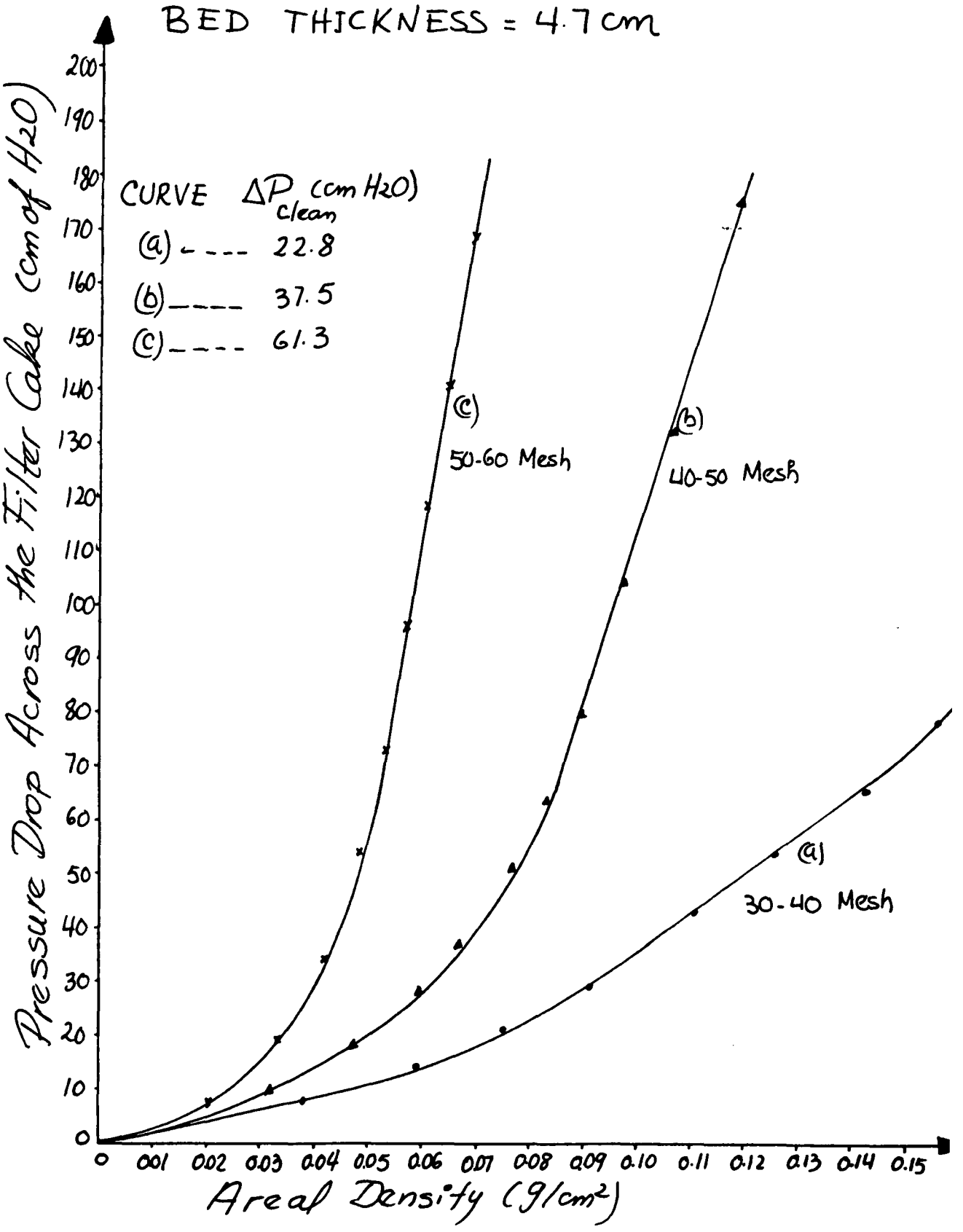

Figure 7-6 Pressure drop versus areal density of Clinker Cooler cement dust deposit on three sizes of sand. Air at 150°C and 28.67 cm/s .

thickness upon air pressure drop, for deposition of cement at 150° C and at 18.57 and 28.67 cm/s superficial velocity respectively.

The regression lines for the straight sections of the curves shown in the Figures can be represented by the following equations:

"30-40 Mesh Sand," Superficial Velocity = 18.57 cm/s

$$\Delta P_{(cm\ H_2O)} = 539.89\ W_{(grs/cm^2)} - 35.53 \qquad (7\text{-}13)$$

Correlation Coefficient = 0.9926

Points Included: 5 points preceding last

"40-50 Mesh Sand," Superficial Velocity = 18.57 cm/s

$$\Delta P_{(cm\ H_2O)} = 1753.39\ W_{(grs/cm^2)} - 110.65 \qquad (7\text{-}14)$$

Correlation Coefficient = 0.9979

Points Included: 5 points preceding last

"50-60 Mesh Sand," Superficial Velocity = 18.57 cm/s

$$\Delta P_{(cm\ H_2O)} = 3474.3\ W_{(grs/cm^2)} - 159.36 \qquad (7\text{-}15)$$

Correlation Coefficient = 0.9956

Points Included: Last six

"30-40 Mesh Sand," Superficial Velocity = 28.67 cm/s

$$\Delta P_{(cm\ H_2O)} = 731.3\ W_{(grs/cm^2)} - 37.4681 \qquad (7\text{-}16)$$

Correlation Coefficient = 0.9999

Points Included: Four Points preceding the last two

"40-50 Mesh Sand," Superificial Velocity = 28.67 cm/s

$$\Delta P_{(cm\ H_2O)} = 3189.4\ W_{(grs/cm^2)} - 203.6 \qquad (7\text{-}17)$$

Correlation Coefficient = 0.9929

Points Included: Last six

"50-60 Mesh Sand," Superficial Velocity = 28.67 cm/s

$$\Delta P_{(cm\ H_2O)} = 6167.6\ W_{(grs/cm^2)} - 257.35 \qquad (7\text{-}18)$$

Correlation Coefficient = 0.9993

Points Included: Last six

Figures 7-5 and 7-6 show a gradual increase in speed of cake formation when the sand size is decreased from 30-40 Mesh to 40-50 and 50-60 Mesh.

Visual observation of the cakes formed with this dust provided the following information:

The cakes formed upon 30-40 Mesh had very irregular surfaces, with huge pinholes. The roots of the cakes penetrated about 10 grains of sand into the bed.

A considerable amount of dust had to be deposited in order to block the passage of particles which were arriving at the surface. The cakes were not coherent and immediately collapsed upon fluidization. During deposition of these cakes, there were instances at which the air pressure drop decreased considerably and then began to increase again.

Decreasing the sand size to 40-50 Mesh improved the structure of the cake. The cakes now had flatter surfaces but still with a lot of detectable pinholes. Upon fluidization the cakes collapsed, after some separation from the bed had occurred. Fracture always began at pinholes. The cakes formed at 28.67 cm/s looked a lot more coherent than the ones formed at 18.57. The roots of the cakes penetrated about 4 to 5 sand grains into the bed.

The cakes formed upon 50-60 Mesh sand were much denser

than the ones formed upon 40-50 Mesh sand; for equivalent cake pressure drops the thickness of the cakes on the finer sand were about one third of the thickness of the cakes formed upon 40-50 Mesh sand. The cakes' surfaces now looked less rough and with fewer pinholes. Penetration of the roots was limited to about 3 to 4 sand grains. Upon fluidization, the cakes separated from the bed as a plug, collapsing at higher air velocities. Cakes deposited at higher velocity (28.67 cm/s) appeared to be more coherent and denser than the ones formed at relatively low velocity (18.57 cm/s). Table 7-3 shows the effect of gas velocity upon porosity of the surface cake formed on beds of different particle size (Equations 7-13 through 7-18).

TABLE 7-3: Slopes of Straight-Line-Sections of Pressure Drop Curves: Clinker Cooler Cement Dust

Size of Sand Mesh No.	Superficial Velocity cm/s	Slope (cm of water) (grs/cm^2)
30-40	18.57	539.9
	28.67	731.3
40-50	18.57	1753.4
	28.67	3189.4
50-60	18.57	3474.3
	28.67	6167.6

Table 7-3 illustrates the fact that upon 30-40 Mesh sand the cakes formed at higher velocity (28.67 cm/s) were looser than the ones formed at lower velocity (18.57 cm/s), whereas upon the other two finer sands the opposite occurred.

7.05 Discussion of Horizontal Bed Studies

7.05.1 Capacity of a Horizontal Bed of Sand at 150° C

Dust deposition, at 150° C on a horizontal bed of sand indicates that if conditions are such that a cake forms on the sand surface, the gas pressure drop will vary with dust areal density according to a well defined pattern. For low areal densities the pressure drop across the gravel layer is low and increases slowly with increase in areal density. Further deposition of dust causes the blockage of the large pores in the bed and the formation of a surface filter cake. Soon after this, a threshold areal density is reached whereupon the pressure drop increases abruptly in a close to linear fashion. This increase in pressure drop is so rapid that the filtration will become impractical as soon as the particulate load exceeds the threshold load. The filter capacity can be judged by extrapolating the steeper slope of the curves of pressure drop versus areal density back to zero pressure drop. Table 7-4 summarizes the horizontal bed capacities for the filtration systems tested.

In general an increase in sand size increased the capacity of the filter. This effect was considerably more pronounced with Con Edison fly ash than with the other two dusts.

An increase in capacity with increasing velocity would imply that the dust particles penetrate deeper into the bed and that cakes formed at different velocities had similar porosities. A capacity decrease on the other hand would imply

TABLE 7-4: Horizontal Bed Filter Capacities at 150° C

Dust	Sand Size	Superficial Velocity cm/s	Wc (grs/cm^2)	ΔPwc (cm H_2O)
Consolidated	30-40 Mesh	18.57	0.0814	13.8
	30-40 Mesh	28.67	0.0707	24.1
Edison				
	40-50 Mesh	18.57	0.0183	3.6
	40-50 Mesh	28.67	0.0100	4.5
Coal				
	50-60 Mesh	18.57	0.0137	8.9
Fly Ash	50-60 Mesh	28.67	0.0022	2.8
Commonwealth	30-40 Mesh	18.57	0.0651	27.7
	30-40 Mesh	28.67	0.0496	32.5
Edison				
	40-50 Mesh	18.57	0.0560	24.5
Coal	40-50 Mesh	28.67	0.0471	31.1
Fly Ash	50-60 Mesh	18.57	0.0503	19.3
	50-60 Mesh	28.67	0.0365	30.9
Clinker	30-40 Mesh	18.57	0.0658	9.4
	30-40 Mesh	28.67	0.0512	11.8
Cooler				
	40-50 Mesh	18.57	0.0631	26.5
Cement	40-50 Mesh	28.67	0.0638	32.6
Dust	50-60 Mesh	18.57	0.0459	28.8
	50-60 Mesh	28.67	0.0417	33.8

Where: Wc = threshold areal density, used for defining the capacity of a horizontal gravel bed filter

ΔPwc = Cake Pressure Drop at Wc.

that cake porosity is reduced by increasing deposition velocity. Our data show that the second effect prevails over the first. In most cases an increase in velocity provoked the formation of denser cakes. Although we did not change the length of the gravel layer, an increase in length, is expected to increase capacity. The data shown in Table 7-4 suggests that if one wants to take advantage of the expected increase in filtration efficiency provided by higher dust areal densities, care must be taken to avoid operation at conditions which will cause a quick approach to the threshold areal density for rapid increase in pressure drop.

7.05.2 Phenomenological Analysis of Horizontal Bed Data

The experimental data obtained in our 150^{o} C horizontal bed of sand could provide useful information about the conditions which determine the speed of formation of a surface filter cake in a gravel filter. A comparison of the three filtration systems explored will be made, with an attempt to identify the causes for dissimilarities in behavior.

7.05.21 Aerodynamic Reaction in the Formation of a Filter Cake

After the roots of a cake have been established the resistance to gas flow is mainly determined by the cake itself. At this moment the aerodynamic regime is determined by the particle Reynold's number based on the dust particle diameter. A combination of Equations 4-67, 4-79 and 4-93 gives the laminar regime relation for the prediction of the gas pressure drop through a filter cake.

$$\Delta P = \frac{s \mu (1-\epsilon_c) \; V \; W}{D_p^{\,2} \; \epsilon_c^{\,3} \; \rho_t} \qquad (7\text{-}19)$$

This equation predicts that for constant gas velocity and viscosity, the deposition of a given dust will originate a linear relation between gas pressure drop and dust areal density. (This implicitly assumes that the porosity of the cake does not change during deposition.)

For a given dust and gas at a fixed temperature and pressure Equation (7-19) could be rewritten as:

$$\Delta P = Kc \; \frac{(1-\epsilon_c)}{\epsilon_c^{\,3}} \; V \; W \qquad (7\text{-}20)$$

Where: Kc = constant

Equation (7-20) shows that an increase in slope will be caused by an increase in gas velocity or by a reduction in cake porosity. Parallel lines at constant velocity imply cakes of the same porosity.

All the curves shown in Figures 7-1 through 7-6 indicate that after an initial period, corresponding to the formation of the roots of the filter cakes, the pressure drop varied linearly with areal density. This behavior suggests that the aerodynamic regime was laminar and that in fact no compaction effects were present. (In some cases at very high pressure drops some reduction in porosity was observed.)

The initial pressure drops (clean bed pressure drops) shown in Figures 7-1 through 7-6 were directly proportional to superficial velocity and inversely proportional to the

square of the particle diameter as predicted by the Carman-Kozeny relation for laminar flow in packed beds (Equation 4-80).

7.05.22 Effect of Sand Size and Deposition Velocity Upon Speed of Formation of Surface Filter Cakes

The three dusts tested formed cakes whose structures depended upon sand size in completely different ways.

An increase in deposition velocity provoked similar effects in the three filtration systems tested.

a) Consolidated Edison Fly Ash

As Figure 7-1 illustrates, at 150^{o} C and at a superficial velocity of 18.57 cm/s it was not possible to form a filter cake upon 20-30 mesh sand. The Figure also shows that the cakes formed upon 30-40, 40-50 and 50-60 mesh sand had almost the same porosity (the straight-line sections of the curves were almost parallel); however, there was a drastic acceleration in cake formation when the sand size was reduced from 30-40 to 40-50 mesh. A further reduction in sand size provided an additional acceleration, although this time the effect was considerably weaker.

The bigger pore volume and smaller tortuosity of the 30-40 mesh sand implied that larger amounts of dust were needed for the establishment of coherent roots, which led to the formation of the surface filter cakes upon this sand. Notice that all cakes with this dust, upon fluidization, separated clearly from the sand surface before collapsing.

In light of this behavior, one is tempted to assume that

the autohesivity of this dust is great while its adhesivity to sand is also sufficient to establish a cake without the building up of very deep roots in the sand.

With this assumption, a possible explanation for the drastic difference in speed of cake formation upon the sand beds of different particle size may be advanced. With large pore volume (i.e., with 30-40 mesh sand) the adhesivity of a dust plays a more important role in the establishment of the roots than its autohesivity. With larger pore volumes a relatively larger amount of dust particles must adhere to sand grains before bridging between dust particles begin to take place. With small pore volumes (i.e., 40-50 mesh sand), dust autohesivity begins to gain importance as soon as a few particles are captured by sand granules.

As Figure 7-2 illustrates, an increase in deposition velocity showed the same trend although this time the cakes were formed at faster rates. The porosity of the cakes decreased with increasing velocity, this effect being more pronounced with the finer sands (40-50 and 50-60 mesh). Apparently the increase in inertial impaction originating from the increase in velocity, provoked the increase in speed of cake establishment.

b) Commonwealth Edison fly ash

As can be seen in Figure 7-3 the cakes deposited at 18.57 cm/s upon the three sand beds had similar porosities. The gradual, small increase in cake formation speed suggests a relatively poor adhesivity of the dust with sand (at least

at the conditions tested). Figure 7-4 shows that the effect of increasing deposition velocity with this system was identical to the one observed with Con Edison Fly Ash (decrease in cake porosity and acceleration in cake formation).

c) Clinker Cooler Cement Dust

Figures 7-5 and 7-6 show that a decrease in sand size originated a gradual increase in speed of cake formation and a decrease in porosity. These phenomena are consistent with the appearance of the cakes formed with this dust. On 30-40 mesh sand big pinholes were observed on the cakes surfaces; a reduction in sand size originated denser cakes with smaller pinholes. The deposits observed on 30-40 mesh sand were not coherent, and again adhesivity with sand seemed to be poor.

The system's reaction to an increase in deposition velocity was similar to the effect observed with the two coal fly ashes.

d) General Conclusions from the Horizontal Bed Studies

The process of deposition of dust in a gravel bed and in the subsequent formation of a filter cake on its surface is complex. This complexity greatly limits the possibility of performing a systematic comparison of the behavior of filtration systems which differ from one another in several characteristics.

The main features of our horizontal bed studies could be summarized as follows:

a) A horizontal bed of sand is a useful tool for determining the maximum size of a given gravel which will

allow the formation of a stable surface filter cake of a given dust under preselected operating conditions.

b) Visual observation of the cakes formed, at 150° C upon sand beds of different particle size, suggests that if high efficiency operation is required, at velocities within the range explored, a sand size close to 40-50 mesh should be used.

c) Due to the effect of different particle size, density and shape, and due to differences in adhesivity and autohesivity and to possible differences in redispersion during the experiments, the porosities of the cakes formed with the dusts tested varied according to the following sequence:

$$\epsilon_{C.E.C.F.A.} < \epsilon_{C.W.E.C.F.A.} < \epsilon_{C.C.C.D}$$

Where:

C.E.C.F.A. stands for Consolidated Edison Coal Fly Ash

C.W.E.C.F.A. stands for Commonwealth Edison Coal Fly Ash

C.C.C.D. stands for Clinker Cooler Cement Dust

d) In general, cakes formed at higher velocities were denser than those formed at low velocity. This effect was more pronounced as the sand particle size was reduced.

e) The analysis of the experimental data obtained in our horizontal bed of sand suggests that it is reasonable to hypothesize that the relative adhesivities of the three dusts tested with sand can be described by the following sequence:

Adhesivity C.E.C.F.A.-sand > Adhesivity C.W.E.C.F.A.-sand > Adhesivity C.C.C.D.-sand

CHAPTER 8.0: ANALYSIS OF EXPERIMENTAL DATA

8.01. Horizontal Bed vs. Panel Bed: The Cake Deposition Paradox.

In Chapter 7.0 we presented and discussed the data obtained during the deposition of three dusts upon a horizontal bed of sand at 150^{o} C; it was then indicated that such studies could be valuable for saving research effort in panel bed filtration (i.e., the maximum size of a given granular material which would provoke the formation of a stable filter cake of a given dust, at preselected operating conditions, can be determined). The idea is that pressure drop data and appearance of cakes formed upon the horizontal beds of sand of different particle size, and at different velocities, could be used for selecting the operating conditions at which the panel bed would efficiently collect the respective dusts.

Chapter 6.0 summarized the results obtained in our laboratory panel bed for the filtration of two coal fly ashes and of a cement dust. Our prediction, based on the horizontal bed data, proved to be useful to the extent that operating conditions which provoked stable cake formation in the horizontal bed also provided high-efficiency filtration in the panel bed. We were puzzled, however, when we observed that the cakes deposited in the panel bed did not

resemble the onesformed in the horizontal bed. Since these differences in cake structure are of fundamental importance in determining the panel bed's capabilities and in understanding its operation, we made a detailed comparison of the data obtained in the two situations.

In Chapter 5.0 we estimated the air velocities at the sand surfaces in the dirty side of the panel bed and with the pressure drop data presented in Chapter 6.0, we were able to plot the dust areal densities (based on the amount of dust spilled from puffback and on the estimated free sand surface exposed to gas flow in the dirty side of the panel) as a function of the cake pressure drops. Figure 8-1 shows such a plot for Con Edison Fly Ash on 40-50 mesh sand, the curves shown in Figures 7-1 and 7-2 for the same filtration system and for similar velocities in the horizontal bed were also plotted in Figure 8-1 for performing the comparison.

Figures 8-2 and 8-3 show similar curves for Commonwealth Edison fly ash and Clinker Cooler cement dust. (The corresponding horizontal bed data were also included).

It can be seen in the Figures, that in general the cakes formed on the horizontal bed were less porous than the ones formed in the panel bed. This difference was specially marked with Con Edison fly ash (Figure 8-1). Visual observation of the cakes formed with this ash in the panel bed taught us that the unblemished cakes formed with this ash in the horizontal bed were no longer present.

The cakes surface looked highly irregular and full of

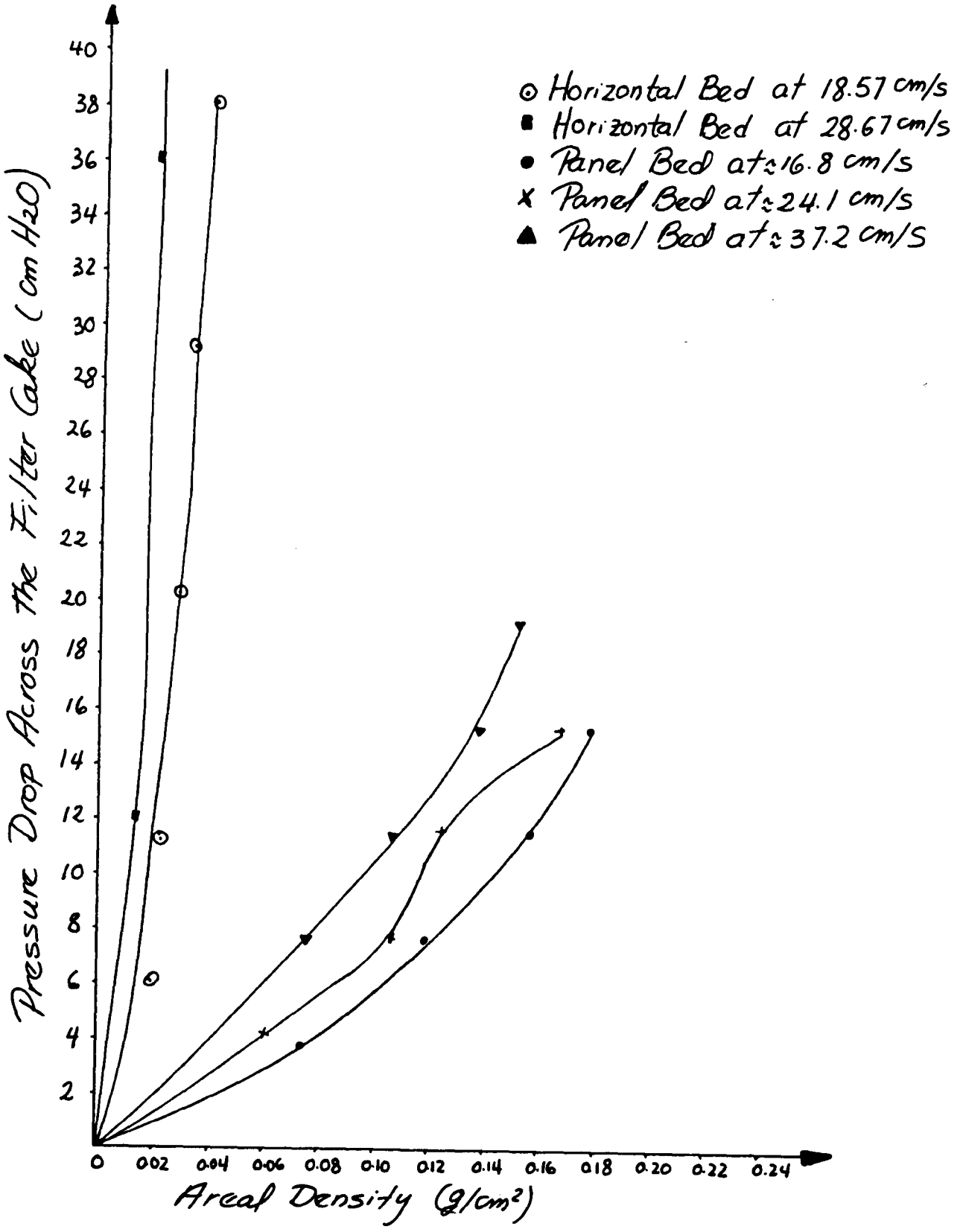

Figure 8-1 Panel Bed versus Horizontal Bed. Pressure drop versus areal density of Con Edison fly ash deposit on 40-50 mesh sand. Air at 150 °C.

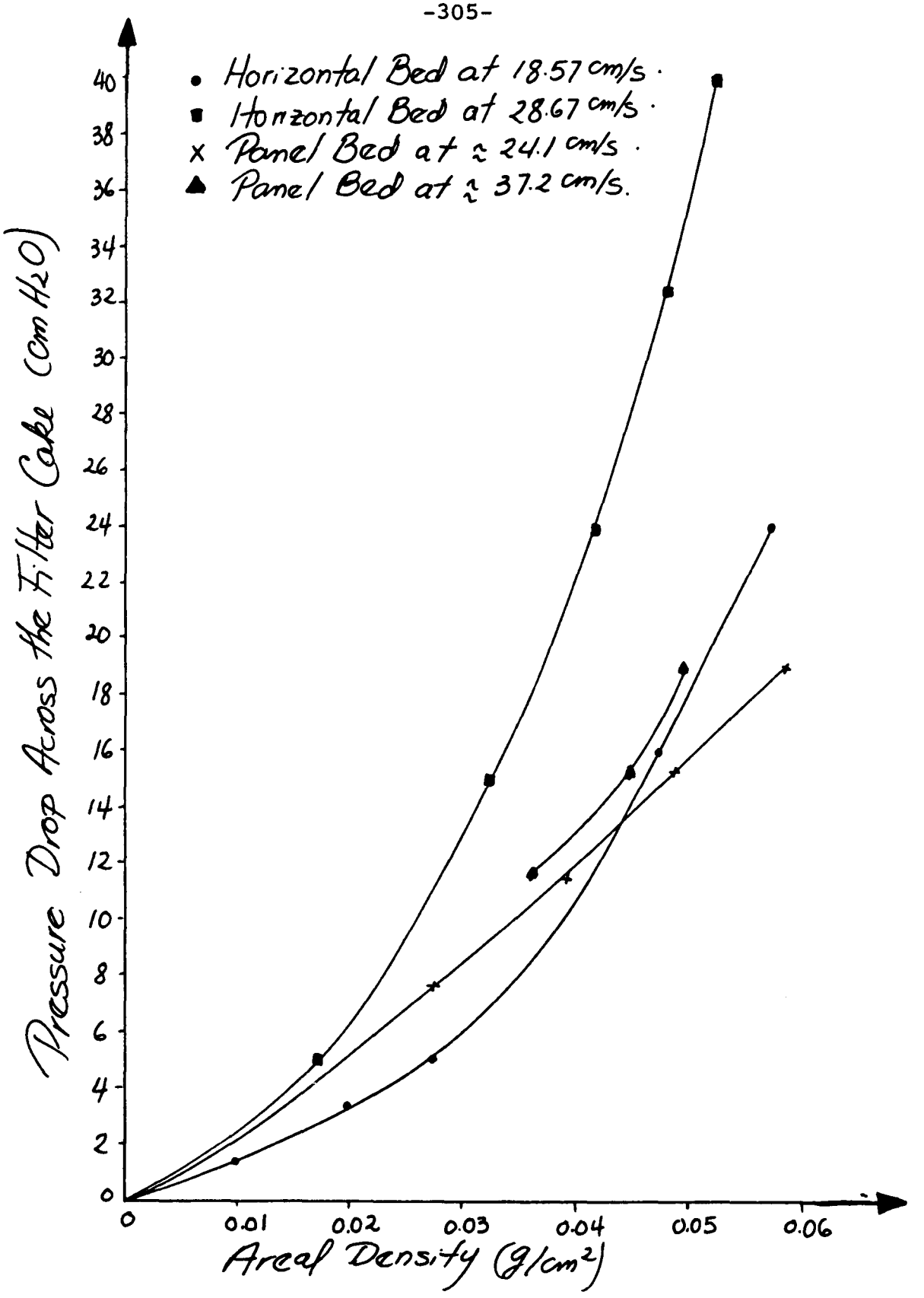

Figure 8-2 Panel Bed versus Horizontal Bed. Pressure drop versus areal density of Commonwealth Edison fly ash deposit on 40-50 mesh sand. Air at 150 °C.

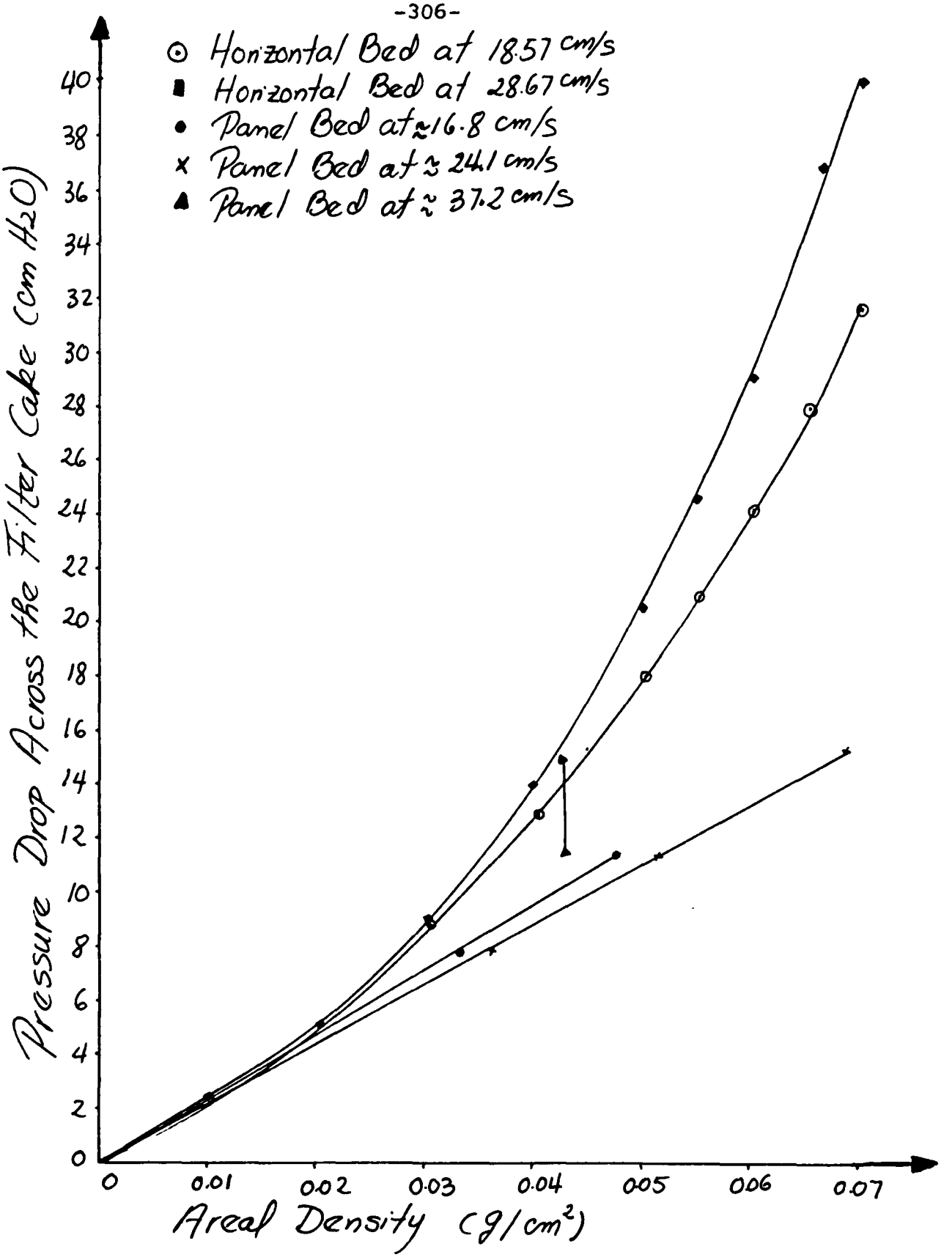

Figure 8-3 Panel Bed versus Horizontal Bed. Pressure drop versus areal density of Clinker Cooler cement dust deposit on 40-50 mesh sand. Air at 150 °C.

pinholes, and in general the cakes were looser than the ones formed in the horizontal bed.

Paretsky (1972) deposited the same fly ash on 20-30 mesh sand in a horizontal bed and in a representative section of a panel bed filter and observed the same phenomenon. He attributed it to a difference in porosity between the two sand beds. He measured a porosity of 0.43 in the horizontal bed and estimated a porosity between 0.55 and 0.61 for the sand in the section of the panel.

Based on the clean bed pressure drops reported in Chapters 6.0 and 7.0 and through the use of Ergun's Equation (Equation 4-82), we have estimated a porosity between 0.41 and 0.42 for the horizontal bed and about 0.49 for the panel bed. These calculations, shown in the Appendix to Chapter 8.0, were performed with the average values of the clean bed pressure drops through the 40-50 Mesh sand beds at 150^{o} C. Apparently puffback in the panel bed filter loosens the bed to an ultimate porosity which is higher than the one obtained by tapping the horizontal bed at the minimum fluidization velocity.

Besides the porosity difference between the two situations, dust is deposited in the horizontal bed from a relatively undisturbed air stream, and on a flat sand surface, while in the panel bed dust is deposited on a curved sand surface and after a 90^{o} turn of the airflow. These two factors contribute to the formation of a non-uniform cake in the panel bed and could aid in the explanation of the observed phenomenon.

It was gratifying to be able to collect this coal fly ash at such high efficiencies and with such low pressure drops (i.e., at such high capacities). Apparently the roots of the cake in the sand bed were denser than the surface cake itself and at the conditions tested they effectively controlled dust penetration.

A situation like the one shown in Figure 7-1 for the finer sands would guarantee high collection efficiency in the panel bed, but it would limit its capacity in such a way that filtration in the device could become impractical.

We indicated in Chapter 5.0 that Commonwealth Edison Fly ash and Clinker Cooler cement dust appeared to have stronger agglomerating tendencies than Con Edison fly ash, and indeed we were expecting to be able to form more compact and stable cakes with these two dusts. The results obtained in the horizontal bed (Chapter 7.0) showed just the opposite to what we expected.

A comparison between Figures 8-1, 8-2 and 8-3 shows that the cakes formed with Commonwealth Edison fly ash and cement dust in the panel bed were considerably denser than the ones formed with Con Edison fly ash, and even when they were looser than the ones formed on the horizontal bed, the difference was negligible if compared to the one observed with Con Edison Fly Ash.

It is understandable to expect different cake structures if the shape and porosity of the deposition surface is modified, but it is a contradiction to observe a modification

of the structure of the cake which does not correspond with the alteration suffered in the deposition surface. In other words, through pressure drop measurements we recognize that porosity in the panel bed is higher than in the horizontal bed and consequently for similar operating conditions we foresee a reduction in cake density rather than an increase.

We, therefore, believe that the two deposition processes were intrinsically different or in other words, that something in the operating procedure was causing that the solid mixtures which were landing on the two sand surfaces were substantially different. The main difference of the two deposition processes was the mode of dust redispersion:

a) In the horizontal bed we simply fed dust to a funnel provided with a 100-mesh screen and shaked it with the help of an electrical vibrator.

b) In the panel bed dust was charged to a cylinder provided with a raking mechanism and the dust after being fed with a screw conveyor into a high pressure chamber was further redispersed by being forced to pass through a critical orifice.

We believe that for dusts with strong agglomerating tendencies (i.e., cement and commonwealth fly ash) the procedure used in horizontal bed deposition did not produce a cloud of individual particles, and that agglomerates were fed to the bed. This would explain the formation of loose cakes with these dusts in the horizontal bed.

On the other hand, in panel bed deposition, with much

better redispersion, we formed denser cakes with the two aforementioned dusts on looser sand beds with curved surfaces. If our hypothesis is correct, horizontal bed deposition of these dusts with efficient dust redispersion would have resulted in surface cakes much denser than the ones formed with Con Edison Fly Ash. That is to say that the trends shown in Figures 7-1 through 7-6 would have been different.

Since we cannot know the difference in dust redispersion which was present while Commonwealth Edison fly ash and cement were deposited on the horizontal bed, we cannot predict at this time the trends in cake structure if each dust were well redispersed; however, the data obtained in the panel bed filter suggest that the autohesivity of these two dusts is higher than the autohesivity of Con Edison fly ash.

8.02 Analysis of the Penetration Trends in 150^{o} C Panel Bed Filtration

A total of four filtration systems were tested in our laboratory panel bed at 150^{o} C. The penetration trends observed in the tests conducted with 40-50 mesh angular sand will be outlined indicating all the collateral phenomena observed during these runs.

8.02.1 General Trends

a) Con Edison Fly Ash:

The filtration pattern of this dust in the panel bed could be summarized as follows:

1. At fixed cleaning intensity, dust penetration increased with increasing filtration velocity; a sharp break

in this trend occurred between 11.12 and 17.2 cm/s (superficial velocity).

2. At fixed velocity, an increase in cleaning intensity does not much affect dust penetration if the filtration velocity is kept below a critical value (velocity at which a drastic deterioration of performance occurs). At higher velocities an increase in cleaning intensity greatly improves the filter's collection efficiency.

3. An increase in dust areal densities generally improve the performance of the filter; however, dust reentrainment originated from cake rupture at relatively high pressure drops reaches a level at which the net effect of further dust deposition without cleaning is a reduction in the cumulative efficiency of the filter.

During these filtration runs we always observed a sudden decrease in pressure drop at high cake densities. This phenomenon usually occurred at a cake pressure drop of about 14.5 cm of H_2O. This disturbance was reproducible and cause a reduction in pressure drop between 2 and 3 cm of H_2O. It was always possible to continue the filtration run (until the preselected cake pressure drop was reached) without a repetition of the phenomenon.

Figures 6-2, 6-3, 6-5 and 6-6 show that increasing the cake pressure drop beyond the point at which a deterioration in performance resulting from dust reentrainment begins to appear, provides an increase in collection efficiency. In most cases, however, a further increase in areal density

suggests that at some point a maximum thickness of filter cake, beyond which it would not be prudent to go, will be reached.

We believe that this phenomenon occurs when unstable cakes gain stability as a result of compaction. This observation is consistent with the faster increase in pressure drops, at high dust areal densities, shown in Figure 8-1.

For this filtration system, higher areal densities before cleaning always implied higher sand spills at a fixed puffback intensity. This implies that the decrease in permeability provoked by the presence of the cakes offset the increase in soil strength resulting from the binding of sand grains by the fly ash deposits.

b) Commonwealth Edison Fly Ash

The filtration pattern of this somewhat finer fly ash in the panel bed could be described as follows:

1. At fixed cleaning intensity, dust penetration decreased with increasing filtration velocity, although no sharp break in this trend was observed.

2. At fixed velocity, an increase in cleaning intensity produced a deterioration in the filtration performance of the panel bed. This effect was considerably more pronounced at intermediate velocities (11.12 cm/s) than at high velocity (17.2 cm/s).

3. At fixed velocity and cleaning intensity, an increase in cake thickness (areal density) improved the performance of the filter up to a point at which a sharp

deterioration occurred. This behavior was observed just while working at intermediate velocities (11.12 cm/s). At high velocities (17.2 cm/s) thicker cakes produced a slight increase in dust penetration. With this dust, we never observed sudden decreases in pressure drops.

In most cases an increase in areal density did not much affect the amount of sand spilled at a fixed puffback intensity.

c) Clinker Cooler Cement Dust

The filtration pattern of this dust in the panel bed could be summarized as follows:

1. At fixed cleaning intensity, an increase in filtration velocity provided a slight increase in performance.

2. For intermediate velocity filtration (11.12 cm/s) an increase in puffback intensity produced a sharp increase in dust penetration. At high velocities (17.2 cm/s) the same increase in cleaning intensity did not much affect the filtration efficiency.

3. At a fixed velocity and cleaning intensity, thicker cakes provided better efficiencies up to a point at which an indication of deterioration in performance began to be observed. This was tested just at the intermediate velocity. At low and high velocities, for the range of cake pressure drops explored, thicker cakes always provided better efficiencies. At a fixed velocity and cleaning intensity the amount of sand spilled at different areal densities did not vary considerably. (The sand spills produced during puffback with this filtration system were not as uniform as

the ones produced with the previous systems.)

8.02.2 Comparative Analysis of Penetration Trends

A comparison between the filtration performance of the panel bed with the three dusts tested could give us some insights about its mechanism of operation. The fact that we were able to achieve very high collection efficiencies in the filtration of three dusts of different characteristics at similar operating conditions, complicates the process of identification of the variables which might have been causing differences in penetration trends.

A sand size which proved to be able to provoke the formation of surface filter cakes at 150^{o} C with the three dusts tested was selected (40-50 mesh sand); consequently, the panel bed was operated under cake filtration mode; most of the time. Sieving, the most important collection mechanism in cake filtration was responsible for the high efficiencies obtained. This collection mechanism depends fundamentally on the structure and stability of the cakes formed, and as a result it was of first priority to explore the operating variables which could affect the cakes' structures. If cleaning (puffback) is controlled in such a way as to always leave roots of the dust being filtered close to the surface of the filter, clean bed filtration should be of secondary importance (i.e., the pores of the sand bed would be clogged soon after a filtration cycle starts).

Table 8-1 illustrates the variables which could affect the performance of the panel bed filter of a fixed geometry

(fixed dimensions and louver shape).

TABLE 8-1: Variables which Affect Efficiency of Collection in a Panel Bed Filter of Fixed Geometry

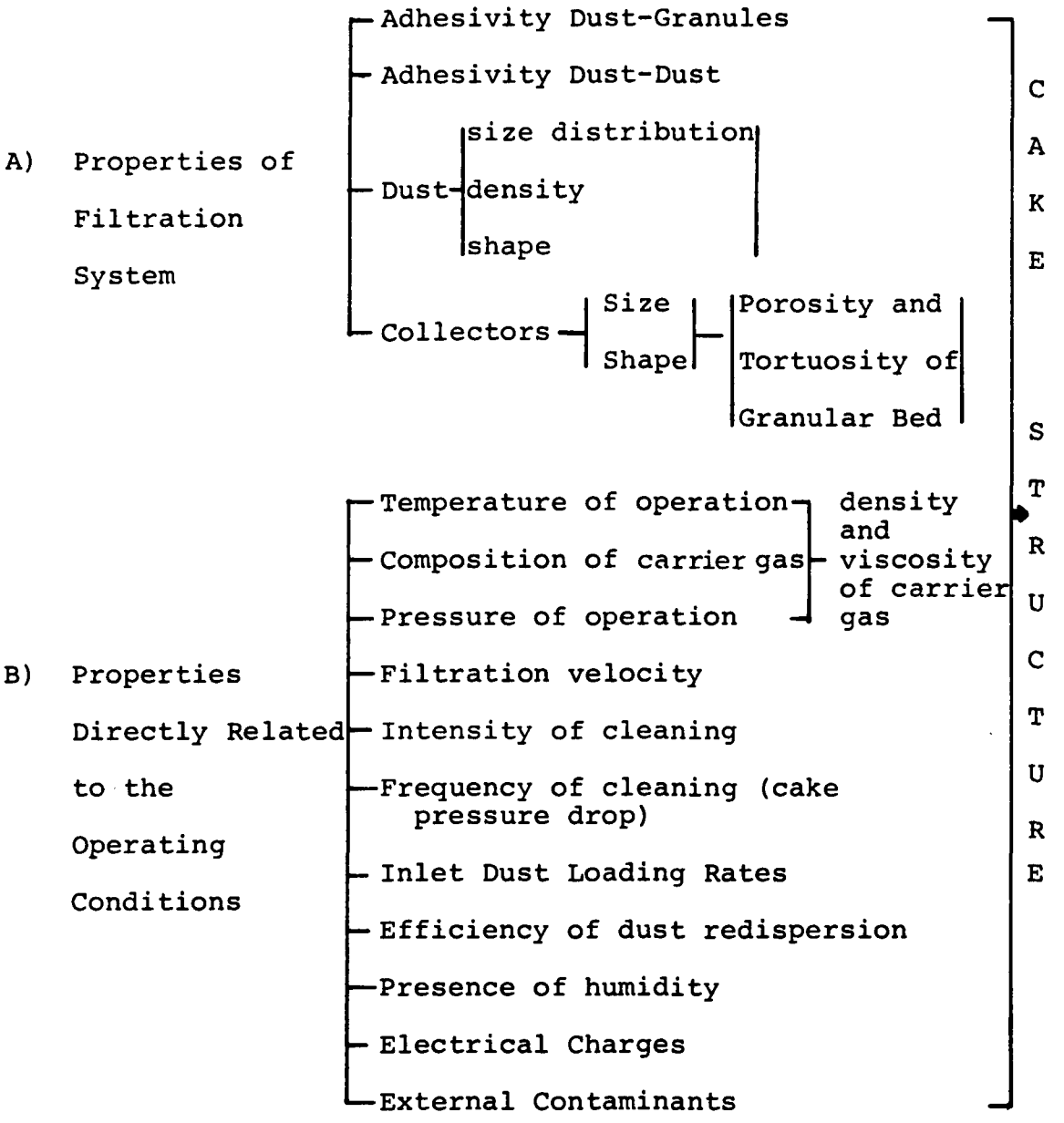

In our experiments, we explored the effect of the properties of the filtration system and fixed all the

variables directly related to the operating conditions excepting:

a) Filtration velocity; b) Frequency of cleaning (cake pressure drops); and c) Intensity of cleaning (Puffback pressure).

After the initial exploratory runs the sand type and size was also fixed: 40-50 mesh angular silica sand. As a result the porosity and tortuosity of the granular bed were also kept approximately constant.

Our results show that Con Edison fly ash was filtered at higher efficiencies than the other two dusts. This was specially true when the filter was operated at low or intermediate velocities (7.75 and 11.12 cm/s). At higher velocities (17.2 cm/s); however, it was necessary to increase the cleaning intensity in order to provide efficiencies which were just comparable to the ones obtained with the other two dusts. For the conditions used in these experiments (dust size and density, collector size, filtration velocity and gas viscosity) the main mechanism of clean bed collection, is inertial impaction and this should increase with increasing filtration velocity; therefore, we cannot attribute the decrease in performance with increasing velocity to a decrease in clean bed filtration.

A possible explanation of this phenomenon is that probably some particles were bouncing back upon collision and therefore were able to penetrate deep into the bed (or eventually all the way through). This would delay the

formation of the highly efficient surface cake and would provoke the formation of unstable roots. The effect of higher drag forces exerted on previously collected particles could weaken the roots of the cake (seepage dust penetration) and this could at higher pressure drops provoke the rupture of the cakes (pinhole plug penetration). We believe that dust re-entrainment resulting from cake instability was the main responsible for the increase in penetration at higher velocities. The fact that an increase in puffback intensity sharply improved filtration performance is a clear indication that dust had penetrated deep into the bed, and on the other hand it also shows that penetration of Con Edison fly ash in the panel bed under these conditions was a gradual phenomenon.

The lower efficiencies obtained with Commonwealth Edison fly ash at the lower velocities were expected since this fly ash had noticeably larger proportion of fine particles ($< 5 \mu m$). It was a surprise, however, to observe a considerable increase in penetration with increasing puffback intensity. This phenomenon suggests that the decrease in efficiency was not provoked by gradual deeper penetration of an unstable cake but by the penetration of very fine material mainly during the initial period of filtration (clean bed filtration). This also suggests that probably the front of dust penetrated deeper into the bed than did Con Edison fly ash, something which indicates that the adhesivity of this dust with sand was lower than the adhesivity of Con Edison fly ash.

In other words, the Commonwealth Edison fly ash gave cakes with deeper roots, and its filtration was more sensitive to puffback, because removal of all of the roots gave rise to clean bed filtration at the start of the next cycle.

If our hypothesis is correct, an increase in filtration velocity of the same magnitude as the one which before had sharply deteriorated the performance of the filter should not cause the same effect with this fly ash. It was gratifying to observe than an increase in filtration velocity instead of causing a deterioration in performance increased the collection efficiency. Apparently the cakes formed at higher velocities were less porous than the ones formed at low velocity and impeded excessive penetration of fine material.

Fine dust penetration during clean bed filtration, the main effect responsible for low efficiencies at the lower velocities, must have decreased substantially in order to provide the increase in performance at higher velocities. Apparently due to higher inertia the collection of finer particles was enhanced. The fact that at the highest velocity tested (17.2 cm/s) an increase in puffback intensity did not much change the cumulative collection efficiency suggests that dust re-entrainment, possibly through the pinhole plug mechanism, is beginning to act and is causing deeper penetration of dust.

We thought that raw cement, with its coarser particle size and with its strong agglomerating tendencies, was going

to be easier to filter than the two coal fly ashes at similar operating conditions. However, our results show that at low and intermediate velocity the collection efficiencies were lower than the ones obtained with Con Edison fly ash; nevertheless, they were much better than the ones obtained with Commonwealth Edison fly ash. Apparently, the cakes formed at these lower velocities with these coarser particles were loose enough as to permit the passage of relatively coarse material. At the intermediate velocity (11.12 cm/s) an increase in puffback intensity provoked a sharp increase in penetration. This resembles the behavior of Commonwealth Edison fly ash at this velocity and suggests both that the roots penetrate deep into the bed and that clean bed filtration at this velocity is not very efficient with this dust. (Something which suggests that the adhesivity of this dust with sand is much lower than the adhesivity of Con Edison fly ash.)

An increase in filtration velocity did not deteriorate the collection capability of the panel bed, and in fact a slight improvement was achieved. This reflects the fact that at higher velocity clean bed filtration is enhanced (higher inertia) and that the cakes formed were less porous. Tests performed at the highest velocity (17.2 cm/s) showed that an increase in puffback intensity did not much affect efficiency, indicating that the roots were now deeper probably as a result of increase collection at deeper locations in the bed or as a result of increasingly important dust re-entrainment

penetration mechanism (seepage and pinhole plugpenetration).

8.03 Model for Granular Bed Filtration

The analysis of the phenomena observed during this investigation could be summarized by postulating the different situations that one can encounter in cake filtration with granular beds.

As a result of the complexity involved in dust deposition and cake formation upon granular beds, and the lack of sufficient theoretical tools which would allow the prediction of the performance of a preselected granular bed in the filtration of a given dust mixture, at given operating conditions, we have to simplify the numerous different situations which could exist by postulating the extreme cases which may be encountered.

Lee (1975) classified the granular bed filtration process into three types--the clean bed filtration, the rooting cake filtration, and the surface cake filtration. Figure 3-19 illustrates Lee's view of granular bed filtration.

The clean bed filtration is the stage in which the granules are basically clean, or if they carry some adhering dust, the dust is not heavy enough to form a thick layer over the surface. In the clean bed filtration, the major filtration mechanism is adhesion and the efficiency will be relatively very poor.

In the rooting cake filtration process, the front and rear of the granules will be filled with dust, and the dust tends to form a continuous phase within the granules. During

this process the efficiency will increase markedly yet the pressure drop will not change much. In rooting cake filtration, adhesion and straining would interact as the collection mechanisms.

After the roots of the cake have been established, the filter cake will grow above the bed's surface. The efficiency will increase to such an extent that most of the dust will be stopped by sieving at the bed surface. Lee (1975) postulates that during this process the penetration will be inversely proportional to the thickness of the filter cake.

According to Lee (1975), filter cakes formed at high velocity are denser than the ones formed at low velocity, but their surfaces will have more and larger pinholes. He concludes that the combination of these dissimilarities will counteract, and that therefore the prediction of collection efficiency and pressure drop increase will be a difficult task.

Although Lee points out that the efficiency of surface cake filtration depends on the porosity of the filter cake, the number and size of pinholes, the velocity of the air and the adhesion and autohesion of the dust, he does not present the extreme cases which could be originated from a variation of the filtration conditions in granular bed filtration and does not consider dust re-entrainment as an important penetration mechanism during cake filtration.

We recognize the merit of the model presented by Lee and accept its fundamental features. We shall, however, explore

the effect of adhesion and autohesion upon the three aforementioned granular bed filtration processes. Emphasis will be given to the effect of these properties upon efficiency and pressure drop.

We shall assume that the differences between the filtration systems to be considered are of such magnitudes which permit at some operating condition the formation of surface filter cakes upon a granular bed of fixed properties. In other words, we shall analyze the performance of a preselected granular bed in the filtration of different dusts which all form a surface filter cake upon the granular bed.

Figures 8-4 through 8-7 illustrate the extreme cases that we may encounter.

Figure 8-4 shows the process of formation of a surface cake with a dust with poor adhesivity and autohesivity. Efficiency during clean bed filtration will be poor, and loose roots will be established across a considerable thickness of the granular bed. During rooting-cake filtration adhesion and straining will interact although not so efficiently as a result of the lack of coherency in the roots. The surface cake will eventually form, and it will be very loose and with an irregular surface full of peaks and valleys. Dust penetration during cake filtration may be by straight-through penetration (fine particles) or as a result of dust re-entrainment through two different mechanisms:
a) Seepage penetration: As a result of the permanent action of the drag force exerted by the flowing gas upon unstable

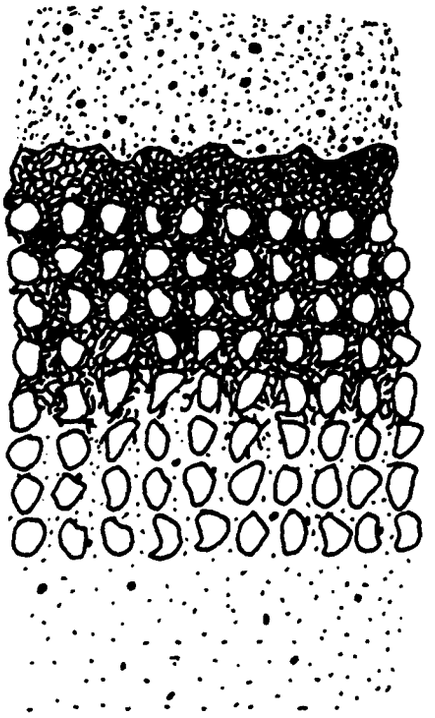

Figure 8-4 Formation of a Surface Cake with a Dust of Poor Adhesivity and Autohesivity

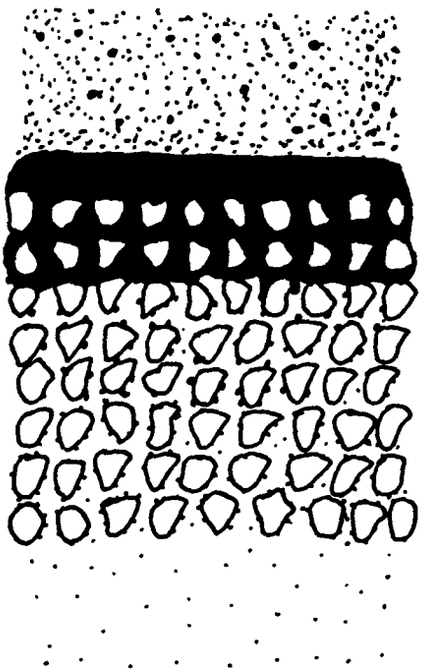

Figure 8-5 Formation of a Surface Cake with a Dust of Good Adhesivity and Autohesivity

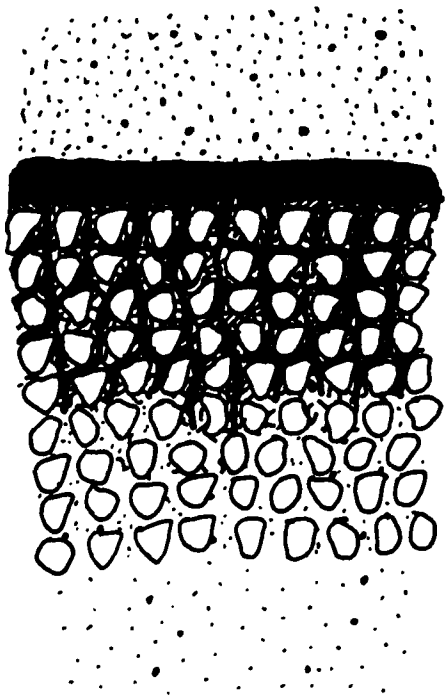

FORMATION OF
A SURFACE CAKE
WITH A DUST OF
POOR ADHESIVITY
AND GOOD AUTOHESIVITY

Figure 8-6 Formation of a Surface Cake with a Dust of Poor Adhesivity and Good Autohesivity

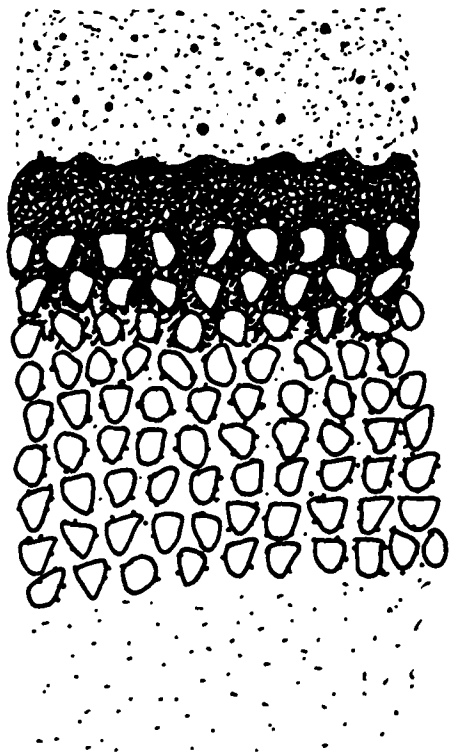

FORMATION OF
A SURFACE CAKE
WITH A DUST OF
GOOD ADHESIVITY
AND POOR AUTOHESIVITY

Figure 8-7 Formation of a Surface Cake with a Dust of Good Adhesivity and Poor Autohesivity

roots, small chunks of dust particles will be separated from the roots located deep within the bed and will become reentrained.

b) Pinhole plug penetration: As a result of the effect of gas pressure drop and velocity upon dust particles located just above the pores of the sand bed (weakest position in the cake), a plug of dust particles may be dislodged from the cake and begin penetrating the sand bed. If the plug collapses (becomes redispersed) some particles will rapidly find their way through the unstable roots and some will be collected at deeper positions within the bed. These holes will connect the cake-sand bed interface with the cake surface and this will also enhance further penetration by the straight-through penetration mechanism.

A situation like the one just described will provide a filter with relative large capacity and relative low efficiency.

An increase in deposition velocity with a filtration system with these characteristics will provide an increase in efficiency during clean bed filtration if inertial impaction predominates as the collection mechanism. This would imply the formation of relatively shallower and denser roots and a cake with a more stable structure (less porous). However, seepage penetration will increase as a result of the increasing velocity, and further dust deposition on a less porous cake will cause a faster increase in pressure drop and probably a faster approach to the resistance of the weakest points at

the interface enhancing therefore pinhole-plug penetration. The overall effect would be a decrease in the filter's capacity and efficiency.

Figure 8-5 illustrates the process of formation of a filter cake with a dust with good adhesivity and autohesivity. Efficiency during clean bed filtration will be good and roots which are shallow and dense will be rapidly established. At this point efficiency will sharply increase and so will the gas pressure drop. A dense surface filter cake with great stability will be quickly formed, and filtration efficiency and pressure drop will rise again. The main collection mechanism will almost always be straining.

A granular filter operating under such conditions will provide excellent efficiencies even for very fine dust particles ($< 1\ \mu m$) but will have a very small capacity.

An increase in deposition velocity will accelerate the process just described.

Dust re-entrainment by the seepage penetration mechanism will be minimum; while pinhole plug penetration will be encountered if the filter is operated at very high cake pressure drops.

Figure 8-6 shows the process of cake formation with a dust of poor adhesivity and good autohesivity. Under these conditions clean bed filtration will be poor and the process of roots establishment will be slow. The roots once formed will extend deep into the bed and will be unstable but relatively dense. At this point the pressure drop and

efficiency will start to increase as sieving gains importance.

Eventually a dense surface cake will begin to form. This cake will be highly efficient as long as the roots close to it do not deteriorate.

With a situation like this, dust re-entrainment by seepage penetration will be always present, and pinhole-plug penetration may not exert a major influence as long as the roots close to the cake surface remain coherent.

An increase in filtration velocity with a system like the one just described will improve clean bed filtration if inertial impaction is the main collection mechanism. This would imply an acceleration in the establishment of the roots, which this time will be shallower and denser. Re-entrainment by seepage will be greatly enhanced.

The surface cake will be formed faster and will be less porous; this would provoke a rapid increase in pressure drop and efficiency. Further dust deposition will provoke a fast increase in pressure drop and in efficiency up to a point at which the combined effects of pressure drop and velocity, coupled with the presence of unstable roots, could greatly enhance the formation of pinholes all over the cake surface. The situation at this moment could degenerate in a sharp deterioration of the filter's performance resulting from excessive dust re-entrainment and straight-through penetration. The capacity and efficiency of a granular filter working with a filtration system like the one just described would be between those of granular filters which operate with the two previously described filtration systems.

Figure 8-7 illustrates the process of formation of a filter cake with a dust of good adhesivity and poor autohesivity. Under these conditions clean bed filtration will be efficient and will provoke the rapid formation of shallow, stable and not too dense roots. The pressure drop will increase slowly and efficiency will be considerably enhanced. The cake once formed will provide a further increase in efficiency and a moderate increase in pressure drop. Dust re-entrainment from seepage penetration under these conditions should not be an important penetration mechanism; however, pinhole-plug penetration must be considered. If the cake pressure drops are kept below a certain critical value pinhole-plug penetration should not sharply deteriorate the filter's performance.

An increase in deposition velocity would improve clean bed filtration if inertial impaction is the main collection mechanism. The roots will be quickly established and the cake will be denser. This would cause an increase in pressure drop and in efficiency. Seepage penetration should increase moderately.

Further dust deposition would increase efficiency up to a point at which the combined effect of pressure drop and velocity could provoke the rupture of the cake at different positions on its surface and this effect combined with very shallow roots would cause a drastic deterioration in filtration performance.

If operated with caution this filter could provide high efficiency and capacity.

8.04 Model for Panel Bed Filtration

The panel bed filter was conceived as a granular filter which should work under cake filtration conditions in order to provide high collection efficiency in the filtration of a variety of dusts of different characteristics.

Since a rapid establishment of a surface cake constitutes a fundamental feature in its operation, its design is best suited for the filtration of relatively concentrated solid-gas mixtures. This mode of operation requires the periodic removal of the cakes whenever resistance to gas throughput increases to an unacceptable level. Puffback cleaning was then incorporated to the design providing an efficient way of cake removal and permitting therefore the cyclic operation of the device.

The three granular bed filtration processes described in the preceeding subsection are present in panel bed filtration. However, a proper design should minimized the influence of the least efficient filtration process; in other words, the operation of the filter must be directed toward the elimination of clean bed filtration.

Puffback cleaning, if properly monitored, can provide an efficient way of performing this task. If its intensity is such that it just removes the surface filter cake and some of the cake's roots, the formation of a new cake in a subsequent filtration cycle will be accelerated. In other words, a good puffback would leave some dust roots close to the sand surface and would therefore considerably decrease

the effect of the relatively inefficient clean bed filtration process.

Experience gathered by Squires (Squires and Pfeffer, 1970), Paretsky (1972), Lee (1975) and throughout this investigation indicates that after a few filtration cycles, puffback provides an almost constant preloading of the filter. A very important feature of this phenomenon is that the roots of dust left near the filter's surface may provide a considerable increase in filtration performance but do not provoke a sharp increase in the initial pressure drop.

Under these conditions, sieving becomes the main collection mechanism in panel bed filtration and what really becomes important is to avoid that further dust deposition causes reentrainment of previously collected particles. In other words, we must try to preserve the stability of the roots and cake.

8.04.1 Panel Bed Filter: Efficiency vs Capacity

In Chapter 7.0 of this dissertation we indicated that for a given dust there exists a maximum size of a given granular material which would provoke the formation of a stable surface filter cake. The results obtained during deposition of three different dusts upon horizontal beds of sand of different particle size indicated that the finer the sand the quicker the cake is formed. It was also observed that a reduction in sand size bellow the "maximum," provoked the formation of denser cakes with shallower roots. Denser cakes always had flatter surfaces. It was then pointed out

that the difference in the acceleration of cake formation resulting from the reduction in sand size while depositing the different dusts should be attributed to differences in adhesivity and autohesivity of the filtration systems studied.

In the panel bed, the size of the granules for the filtration of a given dust should be such as to provoke the formation of surface filter cakes whose roots do not extend beyond the width of the front louver plate. Deeper roots would not be stable since the downward movement of the sand resulting from puffback would tend to redisperse them originating a source of penetration by reentrainment and an accumulation of dust at the bottom of the filter. This last phenomenon will cause flow distribution problems and eventually the saturation of the bed.

Once we have found a granular material of a size which fullfill the above requirements, a further reduction in size will produce an increase in efficiency at the expense of a reduction in capacity. In other words, for constant velocity filtration and for a preselected total pressure drop before cleaning, the filter with the smaller sand would collect a smaller amount of dust in a filtration cycle; and this would necessarily imply an increase in the frequency of cleaning.

A practical limitation in the frequency of cleaning could determine that this increase in efficiency can only be obtained at the expense of a higher pressure drop (higher operating costs). On the other hand, it might be that operation at higher cake pressure drops imply the rupture of

the cakes and therefore the enhancement of dust penetration by reentrainment. A consideration of these factors should determine if this further reduction in size is advantageous or not.

A comparison between the cakes formed in the horizontal bed of sand and the panel bed filter during the deposition of three different dusts upon 40-50 mesh sand at 150° C and at similar velocities, indicates the presence of phenomena which determine that the cakes in the panel bed are less porous. In Section 8.01 we discussed the possible causes for this difference and suggested that apparently the cakes formed in the panel bed had roots which are denser than the cakes themselves. This might have occurred if one of the following situations was present.

a) It might be that the porosity in the first few layers of the sand surfaces is higher than in the rest of the sand contained on the louver plates. (During puffback the sand between the louver plates moves upwardly in a curved fashion.)

b) It might be that the curve-shaped free sand surfaces, which result from puffback, provoke the formation of cakes which are looser than those formed on flat sand surfaces.

If our hypothesis is correct, the panel bed filter might provide capacities much higher than a horizontal bed of sand and achieve comparable collection efficiencies.

8.04.2 The Role of Adhesion and Autohesion in Panel Bed Filtration at 150° C

In Chapter 7.0 of this dissertation we hypothesized that

the relative adhesivities of the three dusts tested with sand at 150° C could be described by the following sequence.

Adhesivity C.E.C.F.A.-Sand > Adhesivity C.W.E.C.F.A.-Sand > Adhesivity C.C.C.D.-Sand

Where:

C.E.C.F.A. stands for Consolidated Edison Coal Fly Ash

CW.F.C.F.A. stands for Commonwealth Edison Coal Fly Ash

C.C.C.D. stands for Clinker Cooler Cement Dust

In Section 8.01 we hypothesized that the autohesivity of Consolidated Edison Fly Ash was smaller than the autohesivities of the other two dusts.

In Section 8.03 we suggested a model for granular bed filtration which considers the three basic filtration processes --the clean bed filtration, the rooting cake filtration, and the surface cake filtration for the extreme cases which could be originated from a variation of the adhesivity and autohesivity of the filtration system. This model considers dust reentrainment as an important penetration mechanism during cake filtration.

We shall analyze now the penetration trends obtained in our 150° C laboratory panel bed filter trying to identify each filtration system with our filtration model.

A) Consolidated Edison Fly Ash

This dust according to our hypotheses has the highest adhesivity and the lowest autohesivity of the three dusts tested. Its relatively high adhesivity was suggested by the following experimental observations:

a) At relatively low velocity (7.75 cm/s) the highest efficiency was obtained and an increase in puffback intensity did not much affect penetration. This phenomenon is consistent with the fact that the surface cakes were quickly formed and that the roots of the cake were very shallow. (This fact was observed in the laboratory panel bed by removing a small section of the cake with a needle, fly ash penetration at this velocity amounted to 2 or 3 grains of sand.)

b) At intermediate velocities (11.12 cm/s) the efficiency decreased; although an increase in puffback intensity did not much affect dust penetration. Under these operating conditions, inertial impaction is the main collection mechanism during clean bed filtration and therefore efficiency during this process should increase and specially so for a dust of high adhesivity. At this higher velocity; however, a cake of low autohesivity might begin to break and dust penetration by the pinhole plug mechanism could offset the increase in efficiency resulting during clean bed filtration. The fact that an increase in puffback intensity did not much affect penetration implies that the cakes were quickly formed and the roots were very shallow.

Its relatively low authohesivity was suggested by the following experimental observations.

a) Penetration increased with filtration velocity and a drastic deterioration in performance occurred somewhere in between 11.12 and 17.2 cm/s. The data at 17.2 cm/s and low

puffback intensity (170.3 kPa) imply that dust reentrainment provoked a sharp deterioration in performance, for a dust of high adhesivity this means that the autohesivity was low enough as to provoke a drastic rupture of the quickly formed cakes. The increase in efficiency at higher puffback intensities suggests that: a) Dust reentrainment from pinhole plug penetration was a gradual phenomenon (this suggest once more that the adhesivity of this dust was high) or in other words, the chunks of dust dislodged from the surface of the filter were recollected at deeper positions in the bed; b) the high puffback intensity was strong enough as to move the front of dust back to the surface.

b) At high cake areal densities, at all filtration velocities tested, a sudden decrease in air pressure drop was observed.

The behavior of this filtration system in the panel bed resembles the behavior of system (d) of our filtration model A dust with good adhesivity but poor autohesivity.

B) Commonwealth Edison Coal Fly Ash

This dust according to our hypotheses has a relatively low adhesivity and a relatively high autohesivity.

Its relatively low adhesivity was suggested by the following experimental observations:

a) The cakes formed with this dust upon 40-50 mesh sand had deep roots the depth of which decreased with increasing velocity. For a dust of low adhesivity clean bed filtration is relatively poor, consequently the presence of

roots in the granular bed at the beginning of a filtration cycle should improve the filtration performance.

The data obtained with this dust at the intermediate velocity (Table 6-16) showed a sharp deterioration in filtration performance when the puffback pressure was increased in 34.4 kPa. This suggests that the stronger puffback was removing most of the roots established during the previous filtration cycle. This fact implies higher penetration for a dust of relatively poor adhesivity. The data obtained at the highest velocity tested (17.2 cm/s) showed a slight increase in penetration with higher puffback intensities. Apparently, as a result of higher inertia the roots were shallower and the effect of leaving a relatively clean bed after a stronger puffback was not that drastic.

b) In general an increase in penetration was observed with decreasing deposition velocity; phenomenon which is consistent with a dust of poor adhesivity. Clean bed penetration is enhanced by a decrease in inertial impaction. This phenomenon was more pronounced at the lowest velocity tested.

Its relatively high autohesivity was suggested by the following experimental observations:

a) An increase in deposition velocity caused a decrease in dust penetration even at the highest velocity tested (17.2 cm/s) and at the highest cake pressure drop explored (19.05 cm of H_2O). This phenomenon is consistent with the resistance to cake rupture resulting from a relatively strong autohesivity.

b) No sudden decreases in air pressure drops were observed throughout the range of areal densities explored.

The behavior of this filtration system in the panel bed resembles the behavior of system (c) of our filtration model: "A dust with poor adhesivity and good autohesivity."

C) Clinker Cooler Cement Dust

This dust according to our hypotheses has the lowest adhesivity and a relatively high autohesivity.

In general, the trends observed with this dust resembled those obtained with Commonwealth Edison Coal Fly Ash. The data obtained in the horizontal bed coupled with the fact that even having the coarsest size distribution (mass median diameter = 38.2 micrometers) provided efficiencies sometimes comparable to the ones obtained with Commonwealth fly ash made us believe that its adhesivity with sand at 150^{o} C is the lowest among the three dusts tested.

CHAPTER 9.0: CONCLUSIONS

1. The results obtained in a small laboratory panel bed filter, with wishbone louvers, at 150° C, shows that cake filtration in this device affords high collection efficiencies (beyond 99.9%, overall and on a weight basis) in the filtration of dusts with different characteristics and with practicable gas throughput and pressure drop.

Most experiments were with 40-50 mesh angular sand, but a few experiments have been conducted with 40-50 mesh silicon carbide and coarser sands. The face velocity was varied from about 8 to 20 cm/s. The pressure drop across the filter cakes formed was varied from about 3.8 to 19 cm of water. Almost all of our experiments have used dust loadings of about 6 to 10 grams/m^3.

2. A comparison between Lee's work at room temperature and our investigation at 150° C shows that the auto- and/or adhesivity of Consolidated Edison coal fly ash decreased substantially with the increase in temperature. We could not produce a coherent deposit of this fly ash at 150° C upon 20-30 mesh sand, a size for which such a deposit is easily made at room temperature. We believe it probable that the major effect bringing about a decrease in auto- and/or adhesivity is elimination of capillary forces arising from the presence of moisture.

Wu's work, in a horizontal bed of sand with the same fly

ash, suggests that a further increase in temperature would not cause another striking difference in cake structure. (At least not up to 315.6° C, the highest temperature tested.)

3. The wishbone louvers were found to be appropriate for high efficiency panel bed filtration of dusts with different characteristics. This louver design guarantees that the dirty sand contained between two louver plates cannot fall down into the bed during puffback.

4. In the panel bed filter the size of the granules for the filtration of a given dust at some preselected conditions should be such as to provoke the formation of surface filter cakes whose roots do not extend beyond the width of the front louver plate.

5. Our laboratory panel bed filter with wishbone louvers and working with 40-50 mesh angular sand at 150° C provided high collection efficiencies (beyond 99.9 Wt%) in the filtration of Consolidated Edison coal fly ash, Commonwealth Edison coal fly ash and Clinker Cooler cement dust without having to modify the range of operating conditions. The data with these filtration systems suggest that a superficial filtration velocity of 11 cm/s is a practicable design velocity. This velocity corresponds to a filtration velocity at the free sand surfaces of about 24 cm/s. The clean bed pressure drop under these conditions would be about 9 cm of H_2O. The frequency of cleaning should be equivalent to a pressure drop across the filter cake between 12 and 15 cm of H_2O.

The spills of sand originated from an efficient puffback cleaning of the filter under these conditions imply the need of a sand recycle system handling between 8 to 11 kilograms of sand per kilogram of dust removed.

6. The determination of the particle size distribution of Consolidated Edison coal fly ash at the outlet of the 150° C panel bed filter operating at 11.12 cm/s, with 40-50 mesh sand allowed the estimation of efficiencies between 98.8 and 99.63 % on a weight basis, in the collection of submicron particles (0.3-1.0 μm). The particle counting procedure under an optical microscope with a 1000X magnification disclosed the fact that under these operating conditions the panel bed under cake filtration operated as an absolute filter for particles bigger than about 5 micrometers.

7. The penetration trends obtained with the three filtration systems explored in our laboratory panel bed at 150° C may be summarized by indicating the similarities and dissimilarities in behavior.

The similarities observed were:

a. The three dusts tested formed coherent deposits upon 40-50 mesh angular sand all of which provided high filtration efficiencies (beyond 99.9 Wt%).

b. In the range of operating conditions tested, dust reentrainment by seepage and/or pinhole plug penetration mechanisms appeared to be of importance in cake filtration with the three dusts.

c. For the three dusts tested, an increase in filtration

cycle time (higher cake pressure drops) produced a decrease in dust penetration. However, the extent of the improvements and the limit in this trend were different for the three different dusts.

d. Puffback cleaning of similar intensities always avoided excessive dust penetration and afforded steady state operation after a few filtration cycles.

The disimilarities observed were:

a. The cakes formed with Commonwealth Edison coal fly ash and Clinker Cooler cement dust were denser than the ones formed with Consolidated Edison coal fly ash.

b. The roots of the cakes formed with Consolidated Edison fly ash were shallower than the ones formed with the other two dusts.

c. Penetration of Consolidated Edison fly ash increased with increasing deposition velocity and a sharp break in this trend occurred somewhere between 11.12 and 17.2 cm/s. Penetration of the other two dusts decreased with increasing velocities. (No sharp break in this trend was observed in the range of velocities tested.)

d. An increase in puffback intensity while filtering Consolidated Edison fly ash at low and intermediate velocities (7.75 and 11.12 cm/s) did not much affect penetration. The same increase in puffback pressure while filtering the other two dusts at same velocities produced a considerable increase in penetration.

e. The cakes formed with Consolidated Edison coal fly

ash were less stable than the ones formed with the other two dusts. Cake rupture as a result of the effects of increasing velocity and pressure drop was easier with this fly ash.

f. For a fixed puffback pressure, an increase in the areal density of the cakes formed with Consolidated Edison fly ash, provoked a considerable increase in the amount of sand spilled, with the other two dusts an increase in areal density did not much affect sand spills.

8. A model for granular bed filtration was suggested. This model considers three processes during granular bed filtration.

a. Clean Bed Filtration: This is the stage in which the granules are basically clean. The major collection mechanism is adhesion and the efficiency will be relatively poor.

b. Rooting Cake Filtration: This is the stage in which the foundation of a surface filter cake is formed. Adhesion and straining will interact providing an increase in efficiency.

c. Cake Filtration: Once a surface filter cake is formed sieving constitutes the main collection mechanism. Efficiency during this process will increase markedly.

During this process three penetration mechanisms were suggested:

c-1. Straight-through Penetration: Extremely fine particles may penetrate the cake and roots without being collected.

c-2. Seepage Penetration: As a result of the effect of

the drag force exerted by the flowing gas, small chunks of dust particles might be separated from the roots located deep within the bed and could eventually penetrate the filter.

c-3. Pinhole Plug Penetration: As a result of the combined effect of gas pressure drop and velocity upon dust particles located just above the pores of the sand bed (weakest positions in the cake), a plug of dust particles may be dislodged from the cake and begin penetrating the sand bed.

Four extreme cases which might be encountered in cake filtration as a result of differences between the adhesivity and autohesivity of the filtration system were suggested. The relative effects of the aforementioned penetration mechanisms were discussed in each of the extremes. The effects of increasing deposition velocity and cycle time were also discussed.

9. A comparison between the cakes formed in a horizontal bed of sand and the panel bed filter suggests that the panel bed filter might provide capacities much higher than a horizontal bed of sand and achieve comparable collection efficiencies.

10. A horizontal bed of sand was found to be a useful tool for obtaining the maximum size of a granule which would provoke the formation of a stable surface cake of a given dust at preselected operating conditions. However, the translation of trends in dust deposition and cake structure obtained in a horizontal bed of sand, into parameters of a

different granular filter must take into consideration possible differences in the deposition processes, especially with dusts which have noticeable differences in autohesivity.

11. The results obtained in a 150° C horizontal bed of sand and in our 150° C laboratory panel bed allowed us to hypothesize that the relative adhesivities of the three dusts tested might be described by the following sequence:

Adhesivity C.E.C.F.A.Sand > Adhesivity CW.E.C.F.A.Sand > Adhesivity C.C.C.D.Sand

12. An analysis of the penetration trends observed in 150° C panel bed filtration allowed us to hypothesized that the autohesivity of Consolidated Edison coal fly ash might be smaller than the autohesivities of the other two dusts.

13. Lee's work in a 3.068 m tall panel bed filter suggests that puffback cleaning can be used in a commercial size panel bed withouth the risk of causing non-uniform cleaning.

APPENDIX A: "APPENDIX TO CHAPTER 6.0"

TABLE 6a-1

PANEL BED FILTER

PENETRATION DATA AT 150°C

FILTRATION SYSTEM: DUST= Fly Ash +80 Mesh (Con Edison)
GRANULES= Angular Sand 40-50 Mesh U.S. Std.

SUPERFICIAL VELOCITY= 7.75cm/sec (15.2ft/min)

PUFFBACK TANK: VOLUME= 206cm^3; PRESSURE= 170.3x10^3 Pa (10 psig)

PRESSURE DROP DUE TO FILTER CAKE BEFORE CLEANING= 3.81cm of H_2O

CYCLE #	ΔP_i cm of H_2O	ΔP_f cm of H_2O	t (min)	Dust from Puffback (grs)	Granules from Puff-back (grs)	Dust at bottom of panel(grs)	(Dust/Granule) from Puffback
1	6.5	10.3	25.0	4.8	37.2	1.5	0.13
2	7.0	10.8	20.8	7.8	47.9	2.0	0.16
3	7.2	11.0	12.7	8.8	54.8	1.8	0.16
4	7.2	11.0	14.6	8.3	50.2	2.0	0.11
5	7.4	11.3	13.1	7.7	44.9	1.9	0.17
6	7.7	11.5	12.6	8.7	53.9	1.7	0.16
7	7.7	11.5	12.0	8.8	54.1	1.9	0.16
8	7.7	11.5	11.9	8.1	51.4	1.7	0.16
9	7.7	11.5	12.5	8.2	51.3	1.6	0.16
10	7.7	11.5	11.0	7.2	38.6	1.4	0.19

Top Filter Paper
Weight Gain (1-3)= 0.2 mgrs

Bottom Filter Paper
Weight Gain (1-3)= 0.2mgrs

Penetration (1-3)
(wt%)= 0.022

Average time per cycle (1-3)= 19.5min

Average total Dust Collected
per cycle (1-3)=8.87 grs

Average Inlet Dust Loading
(1-3)=4.21 grs/m^3

Top Filter Paper
Weight gain(4-10)= 0.6 mgrs

Bottom Filter Paper
Weight gain (4-10)= 0.6 mgrs

ΔP_i (11^{th}Cycle)= 7.7 cm of H_2O

Pepetration (4-10) (wt%)= 0.025

Average time per cycle(4-10)= 12.5min

Average Total Dust Collected
per cycle (4-10)= 9.88grs

Average Inlet Dust Loading
(4-10)= 7.32grs/m^3

TABLE 6a-2

PANEL BED FILTER

PENETRATION DATA AT 150°C

FILTRATION SYSTEM: DUST= Fly Ash +80 Mesh (Con Edison)
GRANULES= Angular Sand 40-50 Mesh U.S. Std.

SUPERFICIAL VELOCITY= 7.7 cm/sec (15.2ft/min)

PUFFBACK TANK: VOLUME= 206cm^3; PRESSURE= 170.3x10^3 Pa (10 psig)

PRESSURE DROP DUE TO FILTER CAKE BEFORE CLEANING= 7.62cm of H_2O

CYCLE #	ΔP_i cm of H_2O	ΔP_f cm of H_2O	t (min)	Dust from Puffback (grs)	Granules from Puff-back (grs)	Dust at bottom of panel(grs)	(Dust/Granule) from Puffback
1	6.7	14.4	20.5	10.6	83.1	3.3	0.13
2	7.2	14.8	19.5	13.8	93.5	3.7	0.15
3	7.2	14.8	18.5	13.1	79.1	3.6	0.17
4	7.2	14.8	18.5	11.7	59.9	2.9	0.20
5	7.4	15.1	24.3	13.3	70.1	3.4	0.19
6	7.7	15.4	18.9	12.6	65.7	2.7	0.19
7	7.9	15.6	20.3	13.3	63.9	2.5	0.21
8	8.2	15.8	21.2	13.6	67.8	2.4	0.20
9	8.2						
10							

Top Filter Paper
Weight Gain (1-3)= 0.2 mgrs

Bottom Filter Paper
Weight Gain (1-3)= 0.2mgrs

Penetration (1-3)
(wt%)= 0.0127

Average time per cycle (1-3)=19.5 min

Average total Dust Collected
per cycle (1-3)=15.37grs

Average Inlet Dust Loading
(1-3)=7.62 grs/m^3

Top Filter Paper
Weight gain(4-10)= 0.3 mgrs

Bottom Filter Paper
Weight gain (4-10)= 0.3 mgrs

ΔP_i (9 thCycle)= 8.2 cm of H_2O

Penetration (4-10) (wt%)= 0.011

Average time per cycle(4-10)=20.6 min

Average Total Dust Collected
per cycle (4-10)= 15.7grs

Average Inlet Dust Loading
(4-10)=7.03 grs/m^3

TABLE 6a-3

PANEL BED FILTER

PENETRATION DATA AT 150°C

FILTRATION SYSTEM: DUST= Coal Fly Ash +80 Mesh (Con Edison)
GRANULES= Angular Sand 40-50 Mesh U.S. Std.

SUPERFICIAL VELOCITY= 7.7 cm/sec (15.2 ft/min)

PUFFBACK TANK: VOLUME= 206 cm^3; PRESSURE= 170.3×10^3 Pa (10 psig)

PRESSURE DROP DUE TO FILTER CAKE BEFORE CLEANING= 11.4 cm of H_2O

CYCLE #	ΔP_i cm of H_2O	ΔP_f cm of H_2O	t (min)	Dust from Puffback (grs)	Granules from Puff-back (grs)	Dust at bottom of panel(grs)	(Dust/Granule) from Puffback
1	7.7	19.2	10.3	11.5	74.6	2.4	0.15
2	7.7	19.2	15.5	17.0	138.2	2.3	0.12
3	7.7	19.2	13.4	15.7	126.1	3.7	0.12
4	7.9	19.4	14.3	16.2	136.5	2.3	0.12
5	7.7	19.2	14.3	16.2	145.8	3.4	0.11
6	7.7	19.2	19.9	16.4	130.2	4.0	0.13
7	7.9	19.4	25.6	16.8	144.4	3.1	0.12
8	7.7	19.2	17.0	18.1	121.6	4.3	0.15
9	7.9	19.4	10.8	17.0	133.9	3.9	0.13
10	7.4	19.0	17.1	17.8	137.2	3.6	0.13

Top Filter Paper
Weight Gain (1-3)= 0.2 mgrs

Bottom Filter Paper
Weight Gain (1-3)=0.45 mgrs

Penetration (1-3)
(wt%) = 0.018

Average time per cycle (1-3) = 13.1 min

Average total Dust Collected
per cycle (1-3) = 17.5 grs

Average Inlet Dust Loading
(1-3) = 12.4 grs/m^3

Top Filter Paper
Weight gain(4-10) = 0.5 mgrs

Bottom Filter Paper
Weight gain (4-10) = 0.9 mgrs

ΔP_i (11^{th} cycle) = 7.6 cm of H_2O

Penetration (4-10) (wt%) = 0.0143

Average time per cycle(4-10) = 17.0 min

Average Total Dust Collected
per cycle (4-10) = 20.4 grs

Average Inlet Dust Loading
(4-10) = 11.1 grs/m^3

TABLE 6a-4

PANEL BED FILTER

PENETRATION DATA AT 150°C

FILTRATION SYSTEM: DUST= Coal Fly Ash +80 Mesh (Con Edison)
GRANULES= Angular Sand 40-50 Mesh U.S. Std.

SUPERFICIAL VELOCITY=7.7 cm/sec (15.2ft/min)

PUFFBACK TANK: VOLUME= 206cm^3; PRESSURE= 170.3x10^3 Pa (10psig)

PRESSURE DROP DUE TO FILTER CAKE BEFORE CLEANING=15.2 cm of H_2O

CYCLE #	ΔP_i cm of H_2O	ΔP_f cm of H_2O	t (min)	Dust from Puffback (grs)	Granules from Puff-back (grs)	Dust at bottom of panel(grs)	(Dust/Granule) from Puffback
1	7.9	23.3	14.3	17.7	148.5	3.5	0.12
2	8.2	23.5	19.3	19.6	143.8	4.1	0.14
3	8.4	23.8	17.6	20.1	167.6	3.7	0.12
4	8.2	23.5	22.3	19.1	151.9	4.5	0.13
5	8.2	23.5	19.9	19.7	146.0	4.6	0.13
6	7.9	23.3	20.3	18.5	140.3	4.6	0.13
7	8.2	23.5	19.3	18.6	124.7	4.5	0.15
8	8.9	24.7	18.8	19.4	120.0	4.5	0.16
9	8.9	24.2	18.0	18.5	132.7	3.6	0.14
10	8.9	24.2	17.0	19.1	149.3	3.4	0.13

Top Filter Paper
Weight Gain (1-3)=0.1 mgrs

Bottom Filter Paper
Weight Gain (1-3)=0.3 mgrs

Penetration (1-3)
(wt%)= 0.0085

Average time per cycle (1-3)=17.1 min

Average total Dust Collected
per cycle (1-3)=22.9 grs

Average Inlet Dust Loading
(1-3)=12.4 grs/m^3

Top Filter Paper
Weight gain(4-10)=0.4 mgrs

Bottom Filter Paper
Weight gain (4-10)=0.6 mgrs

ΔP_i(11thCycle)=8.9 cm of H_2O

Penetration (4-10) (wt%)=0.009

Average time per cycle(4-10)=19.4 min

Average Total Dust Collected
per cycle (4-10)=23.2 grs

Average Inlet Dust Loading
(4-10)=11.1 grs/m^3

TABLE 6a-5

PANEL BED FILTER

PENETRATION DATA AT 150°C

FILTRATION SYSTEM: DUST= Coal Fly Ash +80 Mesh (Con Edison)
GRANULES= Angular Sand 40-50 Mesh U.S. Std.

SUPERFICIAL VELOCITY=11.12cm/sec (21.9ft/min)

PUFFBACK TANK: VOLUME= 206cm^3; PRESSURE= 170.3x10^3 Pa (10 psig)

PRESSURE DROP DUE TO FILTER CAKE BEFORE CLEANING= 7.62cm of H_2O

CYCLE #	ΔP_i cm of H_2O	ΔP_f cm of H_2O	t (min)	Dust from Puffback (grs)	Granules from Puff-back (grs)	Dust at bottom of panel(grs)	(Dust/Granule) from Puffback
1	6.5	12.2	25.0	6.4	33.3	3.9	0.19
2	8.2	15.7	20.0	12.5	54.0	4.0	0.23
3	9.4	16.8	17.0	13.2	64.9	4.5	0.20
4	10.1	17.5	17.0	12.5	60.2	4.0	0.21
5	10.3	17.8	16.0	12.5	65.4	3.7	0.19
6	10.6	18.0	16.0	11.6	60.9	3.7	0.19
7	10.8	18.2	14.0	12.2	64.1	2.9	0.19
8	11.0	18.5	15.0	12.1	63.0	3.3	0.19
9	11.3	18.7	15.0	11.2	58.5	3.1	0.19
10	11.5	19.0	17.0	12.1	63.0	3.3	0.19

Top Filter Paper
Weight Gain (1-10)=1.4 mgrs

Bottom Filter Paper
Weight Gain (1-10)=1.3mgrs

P_i(11^{th}Cycle)=11.3 cm of H_2O

Penetration (1-10)
(wt%) = 0.026

Average time per cycle (1-10)=17.2min

Average total Dust Collected
per cycle (1-10)=15.3grs

Average Inlet Dust Loading
(1-10)=5.73grs/m^3

Test conducted with a small leak of puffback air

TABLE 6a-6

PANEL BED FILTER

PENETRATION DATA AT 150°C

FILTRATION SYSTEM: DUST= Coal Fly Ash +80 Mesh (Con Edison)
GRANULES= Angular Sand 40-50 Mesh U.S. Std.

SUPERFICIAL VELOCITY=11.12cm/sec (21.9ft/min)

PUFFBACK TANK: VOLUME= 206cm^3; PRESSURE= 204.7x10^3 Pa (15 psig)

PRESSURE DROP DUE TO FILTER CAKE BEFORE CLEANING= 7.62cm of H_2O

CYCLE #	ΔP_i cm of H_2O	ΔP_f cm of H_2O	t (min)	Dust from Puffback (grs)	Granules from Puff-back (grs)	Dust at bottom of panel(grs)	(Dust/Granule) from Puffback
1	8.4	16.1	5.3	10.1	116.6	3.7	0.09
2	9.4	17.0	11.8	11.4	125.3	3.3	0.09
3	9.6	17.3	8.5	11.5	127.6	2.8	0.09
4	9.6	17.3	11.4	11.5	127.1	2.6	0.09
5	9.6	17.3	8.3	11.6	132.8	2.6	0.09
6	9.8	17.3	5.8	11.9	136.8	2.7	0.09
7	9.8	17.3	9.6	11.7	136.6	2.8	0.09
8	10.1	17.5	5.0	11.6	135.0	2.6	0.09
9	10.1	17.8	4.5	11.6	137.1	2.5	0.08
10	10.1	17.8	4.3	11.6	134.6	2.7	0.09

Top Filter Paper
Weight Gain (1-10)=1.3 mgrs

Bottom Filter Paper
Weight Gain (1-10)=1.3mgrs

P_i(11thCycle)=10.1 cm of H_2O

Penetration (1-10)
(wt%) = 0.027

Average time per cycle (1-10)=7.4 min

Average total Dust Collected
per cycle (1-10)=14.3grs

Average Inlet Dust Loading
(1-10)=12.5grs/m^3

Test conducted with a Small leak of puffback air

TABLE 6a-7

PANEL BED FILTER

PENETRATION DATA AT 150°C

FILTRATION SYSTEM: DUST= Coal Fly Ash +80 Mesh (Con Edison)
GRANULES= Angular sand 40-50 Mesh U.S. Std.

SUPERFICIAL VELOCITY=11.12cm/sec (21.9ft/min)

PUFFBACK TANK: VOLUME= 206cm^3; PRESSURE= 239.2x10^3 Pa (20 psig)

PRESSURE DROP DUE TO FILTER CAKE BEFORE CLEANING= 7.62cm of H_2O

CYCLE #	ΔP_i cm of H_2O	ΔP_f cm of H_2O	t (min)	Dust from Puffback (grs)	Granules from Puff-back (grs)	Dust at bottom of panel(grs)	(Dust/Granule) from Puffback
1	7.7	15.4	6.7	10.6	133.6	3.2	0.08
2	8.6	16.3	10.3	11.8	140.7	3.0	0.08
3	9.1	16.8	10.4	12.6	146.1	2.9	0.09
4	9.4	17.0	8.8	13.5	149.0	3.5	0.09
5	9.4	17.0	6.7	12.2	142.2	3.5	0.09
6	9.4	17.3	9.3	12.5	144.9	3.8	0.09
7	9.6	17.3	7.6	12.6	142.6	3.8	0.09
8	9.6	17.4	8.4	12.6	143.9	4.0	0.09
9	9.6	17.3	6.0	12.8	141.9	3.7	0.09
10	9.6	17.3	5.0	12.2	134.2	3.8	0.09

Top Filter Paper
Weight Gain (1-10)=1.0 mgrs

Bottom Filter Paper
Weight Gain (1-10)=1.3mgrs

P_i(11thCycle)= 9.6 cm of H_2O

Penetration (1-10)
(wt%) = 0.023

Average time per cycle (1-10)=7.9 min

Average total Dust Collected
per cycle (1-10)=16.1grs

Average Inlet Dust Loading
(1-10)=13.1grs/m^3

Test conducted with a small leak of puffback air

TABLE 6a-8

PANEL BED FILTER

PENETRATION DATA AT 150°C

FILTRATION SYSTEM: DUST= Coal Fly Ash +80 Mesh (Con Edison)
GRANULES= Angular Sand 40-50 Mesh U.S. Std.

SUPERFICIAL VELOCITY= 11.1cm/sec (21.9ft/min)

PUFFBACK TANK: VOLUME= 206cm^3; PRESSURE= 170.3x10^3 Pa (10 psig)

PRESSURE DROP DUE TO FILTER CAKE BEFORE CLEANING=3.81 cm of H_2O

CYCLE #	ΔP_i cm of H_2O	ΔP_f cm of H_2O	t (min)	Dust from Puffback (grs)	Granules from Puff-back (grs)	Dust at bottom of panel(grs)	(Dust/Granule) from Puffback
1	8.4	12.2	13.3	3.3	31.6	0.6	0.10
2	9.6	13.4	9.3	5.5	43.0	0.5	0.13
3	10.3	14.2	13.0	7.9	53.2	0.9	0.15
4	10.3	14.2	11.3	5.5	28.5	0.6	0.19
5	12.0	15.8	9.0	5.5	28.6	0.6	0.19
6	12.2	16.1	7.7	6.8	46.4	0.5	0.15
7	12.2	16.1	7.7	6.8	47.6	0.5	0.14
8	12.5	16.3	8.8	7.7	65.5	0.5	0.12
9	12.2	16.1	7.0	7.3	58.1	0.5	0.13
10	12.2	16.1	8.3	6.7	53.3	0.5	0.13

Top Filter Paper
Weight Gain (1-3)=0.3 mgrs

Bottom Filter Paper
Weight Gain (1-3)=0.4 mgrs

Penetration (1-3)
(wt%)=0.055

Average time per cycle (1-3)=11.9 min

Average total Dust Collected
per cycle (1-3)=6.23 grs

Average Inlet Dust Loading
(1-3)=3.4 grs/m^3

Top Filter Paper
Weight gain(4-10)=0.4 mgrs

Bottom Filter Paper
Weight gain (4-10)=0.4 mgrs

ΔP_i(11thCycle)=12.2 cm of H_2O

Penetration (4-10) (wt%)=0.023

Average time per cycle(4-10)=8.5 min

Average Total Dust Collected
per cycle (4-10)=7.14 grs

Average Inlet Dust Loading
(4-10)= 5.4 grs/m^3

TABLE 6a-9

PANEL BED FILTER

PENETRATION DATA AT 150°C

FILTRATION SYSTEM: DUST= Coal Fly Ash +80 Mesh (Con Edison)
GRANULES= Angular Sand 40-50 Mesh U.S. Std.

SUPERFICIAL VELOCITY= 11.1cm/sec (21.9ft/min)

PUFFBACK TANK: VOLUME= 206cm^3; PRESSURE= 170.3x10^3 Pa (10 psig)

PRESSURE DROP DUE TO FILTER CAKE BEFORE CLEANING=7.62 cm of H_2O

CYCLE #	ΔP_i cm of H_2O	ΔP_f cm of H_2O	t (min)	Dust from Puffback (grs)	Granules from Puff-back (grs)	Dust at bottom of panel(grs)	(Dust/Granule) from Puffback
1	10.8	18.5	18,0	8.95	95.4	1.0	0.09
2	11.8	19.4	17.0	12.70	115.4	0.9	0.11
3	11.8	19.4	12.3	11.2	88.6	0.9	0.13
4	12.0	19.7	11.8	11.2	81.0	0.8	0.14
5	12.5	20.2	11.0	11.8	94.5	0.8	0.12
6	12.5	20.2	13.0	11.6	89.7	0.5	0.13
7	12.7	20.3	12.3	12.0	102.3	0.6	0.12
8	12.2	19.9	12.0	12.6	99.0	0.6	0.13
9	12.7	20.4	11.3	10.9	90.2	0.6	0.12
10	12.7	20.4	12.3	11.6	86.5	0.7	0.13

Top Filter Paper
Weight Gain (1-3)= 0.3 mgrs

Bottom Filter Paper
Weight Gain (1-3)= 0.5mgrs

Penetration (1-3)
(wt%)= 0.083

Average time per cycle (1-3)=15.8 min

Average total Dust Collected
per cycle (1-3)=11.88grs

Average Inlet Dust Loading
(1-3)= 4.9 grs/m^3

Top Filter Paper
Weight gain(4-10)= 0.7 mgrs

Bottom Filter Paper
Weight gain (4-10)= 1.1 mgrs

ΔP_i(11thCycle)= 12.7cm of H_2O

Penetration (4-10) (wt%)= 0.03

Average time per cycle(4-10)=11.95min

Average Total Dust Collected
per cycle (4-10)=12.33grs

Average Inlet Dust Loading
(4-10)= 6.7 grs/m^3

TABLE 6a-10

PANEL BED FILTER

PENETRATION DATA AT 150°C

FILTRATION SYSTEM: DUST= Coal Fly Ash +80 Mesh (Con Edison)
GRANULES= Angular Sand 40-50 Mesh U.S. Std.

SUPERFICIAL VELOCITY= 11.1cm/sec (21.9ft/min)

PUFFBACK TANK: VOLUME= 206cm^3; PRESSURE= 170.3x10^3 Pa (10 psig)

PRESSURE DROP DUE TO FILTER CAKE BEFORE CLEANING=11.43cm of H_2O

CYCLE #	ΔP_i cm of H_2O	ΔP_f cm of H_2O	t (min)	Dust from Puffback (grs)	Granules from Puff-back (grs)	Dust at bottom of panel(grs)	(Dust/Granule) from Puffback
1	9.4	20.9	20.3	10.7	89.5	1.2	0.12
2	11.0	22.6	19.0	14.8	112.7	1.0	0.13
3	11.0	22.6	17.0	14.4	108.3	0.8	0.13
4	11.0	22.6	15.3	12.8	94.8	0.7	0.14
5	11.3	22.8	16.8	14.1	113.0	0.7	0.12
6	11.5	23.0	14.8	14.8	116.8	0.5	0.13
7	11.5	23.0	12.3	13.1	94.6	0.6	0.14
8	11.8	23.3	12.3	14.5	115.5	0.7	0.13
9	11.5	16.3	8.0	11.2	95.5	0.7	0.12
10	11.5						

Top Filter Paper
Weight Gain (1-3)= 0.1 mgrs

Bottom Filter Paper
Weight Gain (1-3)= 0.2mgrs

Top Filter Paper
Weight gain(4-10)= 0.3 mgrs

Bottom Filter Paper
Weight gain (4-10)= 0.3 mgrs

ΔP_i(11thCycle)= cm of H_2O

Penetration (1-3) (wt%)= 0.012

Average time per cycle (1-3)= 18.8min

Average total Dust Collected per cycle (1-3)= 14.3grs

Average Inlet Dust Loading (1-3)=4.92 grs/m^3

Penetration (4-10) (wt%)= 0.0104

Average time per cycle(4-10)=14.25min

Average Total Dust Collected per cycle (4-10)= 14.5grs

Average Inlet Dust Loading (4-10)= 6.6 grs/m^3

TABLE 6a-11

PANEL BED FILTER

PENETRATION DATA AT 150°C

FILTRATION SYSTEM: DUST= Coal Fly Ash +80 Mesh (Con Edison)
GRANULES= Angular Sand 40-50 Mesh U.S. Std.

SUPERFICIAL VELOCITY= 11.1cm/sec (21.9ft/min)

PUFFBACK TANK: VOLUME= 206cm^3; PRESSURE= 170.3x10^3 Pa (10 psig)

PRESSURE DROP DUE TO FILTER CAKE BEFORE CLEANING=15.24cm of H_2O

CYCLE #	ΔP_i cm of H_2O	ΔP_f cm of H_2O	t (min)	Dust from Puffback (grs)	Granules from Puff-back (grs)	Dust at bottom of panel(grs)	(Dust/Granule) from Puffback
1	9.1	25.4	14.0	16.3	121.9	2.3	0.13
2	11.0	26.4	14.3	19.2	122.0	1.6	0.16
3	11.8	27.1	14.0	19.7	139.0	1.9	0.14
4	12.0	27.4	11.4	16.4	106.8	1.9	0.15
5	12.2	27.8	12.8	18.0	115.3	1.7	0.16
6	12.2	27.6	15.8	17.4	105.4	2.0	0.17
7	12.0	27.4	17.8	17.7	105.5	1.9	0.17
8	12.5	27.8	17.2	20.1	119.5	1.7	0.17
9	12.2	27.6	15.8	18.7	106.5	2.0	0.18
10	11.8	27.1	17.7	18.1	99.9	1.8	0.18

Top Filter Paper
Weight Gain (1-3)= 0.4 mgrs

Bottom Filter Paper
Weight Gain (1-3)= 0.4mgrs

Penetration (1-3) (wt%) = 0.02

Average time per cycle (1-3)=14.1 min

Average total Dust Collected per cycle (1-3)=20.33grs

Average Inlet Dust Loading (1-3)= 9.3 grs/m^3

Top Filter Paper
Weight gain(4-10)= 0.9 mgrs

Bottom Filter Paper
Weight gain (4-10)= 1.3 mgrs

ΔP_i (11thCycle)= 11.8cm of H_2O

Penetration (4-10) (wt%) = 0.023

Average time per cycle(4-10)=15.5 min

Average Total Dust Collected per cycle (4-10)=19.91grs

Average Inlet Dust Loading (4-10)= 8.3 grs/m^3

TABLE 6a-12

PANEL BED FILTER

PENETRATION DATA AT 150°C

FILTRATION SYSTEM: DUST= Coal Fly Ash +80 Mesh (Con Edison)
GRANULES= Angular Sand 40-50 Mesh U.S. Std.

SUPERFICIAL VELOCITY=17.2 cm/sec (33.8ft/min)

PUFFBACK TANK: VOLUME= 206cm^3; PRESSURE= 170.3x10^3 Pa (10 psig)

PRESSURE DROP DUE TO FILTER CAKE BEFORE CLEANING=7.62 cm of H_2O

CYCLE #	ΔP_i cm of H_2O	ΔP_f cm of H_2O	t (min)	Dust from Puffback (grs)	Granules from Puff-back (grs)	Dust at bottom of panel(grs)	(Dust/Granule) from Puffback
1	11.5	19.0	16.0	4.7	39.7	2.1	0.12
2	14.6	22.3	18.6	6.7	59.2	1.7	0.11
3	15.8	23.5	17.0	8.0	59.8	1.6	0.13
4	16.6	24.2	17.0	7.1	48.5	1.3	0.15
5	16.3	24.0	13.7	7.2	50.6	1.1	0.14
6	16.6	24.5	12.1	7.3	54.2	1.0	0.13
7	16.8	24.5	12.0	7.1	54.6	1.0	0.13
8	17.0	24.5	11.2	6.7	54.9	1.0	0.12
9	17.0	25.0	11.4	6.7	50.3	1.0	0.13
10	17.7	25.4	11.8	6.6	50.9	0.9	0.13

Top Filter Paper
Weight Gain (1-3)= 1.6 mgrs

Bottom Filter Paper
Weight Gain (1-3)=2.3 mgrs

Penetration (1-3) (wt%)= 0.23

Average time per cycle (1-3)= 17.2min

Average total Dust Collected per cycle (1-3)=8.27 grs

Average Inlet Dust Loading (1-3)= 2.01grs/m^3

Top Filter Paper
Weight gain(4-10)= 4.1 mgrs

Bottom Filter Paper
Weight gain (4-10)= 6.5 mgrs

ΔP_i(11thCycle)= 18.0cm of H_2O

Penetration (4-10) (wt%)= 0.276

Average time per cycle(4-10)=12.73min

Average Total Dust Collected per cycle (4-10)= 8.0 grs

Average Inlet Dust Loading (4-10)= 2.63grs/m^3

Test conducted with a small leak of puffback air

TABLE 6a-13

PANEL BED FILTER

PENETRATION DATA AT 150°C

FILTRATION SYSTEM: DUST= Coal Fly Ash +80 Mesh (Con Edison)
GRANULES= Angular Sand 40-50 Mesh U.S. Std.

SUPERFICIAL VELOCITY= 17.2cm/sec (33.8ft/min)

PUFFBACK TANK: VOLUME= 206cm^3; PRESSURE= 204.7x10^3 Pa (15 psig)

PRESSURE DROP DUE TO FILTER CAKE BEFORE CLEANING= 7.62cm of H_2O

CYCLE #	ΔP_i cm of H_2O	ΔP_f cm of H_2O	t (min)	Dust from Puffback (grs)	Granules from Puff-back (grs)	Dust at bottom of panel(grs)	(Dust/Granule) from Puffback
1	10.1	17.8	21.8	8.1	94.8	2.5	0.09
2	14.2	21.8	16.8	8.8	103.8	1.6	0.08
3	15.6	23.3	14.8	9.5	105.1	1.2	0.09
4	16.8	24.5	13.3	8.7	89.1	1.4	0.10
5	16.1	23.8	13.0	7.8	90.1	1.2	0.09
6	16.1	23.8	13.0	7.8	86.6	1.1	0.09
7	15.8	23.5	12.9	7.5	88.2	1.1	0.09
8	16.1	23.8	12.3	7.4	90.4	1.1	0.08
9	16.1	24.0	11.6	7.4	89.1	1.1	0.08
10	16.1	24.0	12.0	7.1	87.1	1.1	0.08

Top Filter Paper
Weight Gain (1-3)= 1.4 mgrs

Bottom Filter Paper
Weight Gain (1-3)=1.8 mgrs

Penetration (1-3)
(wt%) = 0.148

Average time per cycle (1-3)= 17.8min

Average total Dust Collected
per cycle (1-3)=10.57grs

Average Inlet Dust Loading
(1-3) = 2.48grs/m^3

Top Filter Paper
Weight.gain(4-10)= 2.2 mgrs

Bottom Filter Paper
Weight gain (4-10)= 5.6 mgrs

ΔP_i (11thcycle)= 16.1cm of H_2O

Penetration (4-10) (wt%) = 0.184

Average time per cycle(4-10)=12.6 min

Average Total Dust Collected
per cycle (4-10)= 8.97grs

Average Inlet Dust Loading
(4-10) = 2.97grs/m^3

Test conducted with a small leak of puffback air

TABLE 6a-14

PANEL BED FILTER

PENETRATION DATA AT 150°C

FILTRATION SYSTEM: DUST= Coal Fly Ash +80 Mesh (Con Edison)
GRANULES= Angular Sand 40-50 Mesh U.S. Std.

SUPERFICIAL VELOCITY=17.2 cm/sec (33.8ft/min)

PUFFBACK TANK: VOLUME= 206cm^3; PRESSURE= 239.2x10^3 Pa (20 psig)

PRESSURE DROP DUE TO FILTER CAKE BEFORE CLEANING= 7.62cm of H_2O

CYCLE #	ΔP_i cm of H_2O	ΔP_f cm of H_2O	t (min)	Dust from Puffback (grs)	Granules from Puff-back (grs)	Dust at bottom of panel(grs)	(Dust/Granule) from Puffback
1	13.2	20.9	20.4	7.2	129.2	2.2	0.055
2	13.7	21.4	14.6	8.0	123.8	1.9	0.064
3	14.6	22.3	19.3	8.3	141.1	1.8	0.059
4	14.4	22.1	13.7	7.7	121.6	1.7	0.063
5	14.9	22.6	14.8	7.9	124.6	1.8	0.063
6	14.9	22.6	12.3	7.6	119.9	1.4	0.063
7	15.4	23.0	12.7	7.6	122.6	1.3	0.062
8	15.8	23.5	13.1	7.6	127.0	1.4	0.060
9	15.8	23.5	13.8	8.0	125.8	1.5	0.063
10	15.8	23.5	12.2	7.9	124.2	1.5	0.064

Top Filter Paper
Weight Gain (1-3)= 0.6 mgrs

Bottom Filter Paper
Weight Gain (1-3)=0.6 mgrs

Penetration (1-3)
(wt%) = 0.06

Average time per cycle (1-3)= 18.1min

Average total Dust Collected
per cycle (1-3)= 9.8 grs

Average Inlet Dust Loading
(1-3)=2.26 grs/m^3

Top Filter Paper
Weight gain(4-10)= 1.2 mgrs

Bottom Filter Paper
Weight gain (4-10)= 1.5 mgrs

ΔP_i(11thCycle)= 15.8cm of H_2O

Penetration (4-10) (wt%) = 0.061

Average time per cycle(4-10)=14.69min

Average Total Dust Collected
per cycle (4-10)=9.27 grs

Average Inlet Dust Loading
(4-10) = 2.98grs/m^3

Test conducted with a small leak of puffback air

TABLE 6a-15

PANEL BED FILTER

PENETRATION DATA AT 150°C

FILTRATION SYSTEM: DUST= Coal Fly Ash +80 Mesh (Con Edison)
GRANULES= Angular Sand 40-50 Mesh U.S. Std.

SUPERFICIAL VELOCITY=17.2 cm/sec (33.8ft/min)

PUFFBACK TANK: VOLUME= 206cm^3; PRESSURE= 204.7x10^3 Pa (15 psig)

PRESSURE DROP DUE TO FILTER CAKE BEFORE CLEANING=7.62 cm of H_2O

CYCLE #	ΔP_i cm of H_2O	ΔP_f cm of H_2O	t (min)	Dust from Puffback (grs)	Granules from Puff-back (grs)	Dust at bottom of panel(grs)	(Dust/Granule) from Puffback
1	12.7	20.4	4.8	4.6	140.0	0.6	0.03
2	14.6	22.3	5.3	6.9	160.9	0.6	0.05
3	14.6	22.3	3.4	6.1	147.9	0.7	0.04
4	14.9	22.6	4.6	7.0	141.9	0.7	0.05
5	15.4	23.0	3.7	7.6	158.2	0.9	0.05
6	14.9	22.6	4.8	8.4	171.0	0.5	0.05
7	14.7	22.3	5.2	7.7	171.2	0.7	0.05
8	14.9	22.6	3.0	9.0	177.2	0.4	0.05
9	16.1	23.8	4.2	7.5	148.1	0.5	0.05
10	15.1	22.8	4.0	8.4	171.6	0.3	0.05

Top Filter Paper
Weight Gain (1-3)= 0.5 mgrs

Bottom Filter Paper
Weight Gain (1-3)= 0.4mgrs

Penetration (1-3)
(wt%)= 0.068

Average time per cycle (1-3)= 4.53min

Average total Dust Collected
per cycle (1-3)= 6.5 grs

Average Inlet Dust Loading
(1-3)= 6.0 grs/m^3

Top Filter Paper
Weight gain(4-10)= 0.8 mgrs

Bottom Filter Paper
Weight gain (4-10)= 0.5 mgrs

ΔP_i(11thCycle)= 14.9cm of H_2O

Penetration (4-10) (wt%)= 0.032

Average time per cycle(4-10)= 4.23min

Average Total Dust Collected
per cycle (4-10)= 8.51grs

Average Inlet Dust Loading
(4-10)= 8.41grs/m^3

TABLE 6a-16

PANEL BED FILTER

PENETRATION DATA AT 150°C

FILTRATION SYSTEM: DUST= Coal Fly Ash +80 Mesh (Con Edison)
GRANULES= Angular Sand 40-50 Mesh U.S. Std.

SUPERFICIAL VELOCITY=17.2 cm/sec (33.8ft/min)

PUFFBACK TANK: VOLUME= 206cm^3; PRESSURE= 204.7x10^3 Pa (15 psig)

PRESSURE DROP DUE TO FILTER CAKE BEFORE CLEANING=11.43cm of H_2O

CYCLE #	ΔP_i cm of H_2O	ΔP_f cm of H_2O	t (min)	Dust from Puffback (grs)	Granules from Puff-back (grs)	Dust at bottom of panel(grs)	(Dust/Granule) from Puffback
1	14.0	25.4	9.5	9.5	156.5	1.0	0.06
2	14.4	25.9	4.8	9.1	175.3	1.3	0.05
3	13.7	25.2	4.3	9.6	180.8	1.6	0.05
4	14.2	25.7	11.9	11.1	176.7	1.3	0.06
5	14.4	25.9	6.3	10.6	172.7	1.5	0.06
6	13.9	25.4	8.3	12.4	170.7	1.3	0.07
7	16.1	27.6	6.8	9.7	160.7	0.9	0.06
8	14.2	25.7	6.5	11.6	154.7	0.7	0.07
9	14.8	26.4	4.8	12.0	170.8	2.1	0.07
10	14.9	26.4	7.7	12.3	176.7	1.4	0.07

Top Filter Paper
Weight Gain (1-3)= 0.3 mgrs

Bottom Filter Paper
Weight Gain (1-3)= 0.4mgrs

Penetration (1-3) (wt%) = 0.03

Average time per cycle (1-3)= 6.22min

Average total Dust Collected per cycle (1-3)=10.7 grs

Average Inlet Dust Loading (1-3)= 7.2 grs/m^3

Top Filter Paper
Weight gain(4-10)= 1.6 mgrs

Bottom Filter Paper
Weight gain (4-10)=1.1 mgrs

ΔP_i(11thCycle)= 14.9cm of H_2O

Penetration (4-10) (wt%)= 0.044

Average time per cycle(4-10)=7.48 min

Average Total Dust Collected per cycle (4-10)=12.84grs

Average Inlet Dust Loading (4-10)= 7.17grs/m^3

TABLE 6a-17

PANEL BED FILTER

PENETRATION DATA AT 150°C

FILTRATION SYSTEM: DUST= Coal Fly Ash +80 Mesh (Con Edison)
GRANULES= Angular Sand 40-50 Mesh U.S. Std.

SUPERFICIAL VELOCITY=17.2 cm/sec (33.8ft/min)

PUFFBACK TANK: VOLUME= 206cm^3; PRESSURE= 204.7x10^3 Pa (15 psig)

PRESSURE DROP DUE TO FILTER CAKE BEFORE CLEANING=15.24cm of H_2O

CYCLE #	ΔP_i cm of H_2O	ΔP_f cm of H_2O	t (min)	Dust from Puffback (grs)	Granules from Puff-back (grs)	Dust at bottom of panel(grs)	(Dust/Granule) from Puffback
1	13.0	28.3	10.3	13.4	178.5	1.3	0.08
2	14.2	29.5	11.4	15.9	191.2	0.9	0.08
3	14.2	29.5	9.0	15.1	188.3	1.3	0.08
4	14.4	29.8	9.2	14.8	188.8	1.2	0.08
5	15.1	30.5	9.2	13.9	189.5	1.5	0.07
6	15.1	30.5	7.3	12.9	192.9	1.1	0.07
7	14.2	29.5	7.4	13.1	193.0	1.2	0.07
8	14.9	30.2	7.0	13.3	189.7	1.2	0.07
9	15.1	30.5	9.4	13.7	198.7	1.2	0.07
10	15.1	30.5	7.3	13.9	183.1	1.2	0.08

Top Filter Paper
Weight Gain (1-3)= 0.7 mgrs

Bottom Filter Paper
Weight Gain (1-3)= 0.3mgrs

Penetration (1-3) (wt%) = 0.031

Average time per cycle (1-3)=10.22min

Average total Dust Collected per cycle (1-3)=15.97grs

Average Inlet Dust Loading (1-3)=6.53 grs/m^3

Top Filter Paper
Weight gain(4-10)= 1.0mgrs

Bottom Filter Paper
Weight gain (4-10)= 1.1 mgrs

ΔP_i (11thCycle)= 15.1cm of H_2O

Penetration (4-10) (wt%) = 0.03

Average time per cycle(4-10) = 8.12min

Average Total Dust Collected per cycle (4-10)=14.89grs

Average Inlet Dust Loading (4-10) = 7.66grs/m^3

TABLE 6a-18

PANEL BED FILTER

PENETRATION DATA AT 150°C

FILTRATION SYSTEM: DUST= Coal Fly Ash +80 Mesh (Con Edison)
GRANULES= Angular Sand 40-50 Mesh U.S. Std.

SUPERFICIAL VELOCITY=17.2 cm/sec (33.8ft/min)

PUFFBACK TANK: VOLUME= 206cm^3; PRESSURE= 204.7x10^3 Pa (15 psig)

PRESSURE DROP DUE TO FILTER CAKE BEFORE CLEANING=19.05cm of H_2O

CYCLE #	ΔP_i cm of H_2O	ΔP_f cm of H_2O	t (min)	Dust from Puffback (grs)	Granules from Puff-back (grs)	Dust at bottom of panel(grs)	(Dust/Granule) from Puffback
1	13.9	33.0	12.3	14.1	170.2	1.6	0.08
2	16.1	35.2	9.0	12.0	176.3	0.8	0.07
3	14.2	33.2	10.9	16.1	189.7	1.3	0.08
4	14.6	33.7	10.1	15.4	185.7	1.5	0.08
5	14.9	34.0	12.1	16.2	175.0	1.5	0.09
6	15.6	34.7	8.1	15.2	188.3	1.1	0.08
7	15.1	34.2	8.4	16.3	189.5	1.8	0.09
8	15.1	34.2	9.3	17.4	196.6	1.7	0.09
9	14.9	34.0	12.0	16.9	185.3	1.7	0.09
10	16.3	35.4	9.9	16.5	176.6	1.8	0.09

Top Filter Paper
Weight Gain (1-3)= 0.7 mgrs

Bottom Filter Paper
Weight Gain (1-3)=0.3 mgrs

Penetration (1-3)
(wt%)= 0.022

Average time per cycle (1-3)=10.72min

Average total Dust Collected
per cycle (1-3)=15.3 grs

Average Inlet Dust Loading
(1-3)= 6.0 grs/m^3

Top Filter Paper
Weight gain(4-10)= 0.7 mgrs

Bottom Filter Paper
Weight gain (4-10)= 0.5 mgrs

ΔP_i (11^{th}Cycle)=16.3 cm of H_2O

Penetration (4-10) (wt%)=0.014

Average time per cycle(4-10)= 10.0min

Average Total Dust Collected
per cycle (4-10)=17.86grs

Average Inlet Dust Loading
(4-10)=7.46 grs/m^3

TABLE 6a-19

PANEL BED FILTER

PENETRATION DATA AT 150°C

FILTRATION SYSTEM: DUST= Coal Fly Ash +80 Mesh (Con Edison)
GRANULES= Angular Sand 40-50 Mesh U.S. Std.

SUPERFICIAL VELOCITY= 17.2cm/sec (33.8ft/min)

PUFFBACK TANK: VOLUME= 206cm^3; PRESSURE= 239.3 KPa (20 psig)

PRESSURE DROP DUE TO FILTER CAKE BEFORE CLEANING= 11.4 cm of H_2O

CYCLE #	ΔP_i cm of H_2O	ΔP_f cm of H_2O	t (min)	Dust from Puffback (grs)	Granules from Puff-back (grs)	Dust at bottom of panel (grs)	(Dust/Granule) from Puffback
1	13.7	25.2	11.8	11.5	222.4	0.9	0.05
2	12.7	24.2	8.	12.4	225.1	1.4	0.06
3	13.9	25.4	7.0	9.1	214.5	0.8	0.04
4	14.6	27.6	5.7	12.5	235.7	1.8	0.05
5	14.6	26.2	5.7	13.0	232.4	1.70	0.06
6	14.9	28.3	7.6	15.0	245.3	1.7	0.06
7	15.4	26.9	5.1	10.3	200.9	1.0	0.05
8	15.4						

Top Filter Paper
Weight Gain (1-3)= 0.3 mgrs

Bottom Filter Paper
Weight Gain (1-3)= 0.3mgrs

Top Filter Paper
Weight gain(4- 7)= 0.2 mgrs

Bottom Filter Paper
Weight gain (4-7)= 0.2 mgrs

ΔP_i (8thCycle)= 15.4 cm of H_2O

Penetration (1-3)
(wt%)= 0.02

Average time per cycle (1-3)= 9.2 min

Average total Dust Collected
per cycle (1-3)=12.03grs

Average Inlet Dust Loading
(1-3)= 5.5 grs/m^3

Penetration (4-7) (wt%)= 0.01

Average time per cycle(4-7)= 6. min

Average Total Dust Collected
per cycle (4-10)=13.95grs

Average Inlet Dust Loading
(4-7)=9.73 grs/m^3

TABLE 6a-20

PANEL BED FILTER

PENETRATION DATA AT 150°C

FILTRATION SYSTEM: DUST= Coal Fly Ash +80 Mesh (Con Edison)
GRANULES= Angular Sand 40-50 Mesh U.S. Std.

SUPERFICIAL VELOCITY=20.3 cm/sec (40 ft/min)

PUFFBACK TANK: VOLUME= 206cm^3; PRESSURE= 170.3x10^3 Pa (10 psig)

PRESSURE DROP DUE TO FILTER CAKE BEFORE CLEANING=7.62 cm of H_2O

CYCLE #	ΔP_i cm of H_2O	ΔP_f cm of H_2O	t (min)	Dust from Puffback (grs)	Granules from Puff-back (grs)	Dust at bottom of panel(grs)	(Dust/Granule) from Puffback
1	17.8	25.4	14.0	2.2	20.8	1.3	0.11
2	20.2	27.8	11.0	4.5	37.0	1.0	0.12
3	20.2	27.8	10.8	4.3	35.6	1.1	0.12
4	21.6	29.3	10.6	4.1	25.6	1.3	0.16
5	21.8	29.5	9.2	3.7	21.2	1.1	0.17
6	22.8	30.5	7.9	4.4	34.6	0.9	0.13
7	23.3	30.9	10.0	3.9	24.3	0.7	0.16
8	23.3	29.3	9.6	4.0	31.0	0.7	0.13
9	22.8	28.6	7.3	3.4	20.3	0.6	0.17
10	23.0	30.7	8.0	5.5	35.0	1.1	0.16

Top Filter Paper
Weight Gain (1-3)= 0.4 mgrs

Bottom Filter Paper
Weight Gain (1-3)= 0.4mgrs

Penetration (1-3)
(wt%) = 0.083

Average time per cycle (1-3)=11.93min

Average total Dust Collected
per cycle (1-3)= 4.7 grs

Average Inlet Dust Loading
(1-3)=1.38 grs/m^3

Top Filter Paper
Weight gain(4-10)= 0.8 mgrs

Bottom Filter Paper
Weight gain (4-10)= 1.6 mgrs

ΔP_i (11thCycle)= 23.0cm of H_2O

Penetration (4-10) (wt%)= 0.101

Average time per cycle(4-10)=9.84 min

Average Total Dust Collected
per cycle (4-10)=4.957grs

Average Inlet Dust Loading
(4-10)= 1.3 grs/m^3

TABLE 6a-21

PANEL BED FILTER

PENETRATION DATA AT 150°C

FILTRATION SYSTEM: DUST= Coal Fly Ash +80 Mesh (Con Edison)
GRANULES= Angular Sand 40-50 Mesh U.S. Std.

SUPERFICIAL VELOCITY=20.3 cm/sec (40 ft/min)

PUFFBACK TANK: VOLUME= 206cm^3; PRESSURE= 204.7x10^3 Pa (15 psig)

PRESSURE DROP DUE TO FILTER CAKE BEFORE CLEANING= 7.62cm of H_2O

CYCLE #	ΔP_i cm of H_2O	ΔP_f cm of H_2O	t (min)	Dust from Puffback (grs)	Granules from Puff-back (grs)	Dust at bottom of panel(grs)	(Dust/Granule) from Puffback
1	17.5	25.2	13.4	4.5	64.4	1.2	0.069
2	18.5	25.9	12.3	5.6	71.8	1.1	0.018
3	18.7	26.4	11.6	5.6	59.8	1.1	0.093
4	20.2	27.7	11.0	5.2	61.3	0.9	0.084
5	19.7	27.4	10.8	4.5	48.5	0.8	0.092
6	20.2	27.8	11.2	5.1	57.0	0.8	0.089
7	20.2	27.8	11.5	5.5	63.0	0.8	0.087
8	20.6	28.3	11.3	4.4	44.7	0.8	0.098
9	20.6	28.3	10.6	5.9	65.3	1.0	0.090
10	20.6	28.3	9.5	5.7	65.4	0.7	0.087

Top Filter Paper
Weight Gain (1-3)= 0.4 mgrs

Bottom Filter Paper
Weight Gain (1-3)= 0.5mgrs

Penetration (1-3)
(wt%)= 0.069

Average time per cycle (1-3)=12.43min

Average total Dust Collected
per cycle (1-3)=6.37 grs

Average Inlet Dust Loading
(1-3)= 1.8 grs/m^3

Top Filter Paper
Weight gain(4-10)= 1.5mgrs

Bottom Filter Paper
Weight gain (4-10)= 1.6 mgrs

ΔP_i(11thCycle)= 20.6cm of H_2O

Penetration (4-10) (wt%)= 0.108

Average time per cycle(4-10)=11.3 min

Average Total Dust Collected
per cycle (4-10)= 6.0 grs

Average Inlet Dust Loading
(4-10)= 1.87grs/m^3

TABLE 6a-22

PANEL BED FILTER

PENETRATION DATA AT 150°C

FILTRATION SYSTEM: DUST= Coal Fly Ash +80 Mesh (Con Edison)
GRANULES= Angular Sand 40-50 Mesh U.S. Std.

SUPERFICIAL VELOCITY= 20.3cm/sec (40 ft/min)

PUFFBACK TANK: VOLUME= 206cm^3; PRESSURE= 239.2x10^3 Pa (20 psig)

PRESSURE DROP DUE TO FILTER CAKE BEFORE CLEANING=7.62 cm of H_2O

CYCLE #	ΔP_i cm of H_2O	ΔP_f cm of H_2O	t (min)	Dust from Puffback (grs)	Granules from Puff-back (grs)	Dust at bottom of panel(grs)	(Dust/Granule) from Puffback
1	15.8	23.5	12.4	3.8	114.5	1.1	0.033
2	15.8	23.5	13.0	5.1	131.8	1.1	0.039
3	15.8	23.5	13.6	6.1	144.9	1.3	0.042
4	15.8	23.5	14.1	7.2	107.6	1.5	0.070
5	16.6	24.2	14.2	8.3	117.8	1.7	0.084
6	17.8	25.4	10.6	6.2	96.4	0.8	0.064
7	19.4	26.9	12.0	6.9	120.1	1.1	0.057
8	18.5	26.2	11.8	7.0	116.9	1.0	0.059
9	19.0	26.6	10.5	7.0	118.4	1.0	0.059
10	19.0	26.6	10.6	6.7	114.6	1.0	0.058

Top Filter Paper
Weight Gain (1-3)= 1.0 mgrs

Bottom Filter Paper
Weight Gain (1-3)=0.9 mgrs

Penetration (1-3)
(wt%) = 0.15

Average time per cycle (1-3)= 13.0min

Average total Dust Collected
per cycle (1-3)= 6.16grs

Average Inlet Dust Loading
(1-3)=1.66 grs/m^3

Top Filter Paper
Weight gain(4-10)= 1.4 mgrs

Bottom Filter Paper
Weight gain (4-10)= 2.1 mgrs

ΔP_i (11^{th}Cycle)= 19.0cm of H_2O

Penetration (4-10) (wt%)= 0.089

Average time per cycle(4-10)= 12.3min

Average Total Dust Collected
per cycle (4-10)=8.19 grs

Average Inlet Dust Loading
(4-10)= 2.34grs/m^3

TABLE 6a-23

PANEL BED FILTER

PENETRATION DATA AT 150°C

FILTRATION SYSTEM: DUST= Coal Fly Ash +80 Mesh (Con Edison)
GRANULES=Silicon Carbide 40-50 Mesh U.S. Std.

SUPERFICIAL VELOCITY= 7.7 cm/sec (15.2ft/min)

PUFFBACK TANK: VOLUME= 206cm^3: PRESSURE= 170.3x10^3 Pa (10 psig)

PRESSURE DROP DUE TO FILTER CAKE BEFORE CLEANING=3.81 cm of H_2O

CYCLE #	ΔP_i cm of H_2O	ΔP_f cm of H_2O	t (min)	Dust from Puffback (grs)	Granules from Puff-back (grs)	Dust at bottom of panel(grs)	(Dust/Granule) from Puffback
1	6.7	10.6	14.0	4.0	48.8	0.4	0.08
2	7.2	11.0	13.7	5.6	62.2	0.4	0.09
3	7.4	11.3	13.2	5.6	63.5	0.5	0.09
4	7.4	11.3	12.6	4.8	32.6	0.4	0.15
5	7.7	11.5	13.5	5.1	44.9	0.4	0.11
6	7.9	11.8	7.0	6.1	59.5	0.4	0.10
7	8.2	12.0	8.4	6.1	53.9	0.4	0.11
8	8.2	12.0	10.0	4.8	42.2	0.4	0.11
9	8.2	12.0	10.8	5.4	54.4	0.6	0.10
10	8.0	11.8	11.3	5.4	52.4	0.4	0.10

Top Filter Paper
Weight Gain (1-3)= 0.3 mgrs

Bottom Filter Paper
Weight Gain (1-3)=0.4 mgrs

Penetration (1-3)
(wt%)= 0.062

Average time per cycle (1-3)=13.63min

Average total Dust Collected
per cycle (1-3)= 5.5 grs

Average Inlet Dust Loading
(1-3)= 3.74grs/m^3

Top Filter Paper
Weight gain(4-10)= 0.5mgrs

Bottom Filter Paper
Weight gain (4-10)= 0.5 mgrs

ΔP_i(11thcycle)= 8.2 cm of H_2O

Penetration (4-10) (wt%)= 0.036

Average time per cycle(4-10)= 10.5min

Average Total Dust Collected
per cycle (4-10)= 5.8 grs

Average Inlet Dust Loading
(4-10)= 5.12grs/m^3

TABLE 6a-24

PANEL BED FILTER

PENETRATION DATA AT 150°C

FILTRATION SYSTEM: DUST= Coal Fly Ash +80 Mesh (Con Edison)
GRANULES=Silicon Carbide 40-50 Mesh U.S. Std.

SUPERFICIAL VELOCITY= 7.7 cm/sec (15.2ft/min)

PUFFBACK TANK: VOLUME= 206cm^3; PRESSURE= 170.3x10^3 Pa (10 psig)

PRESSURE DROP DUE TO FILTER CAKE BEFORE CLEANING=7.62 cm of H_2O

CYCLE #	ΔP_i cm of H_2O	ΔP_f cm of H_2O	t (min)	Dust from Puffback (grs)	Granules from Puff-back (grs)	Dust at bottom of panel(grs)	(Dust/Granule) from Puffback
1	7.0	14.6	16.6	7.7	56.2	1.6	0.14
2	7.2	14.9	15.0	10.1	57.7	1.8	0.18
3	8.4	16.1	12.7	9.5	67.9	1.5	0.14
4	7.9	15.6	15.7	8.4	32.4	1.8	0.26
5	9.1	16.8	16.2	11.9	73.8	1.7	0.16
6	8.4	16.1	13.6	9.0	61.9	2.1	0.14
7	8.6	16.3	14.3	9.8	63.7	2.3	0.15
8	8.6	16.3	14.3	9.9	66.7	2.3	0.15
9	8.4	16.1	17.0	10.0	60.2	2.2	0.17
10	8.8	16.5	15.3	10.3	70.3	2.0	0.15

Top Filter Paper
Weight Gain (1-3)= 0.3 mgrs

Bottom Filter Paper
Weight Gain (1-3)=0.3 mgrs

Penetration (1-3) (wt%)= 0.0273

Average time per cycle (1-3)=14.77min

Average total Dust Collected per cycle (1-3)=10.73grs

Average Inlet Dust Loading (1-3)=6.73 grs/m^3

Top Filter Paper
Weight gain(4-10)= 0.5 mgrs

Bottom Filter Paper
Weight gain (4-10)= 0.6 mgrs

ΔP_i (11thCycle)= 8.6 cm of H_2O

Penetration (4-10) (wt%)= 0.019

Average time per cycle(4-10)=15.2 min

Average Total Dust Collected per cycle (4-10)= 11.9grs

Average Inlet Dust Loading (4-10)= 7.3 grs/m^3

TABLE 6a-25

PANEL BED FILTER

PENETRATION DATA AT 150°C

FILTRATION SYSTEM: DUST= Coal Fly Ash +80 Mesh (Con Edison)
GRANULES=Silicon Carbide 40-50 Mesh U.S. Std.

SUPERFICIAL VELOCITY= 7.7 cm/sec (15.2ft/min)

PUFFBACK TANK: VOLUME= 206cm^3; PRESSURE= 170.3x10^3 Pa (10 psig)

PRESSURE DROP DUE TO FILTER CAKE BEFORE CLEANING=11.43cm of H_2O

CYCLE #	ΔP_i cm of H_2O	ΔP_f cm of H_2O	t (min)	Dust from Puffback (grs)	Granules from Puff-back (grs)	Dust at bottom of panel(grs)	(Dust/Granule) from Puffback
1	7.0	18.5	20.3	10.3	68.1	1.4	0.15
2	7.2	18.7	18.8	13.8	79.5	1.9	0.17
3	7.9	19.4	19.3	14.6	83.9	1.7	0.17
4	7.7	19.2	19.4	12.0	62.5	1.8	0.19
5	7.9	19.4	18.4	15.9	90.0	2.2	0.18
6	7.9	19.4	15.3	14.4	88.8	1.6	0.16
7	7.9	19.4	19.3	14.3	87.5	1.6	0.16
8	7.9	19.4	17.0	15.0	90.6	1.6	0.17
9	7.9	19.4	18.8	15.4	89.3	2.0	0.17
10	7.7	19.2	18.3	14.2	79.6	1.9	0.18

Top Filter Paper
Weight Gain (1-3)=0.85 mgrs

Bottom Filter Paper
Weight Gain (1-3)= 0.9mgrs

Penetration (1-3)
(wt%)= 0.06

Average time per cycle (1-3)=19.42min

Average total Dust Collected
per cycle (1-3)=14.57grs

Average Inlet Dust Loading
(1-3)= 6.95grs/m^3

Top Filter Paper
Weight gain(4-10)= 1.3 mgrs

Bottom Filter Paper
Weight gain (4-10)= 1.2 mgrs

ΔP_i (11thCycle)= 7.9 cm of H_2O

Penetration (4-10) (wt%)= 0.031

Average time per cycle(4-10)= 18.1min

Average Total Dust Collected
per cycle (4-10)=16.27grs

Average Inlet Dust Loading
(4-10)= 8.3 grs/m^3

TABLE 6a-26

PANEL BED FILTER

PENETRATION DATA AT 150°C

FILTRATION SYSTEM: DUST= Coal Fly Ash +80 Mesh (Con Edison)
GRANULES= Silicon Carbide 40-50 Mesh U.S. Std.

SUPERFICIAL VELOCITY= 7.7 cm/sec (15.2ft/min)

PUFFBACK TANK: VOLUME= 206cm^3; PRESSURE= 170.3x10^3 Pa (10 psig)

PRESSURE DROP DUE TO FILTER CAKE BEFORE CLEANING= 15.2 cm of H_2O

CYCLE #	ΔP_i cm of H_2O	ΔP_f cm of H_2O	t (min)	Dust from Puffback (grs)	Granules from Puff-back (grs)	Dust at bottom of panel(grs)	(Dust/Granule) from Puffback
1	7.4	23.0	23.8	15.4	88.1	2.5	0.17
2	8.4	23.8	22.7	18.2	92.5	2.5	0.20
3	8.9	24.2	23.8	16.9	76.7	3.0	0.22
4	9.4	24.7	22.0	19.4	101.9	2.8	0.19
5	9.4	24.7	26.6	20.2	117.3	2.9	0.17
6	9.1	24.5	19.9	17.8	98.6	2.0	0.18
7	9.4	24.7	23.9	18.1	89.5	2.5	0.20
8	9.6	25.0	22.1	22.8	109.7	4.0	0.21
9	10.3	25.7	21.1	21.7	117.6	4.7	0.18
10	10.1	25.4	18.9	22.4	122.7	5.0	0.18

Top Filter Paper
Weight Gain (1-3)=0.9 mgrs

Bottom Filter Paper
Weight Gain (1-3)=0.7 mgrs

Penetration (1-3)
(wt%)= 0.04

Average time per cycle (1-3)=23.4 min

Average total Dust Collected
per cycle (1-3)=19.5 grs

Average Inlet Dust Loading
(1-3)= 7.61grs/m^3

Top Filter Paper
Weight gain(4-10)=1.1 mgrs

Bottom Filter Paper
Weight gain (4-10)=1.3 mgrs

ΔP_i(11thCycle)= 10.0 cm of H_2O

Penetration (4-10) (wt%)= 0.021

Average time per cycle(4-10)= 22.1min

Average Total Dust Collected
per cycle (4-10)=23.8 grs

Average Inlet Dust Loading
(4-10)= 9.97grs/m^3

TABLE 6a-27

PANEL BED FILTER

PENETRATION DATA AT 150°C

FILTRATION SYSTEM: DUST=Coal Fly Ash +80 Mesh (Con Edison)
GRANULES= Silicon Carbide 40-50 Mesh U.S. Std.

SUPERFICIAL VELOCITY=11.12cm/sec (21.9ft/min)

PUFFBACK TANK: VOLUME= 206cm^3; PRESSURE= 170.3x10^3 Pa (10 psig)

PRESSURE DROP DUE TO FILTER CAKE BEFORE CLEANING=3.81 cm of H_2O

CYCLE #	ΔP_i cm of H_2O	ΔP_f cm of H_2O	t (min)	Dust from Puffback (grs)	Granules from Puff-back (grs)	Dust at bottom of panel(grs)	(Dust/Granule) from Puffback
1	9.1	13.0	16.2	5.0	37.1	1.4	0.13
2	10.4	14.3	14.8	5.4	38.7	1.3	0.14
3	10.8	14.6	14.3	6.5	50.5	1.1	0.13
4	11.3	15.1	13.8	8.7	83.7	1.4	0.10
5	10.8	14.6	13.0	7.8	78.3	1.3	0.10
6	10.8	14.6	14.5	8.2	70.3	1.6	0.12
7	10.8	14.6	14.8	7.6	76.8	1.4	0.10
8	11.0	14.9	13.6	7.2	70.5	1.4	0.10
9	11.0	14.9	13.8	7.8	73.4	1.4	0.11
10	10.8	14.6	13.4	8.4	75.3	1.5	0.11

Top Filter Paper
Weight Gain (1-3)= 0.7 mgrs

Bottom Filter Paper
Weight Gain (1-3)= 0.9mgrs

Penetration (1-3)
(wt%)= 0.1131

Average time per cycle (1-3)= 15.1min

Average total Dust Collected
per cycle (1-3)= 6.9 grs

Average Inlet Dust Loading
(1-3)= 3.0 grs/m^3

Top Filter Paper
Weight gain(4-10)= 1.2 mgrs

Bottom Filter Paper
Weight gain (4-10)= 1.9 mgrs

ΔP_i(11thCycle)=10.8 cm of H_2O

Penetration (4-10) (wt%)= 0.068

Average time per cycle(4-10)= 13.9min

Average Total Dust Collected
per cycle (4-10)= 9.41grs

Average Inlet Dust Loading
(4-10)= 4.4 grs/m^3

TABLE 6a-28

PANEL BED FILTER

PENETRATION DATA AT 150°C

FILTRATION SYSTEM: DUST= Coal Fly Ash +80 Mesh (Con Edison)
GRANULES= Silicon Carbide 40-50 Mesh U.S. Std.

SUPERFICIAL VELOCITY= 11.1 cm/sec (21.9ft/min)

PUFFBACK TANK: VOLUME= 206cm^3; PRESSURE= 170.3x10^3 Pa (10 psig)

PRESSURE DROP DUE TO FILTER CAKE BEFORE CLEANING= 7.62 cm of H_2O

CYCLE #	ΔP_i cm of H_2O	ΔP_f cm of H_2O	t (min)	Dust from Puffback (grs)	Granules from Puff-back (grs)	Dust at bottom of panel(grs)	(Dust/Granule) from Puffback
1	8.4	16.1	16.7	6.2	40.7	3.0	0.15
2	10.6	18.2	18.4	8.4	51.0	2.7	0.16
3	11.0	18.7	16.6	8.7	45.9	2.3	0.19
4	12.0	19.7	14.5	7.9	30.6	2.6	0.26
5	12.2	19.9	12.1	8.2	35.9	1.8	0.23
6	12.7	20.4	13.5	8.3	40.2	1.7	0.21
7	13.0	20.6	12.1	8.3	38.7	1.7	0.21
8	13.1	20.8	11.5	8.7	44.7	1.5	0.19
9	13.1	20.8	12.3	8.2	37.5	1.6	0.22
10	13.1	20.8	12.7	8.9	42.3	1.6	0.21

Top Filter Paper
Weight Gain (1-3)=0.9 mgrs

Bottom Filter Paper
Weight Gain (1-3)=0.95mgrs

Penetration (1-3)
(wt%)= 0.0865

Average time per cycle (1-3)=17.2 min

Average total Dust Collected
per cycle (1-3)=10.43grs

Average Inlet Dust Loading
(1-3)= 3.9 grs/m^3

Top Filter Paper
Weight gain(4-10)= 1.4 mgrs

Bottom Filter Paper
Weight gain (4-10)=1.7 mgrs

ΔP_i (11thcycle)= 13.1cm of H_2O

Penetration (4-10) (wt%)= 0.064

Average time per cycle(4-10)=12.7 min

Average Total Dust Collected
per cycle (4-10)= 10.1grs

Average Inlet Dust Loading
(4-10)= 5.2 grs/m^3

TABLE 6a-29

PANEL BED FILTER

PENETRATION DATA AT 150°C

FILTRATION SYSTEM: DUST= Coal Fly Ash +80 Mesh (Con Edison)
GRANULES= Silicon Carbide 40-50 Mesh U.S. Std.

SUPERFICIAL VELOCITY=11.12cm/sec (21.9ft/min)

PUFFBACK TANK: VOLUME= 206cm^3; PRESSURE= 170.3x10^3 Pa (10 psig)

PRESSURE DROP DUE TO FILTER CAKE BEFORE CLEANING=11.43cm of H_2O

CYCLE #	ΔP_i cm of H_2O	ΔP_f cm of H_2O	t (min)	Dust from Puffback (grs)	Granules from Puff-back (grs)	Dust at bottom of panel(grs)	(Dust/Granule) from Puffback
1	11.8	23.3	14.1	7.5	62.7	1.2	0.12
2	12.2	23.8	13.9	10.4	72.7	1.1	0.14
3	12.5	24.0	13.3	10.9	66.0	1.1	0.17
4	13.0	24.5	13.9	11.7	62.8	1.4	0.19
5	13.2	24.7	13.0	11.0	62.9	1.2	0.17
6	13.0	24.5	15.0	9.7	48.9	1.2	0.20
7	13.4	25.0	11.5	10.4	50.1	1.2	0.21
8	13.4	25.0	13.0	12.8	77.7	1.7	0.16
9	13.0	24.5	11.3	10.2	62.3	1.0	0.16
10	13.4	25.0	11.6	10.2	47.0	1.1	0.22

Top Filter Paper
Weight Gain (1-3)= 0.5 mgrs

Bottom Filter Paper
Weight Gain (1-3)=0.6 mgrs

Penetration (1-3) (wt%)= 0.05

Average time per cycle (1-3)= 13.8min

Average total Dust Collected per cycle (1-3)= 11.3grs

Average Inlet Dust Loading (1-3)= 5.04grs/m^3

Top Filter Paper
Weight gain(4-10)= 0.6 mgrs

Bottom Filter Paper
Weight gain (4-10)= 0.8 mgrs

ΔP_i (11thcycle)= 13.4cm of H_2O

Penetration (4-10) (wt%)= 0.0242

Average time per cycle(4-10)= 12.7min

Average Total Dust Collected per cycle (4-10)= 12.1grs

Average Inlet Dust Loading (4-10)= 6.14grs/m^3

TABLE 6a-30

PANEL BED FILTER

PENETRATION DATA AT 150°C

FILTRATION SYSTEM: DUST=Coal Fly Ash +80 Mesh (Con Edison)
GRANULES= Silicon Carbide 40-50 Mesh U.S. Std.

SUPERFICIAL VELOCITY=11.12cm/sec (21.9ft/min)

PUFFBACK TANK: VOLUME= 206cm^3; PRESSURE= 170.3x10^3 Pa (10 psig)

PRESSURE DROP DUE TO FILTER CAKE BEFORE CLEANING=15.24cm of H_2O

CYCLE #	ΔP_i cm of H_2O	ΔP_f cm of H_2O	t (min)	Dust from Puffback (grs)	Granules from Puff-back (grs)	Dust at bottom of panel(grs)	(Dust/Granule) from Puffback
1	11.5	26.9	24.0	9.6	55.3	1.3	0.17
2	12.7	28.1	14.3	13.4	70.8	1.2	0.19
3	13.0	28.3	18.0	12.7	54.6	1.7	0.23
4	15.4	30.7	15.4	11.2	36.4	1.6	0.31
5	16.1	31.4	14.4	13.5	48.8	1.2	0.28
6	15.8	31.2	14.0	13.6	55.4	1.2	0.25
7	15.6	31.0	13.3	14.1	58.3	1.1	0.24
8	15.4	30.7	11.0	10.8	33.7	1.1	0.29
9	16.6	32.0	11.5	10.3	33.7	1.4	0.31
10	17.0	32.4	10.9	13.1	54.4	1.3	0.24

Top Filter Paper
Weight Gain (1-3)= 0.4 mgrs

Bottom Filter Paper
Weight Gain (1-3)= 0.5mgrs

Penetration (1-3)
(wt%)= 0.033

Average time per cycle (1-3)=18.7 min

Average total Dust Collected
per cycle (1-3)=13.30grs

Average Inlet Dust Loading
(1-3)=4.59 grs/m^3

Top Filter Paper
Weight gain(4-10)= 0.8 mgrs

Bottom Filter Paper
Weight gain (4-10)= 0.6 mgrs

ΔP_i(11thCycle)= 16.3cm of H_2O

Penetration (4-10) (wt%)= 0.0215

Average time per cycle(4-10)=12.9 min

Average Total Dust Collected
per cycle (4-10)=13.64grs

Average Inlet Dust Loading
(4-10)= 6.81grs/m^3

TABLE 6a-31

PANEL BED FILTER

PENETRATION DATA AT 150°C

FILTRATION SYSTEM: DUST= Coal Fly Ash +80 Mesh Con Edison)
GRANULES= Silicon Carbide 40-50 Mesh U.S. Std.

SUPERFICIAL VELOCITY= 17.2cm/sec (33.8ft/min)

PUFFBACK TANK: VOLUME= 206cm^3; PRESSURE= 204.7x10^3 Pa (15 psig)

PRESSURE DROP DUE TO FILTER CAKE BEFORE CLEANING= 7.62cm of H_2O

CYCLE #	ΔP_i cm of H_2O	ΔP_f cm of H_2O	t (min)	Dust from Puffback (grs)	Granules from Puff-back (grs)	Dust at bottom of panel(grs)	(Dust/Granule) from Puffback
1	14.6	22.3	6.3	6.8	120.7	0.6	0.06
2	14.6	22.6	4.0	7.7	149.0	1.5	0.05
3	13.9	21.8	3.6	7.8	143.6	0.8	0.05
4	17.0	24.7	4.4	8.6	154.2	1.5	0.06
5	15.8	23.5	4.7	10.1	166.3	0.8	0.06
6	15.1	22.8	3.9	9.6	167.7	1.0	0.06
7	16.1	23.8	4.8	9.6	162.4	1.6	0.06
8	16.1	23.8	5.4	9.7	160.5	1.0	0.06
9	16.1	23.8	3.0	9.1	163.3	1.1	0.06
10	15.8	23.5	4.5	9.6	167.8	1.4	0.06

Top Filter Paper
Weight Gain (1-3)= 1.4 mgrs

Bottom Filter Paper
Weight Gain (1-3)= 1.1mgrs

Penetration (1-3)
(wt%)= 0.15

Average time per cycle (1-3)=4.63 min

Average total Dust Collected
per cycle (1-3)= 8.4 grs

Average Inlet Dust Loading
(1-3)= 7.58 grs/m^3

Top Filter Paper
Weight gain(4-10)= 2.7 mgrs

Bottom Filter Paper
Weight gain (4-10)= 1.7 mgrs

ΔP_i (11^{th}Cycle)= 15.8cm of H_2O

Penetration (4-10) (wt%)= 0.086

Average time per cycle(4-10)=4.4 min

Average Total Dust Collected
per cycle (4-10)=10.67grs

Average Inlet Dust Loading
(4-10)=10.13grs/m^3

TABLE 6a-32

PANEL BED FILTER

PENETRATION DATA AT 150°C

FILTRATION SYSTEM: DUST= Coal Fly Ash +80 Mesh (Con Edison)
GRANULES= Silicon Carbide 40-50 Mesh U.S. Std.

SUPERFICIAL VELOCITY=17.2 cm/sec (33.8ft/min)

PUFFBACK TANK: VOLUME= 206cm^3; PRESSURE= 204.7x10^3 Pa (15 psig)

PRESSURE DROP DUE TO FILTER CAKE BEFORE CLEANING=11.43cm of H_2O

CYCLE #	ΔP_i cm of H_2O	ΔP_f cm of H_2O	t (min)	Dust from Puffback (grs)	Granules from Puff-back (grs)	Dust at bottom of panel(grs)	(Dust/Granule) from Puffback
1	15.1	26.6	8.5	8.6	145.1	1.1	0.06
2	15.8	27.4	8.8	11.6	148.5	1.5	0.08
3	17.0	28.6	5.5	13.8	178.3	1.5	0.08
4	16.8	28.3	7.6	13.1	183.8	1.4	0.07
5	15.8	27.4	6.1	12.4	190.6	1.3	0.07
6	15.1	26.6	5.2	13.2	192.8	1.3	0.07
7	14.9	26.4	6.0	13.5	174.1	2.0	0.08
8	15.6	27.1	6.1	12.7	186.7	1.3	0.07
9	15.6 2puffbacks	36.0	<2	20.1 4.1	165.0 104.3	5.4	-
10	16.3	28.1	7.2	14.5	194.8	2.0	0.07

Top Filter Paper
Weight Gain (1-3)= 1.5 mgrs

Bottom Filter Paper
Weight Gain (1-3)= 1.0mgrs

Top Filter Paper
Weight gain(4-10)= 2.2 mgrs

Bottom Filter Paper
Weight gain (4-10)= 2.0 mgrs

ΔP_i(11thCycle)= 16.3cm of H_2O

Penetration (1-3) (wt%) = 0.096

Average time per cycle (1-3)= 7.58min

Average total Dust Collected per cycle (1-3)=12.7 grs

Average Inlet Dust Loading (1-3)= 7.0 grs/m^3

Penetration (4-10) (wt%)= 0.054

Average time per cycle(4-10)= 6.37min

Average Total Dust Collected per cycle (4-10)=16.33grs

Average Inlet Dust Loading (4-10)=10.71grs/m^3

TABLE 6a-33

PANEL BED FILTER

PENETRATION DATA AT 150°C

FILTRATION SYSTEM: DUST= Coal Fly Ash +80 Mesh (Con Edison)
GRANULES= Silicon Carbide 40-50 Mesh U.S. Std.

SUPERFICIAL VELOCITY=17.2 cm/sec (33.8ft/min)

PUFFBACK TANK: VOLUME= 206cm^3; PRESSURE= 204.7x10^3 Pa (15 psig)

PRESSURE DROP DUE TO FILTER CAKE BEFORE CLEANING=15.24cm of H_2O

CYCLE #	ΔP_i cm of H_2O	ΔP_f cm of H_2O	t (min)	Dust from Puffback (grs)	Granules from Puff-back (grs)	Dust at bottom of panel(grs)	(Dust/Granule) from Puffback
1	14.4	29.8	12.6	12.1	153.8	1.4	0.08
2	15.6	31.0	8.0	14.3	184.3	1.5	0.08
3	14.9	30.2	8.3	15.6	196.7	1.9	0.08
4	14.9	30.2	11.6	15.3	194.7	2.0	0.08
5	15.6	31.0	12.3	16.6	192.3	1.9	0.09
6	14.9	30.2	12.2	16.9	206.1	1.9	0.08
7	17.5	32.9	8.7	13.5	185.4	1.5	0.07
8	15.8	31.2	8.6	15.6	189.6	1.3	0.08
9	15.8	31.2	11.1	16.7	201.5	2.1	0.08
10	15.8	31.2	11.4	17.1	208.5	2.5	0.08

Top Filter Paper
Weight Gain (1-3)=1.2 mgrs

Bottom Filter Paper
Weight Gain (1-3)=1.1 mgrs

Penetration (1-3)
(wt%) = 0.072

Average time per cycle (1-3)=9.65 min

Average total Dust Collected
per cycle (1-3)=15.6 grs

Average Inlet Dust Loading
(1-3)=6.76 grs/m^3

Top Filter Paper
Weight gain(4-10)= 2.5 mgrs

Bottom Filter Paper
Weight gain (4-10)= 1.7 mgrs

ΔP_i(11thCycle)= 15.8cm of H_2O

Penetration (4-10) (wt%) = 0.049

Average time per cycle(4-10)=10.84min

Average Total Dust Collected
per cycle (4-10)=17.84grs

Average Inlet Dust Loading
(4-10)= 6.88grs/m^3

TABLE 6a-34

PANEL BED FILTER

PENETRATION DATA AT 150°C

FILTRATION SYSTEM: DUST= Coal Fly Ash + 80 Mesh (Commonweelth Edison)
GRANULES= Angular Sand 40-50 Mesh U.S. Std.

SUPERFICIAL VELOCITY= 11.12cm/sec (21.9 ft/min)

PUFFBACK TANK: VOLUME= 206cm^3; PRESSURE= 170.3 kPa (-10 psig)

PRESSURE DROP DUE TO FILTER CAKE BEFORE CLEANING= 15.24cm of H_2O

CYCLE #	ΔP_i cm of H_2O	ΔP_f cm of H_2O	t (min)	Dust from Puffback (grs)	Granules from Puff-back (grs)	Dust at bottom of panel(grs)	(Dust/Granule) from Puffback
1	8.88	24.12	3.97	4.8	58.8	0.8	0.082
2	10.08	25.32	4.33	5.1	62.1	0.7	0.082
3	10.08	25.32	5.	4.9	60.1	0.7	0.082
4	10.32	28.56	6.57	5.4	59.2	0.9	0.091
5	10.8	26.04	7.48	5.1	58.2	0.7	0.088
6	10.56	25.8	5.88	5.1	59.9	0.7	0.085
7	10.8	26.04	5.2	5.5	61.1	0.7	0.09
8	10.8	26.04	3.68	5.1	58.7	0.7	0.087
9	10.8	26.04	4.66	5.1	57.	1.	0.09
10	10.8	26.04	6.	5.2	62.7	0.8	0.083

Top Filter Paper
Weight Gain (1-3)= 0.4 mgrs

Bottom Filter Paper
Weight Gain (1-3)= 0.4 mgrs

Penetration (1-3) (wt%) = 0.0689

Average time per cycle (1-3)= 4.43 min

Average total Dust Collected per cycle (1-3)= 5.67grs

Average Inlet Dust Loading (1-3)= 8.25grs/m^3

Top Filter Paper
Weight gain(4-10)= 0.6 mgrs

Bottom Filter Paper
Weight gain (4-10)= 0.6 mgrs

ΔP_i (11th Cycle)= 10.8cm of H_2O

Penetration (4-10) (wt%) = 0.0418

Average time per cycle(4-10)= 5.64min

Average Total Dust Collected per cycle (4-10)= 6. grs

Average Inlet Dust Loading (4-10)= 6.87grs/m^3

TABLE 6a-35

PANEL BED FILTER

PENETRATION DATA AT 150°C

FILTRATION SYSTEM: DUST= Coal Fly Ash + 80 Mesh (Commonwealth Edison)
GRANULES= Angular Sand 40-50 Mesh U.S. Std.

SUPERFICIAL VELOCITY=11.12cm/sec (21.9ft/min)

PUFFBACK TANK: VOLUME= 206cm^3; PRESSURE= 204.7 kPa (15 psig)

PRESSURE DROP DUE TO FILTER CAKE BEFORE CLEANING=15.24cm of H_2O

CYCLE #	ΔP_i cm of H_2O	ΔP_f cm of H_2O	t (min)	Dust from Puffback (grs)	Granules from Puff-back (grs)	Dust at bottom of panel(grs)	(Dust/Granule) from Puffback
1	9.6	24.96	4.65	4.8	109.8	0.5	0.044
2	10.08	25.44	3.	4.9	105.6	0.5	0.046
3	10.32	25.56	5.08	5.1	114.8	0.5	0.044
4	10.8	26.04	5.2	5.	115.4	0.4	0.043
5	10.32	27.56	5.05	5.1	115.3	0.5	0.044
6	10.56	27.36	4.18	5.5	115.4	0.5	0.048
7	10.8	26.04	4.78	5.4	115.9	0.5	0.047
8	10.8	26.04	3.84	5.4	115.2	0.5	0.047
9	10.56	25.8	4.58	5.4	122.4	0.5	0.044
10	10.8	26.04	5.33	5.3	122.2	0.4	0.047

Top Filter Paper
Weight Gain (1-3)= 1.2 mgrs

Bottom Filter Paper
Weight Gain (1-3)= 1.1 mgrs

Penetration (1-3) (wt%)= 0.2066

Average time per cycle (1-3)= 4.24 min

Average total Dust Collected per cycle (1-3)= 5.43 grs

Average Inlet Dust Loading (1-3)= 8.27 grs/m^3

Top Filter Paper
Weight gain(4-10)= 2.6 mgrs

Bottom Filter Paper
Weight gain (4-10)= 2.4 mgrs

ΔP_i (11^{th}cycle)= 10.8 cm of H_2O

Penetration (4-10) (wt%)= 0.1812

Average time per cycle(4-10)= 4.71 min

Average Total Dust Collected per cycle (4-10)= 5.77 grs

Average Inlet Dust Loading (4-10)= 7.91 grs/m^3

TABLE 6a-36

PANEL BED FILTER

PENETRATION DATA AT 150°C

FILTRATION SYSTEM: DUST= Coal Fly Ash + 80 Mesh (Commonwealth Edison)
GRANULES= Angular Sand 40-50 Mesh U.S. Std.

SUPERFICIAL VELOCITY= 11.12cm/sec (21.9 ft/min)

PUFFBACK TANK: VOLUME= 206cm^3; PRESSURE= 170.3 kPa (10 psig)

PRESSURE DROP DUE TO FILTER CAKE BEFORE CLEANING= 7.62cm of H_2O

CYCLE #	ΔP_i cm of H_2O	ΔP_f cm of H_2O	t (min)	Dust from Puffback (grs)	Granules from Puff-back (grs)	Dust at bottom of panel(grs)	(Dust/Granule) from Puffback
1	9.36	17.04	3.63	2.6	54.3	0.3	0.048
2	9.6	17.28	3.35	3.3	70.2	0.3	0.047
3	10.08	17.76	3.92	2.8	57.5	0.4	0.049
4	10.56	18.24	4.21	3.1	57.2	0.4	0.054
5	10.08	17.76	3.1	2.9	61.5	0.3	0.047
6	10.32	18.52	2.03	3.	62.5	0.4	0.048
7	10.32	18.	2.	3.	59.8	0.3	0.05
8	10.32	18.	2.4	2.9	59.3	0.3	0.049
9	10.32	18.	3.28	2.9	58.5	0.3	0.05
10	10.56	18.24	3.17	3.1	60.7	0.3	0.051

Top Filter Paper
Weight Gain (1-3)= 0.7 mgrs

Bottom Filter Paper
Weight Gain (1-3)=0.8 mgrs

Penetration (1-3) (wt%)= 0.226

Average time per cycle (1-3)=3.63 min

Average total Dust Collected per cycle (1-3)=3.23 grs

Average Inlet Dust Loading (1-3)=5.74 grs/m^3

Top Filter Paper
Weight gain(4-10)= 0.8 mgrs

Bottom Filter Paper
Weight gain (4-10)=0.9 mgrs

ΔP_i (11^{th} Cycle)=10.32cm of H_2O

Penetration (4-10) (wt%)= 0.1072

Average time per cycle(4-10)=2.88 min

Average Total Dust Collected per cycle (4-10)=3.31 grs

Average Inlet Dust Loading (4-10)= 7.42grs/m^3

TABLE 6a-37

PANEL BED FILTER

PENETRATION DATA AT 150°C

FILTRATION SYSTEM: DUST=Coal Fly Ash + 80 Mesh (Commonwealth Edison)
GRANULES=Angular Sand 40-50 Mesh U.S. Std.

SUPERFICIAL VELOCITY=11.12cm/sec (2.19ft/min)

PUFFBACK TANK: VOLUME= 206cm^3; PRESSURE=170.3 kPa (10 psig)

PRESSURE DROP DUE TO FILTER CAKE BEFORE CLEANING=11.4 cm of H_2O

CYCLE #	ΔP_i cm of H_2O	ΔP_f cm of H_2O	t (min)	Dust from Puffback (grs)	Granules from Puff-back (grs)	Dust at bottom of panel(grs)	(Dust/Granule) from Puffback
1	8.64	20.04	5.3	3.7	50.	0.6	0.074
2	10.08	21.48	2.33	4.3	54.6	0.5	0.079
3	10.08	21.48	2.53	4.3	54.4	0.9	0.079
4	10.08	21.48	4.3	4.	51.7	0.7	0.077
5	10.08	21.48	4.07	4.3	56.1	0.8	0.077
6	10.08	21.48	5.15	4.3	56.6	0.8	0.076
7	10.08	21.48	6.	4.6	58.1	0.8	0.079
8	10.08	21.48	3.78	4.1	56.2	0.7	0.073
9	10.08	21.48	3.22	4.3	56.2	0.75	0.077
10	10.08	21.48	3.	4.3	57.8	0.6	0.074

Top Filter Paper
Weight Gain (1-3)= 0.5 mgrs

Bottom Filter Paper
Weight Gain (1-3)= 0.6mgrs

Penetration (1-3) (wt%) = 0.1126

Average time per cycle (1-3)= 3.39min

Average total Dust Collected per cycle (1-3)= 4.77grs

Average Inlet Dust Loading (1-3)= 9.08grs/m^3

Top Filter Paper
Weight gain(4-10)= 0.9 mgrs

Bottom Filter Paper
Weight gain (4-10)= 1.1 mgrs

ΔP_i (11^{th}Cycle)=10.08cm of H_2O

Penetration (4-10) (wt%) = 0.0835

Average time per cycle(4-10)=4.22 min

Average Total Dust Collected per cycle (4-10)= 5.01grs

Average Inlet Dust Loading (4-10)= 7.67grs/m^3

TABLE 6a-38

PANEL BED FILTER

PENETRATION DATA AT 150°C

FILTRATION SYSTEM: DUST=Coal Fly Ash + 80 Mesh (Commonwealth Edison)
GRANULES= Angular Sand 40-50 Mesh U.S. Std.

SUPERFICIAL VELOCITY= 11.1 cm/sec (21.9 ft/min)

PUFFBACK TANK: VOLUME= 206cm^3; PRESSURE= 170.3 kPa (10 psig)

PRESSURE DROP DUE TO FILTER CAKE BEFORE CLEANING=19.05cm of H_2O

CYCLE #	ΔP_i cm of H_2O	ΔP_f cm of H_2O	t (min)	Dust from Puffback (grs)	Granules from Puff-back (grs)	Dust at bottom of panel(grs)	(Dust/Granule) from Puffback
1	9.6	30.	2.98	4.5	34.1	0.6	0.132
2	11.76	32.88	5.05	6.8	66.6	0.7	0.102
3	12.	31.08	4.68	5.8	68.	0.6	0.085
4	11.28	30.48	7.42	6.3	72.	0.6	0.088
5	11.28	30.36	6.18	6.4	79.3	0.7	0.081
6	11.28	30.36	5.9	6.1	71.8	0.7	0.085
7	11.28	30.36	5.15	6.2	72.3	0.7	0.086
8	11.28	30.36	7.	6.2	71.4	0.7	0.087
9	11.04	30.12	8.55	6.2	71.6	0.7	0.087
10	11.04	30.12	3.4	6.6	87.6	0.6	0.075

Top Filter Paper
Weight Gain (1-3)= 0.6 mgrs

Bottom Filter Paper
Weight Gain (1-3)= 0.7mgrs

Penetration (1-3)
(wt%) = 0.1003

Average time per cycle (1-3)=4.24 min

Average total Dust Collected
per cycle (1-3) = 6.33grs

Average Inlet Dust Loading
(1-3) = 9.64grs/m^3

Top Filter Paper
Weight gain(4-10)= 1.9 mgrs

Bottom Filter Paper
Weight gain (4-10)= 1.8 mgrs

ΔP_i (11thCycle)= 11.04cm of H_2O

Penetration (4-10) (wt%) = 0.1113

Average time per cycle(4-10) = 6.23 min

Average Total Dust Collected
per cycle (4-10)=6.96 grs

Average Inlet Dust Loading
(4-10) = 7.21grs/m^3

TABLE 6a-39

PANEL BED FILTER

PENETRATION DATA AT 150°C

FILTRATION SYSTEM: DUST= Coal Fly Ash + 80 Mesh (Commonwealth Edison)
GRANULES= Angular Sand 40-50 Mesh U.S. Std.

SUPERFICIAL VELOCITY=17.2 cm/sec (33.8ft/min)

PUFFBACK TANK: VOLUME= 206cm^3; PRESSURE=170.3 kPa (10 psig)

PRESSURE DROP DUE TO FILTER CAKE BEFORE CLEANING=11.43cm of H_2O

CYCLE #	ΔP_i cm of H_2O	ΔP_f cm of H_2O	t (min)	Dust from Puffback (grs)	Granules from Puff-back (grs)	Dust at bottom of panel(grs)	(Dust/Granule) from Puffback
1	14.88	26.16	2.53	3.1	53.4	0.3	0.059
2	17.04	28.44	2.28	3.8	58.3	0.3	0.065
3	17.04	28.44	2.43	4.1	61.5	0.4	0.067
4	18.	29.4	2.32	3.7	61.7	0.5	0.06
5	17.28	28.56	2.72	4.2	62.3	0.4	0.067
6	17.52	29.04	2.4	4.1	64.2	0.4	0.064
7	17.52	29.04	2.33	4.	62.1	0.4	0.064
8	17.76	29.28	2.57	3.7	61.8	0.3	0.06
9	17.52	28.92	2.25	3.8	61.3	0.4	0.062
10	17.52	28.92	2.33	3.8	61.6	0.4	0.062

Top Filter Paper
Weight Gain (1-3) = 0.4 mgrs

Bottom Filter Paper
Weight Gain (1-3) = 0.4 mgrs

Penetration (1-3)
(wt%) = 0.0977

Average time per cycle (1-3) = 2.41 min

Average total Dust Collected
per cycle (1-3) = 4. grs

Average Inlet Dust Loading
(1-3) = 6.94 grs/m^3

Top Filter Paper
Weight gain (4-10) = 0.7 mgrs

Bottom Filter Paper
Weight gain (4-10) = 0.6 mgrs

ΔP_i (11th Cycle) = 17.52cm of H_2O

Penetration (4-10) (wt%) = 0.0633

Average time per cycle (4-10) = 2.41 min

Average Total Dust Collected
per cycle (4-10) = 4.3 grs

Average Inlet Dust Loading
(4-10) = 7.44 grs/m^3

TABLE 6a-40

PANEL BED FILTER

PENETRATION DATA AT 150°C

FILTRATION SYSTEM: DUST= Coal Fly Ash + 80 Mesh (Commonwealth Edison)
GRANULES= Angular Sand 40-50 Mesh U.S. Std.

SUPERFICIAL VELOCITY= 17.2cm/sec (33.8ft/min)

PUFFBACK TANK: VOLUME= 206cm^3; PRESSURE= 204.7 kPa (15 psig)

PRESSURE DROP DUE TO FILTER CAKE BEFORE CLEANING=11.43cm of H_2O

CYCLE #	ΔP_i cm of H_2O	ΔP_f cm of H_2O	t (min)	Dust from Puffback (grs)	Granules from Puff-back (grs)	Dust at bottom of panel(grs)	(Dust/Granule) from Puffback
1	14.16	25.44	2.28	3.6	106.4	0.4	0.034
2	15.6	27.12	2.93	4.1	107.4	0.5	0.038
3	16.32	27.84	2.7	4.	109.8	0.4	0.036
4	16.56	28.08	1.72	4.5	102.7	0.5	0.044
5	15.84	27.24	2.07	3.8	99.4	0.5	0.038
6	16.56	27.84	2.4	3.8	101.5	0.4	0.037
7	16.08	27.48	2.37	4.3	101.5	0.4	0.042
8	16.56	27.48	2.53	3.8	103.8	0.3	0.037
9	16.08	27.48	2.6	4.3	106.4	0.4	0.04
10	16.32	27.72	3.1	4.2	107.1	0.3	0.039

Top Filter Paper
Weight Gain (1-3)= 0.2 mgrs

Bottom Filter Paper
Weight Gain (1-3)= 0.2 mgrs

Penetration (1-3)
(wt%)= 0.045%

Average time per cycle (1-3)= 2.64min

Average total Dust Collected
per cycle (1-3)=4.33 grs

Average Inlet Dust Loading
(1-3)= 6.87grs/m^3

Top Filter Paper
Weight gain(4-10)= 0.8 mgrs

Bottom Filter Paper
Weight gain (4-10)= 0.6 mgrs

ΔP_i (11^{th}Cycle)=16.56cm of H_2O

Penetration (4-10) (wt%)= 0.065%

Average time per cycle(4-10)= 2.4 min

Average Total Dust Collected
per cycle (4-10)= 4.5 grs

Average Inlet Dust Loading
(4-10)= 7.84grs/m^3

TABLE 6a-41

PANEL BED FILTER

PENETRATION DATA AT 150°C

FILTRATION SYSTEM: DUST= Coal Fly Ash + 80 Mesh (Commonwealth Edison)
GRANULES= Angular Sand 40-50 Mesh U.S. Std.

SUPERFICIAL VELOCITY= 17.2cm/sec (33.8ft/min)

PUFFBACK TANK: VOLUME= 206cm^3; PRESSURE= 170.3 kPa (10 psig)

PRESSURE DROP DUE TO FILTER CAKE BEFORE CLEANING=15.2 cm of H_2O

CYCLE #	ΔP_i cm of H_2O	ΔP_f cm of H_2O	t (min)	Dust from Puffback (grs)	Granules from Puff-back (grs)	Dust at bottom of panel(grs)	(Dust/Granule) from Puffback
1	14.64	29.76	3.33	4.4	68.4	0.4	0.064
2	16.56	31.68	3.2	4.5	64.5	0.5	0.07
3	17.04	32.4	3.44	4.9	67.5	0.5	0.073
4	18.	33.12	3.5	5.	64.8	0.4	0.077
5	17.52	32.28	3.2	4.8	64.5	0.4	0.074
6	17.52	32.28	3.65	4.9	64.7	0.3	0.076
7	18.	33.24	4.08	4.8	59.8	0.4	0.08
8	18.24	33.24	2.76	4.6	61.	0.4	0.075
9	18.24	34.56	2.89	5.	62.2	0.4	0.08
10	18.24	33.6	3.23	4.9	62.8	0.4	0.078

Top Filter Paper
Weight Gain (1-3)=0.5 mgrs

Bottom Filter Paper
Weight Gain (1-3)=0.3 mgrs

Penetration (1-3) (wt%)= 0.0772

Average time per cycle (1-3)=3.32 min

Average total Dust Collected per cycle (1-3)=5.07 grs

Average Inlet Dust Loading (1-3)=6.37 grs/m^3

Top Filter Paper
Weight gain(4-10)=0.9 mgrs

Bottom Filter Paper
Weight gain (4-10)=0.7 mgrs

ΔP_i (11thCycle)=18.24cm of H_2O

Penetration (4-10) (wt%)= 0.0639

Average time per cycle(4-10)=3.33 min

Average Total Dust Collected per cycle (4-10)=5.24 grs

Average Inlet Dust Loading (4-10)=6.58 grs/m^3

TABLE 6a-42

PANEL BED FILTER

PENETRATION DATA AT 150°C

FILTRATION SYSTEM: DUST= Coal Fly Ash + 80 Mesh (Commonwealth Edison)
GRANULES= Angular Sand 40-50 Mesh U.S. Std.

SUPERFICIAL VELOCITY=17.2 cm/sec (33.8 ft/min)

PUFFBACK TANK: VOLUME= 206cm^3; PRESSURE= 170.3 kPs (10 psig)

PRESSURE DROP DUE TO FILTER CAKE BEFORE CLEANING=19.05cm of H_2O

CYCLE #	ΔP_i cm of H_2O	ΔP_f cm of H_2O	t (min)	Dust from Puffback (grs)	Granules from Puff-back (grs)	Dust at bottom of panel(grs)	(Dust/Granule) from Puffback
1	13.92	33.36	3.52	6.	72.9	0.7	0.082
2	18.	36.96	4.46	6.7	67.7	0.6	0.099
3	18.	36.92	5.73	5.8	65.5	0.5	0.089
4	18.72	37.92	4.37	5.5	62.8	0.4	0.088
5	18.	37.44	2.31	5.5	64.4	0.6	0.085
6	18.48	37.56	4.37	4.9	60.7	0.4	0.081
7	18.96	38.04	3.59	5.4	64.2	0.6	0.084
8	18.72	37.80	4.04	5.2	64.3	0.6	0.081
9	18.72	37.8	4.31	5.4	63.1	0.6	0.086
10	18.72	37.80	4.35	5.3	63.6	0.5	0.083

Top Filter Paper
Weight Gain (1-3)=0.7 mgrs

Bottom Filter Paper
Weight Gain (1-3)=0.4 mgrs

Penetration (1-3) (wt%)= 0.0794

Average time per cycle (1-3)=4.57 min

Average total Dust Collected per cycle (1-3)=6.77 grs

Average Inlet Dust Loading (1-3)=6.19 grs/m^3

Top Filter Paper
Weight gain(4-10)=1.3 mgrs

Bottom Filter Paper
Weight gain (4-10)=0.7 mgrs

ΔP_i (11thCycle)=18.72cm of H_2O

Penetration (4-10) (wt%)= 0.0717

Average time per cycle(4-10)=3.91 min

Average Total Dust Collected per cycle (4-10)=5.84 grs

Average Inlet Dust Loading (4-10)=6.25 grs/m^3

TABLE 6a-43

PANEL BED FILTER

PENETRATION DATA AT 150°C

FILTRATION SYSTEM: DUST= Coal Fly Ash + 80 Mesh (Commonwealth Edison)
GRANULES= Angular Sand 40-50 Mesh U.S. Std.

SUPERFICIAL VELOCITY= 7.75cm/sec (15.2ft/min)

PUFFBACK TANK: VOLUME= 206cm^3; PRESSURE= 170,3 kPa (10 psig)

PRESSURE DROP DUE TO FILTER CAKE BEFORE CLEANING=11.43cm of H_2O

CYCLE #	ΔP_i cm of H_2O	ΔP_f cm of H_2O	t (min)	Dust from Puffback (grs)	Granules from Puff-back (grs)	Dust at bottom of panel(grs)	(Dust/Granule) from Puffback
1	7.08	18.48	3.15	3.3	58.1	0.5	0.057
2	7.92	19.2	4.48	3.4	59.5	0.5	0.057
3	8.16	19.44	4.18	3.7	59.4	0.5	0.062
4	8.64	19.92	5.09	4.3	66.1	0.7	0.065
5	8.4	19.8	4.05	4.	62.	0.7	0.065
6	8.64	20.4	5.6	4.4	60.6	0.6	0.073
7	8.64	20.16	3.6	4.3	64.4	0.5	0.067
8	8.64	21.36	4.52	4.5	66.4	0.6	0.068
9	8.64	20.16	4.22	4.3	64.7	0.6	0.067
10	8.64	20.16	5.4	4.4	60.9	0.5	0.077

Top Filter Paper
Weight Gain (1-3)=0.8 mgrs

Bottom Filter Paper
Weight Gain (1-3)= 1. mgrs

Penetration (1-3)
(wt%)=0.2214

Average time per cycle (1-3)=3.93 min

Average total Dust Collected
per cycle (1-3)=3.97 grs

Average Inlet Dust Loading
(1-3)=9.36 grs/m^3

Top Filter Paper
Weight gain(4-10)= 1.2 mgrs

Bottom Filter Paper
Weight gain (4-10)=1.6 mgrs

ΔP_i(11thCycle)=8.64 cm of H_2O

Penetration (4-10) (wt%)= 0.1193

Average time per cycle(4-10)= 4.64min

Average Total Dust Collected
per cycle (4-10)= 4.91grs

Average Inlet Dust Loading
(4-10)=9.81 grs/m^3

TABLE 6a-44

PANEL BED FILTER

PENETRATION DATA AT 150°C

FILTRATION SYSTEM: DUST= Cement + 80 Mesh
GRANULES= Angular Sand 40-50 Mesh U.S. Std.

SUPERFICIAL VELOCITY=11.12cm/sec (21.9ft/min)

PUFFBACK TANK: VOLUME= 206cm^3; PRESSURE=170.3 kPa (10 psig)

PRESSURE DROP DUE TO FILTER CAKE BEFORE CLEANING=11.43cm of H_2O

CYCLE #	ΔP_i cm of H_2O	ΔP_f cm of H_2O	t (min)	Dust from Puffback (grs)	Granules from Puff-back (grs)	Dust at bottom of panel(grs)	(Dust/Granule) from Puffback
1	8.64	20.16	12.2	5.15	72.65	0.2	0.071
2	9.72	21.12	4.5	6.	58.7	0.3	0.102
3	9.84	21.36	5.23	6.3	75.5	0.25	0.083
4	9.6	24.	0.67	5.5	67.3	0.3	0.082
5	9.6	21.36	4.52	5.6	62.	0.3	0.09
6	9.6	21.36	5.25	5.4	50.9	0.3	0.106
7	9.84	21.36	3.63	5.4	59.1	0.2	0.091
8	10.08	21.6	4.95	5.6	76.7	0.2	0.073
9	9.84	21.36	3.72	5.2	57.	0.35	0.091
10	9.84	21.36	5.5	5.6	72.4	0.2	0.077

Top Filter Paper
Weight Gain (1-3)= 0.5 mgrs

Bottom Filter Paper
Weight Gain (1-3)= 0.9 mgrs

Penetration (1-3)
(wt%)= 0.1125

Average time per cycle (1-3)=7.3 min

Average total Dust Collected
per cycle (1-3)=6.07 grs

Average Inlet Dust Loading
(1-3)=5.36 grs/m^3

Top Filter Paper
Weight gain(4-10)= 0.4 mgrs

Bottom Filter Paper
Weight gain (4-10)= 0.5 mgrs

ΔP_i (11^{th} cycle)=9.84 cm of H_2O

Penetration (4-10) (wt%)= 0.0328

Average time per cycle(4-10)=4.03 min

Average Total Dust Collected
per cycle (4-10)=5.74 grs

Average Inlet Dust Loading
(4-10)=9.2 grs/m^3

TABLE 6a-45

PANEL BED FILTER

PENETRATION DATA AT 150°C

FILTRATION SYSTEM: DUST= Cement + 80 Mesh
GRANULES= Angular Sand 40-50 Mesh U.S. Std.

SUPERFICIAL VELOCITY=11.12cm/sec (21.9ft/min)

PUFFBACK TANK: VOLUME= 206cm^3; PRESSURE= 204.7 kPa (15 psig)

PRESSURE DROP DUE TO FILTER CAKE BEFORE CLEANING=11.43cm of H_2O

CYCLE #	ΔP_i cm of H_2O	ΔP_f cm of H_2O	t (min)	Dust from Puffback (grs)	Granules from Puff-back (grs)	Dust at bottom of panel(grs)	(Dust/Granule) from Puffback
1	9.12	20.4	7.	5.7	116.2	0.3	0.049
2	9.36	20.76	3.47	5.4	108.3	0.7	0.05
3	10.08	21.48	3.25	5.4	111.3	0.5	0.049
4	9.6	21.12	4.	5.3	114.2	0.5	0.046
5	9.36	20.76	5.4	5.1	99.8	0.5	0.051
6	9.36	20.76	4.51	5.1	110.5	0.6	0.046
7	9.36	20.64	5.17	5.1	115.2	0.4	0.044
8	9.36	20.76	5.78	5.0	97.7	0.4	0.051
9	9.36	20.76	6.9	5.1	112.3	0.5	0.045
10	9.36	20.76	6,23	5.1	111.9	0.4	0.046

Top Filter Paper
Weight Gain (1-3)=0.2 mgrs

Bottom Filter Paper
Weight Gain (1-3)=0.4 mgrs

Penetration (1-3)
(wt%)= 0.0488

Average time per cycle (1-3)=4.57 min

Average total Dust Collected
per cycle (1-3)=6.0 grs

Average Inlet Dust Loading
(1-3)=8.48 grs/m^3

Top Filter Paper
Weight gain(4-10)=0.9 mgrs

Bottom Filter Paper
Weight gain (4-10)=1.0 mgrs

ΔP_i (11^{th} Cycle)=9.36 cm of H_2O

Penetration (4-10) (wt%)=0.0711

Average time per cycle(4-10)=5.43 min

Average Total Dust Collected
per cycle (4-10)=5.59 grs

Average Inlet Dust Loading
(4-10)=6.82 grs/m^3

TABLE 6a-46

PANEL BED FILTER

PENETRATION DATA AT 150°C

FILTRATION SYSTEM: DUST= Cement + 80 Mesh
GRANULES= Angular Sand 40-50 Mesh U.S. Std.

SUPERFICIAL VELOCITY=11.12cm/sec (21.9ft/min)

PUFFBACK TANK: VOLUME= 206cm^3; PRESSURE=170.3 kPa (10 psig)

PRESSURE DROP DUE TO FILTER CAKE BEFORE CLEANING=7.62 cm of H_2O

CYCLE #	ΔP_i cm of H_2O	ΔP_f cm of H_2O	t (min)	Dust from Puffback (grs)	Granules from Puffback (grs)	Dust at bottom of panel(grs)	(Dust/Granule) from Puffback
1	9.12	19.2	4.2	3.3	59.9	0.2	0.052
2	9.84	17.52	3.5	3.2	52.1	0.2	0.061
3	9.84	17.76	2.57	3.4	55.8	0.2	0.061
4	9.96	17.64	3.62	3.6	65.8	0.2	0.055
5	9.84	17.52	2.42	3.3	69.2	0.2	0.048
6	9.84	17.52	2.42	3.3	57.4	0.2	0.058
7	9.96	20.88	3.52	5.1	74.8	0.2	0.068
8	9.84	17.52	2.69	3.4	71.1	0.2	0.048
9	9.84	17.4	4.57	4.	58.3	0.2	0.069
10	9.84	17.52	2.28	4.2	62.8	0.2	0.067

Top Filter Paper
Weight Gain (1-3)=0.3 mgrs

Bottom Filter Paper
Weight Gain (1-3)=0.4 mgrs

Penetration (1-3)
(wt%)= 0.0976

Average time per cycle (1-3)=3.42 min

Average total Dust Collected
per cycle (1-3)= 3.5 grs

Average Inlet Dust Loading
(1-3)=6.6 grs/m^3

Top Filter Paper
Weight gain(4-10)=0.7 mgrs

Bottom Filter Paper
Weight gain (4-10)=0.7 mgrs

ΔP_i(11thCycle)=9.84 cm of H_2O

Penetration (4-10) (wt%)= 0.0698

Average time per cycle(4-10)=3.07 min

Average Total Dust Collected
per cycle (4-10)=4.03 grs

Average Inlet Dust Loading
(4-10)=8.49 grs/m^3

TABLE 6a-47

PANEL BED FILTER

PENETRATION DATA AT 150°C

FILTRATION SYSTEM: DUST= Cement + 80 Mesh
GRANULES= Angular sand 40-50 Mesh U.S. Std.

SUPERFICIAL VELOCITY=11.12cm/sec (21.9ft/min)

PUFFBACK TANK: VOLUME= 206cm^3; PRESSURE= 170.3 kPa (10 psig)

PRESSURE DROP DUE TO FILTER CAKE BEFORE CLEANING= 15.2 cm of H_2O

CYCLE #	ΔP_i cm of H_2O	ΔP_f cm of H_2O	t (min)	Dust from Puffback (grs)	Granules from Puff-back (grs)	Dust at bottom of panel(grs)	(Dust/Granule) from Puffback
1	8.88	24.24	3.72	5.8	71.4	0.3	0.081
2	9.36	29.04	7.6	8.7	72.8	0.8	0.12
3	9.36	24.48	4.29	6.5	64.6	0.5	0.101
4	9.84	25.08	5.45	7.6	82.7	0.5	0.092
5	9.36	24.72	5.02	7.1	76.7	0.4	0.093
6	9.6	24.96	4.28	6.3	60.	0.4	0.105
7	9.84	24.96	6.25	7.1	64.2	0.3	0.111
8	9.84	25.08	5.6	7.7	82.8	0.5	0.092
9	9.84	26.64	7.55	7.9	78.5	0.3	0.101
10	10.08	27.6	7.47	7.75	79.2	0.3	0.098

Top Filter Paper
Weight Gain (1-3)= 0.2 mgrs

Bottom Filter Paper
Weight Gain (1-3)=0.4 mgrs

Penetration (1-3)
(wt%) = 0.0389 %

Average time per cycle (1-3)= 5.2 min

Average total Dust Collected
per cycle (1-3)= 7.53grs

Average Inlet Dust Loading
(1-3)= 9.35grs/m^3

Top Filter Paper
Weight gain(4-10)=0.7 mgrs

Bottom Filter Paper
Weight gain (4-10)=0.7 mgrs

ΔP_i (11^{th} Cycle)=9.84 cm of H_2O

Penetration (4-10) (wt%) = 0.0379

Average time per cycle(4-10) = 5.95min

Average Total Dust Collected
per cycle (4-10)= 7.74grs

Average Inlet Dust Loading
(4-10)= 8.4 grs/m^3

TABLE 6a-48

PANEL BED FILTER

PENETRATION DATA AT 150°C

FILTRATION SYSTEM: DUST= Cement + 80 Mesh
GRANULES= Angular Sand 40-50 Mesh U.S. Std.

SUPERFICIAL VELOCITY= 17.2 cm/sec (33.8 ft/min)

PUFFBACK TANK: VOLUME= 206 cm^3; PRESSURE= 170.3 kPa (10 psig)

PRESSURE DROP DUE TO FILTER CAKE BEFORE CLEANING= 11.43 cm of H_2O

CYCLE #	ΔP_i cm of H_2O	ΔP_f cm of H_2O	t (min)	Dust from Puffback (grs)	Granules from Puff-back (grs)	Dust at bottom of panel(grs)	(Dust/Granule) from Puffback
1	12.72	24.24	3.3	4.3	60.3	0.3	0.071
2	14.16	25.44	5.4	5.2	53.7	0.3	0.097
3	14.88	26.16	3.	4.8	49.3	0.3	0.098
4	15.36	26.64	3.58	4.7	66.9	0.4	0.07
5	14.88	26.16	2.97	4.6	49.5	0.3	0.093
6	15.6	27.	3.52	4.8	70.1	0.2	0.069
7	14.4	25.08	1.75	4.4	68.3	0.4	0.064
8	14.64	26.28	4.57	4.6	50.4	0.3	0.091
9	15.36	26.76	2.17	4.5	63.4	0.2	0.071
10	15.12	26.52	2.42	4.4	59.8	0.3	0.074

Top Filter Paper
Weight Gain (1-3)= 0.4 mgrs

Bottom Filter Paper
Weight Gain (1-3)= 0.6 mgrs

Penetration (1-3) (wt%)= 0.0964

Average time per cycle (1-3)= 3.9 min

Average total Dust Collected per cycle (1-3)= 5.07 grs

Average Inlet Dust Loading (1-3)= 5.42 grs/m^3

Top Filter Paper
Weight gain (4-10)= 0.7 mgrs

Bottom Filter Paper
Weight gain (4-10)= 0.7 mgrs

ΔP_i (11th Cycle)= 15.6 cm of H_2O

Penetration (4-10) (wt%)= 0.06

Average time per cycle (4-10)= 3. min

Average Total Dust Collected per cycle (4-10)= 4.87 grs

Average Inlet Dust Loading (4-10)= 6.79 grs/m^3

TABLE 6a-49

PANEL BED FILTER

PENETRATION DATA AT 150°C

FILTRATION SYSTEM: DUST= Cement + 80 Mesh
GRANULES= Angular Sand 40-50 Mesh U.S. Std.

SUPERFICIAL VELOCITY= 17.2 cm/sec (33.8 ft/min)

PUFFBACK TANK: VOLUME= 206 cm^3; PRESSURE= 204.7 kPa (15 psig)

PRESSURE DROP DUE TO FILTER CAKE BEFORE CLEANING= 11.43 cm of H_2O

CYCLE #	ΔP_i cm of H_2O	ΔP_f cm of H_2O	t (min)	Dust from Puffback (grs)	Granules from Puff-back (grs)	Dust at bottom of panel(grs)	(Dust/Granule) from Puffback
1	12.72	24.12	2.2	3.9	91.2	0.2	0.043
2	13.68	25.08	2.8	4.9	88.5	0.2	0.055
3	13.8	25.2	4.12	5.2	91.9	0.2	0.057
4	13.56	26.16	3.08	4.9	100.4	0.2	0.049
5	14.16	25.56	2.94	5.1	102.9	0.3	0.05
6	14.16	25.68	3.92	5.2	103.3	0.2	0.05
7	14.04	25.44	3.79	5.7	115.5	0.2	0.05
8	13.92	25.20	3.55	5.9	109.8	0.2	0.054
9	13.92	25.92	2.62	6.1	114.	0.2	0.054
10	13.68	25.2	3.37	5.5	115.4	0.2	0.048

Top Filter Paper
Weight Gain (1-3)= 0.5 mgrs

Bottom Filter Paper
Weight Gain (1-3)= 0.5 mgrs

Penetration (1-3) (wt%)= 0.1002

Average time per cycle (1-3)= 3.04 min

Average total Dust Collected per cycle (1-3)= 4.87 grs

Average Inlet Dust Loading (1-3)= 6.7 grs/m^3

Top Filter Paper
Weight gain (4-10)= 0.8 mgrs

Bottom Filter Paper
Weight gain (4-10)= 0.8 mgrs

ΔP_i (11^{th} Cycle)= 13.92 cm of H_2O

Penetration (4-10) (wt%)= 0.0587

Average time per cycle (4-10)= 3.32 min

Average Total Dust Collected per cycle (4-10)= 5.7 grs

Average Inlet Dust Loading (4-10)= 7.17 grs/m^3

TABLE 6a-50

PANEL BED FILTER

PENETRATION DATA AT 150°C

FILTRATION SYSTEM: DUST= Cement +80 Mesh
GRANULES= Angular Sand 40-50 Mesh U.S. Std.

SUPERFICIAL VELOCITY= 17.2cm/sec (33.8ft/min)

PUFFBACK TANK: VOLUME= 206cm^3; PRESSURE= 170.3 kPa (10 psig)

PRESSURE DROP DUE TO FILTER CAKE BEFORE CLEANING= 15.24 cm of H_2O

CYCLE #	ΔP_i cm of H_2O	ΔP_f cm of H_2O	t (min)	Dust from Puffback (grs)	Granules from Puff-back (grs)	Dust at bottom of panel(grs)	(Dust/Granule) from Puffback
1	13.68	29.16	5.15	4.2	48.9	0.2	0.085
2	14.4	29.64	3.22	4.2	45.2	0.2	0.092
3	15.36	30.48	2.53	4.6	51.1	0.2	0.09
4	15.6	30.72	4.67	4.6	52.7	0.2	0.087
5	15.36	30.6	3.99	5.	51.8	0.4	0.096
6	15.84	31.08	3.05	4.5	50.2	0.2	0.089
7	15.84	31.08	2.78	4.2	49.	0.2	0.085
8	15.84	31.08	3.18	4.2	49.4	0.2	0.085
9	16.08	32.04	4.13	4.3	48.9	0.2	0.087
10	16.32	31.68	3.13	5.	48.8	0.2	0.102

Top Filter Paper
Weight Gain (1-3)= 0.1 mgrs

Bottom Filter Paper
Weight Gain (1-3)= 0.2mgrs

Penetration (1-3)
(wt%)= 0.0323

Average time per cycle (1-3)= 3.63 min

Average total Dust Collected
per cycle (1-3)= 4.53 grs

Average Inlet Dust Loading
(1-3)= 5.22 grs/m^3

Top Filter Paper
Weight gain (4-10)= 0.2 mgrs

Bottom Filter Paper
Weight gain (4-10)= 0.3 mgrs

ΔP_i (11thcycle)= 16.08cm of H_2O

Penetration (4-10) (wt%)= 0.0219

Average time per cycle(4-10)= 3.56 min

Average Total Dust Collected
per cycle (4-10)= 4.77 grs

Average Inlet Dust Loading
(4-10)= 5.6 grs/m^3

TABLE 6a-51

PANEL BED FILTER

PENETRATION DATA AT 150°C

FILTRATION SYSTEM: DUST= Cement + 80 Mesh
GRANULES= Angular Sand 40-50 Mesh U.S. Std.

SUPERFICIAL VELOCITY=7.75 cm/sec (15.2ft/min)

PUFFBACK TANK: VOLUME= 206cm^3; PRESSURE=170.3 kPa (10 psig)

PRESSURE DROP DUE TO FILTER CAKE BEFORE CLEANING= 7.62cm of H_2O

CYCLE #	ΔP_i cm of H_2O	ΔP_f cm of H_2O	t (min)	Dust from Puffback (grs)	Granules from Puff-back (grs)	Dust at bottom of panel(grs)	(Dust/Granule) from Puffback
1	6.24	13.92	7.3	2.8	66.6	0.1	0.042
2	6.72	14.4	5.25	3.9	65.3	0.4	0.06
3	6.84	14.5	7.38	4.2	60.1	0.3	0.07
4	6.72	14.4	7.5	3.8	71.2	0.5	0.053
5	6.72	14.4	3.85	3.5	58.9	0.4	0.06
6	6.96	14.64	3.52	3.5	65.4	0.4	0.054
7	6.96	14.64	3.23	3.6	68.2	0.2	0.053
8	6.84	14.52	3.	3.5	61.2	0.4	0.057
9	6.96	14.64	2.8	3.4	62.6	0.2	0.054
10	6.96	14.64	3.15	3.3	55.5	0.3	0.06

Top Filter Paper
Weight Gain (1-3)=0.5 mgrs

Bottom Filter Paper
Weight Gain (1-3)=0.7 mgrs

Penetration (1-3)
(wt%)= 0.15%

Average time per cycle (1-3)= 6.64min

Average total Dust Collected
per cycle (1-3)= 3.9 grs

Average Inlet Dust Loading
(1-3)= 5.44grs/m^3

Top Filter Paper
Weight.gain(4-10)=1.1 mgrs

Bottom Filter Paper
Weight gain (4-10)= 1.1 mgrs

ΔP_i(11thCycle)= 7.08cm of H_2O

Penetration (4-10) (wt%)= 0.1191

Average time per cycle(4-10)=3.86 min

Average Total Dust Collected
per cycle (4-10)= 3.86grs

Average Inlet Dust Loading
(4-10)=9.26 grs/m^3

TABLE 6a-52

PANEL BED FILTER

PENETRATION DATA AT 150°C

FILTRATION SYSTEM: DUST= Cement + 80 Mesh
GRANULES=Angular Sand 40-50 Mesh U.S. Std.

SUPERFICIAL VELOCITY=7.75 cm/sec (15.2 ft/min)

PUFFBACK TANK: VOLUME= 206cm^3; PRESSURE= 170.3 kPa (10 psig)

PRESSURE DROP DUE TO FILTER CAKE BEFORE CLEANING=11.43cm of H_2O

CYCLE #	ΔP_i cm of H_2O	ΔP_f cm of H_2O	t (min)	Dust from Puffback (grs)	Granules from Puff-back (grs)	Dust at bottom of panel(grs)	(Dust/Granule) from Puffback
1	6.24	17.76	4.62	3.2	56.6	0.3	0.057
2	6.48	18	4.28	4.5	58.8	0.6	0.077
3	6.72	18.48	6.72	5.1	61.	0.7	0.084
4	7.2	18.72	8.	5.2	72.1	0.8	0.072
5	6.96	18.48	9.27	4.7	66.1	0.7	0.071
6	6.96	18.48	10.6	5.	67.2	0.6	0.074
7	6.96	18.48	7.38	5.	74.9	0.6	0.067
8	6.96	18.48	4.55	4.8	62.5	0.6	0.077
9	7.2	18.72	7.	4.9	65.4	0.5	0.075
10	6.96	18.48	10.6	5.6	68.6	0.8	0.082

Top Filter Paper
Weight Gain (1-3)= 0.3 mgrs

Bottom Filter Paper
Weight Gain (1-3)= 0.4mgrs

Penetration (1-3)
(wt%)= 0.0712

Average time per cycle (1-3)= 5.2 min

Average total Dust Collected
per cycle (1-3)= 4.8 grs

Average Inlet Dust Loading
(1-3)= 8.53 grs/m^3

Top Filter Paper
Weight gain(4-10)= 0.8 mgrs

Bottom Filter Paper
Weight gain (4-10)= 0.8 mgrs

ΔP_i (11thCycle)= 6.96 cm of H_2O

Penetration (4-10) (wt%)=0.0589

Average time per cycle(4-10)= 8.2 min

Average Total Dust Collected
per cycle (4-10)= 5.69 grs

Average Inlet Dust Loading
(4-10)= 6.43 grs/m^3

APPENDIX B: ROUGH ESTIMATION OF POROSITIES

Ergun's Equation :

$$\frac{\Delta P}{L} = \frac{150\,(1-\epsilon)^2 \mu\, V_s}{\epsilon^3\, D_p^2} + \frac{1.75\,(1-\epsilon)\,\rho\, V_s^2}{\epsilon^3\, D_p}$$

For air at 150°C :

$\rho = 0.836$ kg/m^3 (Perry and Chilton (1973),p.3-72)

$\mu = 0.023$ N s /m^2 (Perry and Chilton (1973),p.3-211)

For angular sand :

$\psi = 0.73$ (Sphericity) (Perry and Chilton (1973),p.5-53)

$D_s = 0.03585$ cm (40-50 mesh)(Arithmetic average of the screen openings)

The equivalent spherical diameter is:

$D_p = 0.02617$ cm

Substituting these data into Ergun's Eoustion:

$$\frac{\Delta P}{L} = \frac{(1-\epsilon)^2 V_s\, 513.69\times10^{-4}}{\epsilon^3} + \frac{(1-\epsilon)\, V_s^2\; 0.57\times10^{-4}}{\epsilon^3}$$

Where $\Delta P/L$ is in cm of H_2O /cm and V_s in cm/s

a) HORIZONTAL BED POROSITY

Clean Bed Pressure Drops :

20.77 cm of H_2O at V_s= 18.57 cm/s and at 150°C

Bed Thickness = 4.7 cm (40-50 Mesh angular sand)

37.33 cm of H_2O at V_s= 28.67 cm/s and at 150°C
Bed Thickness = 4.7 cm (40-50 Mesh angular sand)
The pressure drops used were the averages of all the runs.
Solving the equation by trial and error we obtain:

ϵ = 0.4214 At V_s= 18.57 cm/s

ϵ = 0.4088 At V_s= 28.67 cm/s

These results imply that the porosity in the Horizontal Bed varies from about 0.41 to 0.42.

b) PANEL BED FILTER POROSITY

In this rough estimation of the porosity in the panel bed filter, we are going to neglect the effect of the middle and back louvers upon the gas pressure drop.
We shall not considered the 2.54 cm bed of 14-20 Mesh angular sand since its effect upon gas pressure drop is of minor importance.

We shall assume that air travels at the "filtration velocity" for about 1.96 cm and then at the superficial velocity for 2.54 cm. (See Figures 5-2 and 5-5)

The average porosity was then calculated as in the horizontal bed :

$$\Delta P = \frac{(1-\epsilon)^2 V_s \ 513.69\times10^{-4}}{\epsilon^3} + \frac{(1-\epsilon) V_s^2 \ 0.57\times10^{-4}}{\epsilon^3} L_1$$

$$+ \frac{(1-\epsilon)^2 V_f \ 513.69\times10^{-4}}{\epsilon^3} + \frac{(1-\epsilon) V_f^2 \ 0.57\times10^{-4}}{\epsilon^3} L_2$$

Where: L_1= 2.54 cm

L_2= 1.956 cm

V_f= 2.1664 V_s

Clean Bed Pressure Drops :

6.9 cm of H_2O at V_s= 7.75 cm/s and at 150°C

9.2 cm of H_2O at V_s= 11.12 cm/s and at 150°C

13.3 cm of H_2O at V_s= 17.2 cm/s and at 150°C

Solving the equation by trial and error we obtain:

ϵ = 0.4783 at V_s= 7.75 cm/s

ϵ = 0.4869 at V_s= 11.12 cm/s

ϵ = 0.4959 at V_s= 17.2 cm/s

The pressure drops used in these calculations were the averages of all runs.

Our results imply that the porosity in the panel bed varies from about 0.48 to 0.50.

BIBLIOGRAPHY

Arras, K., Berz, W., and Johnston, W.F., "Thirteen Years of Experience in the De-dusting of Clinker Coolers with Gravel Bed Filters," paper presented at the 1972 I.E.E.E. Cement Industry Technical Conference,(1972).

Bird, R.B., Stewart, W.E., and Lightfoot, E.N., "Transport Phenomena", John Wiley & Sons, Inc., New York, (1960).

Bohm, L., Jordan, S., and Schikarski, W., "The Off-Gas Filter System of the SNR-300," paper presented at the 13th A.E.C. Air Cleaning Conference, San Francisco, Ca., (1974).

Bohm,L., Jordan, S., and Schikarski, W., "Experiments of Filtration of Sodium Aerosols by Sand-Bed Filters," paper presented at Conference on Fast Reactor Safety, Beverly Hills, Ca., (1974).

Bohm, L., and Jordan, S., "On the Filtration of Sodium Oxide Aerosol by Multilayer Sand-Bed Filters," Journal Aerosol Science, 7, 311-318, (1975).

Bradley, R.S., Trans. Faraday Soc., 32(8):1088,(1936).

Carman, P.C., "Fluid Flow Through Granular Beds," Trans. I.Ch.E., 15:150-166, (1937).

Corn, M., "The Adhesion of Solid Particles to Solid Surfaces, I- A Review," J.A.P.C.A.,11(11):523, (1961a)

Corn, M., "The Adhesion of Solid Particles to Solid Surfaces, II-", J.A.P.C.A., 11(12):566, (1961b)

Crawford, M., "Air Pollution Control Theory," McGraw-Hill, Inc., New York (1976).

Davies, C.N., "Air Filtration," Academic Press, London-New York (1973).

Dennis, R., "Collection Efficiency as a Function of Particle Size, Shape, and Density: Theory and Experience," J.A.P.C.A., 24(12):1156 (1974).

Engelbrecht, H.L., "The Gravel Bed Filter : A New Approach to Gas Cleaning," J.A.P.C.A., 15(2):43 (1965)

Epstein, B., I & EC., 40:2289 (1948).

Ergun, S., "Fluid Flow Through Packed Columns," C.E.P., 48(2):89 (1952).

First, M.W., "Filters: Prefilters, High Capacity Filters, and High Efficiency Filters; Review, Projection, and Discussion," in Proceedings of the Tenth A.E.C. Air Cleaning Conference, Conf. 680821, pp. 65-78, 142-147, New York (1968).

First, M.W., and Silverman, L., "Predicting the Performance of Cleanable Industrial Fabric Filters," J.A.P.C.A., 13(12):581 (1963).

Foust, A.S., Wenzel, L.A., Clump, C.W., Mauss, L., and Andersen, L.B., "Principles of Unit Operations," John Wiley & Sons, New York (1960).

Frederick, E.R., "How Dust Filter Selection Depends on Electrostatics," Chemical Engineering, June 26 (1961).

Friedlander, S.K., "Mass and Heat Transfer to Single Spheres and Cylinders at Low Reynolds Numbers," A.I.Ch.E.J., 3:43 (1957).

Fuchs, N.A., "The Mechanics of Aerosols," Pergamon Press, London (1964).

Gregg, S.J., and Sing, K.S.W., "The Adsorption of Gases on Porous Solids," in Surface and Colloid Science, Volume 9 (E. Matijevic Editor), John Wiley & Sons, New York (1976).

Gutfinger, C., Abuaf, N., and Tardos, G., Proceedings of the Sixth Scientific Conference of the Israel Ecological Society, Tel-Aviv, June 4-5 (1975).

Gutfinger, C., and Tardos, G., "Theoretical and Experimental Investigation on Granular Bed Dust Filters," TME-314, Technion-Israel Institute of Technology- Haifa, Israel July (1977).

Herdan, G., "Small Particle Statistics," Butterworths, London (1960).

Hirschfelder, J.O., Curtis, C.F., and Bird, R.B., "Molecular Theory of Gases and Liquids," John Wiley & Sons,New York (1954).

Irani, R.R., and Callis, C.F., "Particle Size: Measurement, Interpretation and Application", John Wiley & Sons, New York (1963).

Jackson, M., "Fluidized Beds for Sub-micron Particle Collection," A.I.Ch.E. Symposium Series, 141(70):82 (1974).

Juvinall, R.A., Kessie, R.W., and Steindler, M.J.,"Sand Bed Filtration of Aerosols: A Review of Published Information on their Use in Industrial and Atomic Energy Facilities," ANL-7683, National Technical Information Service, Springfield, Va. (1970).

Kalen, B., and Zenz, F.A., "Filtering Effluent from a Cat Cracker," C.E.P., 68(5):67 (1973).

Kolmogoroff, A.N.,"Uber das Logarithmish Normale Verteilungsgesetz der Dimensionen der Teilchen bei Zerstucke lung", C.R. Dokl Acak. Sci. U.R.S.S. (Akad. Nauk U.S.S.R.) 31(2):99 (1941).

Lee, K.C., "Filtration of Redispersed Power-Station Fly Ash by a Panel Bed Filter with Puffback," Ph.D. Thesis, The City University of New York, N.Y. (1975).

Lee, K.C., Rodon, I., Wu, M.S., Pfeffer, R. and Squires, A.M., "The Panel Bed Filter," Report # RP. 257-2, Electric Power Research Institute, Palo Alto Ca. (1977).

Lee, K.C., private communication, New York City, The City College of New York (1976).

Leith, D.H., "Particle Collection in a Pulse-Jet Fabric Filter, Sc.D. Thesis, Harvard School of Public Health, Boston,Ma. (1975).

Leith, D.H., Rudnick, S.N., and First, M.W., "High-Velocity, High-Efficiency Aerosol Filtration," E.P.A. Report # EPA-600/2-76-020, National Technical Information Service, Springfield, Va. (1976).

Leith, D.H., and First, M.W., "Performance of a Pulse-Jet Filter at High Filtration Velocity: I-Particle Collection," J.A.P.C.A., 27(6):534 (1977).

Leva, M., "Fluidization,"McGraw-Hill Book Co., New York (1959).

Lucas,H.G., and Smith, N.S. Jr., "Multiple-Orifice Feeder for Fine Particles," U.S. Bureau of Mines Report of Investigations, R.I. 7944 (1974).

Lunge, G., "A Theoretical and Practical Treatise on the Manufacture of Sulfuric Acid and Alkali with the Collateral Branches," 1st Edition, Vol. 3, p. 248, Jan van Voorst, London (1880).

McCain, J.D., "Evaluation of Rexnord Gravel Bed Filter," Report # EPA-600/2-76-164, U.S. Environmental Protection Agency, Washington (1976)

Miyamoto, S., and Bohn, H.L., "Filtration of Airborne Particulates by Gravel Filters: I- Initial Collection Efficiency of a Gravel Layer," J.A.P.C.A., 24(11):1051 (1974).

Miyamoto, S., and Bohn, H.L., "Filtration of Airborne Particulates by Gravel Filters:II- Collection Efficiency and Pressure Drop in Filterin Fume," J.A.P.C.A., 25(1):40 (1975).

Muller, A., Proc. Roy. Soc.,A154,624 (1936).

Nielsen, K.A. and Hill, J.C., "Collection of Inertialess Particles on Spheres with Electrical Forces," I.&E.C. Fundamentals, 15, 149 (1976).

Orr, C., " Particulate Technology," Mcmillan Co., New York (1966).

Pall, D.B., I.&E.C., 45, 1197 (1953).

Parestky, L., "Filtration of Aerosols by Granular Beds," Ph.D. Thesis, The City University of New York,N.Y.(1972).

Paretsky, L., Theodore, L., Pfeffer, R., and Squires, A.M., "Panel Bed Filter for Simultaneous Removal of Fly Ash and Sulfur Dioxide: II- Filtration of Dilute Aerosols by Sand Beds," J.A.P.C.A., 21(4):204 (1971).

Payatakes, A.C., Tien, C., and Turian, R.M., "Trajectory Calculation of Particle Deposition in Deep Bed Filtration," A.I.Ch.E.J., 20(5):889 (1974)

Perry, R.H., and Chilton, C.H., (Editors), "Chemical Engineers' Handbook," fifth Edition, McGraw-Hill Book Co., New York (1973).

Prieve, D.C., and Ruckensteins, E., "Effect of London Forces upon the Rate of Deposition of Brownian Particles," A.I.Ch.E.J., 20(6):1178 (1974).

Rajagopalan, R., and Tien, C., "Trajectory Analysis of Deep Bed Filtration with the Sphere in Cell Porous Media Model, A.I.Ch.E.J., 22(3):523 (1976).

Rexnord Co., "Gravel Bed Dust Collector," Bulletin # 203, Air Pollution Control Division, Louisville, Ky. (1976).

Ricca, F., Pisani, C., and Garrone, E., "Adsorption-Desorption Phenomena," Proc. 2nd Intern. Conf.,1971, p. 111 (1972).

Schueler, J.A., "Gravel Bed Filters for Lime Kilns," paper presented at the Convention of the National Lime Association. Hershey, Pa., November 9 (1972).

Snyder, C.A., and Pring, R.T., "Design Considerations in Filtration of Hot Gases," I.&E.C., 47(5):960 (1955)

Spielman, J.P., and Fitzpatrick, J.A., "Theory of Particle Collection under London and Gravity Forces," J. Coll. Interface Sci., 42, 607 (1973).

Squires, A.M., "Method and Apparatus for Treating Fluid and Non-Fluid Materials," U.S. Patent 3,296,775, January 10 (1967).

Squires, A.M., and Pfeffer, R., " Panel Bed Filters for Simultaneous Removal of Fly Ash and Sulfur Dioxide: I-Introduction," J.A.P.C.A., 20(8):534 (1970).

Strauss, W., and Thring, M.W., Journal Iron Steel Institute, 62,196 (1960).

Sundberg, R.E., "The Prediction of Overall Collection Efficiency of Air Pollution Control Devices from Fractional Efficiency Curves," J.A.P.C.A., 24(8):759 (1974).

Tardos, G., Gutfinger, C. and Abuaf, N., "Deposition of Dust Particles in a Fluidized Bed Filter," Israel Journal of Technology, 12, 184 (1974)

Tardos, G., Abuaf, N., and Gutfinger, C., "Diffusional Filtration of Dust in a Fluidized Bed Filter," Atmospheric Environment, 10,389 (1976).

Taub, S.I., "Filtration Phenomena in a Packed Bed Filter," Ph.D. Thesis, Carnegie-Mellon University, Pittsburg, Pa. (1970).

Thomas, J.W., and Yoder, R.E., "Aerosol Size for Maximum Penetration through Fiberglas and Sand Filters," AMA Arch. Ind. Health, 13, p. 545 (1956a).

Thomas, J.W., and Yoder, R.E., "Aerosol Penetration through a Lead Shot Column: A Method of Particle Size Estimation," AMA Arch. Ind. Health, 13, p. 550 (1956b).

Whitman, R.V., and Healy, K.A., "Shear Strength of Sands During Rapid Loadings," Trans. A.S.C.E., 128, 1553 (1963).

Whitman, R.V., Miller, E.T., and Moore, P.J., "Yielding and Locking of Confined Sand," Journal of Soil Mechanics and Foundation Division, Pro. of A.S.C.E., 90 # SM4, p. 57c (1964).

Willeke, K., and Whitby, K.T., "Atmospheric Aerosols: Size Distribution Interpretation," J.A.P.C.A.,25(5):529 (1975).

Williams, C.E., Hatch, T. and Greenburg, L., "Determination of Cloth Area for Industrial Air Filters," Heating,Piping and Air Conditioning Journal, 12(4):259 (1940).

Yu, E.K., "Filtration of Aerosols by Granular Beds," B.S. Ch.E. Research, The City College of New York, N.Y. (1972).

Zenz, F.A., and Othmer, D., "Fluidization and Fluid-Particle Systems," Reinhold Publishing Co., New York (1960).

Zenz, F.A., and Krockta, H., "The Shallow Expandable Bed: A Versatile Processing Tool," A.I.Ch.E. Symposium Series 116(67):245 (1973).

Zimon, A.D., "Adhesion of Dust and Powder," Plenum Press, New York (1969).